United States Nuclear Regulatory Commission Official Hearing Exhibit
In the Matter of: FLORIDA POWER & LIGHT COMPANY (Turkey Point Nuclear Generating, Units 3 and 4)
ASLBP #: 15-935-02-LA-BD01
Docket #: 05000250 & 05000251
Exhibit #: NRC-036-00-BD01 Identified: 1/4/2016
Admitted: 1/4/2016 Withdrawn:
Rejected: Stricken:
Other:
NRC-036
Submitted Nov. 10, 2015

USGS
science for a changing world

Prepared in cooperation with Miami-Dade County

Origins and Delineation of Saltwater Intrusion in the Biscayne Aquifer and Changes in the Distribution of Saltwater in Miami-Dade County, Florida

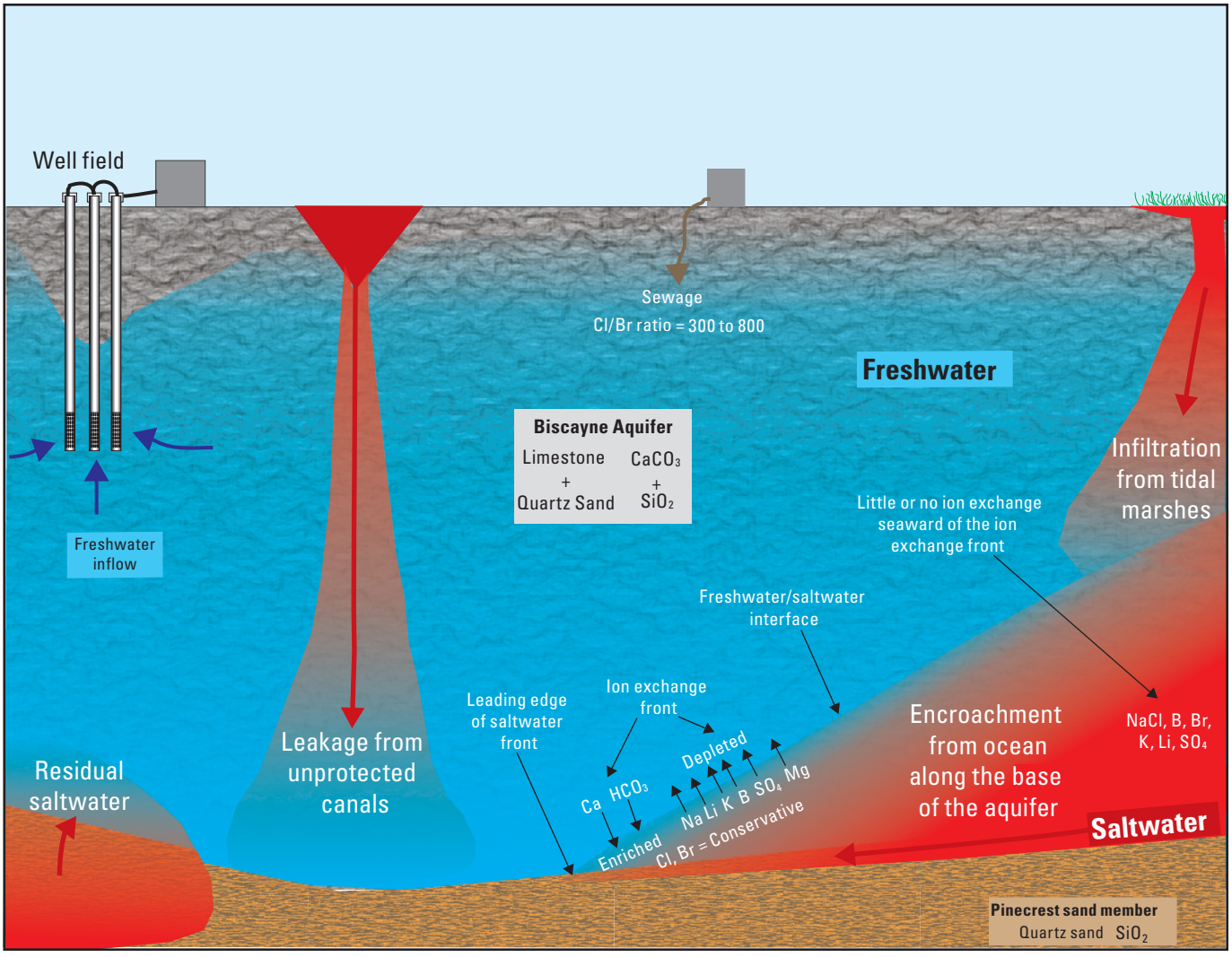

Scientific Investigations Report 2014–5025

U.S. Department of the Interior
U.S. Geological Survey

Cover. Conceptual diagram of sources and mechanisms of the saltwater that has intruded parts of aquifers in southeast Florida, and changes in water chemistry that may result from this intrusion.

Origins and Delineation of Saltwater Intrusion in the Biscayne Aquifer and Changes in the Distribution of Saltwater in Miami-Dade County, Florida

By Scott T. Prinos, Michael A. Wacker, Kevin J. Cunningham, and David V. Fitterman

Prepared in cooperation with Miami-Dade County

Scientific Investigations Report 2014–5025

U.S. Department of the Interior
U.S. Geological Survey

U.S. Department of the Interior
SALLY JEWELL, Secretary

U.S. Geological Survey
Suzette M. Kimball, Acting Director

U.S. Geological Survey, Reston, Virginia: 2014

For more information on the USGS—the Federal source for science about the Earth, its natural and living resources, natural hazards, and the environment, visit http://www.usgs.gov or call 1–888–ASK–USGS.

For an overview of USGS information products, including maps, imagery, and publications, visit http://www.usgs.gov/pubprod

To order this and other USGS information products, visit http://store.usgs.gov

Any use of trade, firm, or product names is for descriptive purposes only and does not imply endorsement by the U.S. Government.

Although this information product, for the most part, is in the public domain, it also may contain copyrighted materials as noted in the text. Permission to reproduce copyrighted items must be secured from the copyright owner.

Suggested citation:
Prinos, S.T., Wacker, M.A., Cunningham, K.J., and Fitterman, D.V., 2014, Origins and delineation of saltwater intrusion in the Biscayne aquifer and changes in the distribution of saltwater in Miami-Dade County, Florida: U.S. Geological Survey Scientific Investigations Report 2014–5025, 101 p., *http://dx.doi.org/10.3133/sir20145025*.

ISSN 2328-0328 (online)

Acknowledgments

The authors would like to acknowledge the contributions of information provided by EAS Engineering, Inc., the Florida Department of Environmental Protection, the Florida Keys Aqueduct Authority, Miami-Dade County Department of Environmental Resource Management, and the South Florida Water Management District. We greatly appreciate the cooperation of the following property owners who allowed us to make measurements on their lands: the AA Baker Group, LTD, the Archdiocese of Miami, Alamo Rent A Car, Barry University, FRS Holdings, Inc., the City of Homestead, Homestead Miami Speedway, Hallandale Beach Elementary School, the Miami-Dade County Department of Public Schools, Miami-Dade County Parks and Recreation Department, the South Florida Water Management District, and Palmer Trinity School. Bob Brown of the Archdiocese of Miami; Edward Swakon of EAS Engineering, Inc.; Dr. Claudius Carnegie, Jorge Corrales, and Greg Mohr of the Miami-Dade County Department of Public Schools; Maria Idia Macfarlane, Sonia Villamil, and Virginia Walsh of the Miami-Dade Water and Sewer Department; and Steve Krupa of the South Florida Water Management District were instrumental in helping us gain access to numerous properties where the time-domain electromagnetic soundings were completed. Maria Idia Macfarlane of the Miami-Dade County Water and Sewer Department helped to oversee much of the well installation. Jorge Corrales helped collect many of the surface geophysical measurements that were made on lands owned by the Miami-Dade County Department of Public Schools. Michael J. Alexander, project manager of the Homestead Miami Speedway, not only provided necessary access to speedway properties for measurements but also helped make necessary contacts with other properties owners in the area. Jim Happell of the University of Miami, Rosenstiel School of Marine and Atmospheric Science, John Stowell of Mount Sopris Instrument Company, and Roy Sonenshein of the National Park Service, Everglades National Park provided substantive reviews.

The authors also would like to acknowledge the contributions of staff members of the U.S. Geological Survey. Michele Markovits helped with many aspects of this study, including the geochemical sampling, geophysical data collection, data entry, and sample preparation and analysis. Adam Foster provided substantive geochemical advice and helped to compile sample results in the database. Robert Valderrama completed most of the processing of time series electromagnetic induction log sets, and Brian Banks collected the most recent logs for these datasets. Ronald Bruce Irvin provided quality assurance of these log sets and partially automated the application of necessary adjustments. Lee Massey and Corey Whittaker helped to collect water samples. Brian Banks, Adrian Castillo, Eric Carlson, and Jeff Robinson helped to collect time-domain electromagnetic soundings. Jeff Robinson also collected many of the borehole logs as the new monitoring wells were being installed and helped to oversee some of the well installation. Ronald Bruce Irvin created the necessary scripts, software, and files to convert the static “Manual Water-Level Measurements in South Florida” website into a dynamic website that serves routinely collected salinity information as well as most of the salinity information collected during this study. The new website has proven to be valuable to local water managers as they seek greater understanding of the changes in the extent and magnitude of saltwater intrusion in the Biscayne aquifer. Ronald Bruce Irvin also oversaw quality assurance for the time-series electromagnetic induction logs used during this study. Michael W. Bradley, Ed Busenberg, Richard H. Coupe, Kim H. Haag, Steven Hinkle, Carole Johnson, Robert Renken, Dorothy Sifuentes, Rick M. Spechler, David Sumner, Kimberly A. Swidarski, Kim Waltenbaugh, and Peggy Widman provided invaluable support during the review, approval, and publication process of this report.

Contents

Abstract....1
Introduction....2
Definition of Terms....2
Purpose and Scope....6
Approach....6
Description of Study Area....6
Hydrologic Controls....6
Topography and Physiography....7
Climate....7
Water Use in Miami-Dade County....7
Hydrogeology/Hydrostratigraphic Framework....10
Previous Studies....11
Origin of Saltwater Intrusion in Southeastern Florida....12
Mechanisms of Saltwater Intrusion....12
Upconing of Relict Saltwater from Previous Sea-Level High Stands....12
Encroachment of Seawater along the Base of the Biscayne Aquifer....13
Infiltration of Saltwater from Saltwater Marshes....13
Seepage from Streams or Canals in which Saltwater has Migrated Inland....13
Effects of Urban and Hydrologic Development on Saltwater Intrusion....16
Predevelopment Conditions....17
Relation of Urban Development to Saltwater Intrusion....17
Data Collection and Analysis....20
Salinity Measurements....21
Time-Series Electromagnetic Induction Logging....21
Comparison of Bulk Resistivity to Specific Conductance of Water and Chloride Concentration....22
Time-Domain Electromagnetic Soundings....22
HEM Survey Analysis....22
Approximate Inland Extent of Saltwater in the Biscayne Aquifer....25
Improved Spatial Coverage and Precision of the Inland Extent of Saltwater....25
Changes between 1995 and 2011....25
Characterization and Distribution of Saltwater in the Biscayne Aquifer....28
Major and Trace Ion Geochemistry....28
Strontium Isotope Age Dating....34
Oxygen and Hydrogen Stable Isotopes....35
Tritium and Uranium Concentration....38
Tritium/Helium-3 Age Dating....38
Sulfur Hexafluoride Age Dating....39
Estimates of Recharge Temperature Based on Dissolved Gases....39
Sources of Saltwater in the Biscayne Aquifer....41
Relict Seawater from Previous Sea-Level High Stands....41
Historical Leakage of Saltwater from Canals....42
The Card Sound Road Canal and FEC Railway Borrow Ditches....43

Miami and Tamiami Canals 47
C–111 Canal....47
Turkey Point Nuclear Power Plant Cooling Canal System....47
Recent Leakage from Canals....47
Card Sound Road Canal....48
Biscayne Canal....48
Snapper Creek Canal 49
Black Creek Canal 51
Princeton Canal....54
Saltwater Encroachment....55
Limitations....56
Summary and Conclusions....64
Selected References....66
Appendix 1. Site Location and Construction Information....76
Appendix 2. Results of Geochemical Sampling....76
Appendix 3. Salinity Profiles Collected from the Card Sound Road Canal 76
Appendix 4. Results of Time-Domain Electromagnetic Soundings....76
Appendix 5. Time-Series Electromagnetic Induction Log (TSEMIL) Dataset Calibration and Processing 77
Appendix 6. Evaluation of Depth of the Biscayne Aquifer by Using TEM Soundings....83
Appendix 7. Description of Installation and Construction of Saltwater Front Monitoring Wells 88
Appendix 8. Geophysical Logs 94
Appendix 9. Hydrostratigraphic Analysis....94
Appendix 10. Geochemical Sampling Methods 96
Appendix 11. Salinity Measurements in Canals 101
Appendix 12. Geographic Information System Files....101

Figures

1. Map showing the location of the study area, well fields, the National Parks, water conservation areas, and the helicopter electromagnetic survey of 2001, Miami-Dade and Broward Counties, Florida....3
2. Map created for the Annual Report of the Surveyor General for 1859, New York, NY, General Land Office, 1859, courtesy of the Geography and Map Division of the Library of Congress....4
3. Map showing the physiographic provinces, location of the cross section shown in figure 7, and locations of rainfall monitoring stations within the study area 8
4. Graph showing estimated total annual precipitation from selected stations in or near Miami-Dade County and documented droughts during 1931 to 2011 9
5. Graph showing estimated population (from U.S. Census Bureau, 2013) and public groundwater withdrawals in Miami-Dade County, Florida....9
6. Chart showing the generalized relation of hydrogeologic, lithostratigraphic, and time-stratigraphic units in Miami-Dade County....10
7. Hydrogeologic section *A*–*A*′ showing hydrostratigraphy of the surficial aquifer system and uppermost part of the intermediate confining unit from west to east across central Miami-Dade County....11

8. Map showing the locations of salinity monitoring sites, time-domain electromagnetic soundings, groundwater-level monitoring wells, and the mapped approximations of the inland extent of saltwater in the Biscayne aquifer in Miami-Dade and southern Broward Counties....15
9. Conceptual diagram of sources and mechanisms of the saltwater that has intruded parts of aquifers in southeast Florida, and changes in water chemistry that may result from this intrusion....16
10. Graph showing salinity of the Biscayne Canal at station BS04, Miami-Dade County, Florida, 1988–2010....17
11. Photograph showing the rapids of the Miami River prior to their destruction by dynamiting to increase drainage of the Everglades....19
12. Photograph showing the first water control structure on the Miami Canal installed in December 1939....19
13. Graph showing chloride concentration in samples from monitoring wells G–355, G–548, G–1351, and G–1354 near the Miami Canal and between 0.6 and 2.4 kilometers northwest of salinity control structure S–26, Miami-Dade County, Florida....20
14. Graph showing the relation between the resistivity of water samples collected in monitoring wells in Miami-Dade County, Florida, and the formation resistivity measured by electromagnetic induction logs in the screened intervals of the same well....23
15. Graph showing the relation between water resistivity and chloride concentration in water samples from monitoring wells in Miami-Dade County, Florida....23
16. Example of a depth slice from the 2001 helicopter electromagnetic survey, Miami-Dade County, Florida....24
17. Map showing the origin and delineation of saltwater intrusion in the Biscayne aquifer and the basis for modifications to its mapped extent....26
18. Graphs showing chloride concentrations in water samples from long-term monitoring wells....27
19. Graph showing the calcium to (bicarbonate + sulfate) ratio and the chloride concentration in groundwater and surface-water samples collected during 2009–2010, Miami-Dade County, Florida....30
20. Graph showing the bromide and chloride concentrations in groundwater and surface-water samples collected during 2009–2010, Miami-Dade County, Florida....30
21. Graph showing the magnesium and chloride concentrations in groundwater and surface-water samples collected during 2009–2010, Miami-Dade County, Florida....31
22. Graph showing the potassium and chloride concentrations in groundwater and surface-water samples collected during 2009–2010, Miami-Dade County, Florida....31
23. Graph showing the sodium and chloride concentrations in groundwater and surface-water samples collected during 2009–2010, Miami-Dade County, Florida....32
24. Graph showing the boron and chloride concentrations in groundwater and surface-water samples collected during 2009–2010, Miami-Dade County, Florida....32
25. Graph showing the sulfate and chloride concentrations in groundwater and surface-water samples collected during 2009–2010, Miami-Dade County, Florida....33

26. Graph showing the calcium and chloride concentrations in groundwater and surface-water samples collected during 2009–2010, Miami-Dade County, Florida 33
27. Graph showing the barium and chloride concentrations in samples 34
28. Graph showing the silica and chloride concentrations in samples 35
29. Graphs showing relations between (*A*) chloride concentration and delta deuterium and (*B*) delta oxygen-18 and delta deuterium in groundwater and surface-water samples collected during 2009–2010, Miami-Dade County, Florida 37
30. Graph showing the $^{3}H/^{3}He$ interpreted piston-flow ages of water samples collected during 2009–2010 in the Miami-Dade County area and dates of documented droughts in south Florida 41
31. Graphs showing the (*A*) average monthly precipitation, daily average air temperature in Miami, Florida, and the range of recharge temperatures of water samples collected from the Biscayne aquifer in Miami-Dade County, Florida, and (*B*) average of daily maximum water levels in selected wells open to the Biscayne aquifer during October 1, 1974, to September 30, 2009 44
32. Graphs showing (*A*) time-series electromagnetic induction log (TSEMIL) dataset and (*B*) chloride concentrations in samples from monitoring well G–3601 and bulk conductivity measured at a depth of 56.1 meters, Biscayne aquifer, Miami-Dade County, Florida 45
33. Graphs showing: (*A*) time-series electromagnetic induction log (TSEMIL) dataset; and (*B*) chloride concentrations in samples from monitoring well G–3701 and bulk conductivity measured at a depth of 24.0 meters, Biscayne aquifer, Miami-Dade County, Florida 46
34. Graph showing salinity of the Snapper Creek Canal at station SP04, 1991–2010, Miami-Dade County, Florida 49
35. Graphs showing: (*A*) time-series electromagnetic induction log (TSEMIL) dataset; and (*B*) chloride concentrations in samples collected from well G–3608 and bulk conductivity measured at a depth of 28.9 meters, Biscayne aquifer, Miami-Dade County, Florida 50
36. Graph showing chloride concentrations in water samples from wells G–896 and G–3608, Miami-Dade County, Florida 52
37. Graph showing water levels in wells G–896 and G–3608, 1996–2011, Miami-Dade County, Florida 52
38. Graphs showing: (*A*) time-series electromagnetic induction log (TSEMIL) dataset; and (*B*) chloride concentrations in water samples from well G–3702 and bulk conductivity measured at a depth of 24.6 meters, Biscayne aquifer, Miami-Dade County, Florida 53
39. Graph showing salinity of the Black Creek Canal at station BL03, 1991–2008 and 2010, Miami-Dade County, Florida 54
40. Graph showing salinity of the Princeton Canal at station PR03, 1991–2008 and 2010, Miami-Dade County, Florida 55
41. Graphs showing: (*A*) time-series electromagnetic induction log (TSEMIL) dataset; and (*B*) chloride concentrations in samples from monitoring well G–3604 and bulk conductivity measured at a depth of 34.7 meters, Biscayne aquifer, Miami-Dade County, Florida 57
42. Graphs showing: (*A*) time-series electromagnetic induction log (TSEMIL) dataset; and (*B*) chloride concentrations in water samples from monitoring well G–3609 and bulk conductivity measured at a depth of 22.7 meters, Biscayne aquifer, Miami-Dade County, Florida 58

43. Graphs showing: (*A*) time-series electromagnetic induction log (TSEMIL) dataset; and (*B*) chloride concentrations in water samples from monitoring well G–3698 and bulk conductivity measured at a depth of 24.5 meters, Biscayne aquifer, Miami-Dade County, Florida 59
44. Graphs showing: (*A*) time-series electromagnetic induction log (TSEMIL) dataset; and (*B*) chloride concentrations in water samples from monitoring well G–3699 and bulk conductivity measured at a depth of 25.3 meters, Biscayne aquifer, Miami-Dade County, Florida 60
45. Graphs showing: (*A*) time-series electromagnetic induction log (TSEMIL) dataset; and (*B*) chloride concentrations in water samples from monitoring well G–3602 and bulk conductivity measured at a depth of 46.9 meters, Biscayne aquifer, Miami-Dade County, Florida 61
46. Graphs showing time-series electromagnetic induction log (TSEMIL) datasets from monitoring wells (*A*) G–3855 and (*B*) G–3856 for November 2007 to April 2008, Biscayne aquifer, Miami-Dade County, Florida 62
47. Graphs showing chloride concentrations in samples from monitoring wells, Miami-Dade County, Florida 63
48. Graph showing salinity of the Mowry Canal at station MW04, 1991–2009 and 2010, Miami-Dade County, Florida 63

Tables

1. Partial history (1881–1978) of canal, structure, and levee installations in south Florida 18
2. Partial history (1899–2001) of well field installations and operations in Miami-Dade County, Florida 19
3. Vertical flows measured in open boreholes prior to well installation, 2009–2011, Miami-Dade County, Florida 21
4. Determination of the strontium-87 to strontium-86 ratio in water samples collected during 2009, in Miami-Dade County, Florida 36
5. Results of tritium/helium-3 age dating of water samples collected during 2009–2010 in Miami-Dade County, Florida 40
6. Differences between ages determined using SF_6 and tritium/helium-3 age dating for samples collected in Miami-Dade County, Florida, during 2009–2010 42
7. Average recharge temperature and chloride concentration of surface-water and groundwater samples collected in Miami-Dade County, Florida during 2009–2010 43

Conversion Factors

SI to Inch/Pound

Multiply	By	To obtain
	Length	
centimeter (cm)	0.3937	inch (in.)
millimeter (mm)	0.03937	inch (in.)
meter (m)	3.281	foot (ft)
kilometer (km)	0.6214	mile (mi)
	Area	
square meter (m^2)	0.0002471	acre
square kilometer (km^2)	247.1	acre
square centimeter (cm^2)	0.001076	square foot (ft^2)
square meter (m^2)	10.76	square foot (ft^2)
square centimeter (cm^2)	0.1550	square inch (ft^2)
square kilometer (km^2)	0.3861	square mile (mi^2)
	Volume	
liter (L)	0.2642	gallon (gal)
cubic meter (m^3)	264.2	gallon (gal)
cubic meter (m^3)	0.0002642	million gallons (Mgal)
cubic centimeter (cm^3)	0.06102	cubic inch (in^3)
liter (L)	61.02	cubic inch (in^3)
cubic meter (m^3)	35.31	cubic foot (ft^3)
	Flow rate	
meter per day (m/d)	3.281	foot per day (ft/d)
meter per year (m/yr)	3.281	foot per year ft/yr)
liter per second (L/s)	15.85	gallon per minute (gal/min)
liter per minute (L/min)	0.2642	gallon per minute (gal/min)
cubic meter per day (m^3/d)	264.2	gallon per day (gal/d)
cubic meter per second (m^3/s)	22.83	million gallons per day (Mgal/d)
	Mass	
gram (g)	0.03527	ounce, avoirdupois (oz)
kilogram (kg)	2.205	pound avoirdupois (lb)
	Radioactivity	
becquerel per liter (Bq/L)	27.027	picocurie per liter (pCi/L)
	Hydraulic conductivity	
meter per day (m/d)	3.281	foot per day (ft/d)
	Hydraulic gradient	
meter per kilometer (m/km)	5.27983	foot per mile (ft/mi)
	Transmissivity*	
meter squared per day (m^2/d)	10.76	foot squared per day (ft^2/d)

Electrical Conductivity and Electrical Resistivity

Multiply	By	To obtain
	Electrical conductivity	
siemens per meter (S/m)	1,000	millisiemens per meter (mS/m)
siemens per meter (S/m)	10,000	microsiemens per centimeter (μS/cm)
	Electrical resistivity	
ohm-meters (ohm-m)	0.001	kiloohm-meters (kohm-m)

Electrical conductivity σ in siemens per meter [S/m] can be converted to electrical resistivity ρ in ohm-meters [ohm m] as follows: $\rho = 1/\sigma$.

Electrical conductivity σ in millisiemens per meter [mS/m] can be converted to electrical resistivity ρ in ohm-meters [ohm m] as follows: $\rho = 1{,}000/\sigma$.

Electrical conductivity σ in microsiemens per centimeter [μS/cm] can be converted to electrical resistivity ρ in ohm-meters [ohm m] as follows: $\rho = 10{,}000/\sigma$.

Electrical resistivity ρ in ohm-meters [ohm m] can be converted to electrical conductivity σ in siemens per meter [S/m] as follows: $\sigma = 1/\rho$.

Electrical resistivity ρ in ohm-meters [ohm m] can be converted to electrical conductivity σ in millisiemens per meter [mS/m] as follows: $\sigma = 1{,}000/\rho$.

Electrical resistivity ρ in ohm-meters [ohm m] can be converted to electrical conductivity σ in microsiemens per centimeter [μS/cm] as follows: $\sigma = 10{,}000/\rho$.

Specific conductance (SC) refers to fluid electrical conductivity corrected to a temperature of 25 °C. The units of specific conductance are usually in microsiemens per centimeter [μS/cm]. The above conversions apply.

Temperature in degrees Celsius (°C) may be converted to degrees Fahrenheit (°F) as follows:

$$°F = (1.8 \times °C) + 32$$

Temperature in degrees Fahrenheit (°F) may be converted to degrees Celsius (°C) as follows:

$$°C = (°F - 32)/1.8$$

Vertical coordinate information is referenced to the National Geodetic Vertical Datum of 1929 (NGVD 29).

Horizontal coordinate information is referenced to the North American Datum of 1983 (NAD 83).

Altitude, as used in this report, refers to distance above the vertical datum.

*Transmissivity: The standard unit for transmissivity is cubic foot per day per square foot times foot of aquifer thickness [$(ft^3/d)/ft^2$]ft. In this report, the mathematically reduced form, foot squared per day (ft^2/d) or meters squared per day (m^2/d), is used for convenience.

Specific conductance is given in microsiemens per centimeter at 25 degrees Celsius (μS/cm at 25 °C).

Concentrations of chemical constituents in water are given either in milligrams per liter (mg/L) or micrograms per liter (μg/L).

Abbreviations

Ar	Argon
ABI	Acoustic borehole image
CCS	Cooling canal system
cc STP/g	Cubic centimeters at standard temperature and pressure per gram
cps	Counts per second
CU-LDEO	Columbia University, Lamont-Doherty Earth Observatory Noble Gas laboratory
EMI	Electromagnetic induction
ENSO	El Niño–Southern Oscillation
FEC	Florida East Coast
FEM	Frequency-domain electromagnetic
FGDC	Federal Geographic Data Committee
FKAA	Florida Keys Aqueduct Authority
FPL	Florida Power and Light
GIS	Geographic information system
GMWL	Global meteoric water line
GWSI	USGS Ground Water Site Inventory system
HEM	Helicopter electromagnetic
^{3}H	Tritium
$^{2}H/^{1}H$	Isotopic ratio of deuterium to hydrogen
Hz	Hertz
kHz	Kilohertz
LEL	Local evaporation line
LSWML	Local saltwater mixing line
Ma	Million years
M-D DERM	Miami-Dade County Department of Environmental Resource Management
M-D PERA	Miami-Dade County Permitting, Environmental, and Regulatory Affairs
N_2	Nitrogen
N_2/Ar	Nitrogen/argon
NOAA	National Oceanic and Atmospheric Administration
OBI	Optical borehole image
ORP	Oxygen Reduction Potential
$^{18}O/^{16}O$	Isotopic ratio of oxygen-18 to oxygen-16
PDF	Portable Document Format
ppm	parts per million
ppt	parts per thousand
pptv	parts per thousand total volume
PSU	Practical salinity units
PVC	Polyvinyl chloride
Q	Quaternary
SF_6	Sulfur hexafluoride
SP	Spontaneous potential
SPR	Single-point resistance
SST	Sea surface temperature
TDS	Total dissolved solids
TEM	Time-domain electromagnetic
TSEMIL	Time-series electromagnetic induction log
USEPA	U.S. Environmental Protection Agency
USGS	U.S. Geological Survey
USGS-SI&T	USGS Stable Isotope and Tritium
USGS-RCL	USGS Reston Chlorofluorocarbon Laboratory
VSMOW	Vienna Standard Mean Ocean Water
WCA	Water Conservation Area

Origins and Delineation of Saltwater Intrusion in the Biscayne Aquifer and Changes in the Distribution of Saltwater in Miami-Dade County, Florida

By Scott T. Prinos, Michael A. Wacker, Kevin J. Cunningham, and David V. Fitterman

Abstract

Intrusion of saltwater into parts of the shallow karst Biscayne aquifer is a major concern for the 2.5 million residents of Miami-Dade County that rely on this aquifer as their primary drinking water supply. Saltwater intrusion of this aquifer began when the Everglades were drained to provide dry land for urban development and agriculture. The reduction in water levels caused by this drainage, combined with periodic droughts, allowed saltwater to flow inland along the base of the aquifer and to seep directly into the aquifer from the canals. The approximate inland extent of saltwater was last mapped in 1995.

An examination of the inland extent of saltwater and the sources of saltwater in the aquifer was completed during 2008–2011 by using (1) all available salinity information, (2) time-series electromagnetic induction log datasets from 35 wells, (3) time-domain electromagnetic soundings collected at 79 locations, (4) a helicopter electromagnetic survey done during 2001 that was processed, calibrated, and published during the study, (5) cores and geophysical logs collected from 8 sites for stratigraphic analysis, (6) 8 new water-quality monitoring wells, and (7) analyses of 69 geochemical samples.

The results of the study indicate that as of 2011 approximately 1,200 square kilometers (km^2) of the mainland part of the Biscayne aquifer were intruded by saltwater. The saltwater front was mapped farther inland than it was in 1995 in eight areas totaling about 24.1 km^2. In many of these areas, analyses indicated that saltwater had encroached along the base of the aquifer. The saltwater front was mapped closer to the coast than it was in 1995 in four areas totaling approximately 6.2 km^2. The changes in the mapped extent of saltwater resulted from improved spatial information, actual movement of the saltwater front, or a combination of both.

Salinity monitoring in some of the canals in Miami-Dade County between 1988 and 2010 indicated influxes of saltwater, with maximum salinities ranging from 1.4 to 32 practical salinity units (PSU) upstream of the salinity control structures. Time-series electromagnetic induction log data from monitoring wells G–3601, G–3608, and G–3701, located adjacent to the Biscayne, Snapper Creek, and Black Creek Canals, respectively, and upstream of the salinity control structures, indicated shallow influxes of conductive water in the aquifer that likely resulted from leakage of brackish water or saltwater from these canals. The determination that saltwater influxes were recent is supported by the similarity in the oxygen and hydrogen stable isotope composition in samples from the Snapper Creek Canal, 1.6 kilometers (km) inland of a salinity control structure, and in samples from well G–3608, which is adjacent to the canal, as well as by the relative ages of the water sampled from well G–3608 and other wells open to the aquifer below the saltwater interface. Historical and recent salinity information from the Card Sound Road Canal, monitoring well FKS8 located adjacent to the canal, and the 2001 helicopter electromagnetic survey indicated that saltwater may occasionally leak from this canal as far inland as 15 km. This leakage may be prevented or reduced by a salinity control structure that was installed in May 2010. Saltwater also may have leaked from the Princeton Canal.

Results of geochemical sampling and analysis indicate a close correspondence between droughts and saltwater intrusion. Tritium/helium-3 apparent (piston-flow) ages determined from samples of saltwater with chloride concentrations of about 1,000 milligrams per liter (mg/L) or greater generally corresponded to a period during which droughts were frequent. Comparison of average daily air temperatures in Miami, Florida, with estimates of recharge temperatures determined from the dissolved gas composition in water samples indicated that saltwater likely entered the aquifer in April or early May when water levels are typically at their lowest during the year. Conversely, most of the samples of freshwater with chloride concentrations less than about 1,000 mg/L indicate recharge temperatures corresponding to air temperatures in mid to late May when rainfall and water levels in the aquifer increase, and the piston-flow ages of these samples correspond to wet years. The piston-flow ages of freshwater samples generally were younger than ages of samples of saltwater.

Saltwater samples that were depleted in boron, magnesium, potassium, sodium, and sulfate, and enriched in calcium relative to the concentrations theoretically produced by freshwater/seawater mixing, generally were found to be associated with areas where saltwater had recently intruded. The calcium to (bicarbonate + sulfate) molar ratios ($Ca/(HCO_3+SO_4)$) of these samples generally were greater than 1. Saltwater samples from some of the monitoring wells, however, indicated little or no enrichment or depletion of these ions relative to the theoretical freshwater/seawater mixing line, and the $Ca/(HCO_3+SO_4)$ molar ratios of these samples generally were less than 1. Results indicated that aquifer materials are approaching equilibrium with seawater at these well locations.

Introduction

The Biscayne aquifer underlying the study area (fig. 1) in Miami-Dade County and southern Broward County in Florida is prone to saltwater intrusion because this area has low land-surface altitude and a low topographic gradient and is bordered to the east and south by sources of saltwater in the Atlantic Ocean, Biscayne Bay, and Florida Bay. The aquifer is part of the surficial aquifer system, is semi-confined, and consists primarily of highly permeable limestone. Prior to development, much of Miami-Dade County was covered by the shallow marshes of the Everglades (fig. 2*A*). Beginning in the early 20th century to provide land for urban development, flood control, irrigation, and agriculture, a large part of the Everglades in this county was drained by a network of uncontrolled or inadequately controlled canals (Leach and others, 1972, p. 23) that extended to the bays and the ocean. This drainage and subsequent water-supply withdrawals reduced water levels in the aquifer. These water-level declines were exacerbated during droughts and allowed saltwater to intrude some water-supply wells and municipal well fields in Miami-Dade County.

In December 1939, the U.S. Geological Survey (USGS) began salinity and water-level monitoring in the Biscayne aquifer. Shortly thereafter, water-resource managers began implementing strategies to mitigate saltwater intrusion. The extent of saltwater intrusion was last mapped in 1995 (Sonenshein, 1997). Since 1995, salinity monitoring has indicated that saltwater has intruded farther inland in some locations and has receded seaward in others. At some locations, data were insufficient to indicate the current extent of saltwater intrusion or to determine whether changes had occurred. Furthermore, information on monitoring well construction indicated that some of the existing monitoring wells cannot provide the quality of information necessary to fully evaluate movement of the saltwater front in the Biscayne aquifer.

To address these concerns, the USGS, in cooperation with Miami-Dade County, began a study in 2008 to: delineate the current extent of saltwater intrusion in the Biscayne aquifer; characterize how the extent has changed since the last mapping effort; improve salinity monitoring in the Biscayne aquifer; and identify the sources of the saltwater to better understand the actions required to prevent or mitigate saltwater intrusion. As part of this effort, eight new monitoring wells were installed in areas where there was insufficient information to identify the location of the front, and data from geophysical tools and techniques were incorporated into the analysis. To improve accessibility of salinity monitoring information to the public, the USGS cooperative water conditions website was enhanced to allow panning, zooming, and layer selections. The improved website, "Saline Intrusion Monitoring, Miami-Dade County, Florida," serves data collected during this study, as well as data from the active salinity monitoring network, and provides the interpreted maps of the inland extent of saltwater intrusion (*http://www.envirobase.usgs.gov/FLIMS/SaltFront/viewer.htm*, U.S. Geological Survey, 2011g). This website allows the USGS to deliver timely hydrologic data, analyses, and decision-support tools concerning saltwater intrusion. The results of this study, summarized in this report: (1) provide needed information regarding the amount and quality of water in Miami-Dade County (2) advance the monitoring network and techniques for determining water quality, and (3) advance understanding of the process of saltwater intrusion, which can affect water availability.

Definition of Terms

The following definitions are used in this report:

- *Brackish water* – Water with chloride concentrations ranging from 251 to 1,000 milligrams per liter (mg/L).
- *Freshwater* – Water meeting the U.S. Environmental Protection Agency (USEPA) secondary drinking water standards for chloride concentrations less than or equal to 250 mg/L (U.S. Environmental Protection Agency, 2011a).
- *Saltwater* – Water having a chloride concentration of greater than or equal to 1,000 mg/L. This value is based on previous mapping efforts in southeast Florida (Klein and Waller, 1985; Koszalka, 1995).
- *Saltwater encroachment* – A specific type of saltwater intrusion that is caused by the gradual lateral movement of saltwater from the sea inland along the base of the aquifer as a result of decreases of the freshwater head in the aquifer relative to sea level.
- *Saltwater front* – The farthest inland extent of saltwater intrusion in the aquifer. In some instances there is brackish water from previous intrusion events or residual connate water that occurs inland of the saltwater front.
- *Saltwater interface* – A zone of transition between intruded saltwater and freshwater in the aquifer. Sometimes this interface is sharp. Often this interface is diffuse and allows mixing between the two masses of water.
- *Saltwater intrusion* – A generic term referring to an influx of saltwater through various pathways into an aquifer.
- *Salinity* – (1) A quantitative term describing the measured concentration of dissolved solids in water expressed as practical salinity units (PSU) or in parts per thousand (ppt). (2) A generic term referring to various types of information describing the concentration of dissolved solids in water. Information may include measurements of the electrical conductivity of water, airborne, borehole, or surface geophysical measurements, or sample results.

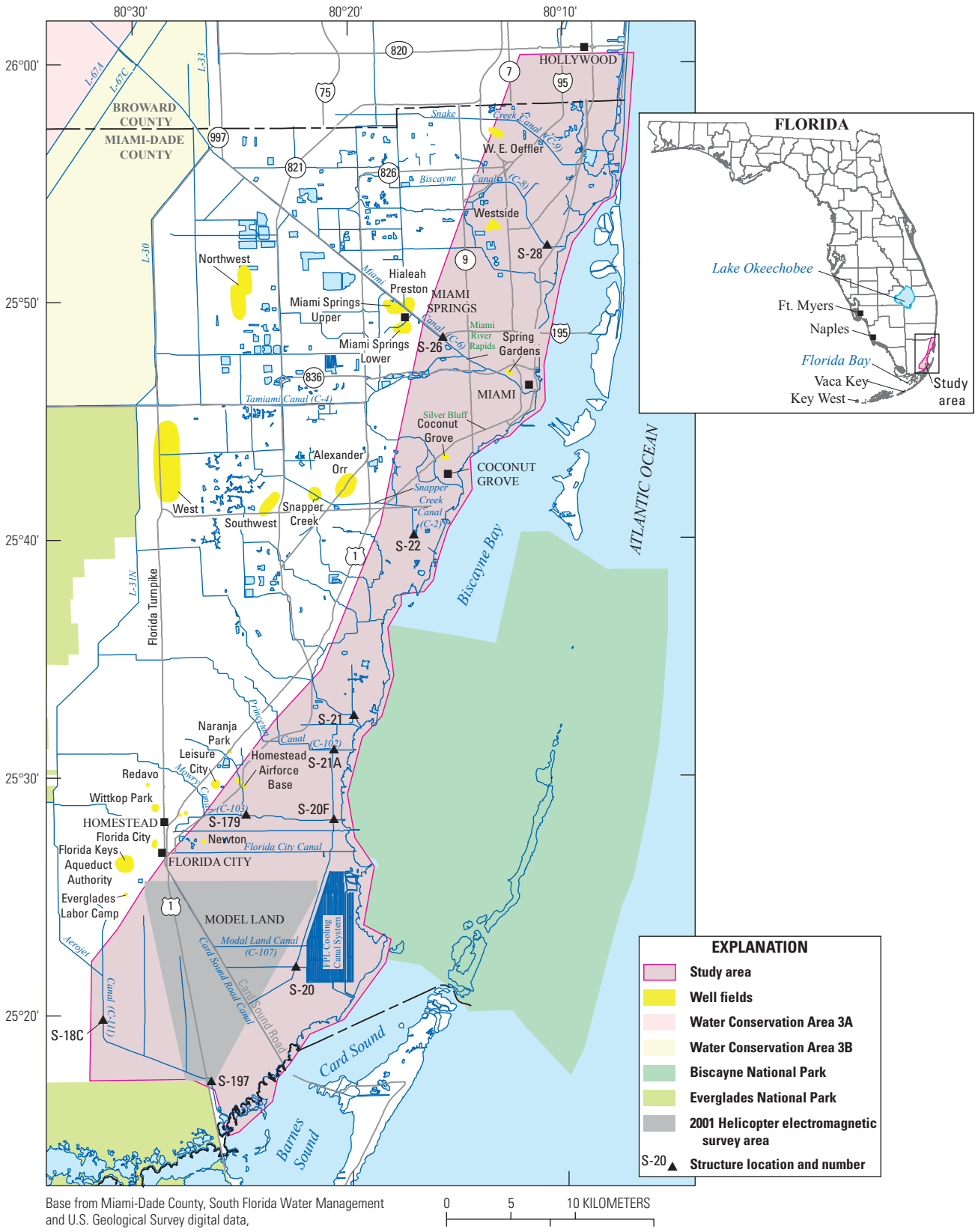

Figure 1. Location of the study area, well fields, the National Parks, water conservation areas, and the helicopter electromagnetic survey of 2001, Miami-Dade and Broward Counties, Florida.

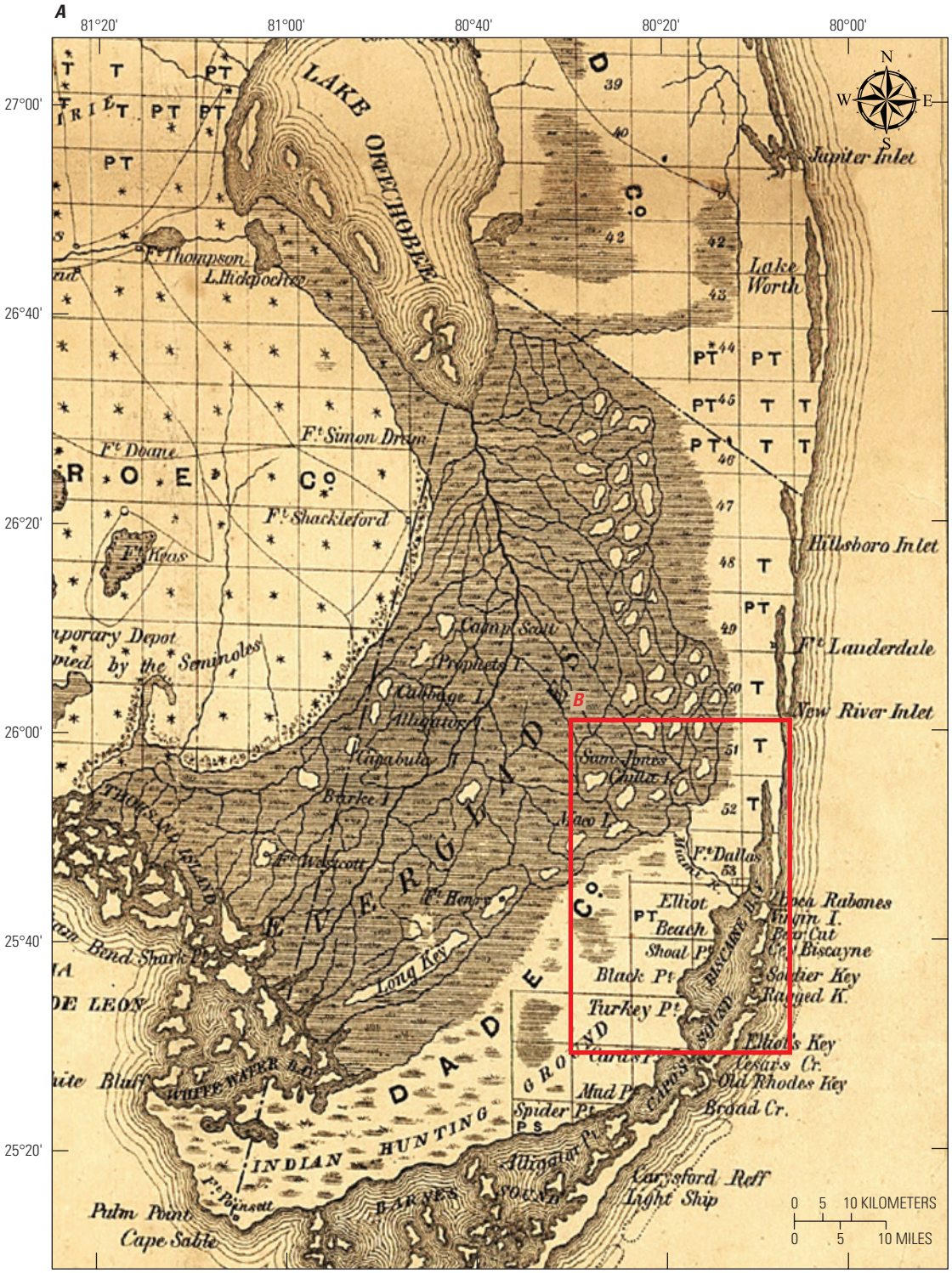

Figure 2. (*A*) Map created for the Annual Report of the Surveyor General for 1859, New York, NY, General Land Office, 1859, courtesy of the Geography and Map Division of the Library of Congress. Latitude and longitude grid georeferenced to the coordinate system of original map to the extent possible, given inaccuracies in original map. (*B*) Digital elevation map showing the topography of the study area in Miami-Dade County and southern Broward County. Altitudes are referenced to the National Geodetic Vertical Datum of 1929 (NGVD 29). Prior to conversion to meters, altitudes were initially referenced to the North American Vertical Datum of 1988 by the Florida Division of Emergency Management by using the results of a light detection and ranging (LIDAR) study (2009), and NGVD 29 altitudes were estimated with a +0.46-meter adjustment factor.

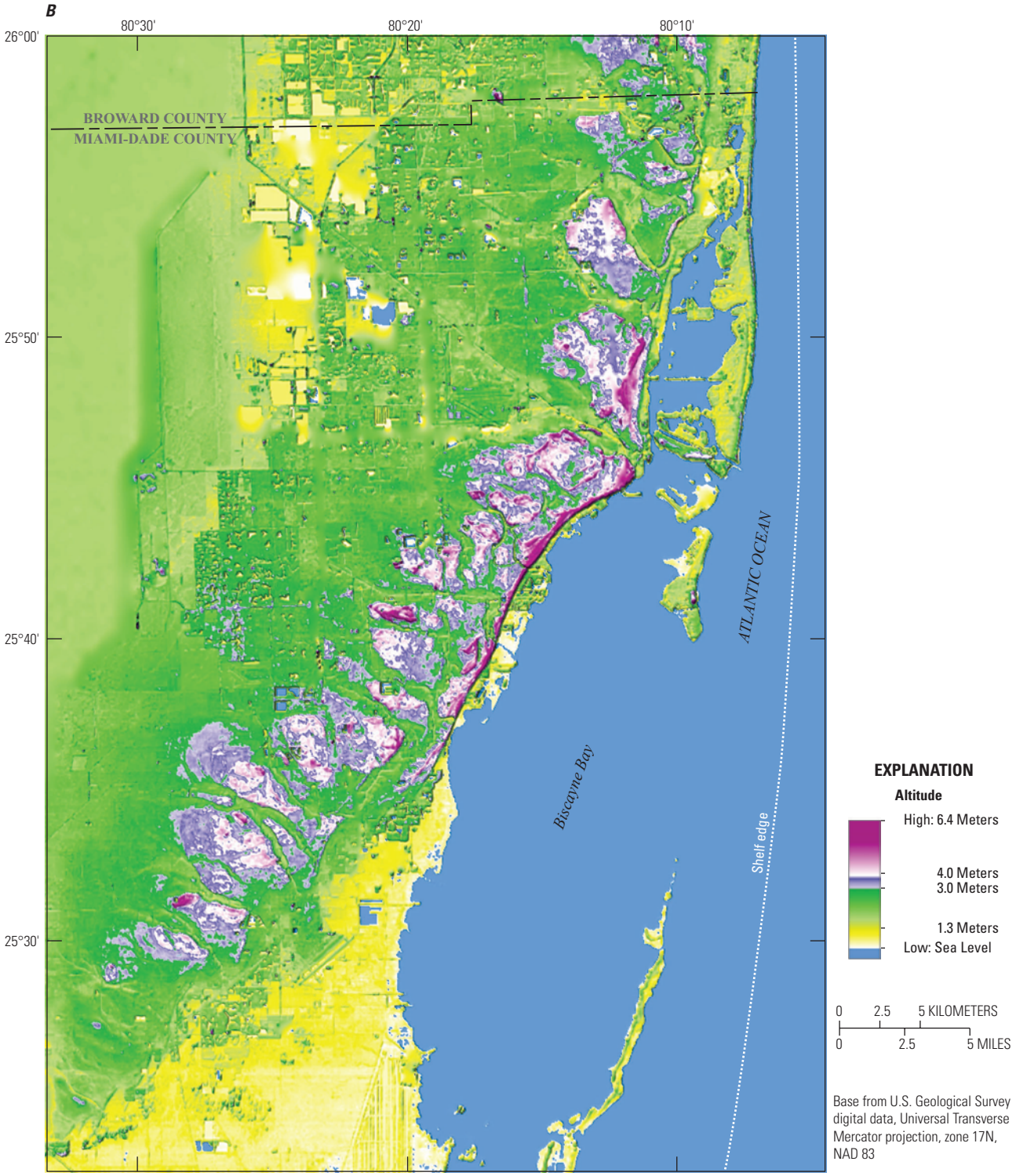

Figure 2. (*A*) Map created for the Annual Report of the Surveyor General for 1859, New York, NY, General Land Office, 1859, courtesy of the Geography and Map Division of the Library of Congress. Latitude and longitude grid georeferenced to the coordinate system of original map to the extent possible, given inaccuracies in original map. (*B*) Digital elevation map showing the topography of the study area in Miami-Dade County and southern Broward County. Altitudes are referenced to the National Geodetic Vertical Datum of 1929 (NGVD 29). Prior to conversion to meters, altitudes were initially referenced to the North American Vertical Datum of 1988 by the Florida Division of Emergency Management by using the results of a light detection and ranging (LIDAR) study (2009), and NGVD 29 altitudes were estimated with a +0.46-meter adjustment factor—Continued.

Purpose and Scope

The purpose of this report is to document the methods used to (1) delineate the current inland extent of saltwater intrusion, (2) examine the origins of saltwater intrusion, and (3) describe the spatial and temporal changes in the distribution of saltwater in the Biscayne aquifer in eastern Miami-Dade County. The analyses presented herein describe how saltwater from Biscayne Bay, Barnes Sound, Card Sound, Florida Bay, or the Atlantic Ocean (fig. 1) has been transported, and may continue to be transported within the Biscayne aquifer. The study area extends westward from the coast as far as is required to describe saltwater in the Biscayne aquifer from these sources.

This report includes discussions of the (1) extent of saltwater intrusion, (2) environmental and anthropogenic causes of saltwater intrusion, (3) temporal and spatial changes in the distribution of saltwater, (4) effects of urban and hydrologic development on saltwater intrusion, (5) types of data collected, collection methods, and analytical methods, and (6) limitations of this analysis. Geophysical data include time-domain electromagnetic (TEM) soundings, a helicopter electromagnetic (HEM) survey, and electromagnetic induction (EMI) logs. A procedure developed during the study for interpretation of EMI log data is presented. TEM soundings also were used to evaluate the depth of the base of the Biscayne aquifer. This effort provided an evaluation of the quality of models developed from geophysical data and of the use of these models to augment existing stratigraphic information. Understanding the depth of the base of the Biscayne aquifer is important to this study because the toe of the wedged-shaped saltwater front typically extends farthest inland at the base of a given aquifer. Water chemistry analyses included determinations of dissolved gas concentrations, major and trace ion concentrations, stable isotope ratios, and tritium/helium-3 ($^3H/^3He$) age dating. These analyses were combined with time-series salinity data and geophysical information to evaluate the sources of saltwater in the aquifer. Information on the construction of the eight new monitoring wells is included in the appendixes, including borehole geophysical log data. Borehole geophysical data were used to enhance the interpretation of the hydrogeology of the Biscayne aquifer in Miami-Dade County. The procedures used to collect, model, and evaluate the TEM soundings collected for this study have been published separately (Fitterman and Prinos, 2011). The calibration and interpretation of the 2001 HEM survey undertaken as part of this study are presented in Fitterman and others (2012).

Approach

Water-quality data, including ongoing salinity and specific conductance monitoring data provided by various organizations, and information from TEM soundings, EMI logs, and a HEM survey, were entered into a geographic information system (GIS). This information was used to construct a map of the current saltwater front. Additional specific conductance and chloride concentration samples were collected from the eight monitoring wells installed as part of this study, as well as from several new wells that had been installed by other organizations. A preliminary map of the saltwater front was completed in October 2008 using data available at that time. A final map was completed in 2011 using the additional data collected during the study and made available from other organizations. Time-series water-quality and time-series electromagnetic induction log (TSEMIL) datasets were used to evaluate the changes that occurred in the location of the saltwater front between 1995 and 2011 and to distinguish between changes in the mapped location of the saltwater front resulting from front movement and changes that likely resulted from improved spatial monitoring network coverage.

To identify the sources of salinity, water-quality samples were collected for evaluation of the analytes alkalinity, barium, boron, bromide, calcium, chloride, fluoride, iron, magnesium, potassium, silica, sodium, strontium, sulfate, sulfur hexafluoride (SF_6), uranium, tritium (^3H); field properties including dissolved oxygen, pH, specific conductance, and temperature; and the isotopic ratios of tritium and helium ($^3H/^3He$), oxygen ($^{18}O/^{16}O$), hydrogen and deuterium ($^2H/^1H$), and strontium ($^{87}Sr/^{86}Sr$). Selected sites were sampled to evaluate the apparent age of the water using $^3H/^3He$ and SF_6 age-dating methods. Selected samples were analyzed to evaluate dissolved gas composition and terrigenic helium concentration. The analytes evaluated for each sample varied and were selected based on well construction, well installation date, sampling methods used, and study needs. The information was interpreted to evaluate whether the saltwater sampled was relict or recent.

Description of Study Area

The study area (fig. 1) is primarily the eastern part of Miami-Dade County, Florida. The northern boundary is in Hallandale Beach in southern Broward County, Florida (fig. 1). The southern boundary is the Florida Bay. Generally the study area extends about 8 to 11 km (6 to 7 miles) inland from the coast or Biscayne Bay. In the southern part of the county, however, the study area extends westward to the Aerojet (C–111) Canal.

Hydrologic Controls

Saltwater intrusion is controlled by factors including (1) climatic conditions that result in wet and dry seasons, droughts, and floods; (2) the distribution of porosity within the sand and karst limestone layers of the Biscayne aquifer, (3) a general eastward and southeastward groundwater-flow direction, (4) freshwater levels in the aquifer relative to sea level, (5) generally low land-surface altitude (fig. 2*B*), (6) a low regional flow gradient, and (7) a water management system including drainage canals, water control structures, pumps, levees, water-supply well fields, and water conservation areas (fig. 1). High permeability surface materials or karst features allow rapid recharge of the aquifer or surface sheet flow when groundwater levels rise above the land surface.

Topography and Physiography

Miami-Dade County is generally flat and poorly drained. The land-surface altitude for approximately 70 percent of the county is below 1.8 m. Figure 2*A* is a historical map showing the predevelopment extent of the everglades. Areas shown as everglades in figure 2*A* correspond to areas that currently have land-surface altitudes of about 0 to 3.0 m (fig. 2*B*). East of the Everglades is the Atlantic Coastal Ridge physiographic province (figs. 2*B* and 3), which ranges in altitude from 2.4 to 7.3 m (Hoffmeister and others, 1967, p. 176; Lietz, 1999). East and south of the Atlantic Coastal Ridge is the low lying (fig. 2*B*) Coastal Marsh and Mangrove physiographic province (fig. 3).

Climate

The wet and dry tropical climate (Hagemeyer, 2012) of south Florida is created by a combination of its latitude and proximity to the ocean and the Gulf of Mexico. Although Miami-Dade County is farther south than most of the United States, buffering from the Atlantic Ocean ensures that summer temperatures rarely exceed 38 °C, and winter temperatures rarely fall below freezing. The highest and lowest temperatures typically occur during August and January, respectively. Daily mean temperature averages about 28 °C in August and 20 °C in January (National Climatic Data Center, 2012). A wet season occurring from mid-May through September of each year is typified by afternoon thunderstorms with relatively heavy rainfall that is augmented by rainfall from tropical storms and hurricanes. During the wet season, solar radiation induces the movement of moist air inland from the ocean (Hagemeyer, 2012), where it combines with evaporating water from the swamps and wet prairies to produce frequent and generally localized thunderstorms. The low humidity and solar radiation occurring during the dry season that extends from October to early May greatly reduce the occurrence of afternoon thunderstorms. Relatively low sea-surface temperatures during December to May also reduce the likelihood of tropical storms; consequently, rainfall during the dry season is caused primarily by the interaction of cold fronts from the north with moist tropical air in the south.

The occurrence of hurricanes, tropical storms, and droughts in south Florida is related to a large extent to the El Niño–Southern Oscillation (ENSO). El Niño periods are characterized by unusually warm sea surface temperatures (SSTs) south of the equatorial eastern Pacific Ocean, whereas La Niña periods are characterized by unusually cool SSTs in this region. El Niño periods tend to draw the jet stream southward, which produces wind shear that hampers the formation of tropical storms and hurricanes but also increases the likelihood of precipitation in south Florida. La Niña periods result in less precipitation and more persistent high pressure systems in south Florida, which increases the potential for droughts (Hagemeyer, 2012). Prolonged droughts in Florida occurred in 1938–39 and 1943–46 (Parker and others, 1955); 1949–57 (Waller, 1985; Bridges and others, 1991, p. 231–238); 1960–63 (Waller, 1985; Bridges and others, 1991, p. 231–238); 1970–77 (Benson and Gardner, 1974; Waller, 1985; Bridges and others, 1991, p. 231–238); 1980–82 (Waller, 1985; Bridges and others, 1991, p. 231–238); 1985 (South Florida Water Management District, 1985), 1989–90 (Trimble and others, 1990), and 1998–2002 (Verdi and others, 2006). Drought periods are shown on a graph of average annual total rainfall during 1931 to 2011 (fig. 4). To construct this graph, average monthly total rainfall at eight long-term monitoring stations was computed and totaled annually. Selected stations had data that were 69 to 97 percent complete for the evaluated period. The following National Oceanic and Atmospheric Administration, National Climatic Data Center stations were used: Everglades (1931–2011), Fort Lauderdale (1931–2011), Hialeah (1941–2011), Homestead Experimental Station (1931–1988), Miami Beach (1941–2011), Miami International Airport (1948–2011), Royal Palm Ranger Station (1949–2011), and Tamiami Trail 40 Mile Bend (1941–2006) (fig. 3). The 1998 to 2002 drought (fig. 4) was not as severe in Miami-Dade County as it was in other areas. During this period, the rainfall in Miami-Dade County was lower than normal only in 2000, and the drought period was shorter (fig. 4) than in other parts of the State. Based on the rainfall data, it appears that the 1985 and 1989–90 drought periods were of longer duration in Miami-Dade County than in other parts of the State and combined to form one extended drought period from 1984 to 1990 (fig. 4).

Water Use in Miami-Dade County

Miami-Dade County's population of 2,496,000 (U.S. Census Bureau, 2010) makes Miami-Dade County one of the most populous counties in the United States. As of 2010, the vast majority of the county's residents lived in an area of approximately 1,550 square kilometers (km^2) that is within about 24 kilometers (km) of the ocean or Biscayne Bay. As the population of Miami-Dade County has increased, demand for freshwater also has increased. The Biscayne aquifer is the principal aquifer for the residents of Miami-Dade County (Miller, 1990). Ninety-nine percent of all groundwater withdrawn in Miami-Dade County in 2005 emanated from the Biscayne aquifer (Marella, 2009). Public groundwater withdrawals generally have increased as population increased during 1965 to 1987 (fig. 5) (Marella, 1999, 2009; R.L. Marella, U.S. Geological Survey, written commun., 1998, 2011; U.S. Census Bureau, 2013). Although population continued to increase at a relatively steady rate during 1993 to 2006, there was only a marginal increase in public groundwater withdrawals during this same period (fig. 5). Since 2006, public groundwater withdrawals have decreased as population has continued to increase. This decrease may be, at least in part, the result of stricter water use restrictions that began in May 2007 when water levels in Lake Okeechobee declined to record minimums. These water use restrictions were still in effect at the time of this report. The Biscayne aquifer is also the primary source of potable water for all residents living in the Florida Keys, Monroe County (Marella, 2009). Water from the Biscayne aquifer is delivered by an aqueduct that extends from the Florida Keys Aqueduct Authority (FKAA) well field west of Florida City south to Key West (fig. 1). Although the

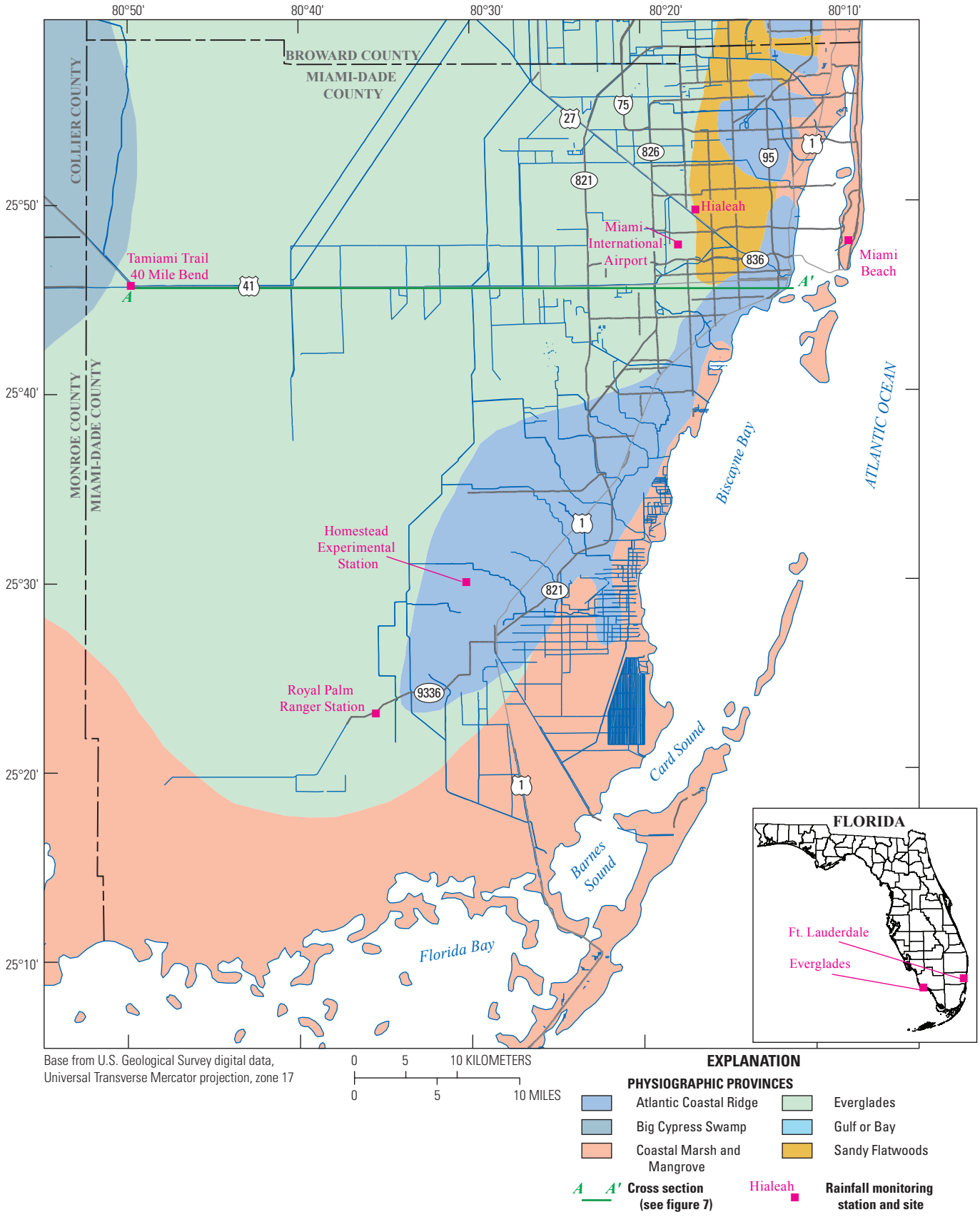

Figure 3. Physiographic provinces, location of the cross section shown in figure 7, and locations of rainfall monitoring stations within the study area. Modified from Lietz (1999).

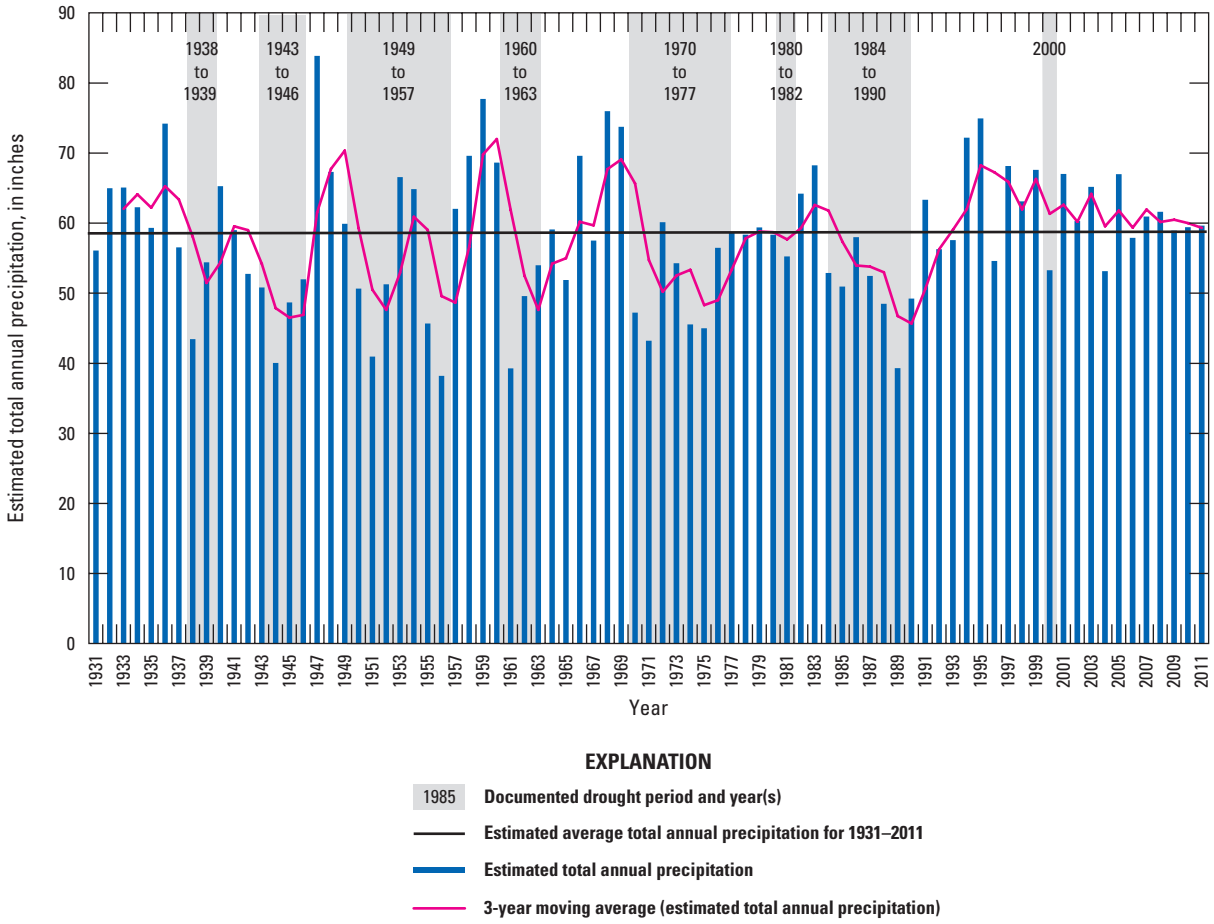

Figure 4. Estimated total annual precipitation from selected stations in or near Miami-Dade County and documented droughts during 1931 to 2011.

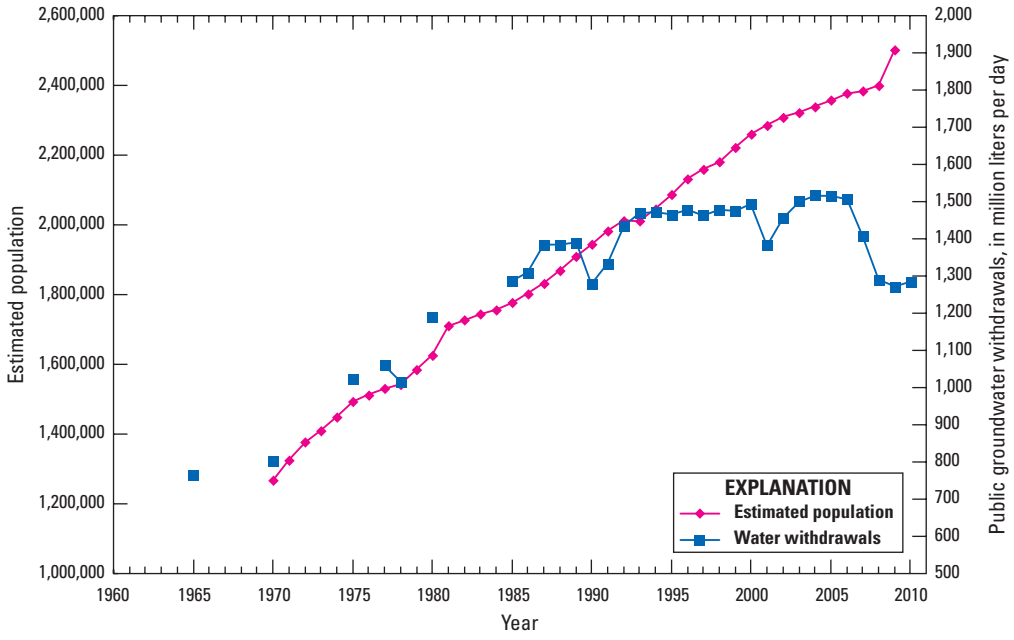

Figure 5. Estimated population (from U.S. Census Bureau, 2013) and public groundwater withdrawals in Miami-Dade County, Florida.

spatial extent of the Biscayne aquifer is limited primarily to Broward, Miami-Dade, and Palm Beach Counties, it provided 33 percent of all public-supply groundwater used in Florida as of 2005 (Marella, 2009).

Hydrogeology/Hydrostratigraphic Framework

The study area is underlain by the surficial aquifer system, the intermediate confining unit, and the Floridan aquifer system (fig. 6). In the study area, the surficial aquifer system corresponds with the Tamiami Formation of Pliocene age; the Fort Thompson Formation, Key Largo Limestone, Miami Limestone, and Pamlico Sand (Schroeder and Klein, 1954) of Pleistocene age, and the Lake Flirt Marl of Holocene age (Parker and Cooke, 1944; Causaras, 1987; Fish and Stewart, 1991; Cunningham and others, 1998; Cunningham and others, 2001; Cunningham and others, 2004; Cunningham and others, 2006a, b).

The surficial aquifer system includes two aquifers: the Biscayne aquifer and the deeper, informally named gray limestone aquifer (Fish and Stewart, 1991). The Biscayne aquifer is wedge-shaped and becomes thinner toward the western part of Miami-Dade County (fig. 7). The deepest part of the Biscayne aquifer is approximately 55 m deep in the northeastern part of the county (Fish and Stewart, 1991). The depth of the base of the Biscayne aquifer in the area of the HEM survey in southern Miami-Dade County varies from about 17 to 30 m (Fish and Stewart, 1991). Fish and Stewart (1991) show that the two aquifers merge with one another in central and northern coastal Miami-Dade County (fig. 7). Both aquifers are composed mostly of highly porous, karstic limestone, and the Biscayne aquifer is by far the more productive of the two. Where the two aquifers are distinct, the top of the gray limestone aquifer is separated from the base of the Biscayne aquifer by an upper semiconfining unit generally composed of quartz sands (figs. 6 and 7). The base of the gray limestone aquifer is separated from the top of the underlying intermediate confining unit by a semiconfining unit (figs. 6 and 7). In the study area (fig. 1), the surficial aquifer system generally has transmissivity values that are greater than 93,000 meters squared per day (m^2/d) (1,000,000 feet squared per day [ft^2/d]) (Fish and Stewart, 1991). One aquifer

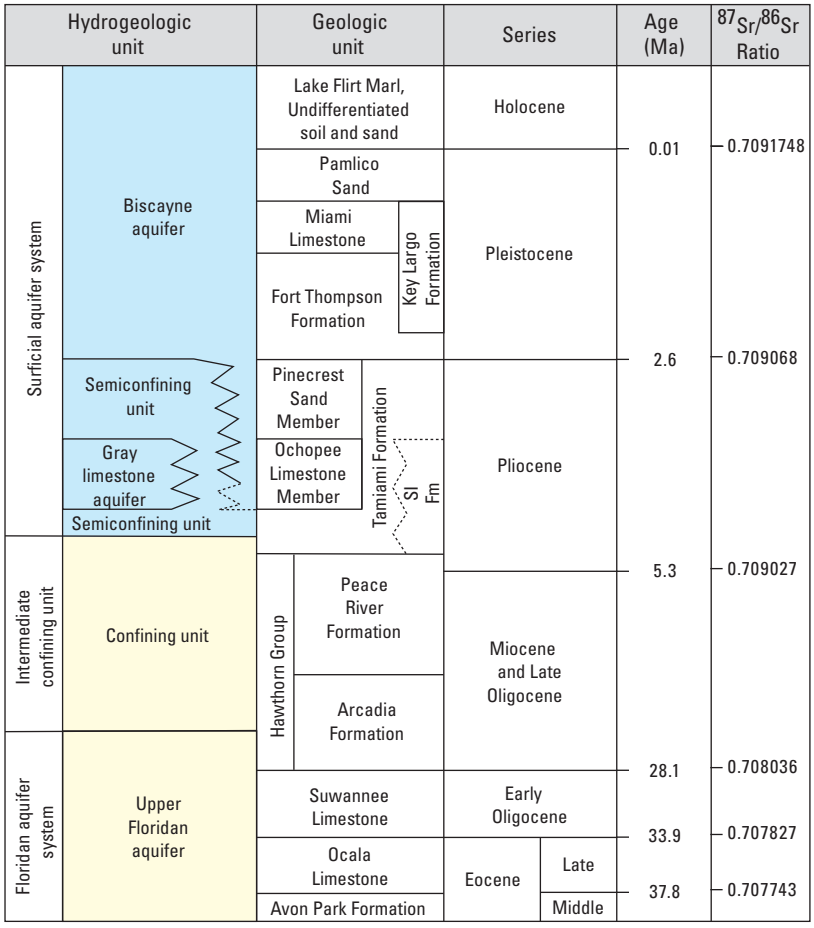

Figure 6. Generalized relation of hydrogeologic, lithostratigraphic, and time-stratigraphic units in Miami-Dade County (based on Causaras, 1987; Fish and Stewart, 1991; Cunningham and others, 2001, 2006a; Reese and Richardson, 2008; Gradstein and others, 2012; and this report). [SI Fm, Stock Island Formation]

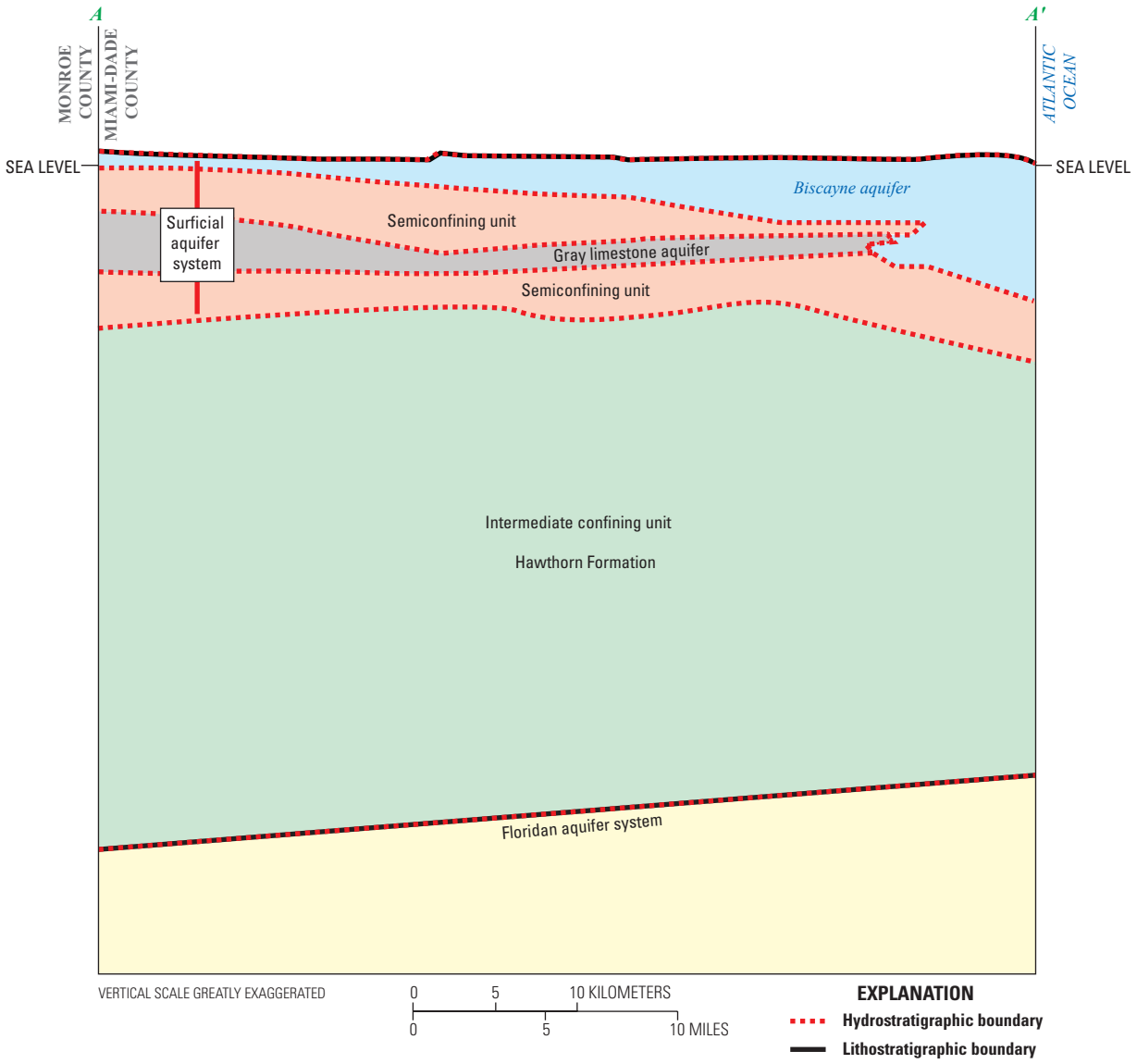

Figure 7. Hydrogeologic section *A–A′* showing hydrostratigraphy of the surficial aquifer system and uppermost part of the intermediate confining unit from west to east across central Miami-Dade County (modified from Fish and Stewart, 1991). Location of cross section shown in figure 3.

test in central Miami-Dade County indicated a transmissivity of 270,000 m^2/d (Fish and Stewart, 1991).

The intermediate confining unit underlies the surficial aquifer system (figs. 6 and 7). The intermediate confining unit is approximately 170 to 240 m thick and is composed of a succession of quartz sand and sandstone, limestone, dolomite, and minor terrigenous mudstone, diatomaceous mudstone, and dolosilt that compose the Late Oligocene–Early Pliocene Hawthorn Group (Fish and Stewart, 1991; Cunningham and others, 2001). In the study area, the intermediate confining unit overlies the Upper Floridan aquifer of the Floridan aquifer system (fig. 6), which is composed primarily of limestone and relatively minor dolomitic limestone and dolomite (Reese, 1994). The intermediate confining unit also can include the lowermost part of the Tamiami Formation (Fish and Stewart, 1991) and the Stock Island Formation.

Previous Studies

The mechanisms of saltwater intrusion and the changes in the hydrology of south Florida that allowed saltwater to intrude large parts of the Biscayne aquifer in Miami-Dade County have been described by Cross and Love (1942), Parker (1945), Parker and others (1955), Kohout and Leach (1964), and Renken and others (2005a). Brown and Parker (1945) provided detailed examinations and a cross section showing saltwater encroached at Silver Bluff in Coconut Grove (fig. 1). Hoy and others (1951) published six cross sections showing changes in the position of the saltwater front in the Miami area between 1946 and 1950. Klein (1957) provided a contour map of the saltwater front near Silver Bluff in Coconut Grove (fig. 1). Schroeder and others (1958) described the Biscayne aquifer in Dade (currently

named Miami-Dade) and Broward Counties and reported that, at that time in southern Broward County near the city of Hollywood, saltwater had not yet encroached as far inland as U.S. Highway 1, which is about 2.4 km from the ocean. Sherwood and Leach (1962) found that the Biscayne aquifer in the vicinity of salinity control structure S–22 on the Snapper Creek Canal (fig. 1) is so permeable that if water levels upstream of the structure are higher than water levels downstream of the structure, then when the structure is closed, water will flow through the aquifer under the structure toward Biscayne Bay.

Sherwood and Klein (1963) evaluated the relation between surface water and groundwater in southeastern Florida and provided a comparison of the water levels in Miami-Dade County near Miami with the inland extent of saltwater in the Biscayne aquifer. The relation of saltwater intrusion to discharge in the Miami River and its tributaries was evaluated by Leach and Grantham (1966). This analysis indicated that water with a chloride concentration of 1,000 parts per million (ppm) occurred in the Miami Canal as far inland as control structure S–26 (fig. 1) about 23 percent of the time and that about 60 percent of the Biscayne aquifer in the vicinity of the Miami Canal and its tributaries could gradually be restored to freshwater conditions if the structure were moved downstream of the confluence of the Tamiami Canal. Kohout and Leach (1964) examined the relation between water control dam operation in the Snake Creek Canal and salinity in the aquifer. Bearden (1974, p. 25) mapped the potentiometric surface in southern Broward County near the city of Hollywood and provided maps showing the extent of saltwater intrusion occurring near unregulated canals.

The USGS mapped the approximate inland extent of saltwater in the Biscayne aquifer in Miami-Dade County in 1951 (Hoy, 1952), 1978 (Swayze, 1980), 1984 (Klein and Waller, 1985), and 1995 (Sonenshein, 1997) and in Broward County in 1990 (Koszalka, 1995). Parker and others (1955) also published a map showing the inland extent of saltwater in the Biscayne aquifer in Miami-Dade County that differs from the map created in 1951 (Hoy, 1952), but the date that this map was created is not provided.

Klein and Ratzlaff (1989) and Sonenshein and Koszalka (1996) evaluated changes in the extent of saltwater intrusion in the Biscayne aquifer in Miami-Dade County. Prior to the current study, little groundwater salinity information was available for the area south of Florida City in southeastern Miami-Dade County; therefore, the line in the map showing the inland extent of saltwater in the Biscayne aquifer plotted by Sonenshein (1997) was dashed in this area to indicate that data were insufficient. Sonenshein (1997) used the interpretations of 15 TEM soundings to augment the information provided by monitoring wells; the majority of these soundings were collected near the Miami Canal. Fitterman and Deszcz-Pan (1998, 2002) and Fitterman and others (1999) interpreted TEM soundings and HEM surveys to evaluate saltwater intrusion in southwestern Miami-Dade County in the Everglades National Park.

Prinos and others (2002) examined the chloride concentrations in USGS monitoring wells during 1974–1999 in the Biscayne aquifer and identified statistically significant increasing trends in chloride concentrations in the data from 40 percent of the wells in this aquifer. Decreasing trends in chloride concentrations were identified in the data from 28 percent of these wells. Data from 32 percent of the monitoring wells showed no quantifiable trend for the period evaluated.

Origin of Saltwater Intrusion in Southeastern Florida

An understanding of the mechanisms of saltwater intrusion and the effects of urban development in southeast Florida is necessary for water management and development of remediation strategies. The management and remediation strategies necessary to prevent saltwater from encroaching inland along the base of the aquifer are different from those needed to prevent saltwater from leaking upward from deeper aquifers. Mitigation of saltwater intrusion, while also addressing the frequently competing needs of flood prevention, agriculture, urban development, public water supply, and ecosystem preservation, has resulted in a complex water management system of canals and water control structures (fig. 8) as well as an extensive saltwater monitoring network.

Mechanisms of Saltwater Intrusion

A number of mechanisms have led to the occurrence of saltwater in the Biscayne aquifer (fig. 9). These mechanisms include (1) upconing of relict or residual saltwater that had been incorporated in relatively impermeable sediments during previous sea-level high stands occurring during interglacial periods (Parker, 1945, p. 533; Bearden, 1974, p. 25), (2) the gradual encroachment of saltwater from the ocean along the base of the aquifer resulting from reductions in freshwater head relative to sea level (Cross and Love, 1942, p. 501), (3) infiltration of saltwater from coastal saltwater mangrove marshes (Matson and Sanford, 1913, p. 59), and (4) the flow of saltwater inland through canals where it leaks into the aquifer (Cross and Love, 1942, p. 501).

Upconing of Relict Saltwater from Previous Sea-Level High Stands

During the Pleistocene, sea levels varied as water was periodically stored or released by growing or melting continental ice sheets. The sand and limestone formations of the Biscayne aquifer consist largely of materials that were deposited while shallow seas covered south Florida. These materials, when first deposited, would have included connate saltwater in the pore fluids. As sea level declined,

saline pore fluids generally were replaced by freshwater that flowed through the aquifer. Some of the less permeable materials, however, may have retained some of the relict saltwater. This source of saltwater was discussed by Parker and others (1955). It is also possible that some strata were intruded again by seawater as sea level rose during later interglacial periods.

Encroachment of Seawater along the Base of the Biscayne Aquifer

The encroachment of seawater along the base of the Biscayne aquifer can be described by the Ghyben-Herzberg relation (Ghyben, 1889; Herzberg, 1901), applied by Brown (1925, p. 17) to coastal aquifers:

$$h = \frac{t}{g-1}, \quad (1)$$

where h is the depth of saltwater below sea level, g is the specific gravity of seawater, t is the height of freshwater above sea level, and the specific gravity of the freshwater is assumed to be 1. This relation describes saltwater encroachment in a homogeneous, unconfined aquifer under hydrostatic conditions. Although the Biscayne aquifer is not homogeneous and flow conditions are not hydrostatic, this relation can be used to derive a coarse approximation of the freshwater head necessary to prevent saltwater intrusion in the Biscayne aquifer. Given a specific gravity of 1.0268 for seawater in the Miami area (Parker and others, 1955, p. 573), the interface between fresh and saltwater in the aquifer will be depressed by approximately 37.3 m for each meter of freshwater head above sea level. The Ghyben-Herzberg relation indicates that the altitude of freshwater must be 0.6 to 1.5 m above sea level to prevent encroachment of saltwater along the base of the aquifer because the base of the Biscayne aquifer ranges from 24 to 55 m below land surface near the east coast of Miami-Dade County (Fish and Stewart, 1991). Altitudes of freshwater in some areas of coastal Miami-Dade County are well below these altitudes (U.S. Geological Survey, 2011f); consequently, some saltwater encroachment has occurred.

The full extent of encroachment predicted by the Ghyben-Herzberg relation does not occur in some parts of the Biscayne aquifer because the relation describes a static balance of densities, rather than the dynamic forces actually occurring within the aquifer (Kohout, 1964). The direction of fresh groundwater flow in the Biscayne aquifer is typically from inland toward the coast, and the gradient increases during periods of recharge. Kohout (1964) determined that saltwater (1) tends to flow inland along the base of the aquifer, (2) becomes less dense and flows upward as it mixes with freshwater at the freshwater-saltwater interface, and then (3) flows back toward the sea along with the freshwater flowing seaward.

Infiltration of Saltwater from Saltwater Marshes

Infiltration of saltwater from saltwater marshes occurs along the southern, southwestern, and southeastern coastlines of Florida, where the land surface is so low that saltwater can flow over land for approximately 1 to 3 km at high tide. The water in these saltwater marshes can become hypersaline as a result of high evaporation rates, and during droughts, reductions in freshwater levels and flows may allow the saltwater in these marshes to migrate inland. Tropical storm or hurricane-driven storm surge or gale-driven seiches may cause the saltwater to flow farther inland than normal, where it could infiltrate the aquifer. Reductions in freshwater levels in the Everglades likely increased the potential for overland flow of this saltwater. Installation of canals also provided a pathway for inland flow of this saltwater. Meyer (1974, p. 28) reported that on the upstream side of water control structure S–18C (fig. 8) in "September 1965 the chloride peaked at 13,370 mg/L as a result of tidal inundation during Hurricane Betsy." S–18C is 9.8 km inland from Florida Bay. Meyer (1974) also reported that the chloride concentration of the water was 10,000 mg/L at least 3.2 km farther upstream from S–18C.

Seepage from Streams or Canals in which Saltwater has Migrated Inland

Parker and others (1955, p. 621) described the potential migration of saltwater up canals in terms of a balance of seawater and freshwater heads. Well-designed salinity control structures can potentially reduce or prevent saltwater encroachment along the base of the aquifer and the seepage of saltwater from canals by retaining sufficient freshwater in the canal to increase the hydraulic head in the canals and in the aquifer adjacent to canals and by directly preventing the flow of saltwater upstream. Salinity control structures in Miami-Dade County, however, have not always prevented saltwater intrusion. The extensive secondary porosity of layers within the Biscayne aquifer potentially can allow saltwater flow around the structures through the aquifer (Leach and Grantham, 1966, p. 25) unless grout walls or other such features were installed to prevent this flow. Between 1988 and 2010 there have been, for example, frequent influxes of water, with a salinity of between 15 and 32 PSU at station BS04 (Maria Idia Macfarlane, Water and Sewer Department, written commun., March 7, 2011; Craig Grossenbacher, Miami-Dade County Permitting, Environmental, and Regulatory Affairs, written commun., July 7, 2010) in the Biscayne Canal (fig. 10), which is upstream of the salinity control structure S–28 (fig. 8).

In the Snake Creek Canal, when the salinity control structure was open, water from the shallow aquifer drained toward the canal, the saltwater front at the base of the Biscayne aquifer moved inland, and leakage of saltwater from the canal into the aquifer was reduced or eliminated

FLORIDA
Lake Okeechobee
Key West
Study area
EXPLANATION
Approximate inland extent of saltwater
1955
1995
2011
Lines are dashed where information was insufficient for an accurate estimate
Time-domain electromagnetic soundings
U.S. Geological Survey groundwater-level monitoring well
S-338
Water-control or salinity-control structure
Salinity monitoring sites by organization
Florida Keys Aqueduct Authority
EAS Engineering, Inc.
U.S. Geological Survey
Miami-Dade County Permitting, Environmental, and Regulatory Affairs
ATLANTIC OCEAN
Biscayne Bay
BROWARD COUNTY
MIAMI-DADE COUNTY
Miami Canal at Water Plant
Miami River
Snake Creek Canal
Biscayne Canal
Little River Canal (C-7)
Miami Canal (C-6)
Comfort Canal (C-5)
Tamiami Canal (C-4)
Coral Gables Canal (C-3)
Snapper Creek Canal (C-100)
Cutler Drain Canal
Arch Creek
C9 Canal near NE 17 Ave
C8 Canal at G-3601
C5 Canal at NW 32 Ct
C2 Canal at G-3608
C2 Canal 150ft upstream of S-22
Canal C100A at SW 72 Ave
Canal C-100A
Canal C-100C
80°10'
80°20'
80°30'
26°00'
25°50'
25°40'

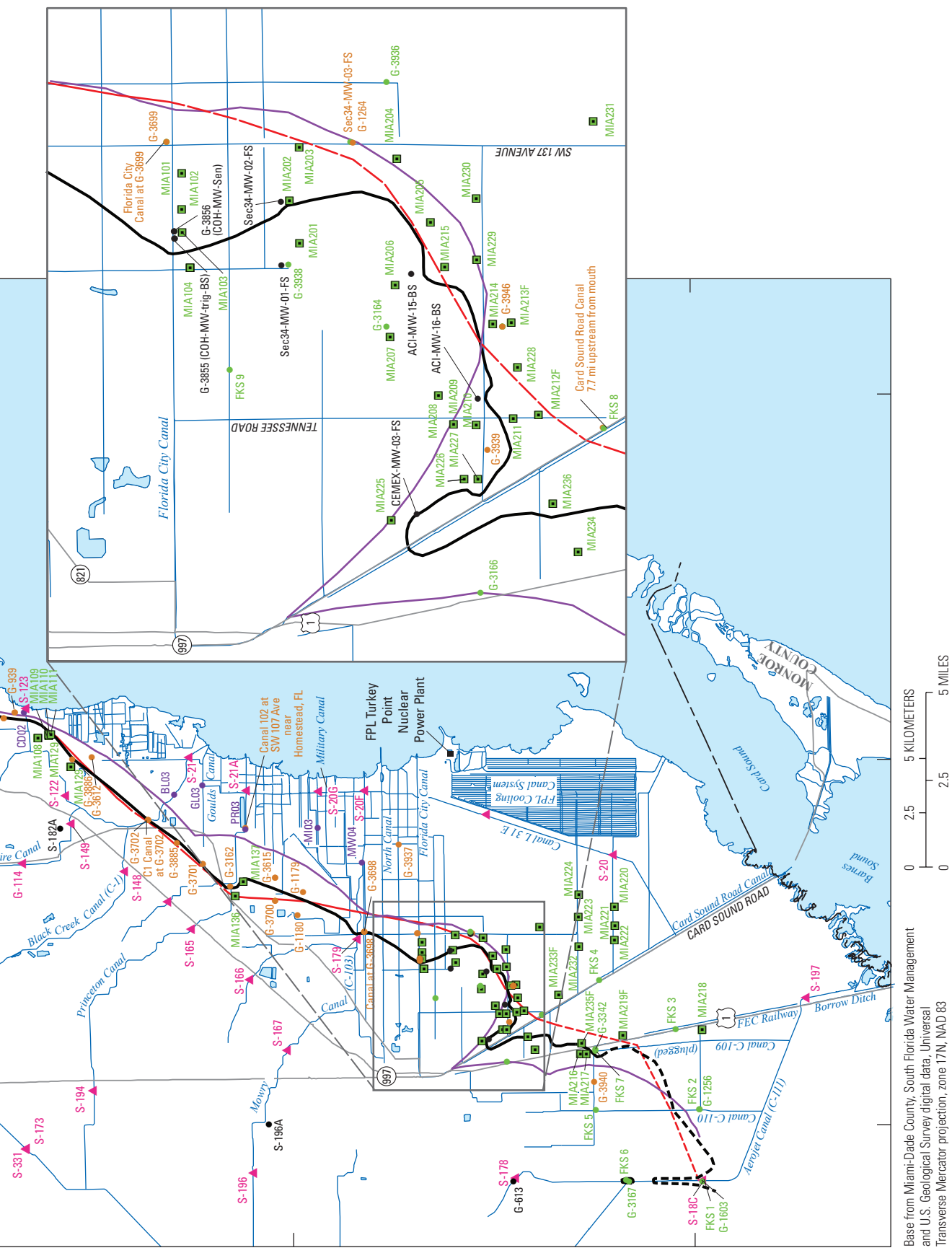

Figure 8. Locations of salinity monitoring sites, time-domain electromagnetic soundings, groundwater-level monitoring wells, and the mapped approximations of the inland extent of saltwater in the Biscayne aquifer in Miami-Dade and southern Broward Counties in 1955, 1995, and 2011. Enlarged version of this figure availabe for download at *http://pubs.usgs.gov/sir/2014/5025/downloads/sir2014-5025_figure08large.pdf.*

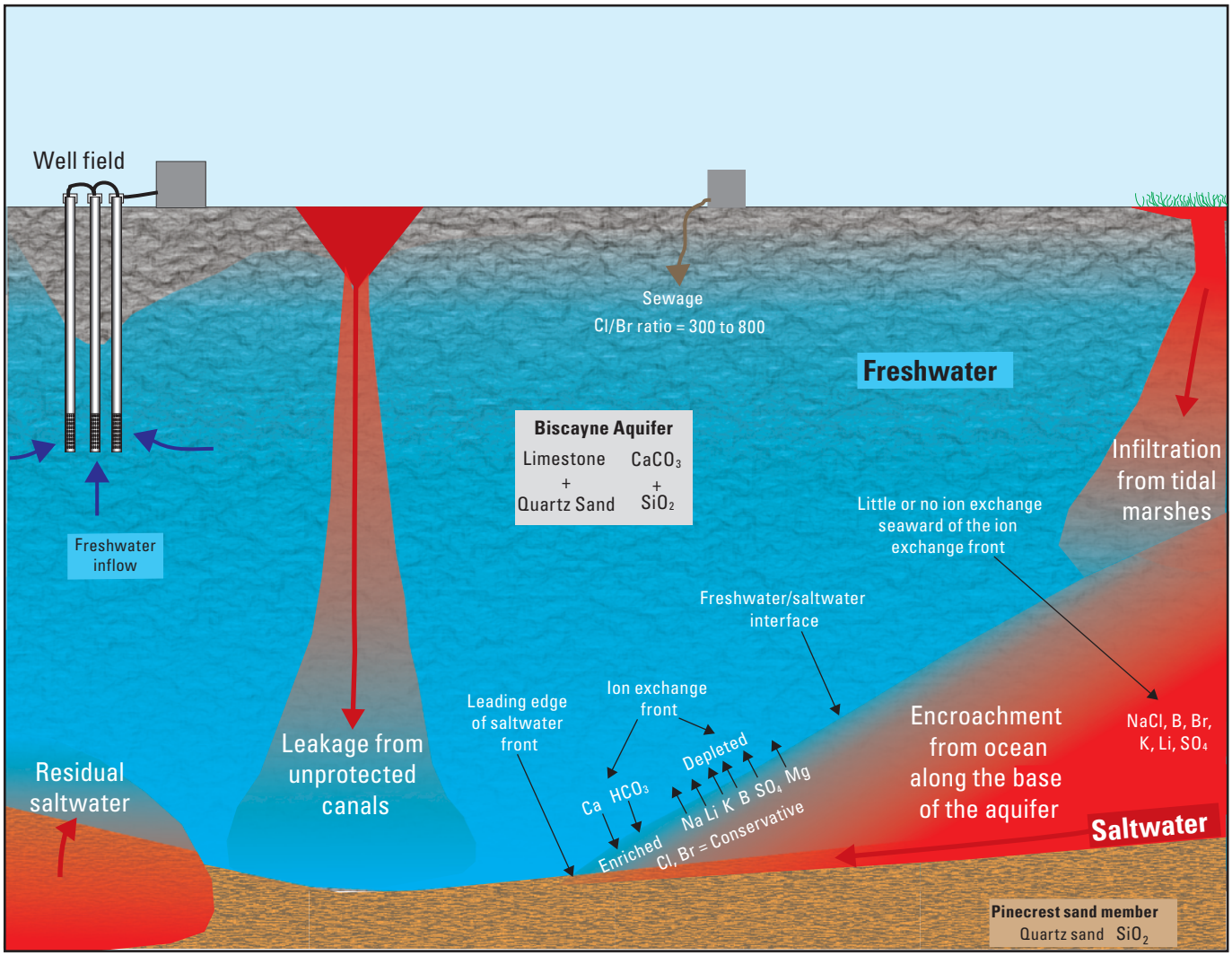

Figure 9. Conceptual diagram of sources and mechanisms of the saltwater that has intruded parts of aquifers in southeast Florida, and changes in water chemistry that may result from this intrusion.

because the flow gradient in the aquifer was primarily toward the canal (Kohout and Leach, 1964, p. 36). Conversely, when the water control structure was closed, the water that was in the canal inland of the dam, whether it was fresh or saline, was pushed horizontally outward into the aquifer. The potential exists, therefore, for intrusion of the aquifer caused by any saltwater trapped upstream of control structures.

The National Oceanic and Atmospheric Administration (NOAA) estimates that mean sea levels at Ft. Myers, Key West, Miami Beach, Naples, and Vaca Key, Florida, have increased at rates of 0.24, 0.22, 0.24, 0.20, and 0.28 m per 100 years, respectively (National Oceanic and Atmospheric Administration, 2012). Relative increases in sea level may exacerbate the encroachment of saltwater along the base of the aquifer and the leakage of saltwater past salinity control structures where it could potentially leak into the aquifer.

Effects of Urban and Hydrologic Development on Saltwater Intrusion

A goal of this study was to examine the environmental and anthropogenic causes of saltwater intrusion in the Biscayne aquifer in eastern Miami-Dade County and to delineate the resulting distribution of saltwater of various ages and sources. This goal was accomplished in part through geochemical evaluations of recharge conditions and ages of water in the aquifer. A detailed understanding of the history of saltwater intrusion provides a valuable framework for evaluating these geochemical results. The following sections provide a summary of predevelopment conditions and events leading to saltwater intrusion in the Biscayne aquifer. Detailed examinations of the history of urban and hydrologic development in the study area are provided by Fletcher (1911), Paige (1986), and Parker and others (1955).

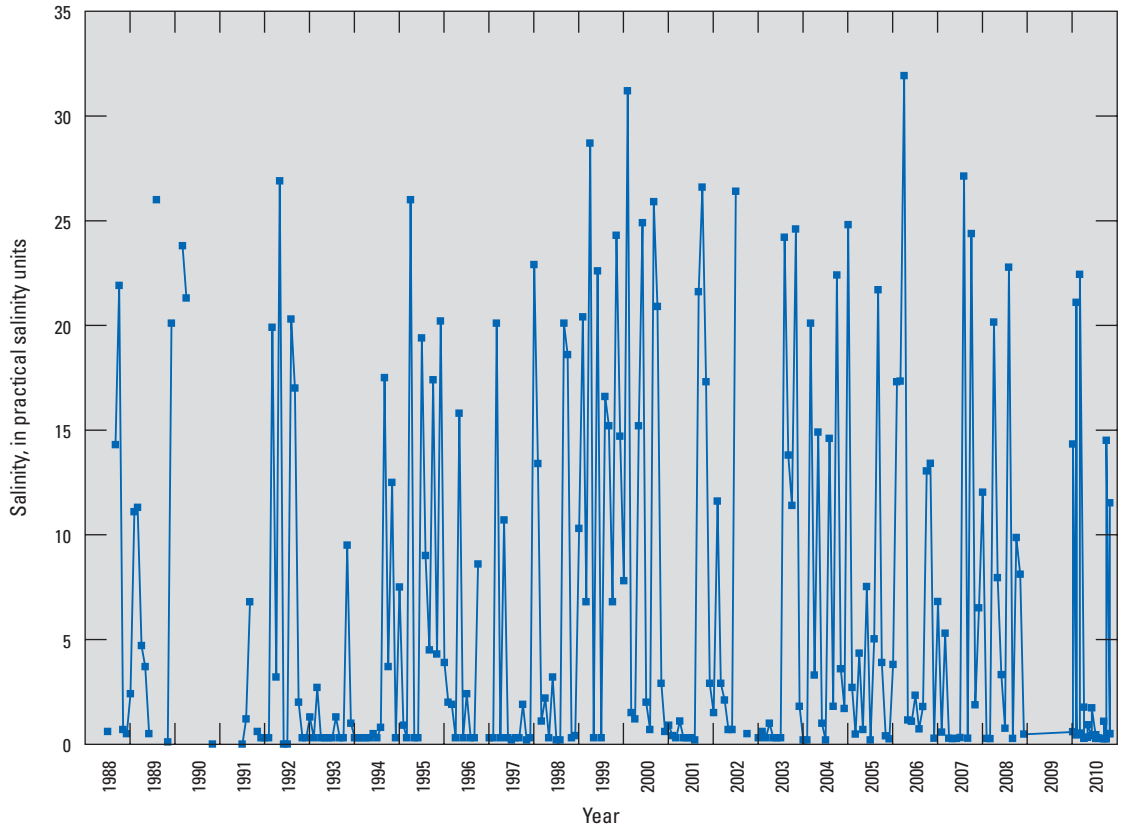

Figure 10. Salinity of the Biscayne Canal at station BS04, Miami-Dade County, Florida, 1988–2010.

Predevelopment Conditions

Prior to development, the freshwater marshes of the Everglades covered approximately 3,000 km^2 of Miami-Dade County, which is most of the land west of the Atlantic Coastal Ridge except for an area in northwestern Miami-Dade County (figs. 2*A* and 3). Most of the southern and eastern coastal parts of the county, approximately 1,030 km^2, were covered with coastal marshes and mangrove swamps (fig. 3). Water levels in the Everglades near Miami are estimated to have been approximately 3 to 4.3 m above NGVD 29 (Shaler, 1890, p. 158; Parker and others, 1955, p. 581; Fish and Stewart, 1991, p. 47). These water levels exceed the estimated minimum freshwater heads (0.6 to 1.5 m) necessary to prevent saltwater encroachment in the Biscayne aquifer. Early residents and visitors describe numerous freshwater springs, onshore near the coast as well as offshore in Biscayne Bay (Fuller, 1904; Munroe and Gilpin, 1930; Parks, 1987). Water levels were sufficiently high prior to development in this area to maintain freshwater in the Biscayne aquifer close to the coast (Parker, 1945). Although the current study did not identify any historical information directly describing the extent of saltwater intrusion in the southernmost parts of Miami-Dade County prior to drainage of the Everglades, the low land-surface altitudes in this area and the existence of coastal saltwater marshes indicate that there may have been at least some saltwater intrusion in this area, which may have been caused by inland flow of saltwater in coastal streams or overwashing of the coast during hurricanes or tropical storms.

Relation of Urban Development to Saltwater Intrusion

Water levels in the Biscayne aquifer near Miami are estimated to be approximately 2.9 m below predrainage conditions based on a comparison of historical information and monitoring-well data (Parker and others, 1955, p. 580; U.S. Geological Survey, 2011f), and this reduction in water levels has resulted in saltwater intrusion in about 1,200 km^2 of the Biscayne aquifer in Miami-Dade County as of 2011. The events that led to this intrusion began in December 1845 when drainage of the Everglades was first proposed by the Florida State Senate (Paige, 1986, p. 138). Between 1850 and 1907, various Federal and State acts were passed to facilitate drainage of the Everglades, and these acts provided authority and resources for the installation of numerous drainage canals. The Miami Canal (table 1; fig. 11) installed beginning in 1908, was one of the first canals in south Florida. Concrete locks and dams that might have helped reduce saltwater intrusion were installed in 1912–13 in many of the canals; however, with a few exceptions, these locks and dams typically were poorly maintained and operated (Parker and others, 1955, p. 587).

Table 1. Partial history (1881–1978) of canal, structure, and levee installations in south Florida.

[km², square kilometers; ?, date uncertain; –, no data]

Begin year	End year	Feature
1881	1896	First canals to drain 400 km² near lake Okeechobee.
1906	1909	Launching of publicly funded dredge ships, Everglades, Okeechobee, Caloosahatchee, and Miami.
1908	1932	Dynamiting of the Miami Rapids, dredging of the Miami Canal.
1910	–	Small 2-m-high earth dike built along part of the southern shoreline of Lake Okeechobee.
1912	1917	Florida City (C–105), Snake Creek (C–9), and Snapper Creek (C–2) Canals.
1919	1928	Tamiami Canal dredged as far west as the L–28 canal.
?	1922	The Model Land (C–107 and C–107S), North (C–104), and Goulds (C–101) Canals.
1922	–	Enlarged Lake Okeechobee dike.
1925	1928	Biscayne (C–8) and Little River (C–7) Canals.
1925	1934	Completion of the Comfort Canal.
1925	1927	many small canals in Miami-Dade County.
1930	1938	Herbert Hoover Dike installed at Lake Okeechobee.
1942	1945	Replacement of first water control structure on Miami Canal by a pneumatic dam. This failed in 1945 and was in turn replaced by a sheet pile structure.
?	1945	Initial Military, Mowry (C–103) canals and FEC Railroad and Card Sound Road borrow ditches.
1945	1946	Sheet pile salinity control structures installed on Coral Gables, Little River, Snapper Creek, Snake Creek, and Tamiami Canals.
1950	1960	Levee system on the western side of the urban development, L–30, L–31N, and L–33 Canals, extension of Little River Canal (C–7), Snake Creek (C–9), and Snapper Creek (C–2) Canals, and installation of salinity control structures S–22, S–27, and S–29.
1960s	–	Expansion of Herbert Hoover Dike.
1960	1968	Aerojet (C–111), Belle Air (C–1N), Black Creek (C–1), Cutler Drain (C–100), L–31E, L–67, and Princeton (C–102) Canals and extension of Biscayne Canal (C–8), Little River (C–7), Mowry (C–103), L–31N Canals, installation of salinity control structures S–20, S–20F, S–21, S–21A, S–28, S–123.
1970	1978	C–109, and C–110 Canals, expansion of Card Sound Road Borrow Ditch to create The Card Sound Road Canal (C–108). Installation of salinity control structures S–26, S–25B, S–25, S–25A, and S–336. C–109 and C–110 not fully completed.

In addition to the drainage caused by canals, withdrawals from the aquifer for public, residential, and industrial water supply increased as population increased (table 2). The first public supply wells were installed in 1899. The well drilled closest to the Miami River became saline within about a year. The Spring Gardens well field was installed in 1907 as a replacement for the first public supply wells, but it started to become saline in 1919 and was replaced by new well fields in Miami Springs and Coconut Grove in 1924 and 1925, respectively (fig. 1, table 2) (Parker and others, 1955, p. 705; South Florida Water Management District, 2010). By 1942 nearly 10,000 domestic, public, and industrial water supply wells had been installed in Miami-Dade County; these wells ranged in depth from a few meters to 37 m or more (Cross and Love, 1942, p. 490).

In 1938–1939 a major drought (fig. 4) exacerbated the effects of changes in the hydrologic system. Some of the wells in the Miami Springs and Hialeah well fields nearest to the Miami Canal, and numerous private water supply wells near tidal canals, began to become saline (Parker and others, 1955, p. 587–691). To protect the well fields, a water control structure was installed in the Miami Canal in 1939 (fig. 12). The control structure leaked considerably, and it had a gate that had to be periodically lifted to allow the passage of barges. It was eventually replaced by better structures. The Coconut Grove well field began to yield saltwater in 1933 and had to be abandoned in 1941. A USGS study by Cross and Love (1942) indicated that (1) saltwater had intruded 3.2 km inland into the Biscayne aquifer and several kilometers farther inland along the Miami Canal, (2) saltwater was leaking from the canals and encroaching along the base of the Biscayne aquifer, (3) groundwater levels near the Miami Canal were below nearby canal stages and were drawing saltwater into the aquifer, and (4) two small lakes that were open to the Miami Canal had become saline, and this saltwater seeped into the aquifer where it flowed downgradient toward the Miami Springs well field.

Parker and others (1955, p. 589–680) write that during the 1943–46 drought, saltwater migrated at least 6 km inland from the mouths of all of the canals, except possibly the Goulds and Mowry Canals, which were not sampled farther inland. In eight of these canals, saltwater migrated 11 to 20 km inland. Between 1944 and 1945, freshwater runoff ceased in several of the shorter canals, and highly saline water was

Table 2. Partial history (1899–2001) of well field installations and operations in Miami-Dade County, Florida.

[–, no data]

Begin year	End year	Feature
1899	–	First city of Miami public water supply wells.
1907	1919	Installation and modifications to the Spring Gardens well field.
1919	–	Spring Gardens Well Field began to yield salty water.
1924	–	Installation of the lower Miami Springs well field (8 wells) as a replacement for the Spring Gardens well field.
1925	1937	Installation (initially two wells) and subsequent modification of the Coconut Grove well field.
1933	–	Coconut Grove well field first became salty.
1936	1954	Installation of Upper Miami Springs well field (4 wells), expanded in 1945, 1949, and 1954 (total of 12 wells).
1936	–	Installation of Hialeah well field (three wells).
1941	–	Coconut Grove well field had to be abandoned because of saltwater encroachment.
1942	–	By this year, an estimated 10,000 domestic, public, and industrial water supply wells had been installed.
1949	1964	Installation of Alexander Orr well field (4 wells) expanded in 1952 and 1964 to total of 10 wells.
1953	1971	Installation of Leisure City well field.
1953	1997	Installation of Southwest well field.
1966	1972	Installation of Preston well field.
1975	–	Installation of Medley and Naranja well fields.
1976	1982	Installation of Snapper Creek and Northwest well fields.
2000	2001	Installation of the Newton well field.

Figure 11. Rapids of the Miami River prior to their destruction by dynamiting to increase drainage of the Everglades. From Smith, 1909. Courtesy of History Miami Archives and Research Center.

Figure 12. First water control structure on the Miami Canal installed in December 1939. This structure leaked considerably and also was opened to allow barges to pass. Photograph from the files of the U.S. Geological Survey.

observed entering the ground "with visible velocity" (Parker and others 1955, p. 630). Parker and others (1955, p. 589–590) indicated that during 1943 to 1946 the greatest advance of saltwater encroachment occurred in the Biscayne aquifer. They found that in a 27-month period between 1943 and 1944 saltwater encroached landward by 610 m, which was a rate of 270 meters per year (m/yr).

In 1945, having received the authority to control water levels in canals within its boundaries through a legislative act, Dade County (currently named Miami-Dade County) began to install numerous salinity control structures that were effective in controlling salinity (Parker and others, 1955, p. 589). During the 1950s and 1960s, additional canals and more technologically advanced control structures were built with the dual purposes of preventing extensive flooding by allowing sufficient drainage during tropical storms and maintaining freshwater heads sufficient to prevent further saltwater intrusion. During the first 2 years of the 1970 to 1977 drought (fig. 4), however, saltwater in the Miami Canal upstream of salinity control structure S–26 came to within 1.6 km of the Miami Springs and Hialeah (currently named the Hialeah-Preston) well fields (Benson and Gardner, 1974) and increased the salinity of samples from wells near the Miami Canal (fig. 13). Although saltwater continues to leak past many of the water control structures in Miami-Dade County, since the late 1970s, the chloride concentration in samples from monitoring wells near the Miami-Canal have decreased (fig. 13), and the changes in the inland extent of saltwater have been relatively minor compared to the changes that occurred between 1904 and 1946 (Parker and others, 1955, p. 589, fig. 169; Renken and others, 2005a, figs. 53–55).

Data Collection and Analysis

Site location and construction information for sites used to evaluate the inland extent of saltwater or the causes of saltwater intrusion in the Biscayne aquifer is provided in appendix 1. Monitoring results from a few of these sites are provided in this report. Monitoring results from the remaining sites are available from the USGS Annual Water Data Reports and National Water Information System—Web interface—Water quality samples for the Nation websites (U.S. Geological Survey, 2011e, f) or from the organizations listed in appendix 1. The results of 69 geochemical samples and 3 replicate samples from 44 sites are provided in appendix 2. Salinity profiles were collected in the Card Sound Road Canal to evaluate the extent to which saltwater can flow inland along this canal (appendix 3). Information concerning the TEM soundings is provided in appendix 4. The methods used to develop TSEMIL datasets are provided in appendix 5. A comparison of the depth of the base of the Biscayne aquifer to the models of TEM soundings is provided in appendix 6. To improve the saltwater monitoring network, eight new monitoring wells (fig. 8) were installed during

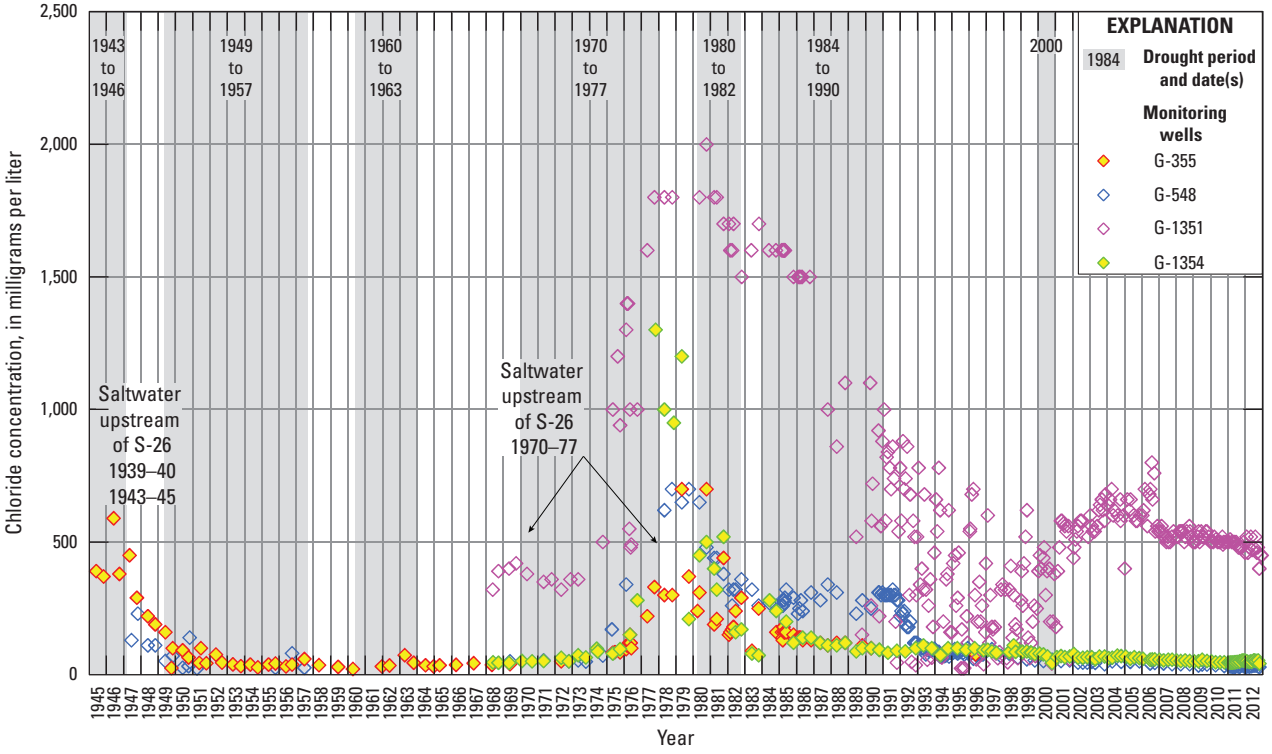

Figure 13. Chloride concentration in samples from monitoring wells G–355, G–548, G–1351, and G–1354 near the Miami Canal and between 0.6 and 2.4 kilometers northwest of salinity control structure S–26, Miami-Dade County, Florida.

this study, and a suite of geophysical logs were collected prior to completion of the wells. Information concerning the installation of these eight monitoring wells and other data collected in these wells are included in appendix 7, and the geophysical logs collected from these wells are provided in appendix 8. The hydrostratigraphic analyses using information from these new wells are included in appendix 9. Sampling methods, sample analyses, and quality assurance are described in appendix 10. Monthly measurements of salinity in canals collected by the Miami-Dade County Permitting, Environmental, and Regulatory Affairs (M-D PERA; Maria Idia Macfarlane, Water and Sewer Department, written commun., March 7, 2011; Craig Grossenbacher, Miami-Dade County Permitting, Environmental, and Regulatory Affairs, written commun., July 7, 2010) are provided in appendix 11.

Salinity Measurements

Salinity data from about 2,000 active or inactive sites within the study area were available for evaluation of the inland extent of saltwater. Most of these sites, however, were not close enough to the saltwater front, or at the necessary depth, to aid in mapping the saltwater front. Numerous sites also were sampled by local and regional organizations. Only those actively monitored sites that were used to map the saltwater front are included in appendix 1 and shown in figure 8.

In some areas, long open-interval wells were the only wells available. Studies in Miami-Dade County and elsewhere have determined that fresh and saltwater within the open intervals of long open-interval wells may mix (Kohout and Hoy, 1963; Oki and Presley, 2008; Shalev and others, 2009). The Biscayne aquifer has been shown to have cyclostratigraphic layers with three alternating forms of porosity (Cunningham and others, 2006b), and some of the layers have been shown to be laterally extensive. As a result, natural head differentials can exist between these layers. Open boreholes that pierce layers with head differentials can allow ambient vertical flow within the borehole. Geophysical logs collected in the boreholes of wells installed during this study near the edge of the saltwater interface in the Biscayne aquifer confirm the occurrence of extreme variations in porosity and vertical ambient flow within the borehole. Heat pulse flowmeter measurements collected in the boreholes of six of the eight new wells (G–3885, G–3886, G–3887, G–3888, G–3947, and G–3949) indicated maximum up-hole or and down-hole vertical flow rates of 2.31 and –5.45 liters per minute (L/min) (table 3) respectively. These flow rates indicate that certain types of samples and measurements from long open-interval wells in the Biscayne aquifer may not be representative of the aquifer.

If long open-interval wells were the only wells available in some areas, data collected from them were used to determine if the saltwater interface occurred in a well. A non-isokinetic thief sampler called a Kemmerer (Lane and others, 2003, p. 33–34) was used by the USGS to sample long open-interval wells to minimize the mixing that could be caused when the well is pumped (Kohout and Hoy, 1963). The Kemmerer captures a sample from the bottom of the well where salinity is likely the greatest.

Each organization involved in the collection of salinity data determined the constituents or parameters to be measured and how those parameters were reported. In some instances, the same organization may have reported results differently through time. Chloride concentrations generally were expressed as either milligrams per liter or parts per million of chloride. Salinity was reported as practical salinity units and also as parts per thousand. The salinity units are approximately equivalent but cannot be directly converted without additional information. These parameters are therefore reported in the same units used by the organizations that provided the data. Metric equivalents are provided where necessary.

Time-Series Electromagnetic Induction Logging

In Miami-Dade County, salinity monitoring wells have been installed with polyvinyl chloride (PVC) casings and annular seal materials that do not impede the induction of electromagnetic energy in the aquifer. EMI logs, which consist of measurements of the bulk conductivity or resistivity of earth materials throughout the depth penetrated by the wells, can be collected in these wells. The radius of investigation is 20 to 100 centimeters (cm) from the center of the borehole (McNeill and others, 1990, p. 1). The freshwater-saturated sand and limestone sediments of the Biscayne aquifer generally have relatively low bulk conductivities (10 to 30 millisiemens per meter [mS/m]), but where the sediments have been intruded by saltwater, bulk conductivity is higher. Therefore, EMI logs can be used to identify the depths at which saltwater occurs in the aquifer. Moreover, because EMI measurements can be collected through PVC casing, the possibility of ambient vertical borehole flow can be eliminated. In south Florida, the USGS began to collect EMI logs from short-screened PVC-cased monitoring wells in 1995.

Table 3. Vertical flows measured in open boreholes prior to well installation, 2009–2011, Miami-Dade County, Florida.

[L/min, liters per minute; m, meter; –, no data]

Local identifier	Maximum up-hole flow rate (L/min)	Depth of maximum up-hole flow (m)	Maximum down-hole flow rate (L/min)	Depth of maximum down-hole flow (m)
G–3885	0.45	16.8	0	–
G–3886	2.31	16.5	–0.72	22.9
G–3887	1.4	15.2	0	–
G–3888	1.48	14.2	0	–
G–3946	0.15	12.6	0	–
G–3947	0	–	–5.45	31.7 to 36.0, 38.1 to 39.3
G–3948	0	–	0	–
G–3949	0.42	25.9	0.04	–

A time series of EMI logs can provide a detailed understanding of the movement of saltwater through the Biscayne aquifer that would not be possible using other methods.

The current study used EMI logs that had been collected in 35 wells in Miami-Dade County. Some of these wells were logged only once, but sets of EMI logs that were collected annually or semiannually are available for the majority of these wells. The EMI logs were used to (1) provide information about the thickness of saltwater occurring in the Biscayne aquifer, (2) evaluate TEM sounding models, (3) calibrate the HEM survey, and (4) provide insights into occurrence of saltwater in the aquifer. As part of the current study, a methodology was developed to process individual EMI logs into a TSEMIL dataset that was used to evaluate relatively small temporal changes in bulk conductivity (appendix 5).

Many of the older wells, from which TSEMIL datasets were collected, do not penetrate beyond the base of the Biscayne aquifer; therefore, if saltwater did occur below the base of the aquifer, it was not shown by these logs. The thickness of the saltwater wedge determined with TSEMIL datasets is therefore based on the thickness of the saltwater lens within the Biscayne aquifer itself. Although figures showing TSEMIL datasets are not provided in this report for all sites where they were used, these datasets are readily available in the USGS online Annual Water Data Reports (U.S. Geological Survey, 2011e).

Comparison of Bulk Resistivity to Specific Conductance of Water and Chloride Concentration

EMI logs collected by the USGS in Miami-Dade County (U.S. Geological Survey, 2011e) indicate that freshwater-saturated materials of the Biscayne aquifer typically vary in bulk resistivity from approximately 35 to 220 ohm-meters (ohm-m) and have an average bulk resistivity of approximately 80 ohm-m. Data from EMI logs and water samples collected during the spring of 2009 from the Biscayne aquifer in Miami-Dade County were used to establish a relation between the bulk resistivity of the formation (including the water and the rock) and the electrical resistivity of the water (fig. 14) (Fitterman and Prinos, 2011). A relation between the chloride concentration in water samples and the resistivity of these water samples (fig. 15) (Fitterman and Prinos, 2011) was combined with the relation between bulk resistivity and water resistivity to determine that parts of the aquifer saturated with saltwater (1,000 mg/L of chloride or more) would have formation resistivities of about 10 ohm-m or less. Bulk resistivities ranging between 10 and 15 ohm-m were considered indicative of the mixing zone at the leading edge of saltwater intrusion and the mapped extent of saltwater intrusion was plotted to be very close to these measurements.

The relation between the bulk resistivity of the formation and the electrical resistivity of the water is affected by variations in porosity and lithology and by potential measurement errors. One type of measurement error is caused by the limitation of induction logging equipment to provide a full response to hydrostratigraphic layers thinner than 4 m (Taylor and others, 1989).

Time-Domain Electromagnetic Soundings

TEM soundings are surface geophysical measurements that have been used extensively in south Florida since 1994 to evaluate the inland extent of saltwater in the Biscayne aquifer (Sonenshein, 1997; Fitterman and others, 1999; Hittle, 1999; Schmerge, 2001; Stewart and others, 2002) and to aid in the calibration and interpretation of results from a December 1994 HEM survey in the Everglades (Fitterman and Deszcz-Pan, 1998). Seventy-nine TEM soundings were collected during 2008 and 2009 to aid in mapping the inland extent of saltwater in the Biscayne aquifer and to provide information to calibrate the HEM survey (fig. 8, appendix 4). Detailed information and the final models developed for each of these TEM soundings are provided in Fitterman and Prinos (2011). Additional information concerning the TEM method in general is provided by Kaufman and Keller (1983), Fitterman (1989), McNeill (1990), and Fitterman and Labson (2005).

HEM Survey Analysis

The 2001 HEM survey processed during this study provided much more detailed information concerning the extent of saltwater than previously existed in the Model Land area (fig. 1). The Model Land area in southeast Miami-Dade County, south of the Florida City Canal and east of U.S. Highway 1, is the location of a wetland restoration project. The survey area covered about 115 km^2 of the southernmost part of the study area (fig. 1). The survey consisted of densely spaced frequency-domain electromagnetic (FEM) measurements collected using an instrument package suspended 30-m below a helicopter. Measurements were collected by passing a sinusoidally varying current through multi-turn transmitter coils. Five horizontal coplanar coil pairs operating at nominal frequencies of 400, 1,500, 6,400, 25,000, and 100,000 hertz (Hz) were used. The conversion of these measured fields to apparent and differential resistivity is described in Fitterman and others (2012). Resistivity-depth functions were obtained from a differential resistivity-depth analysis. These functions were used to create resistivity-depth–slice maps ranging in depth from 5 to 100 m. East-west and north-south cross sections of resistivity that coincided with the flight lines also were created. All of the cross sections and depth slices processed during the current study are provided in Fitterman and others (2012); figure 16 shows an example of the 30-m-depth slice.

The maps and cross sections indicate a relatively sharp transition zone where differential resistivity generally decreased from 70 to 35 ohm-m across a horizontal distance of about 300 to 600 m (Fitterman and others, 2012). Based on information from sampled monitoring wells and TEM

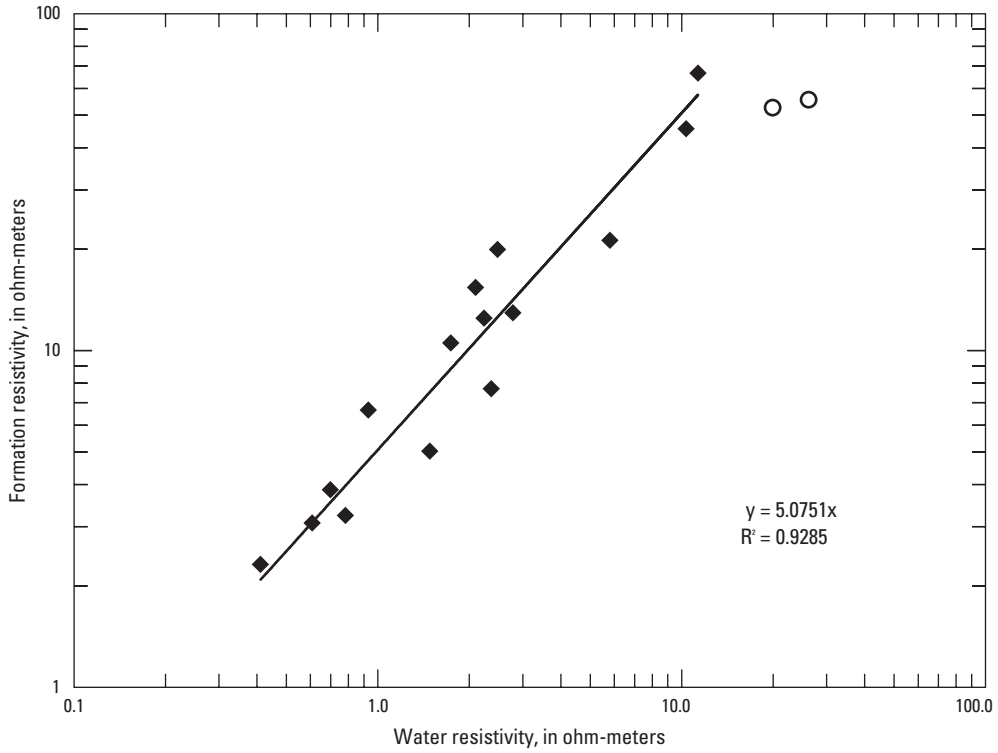

Figure 14. Relation between the resistivity of water samples collected in monitoring wells in Miami-Dade County, Florida, and the formation resistivity measured by electromagnetic induction logs in the screened intervals of the same well. Measurements symbolized by open circles were not used for the regression.

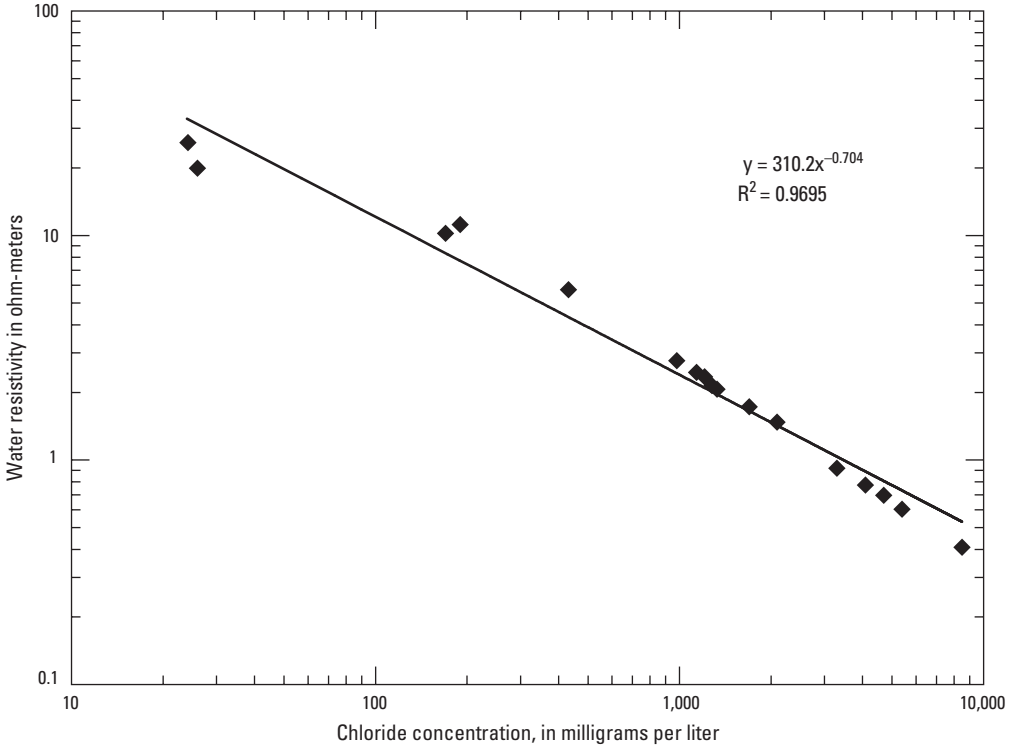

Figure 15. Relation between water resistivity and chloride concentration in water samples from monitoring wells in Miami-Dade County, Florida. From Fitterman and Prinos (2011).

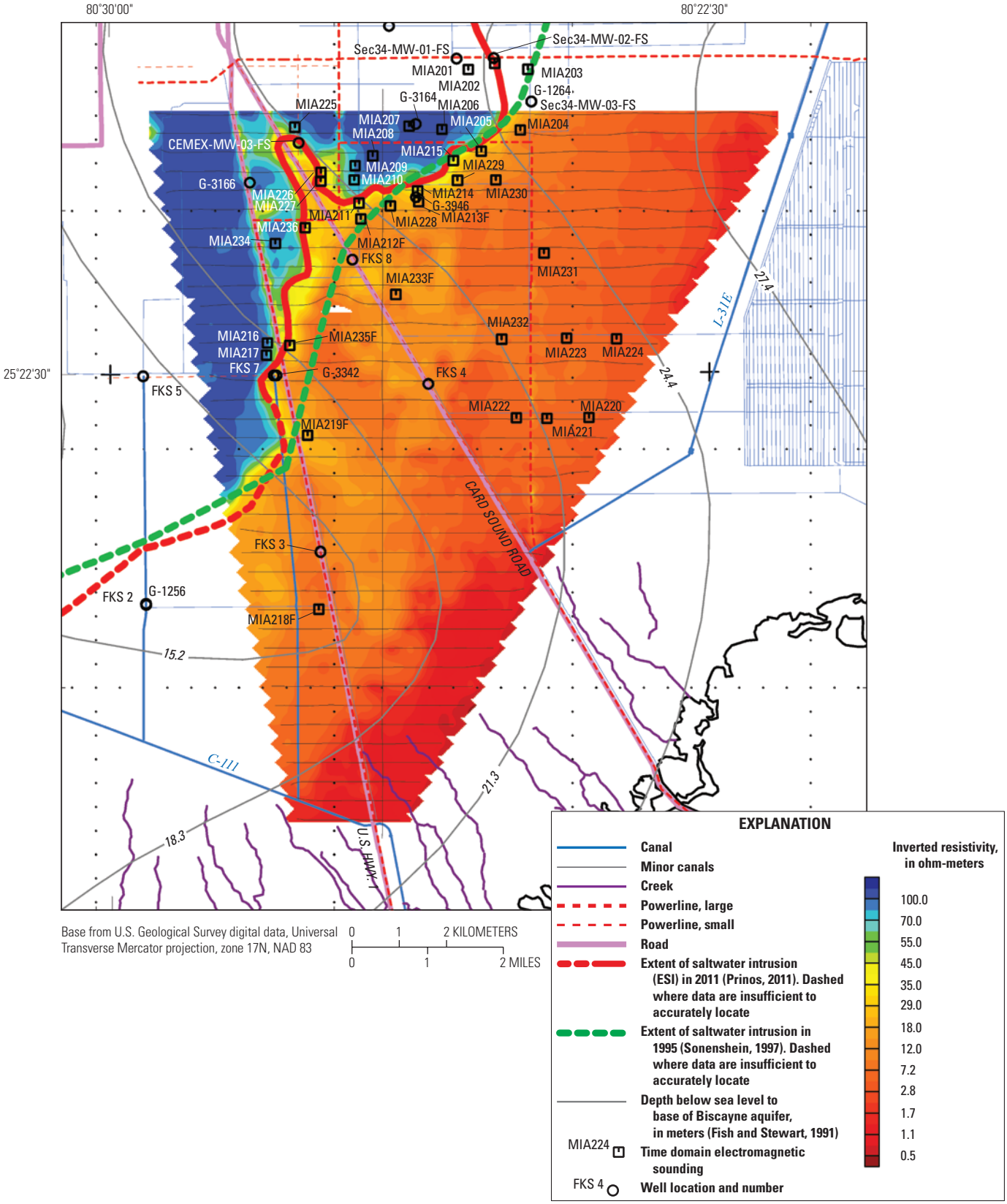

Figure 16. Example of a depth slice from the 2001 helicopter electromagnetic survey, Miami-Dade County, Florida. Modified from Fitterman and others (2012).

soundings collected in this area, this transition zone was interpreted to be the saltwater interface. To determine the inland extent of saltwater in the HEM survey area, the 45-ohm-m differential resistivity contour of each of the depth slices was mapped. This map provided a three-dimensional representation of the saltwater interface. The intersection of this interface with the base of the Biscayne aquifer interpolated from the map of Fish and Stewart (1991) was mapped and represents the inland extent of saltwater in the Biscayne aquifer in 2001. This information was used to create the 2008 preliminary map of the inland extent of saltwater intrusion in this area. Thirty-six additional TEM soundings collected in the spring of 2009 and 4 new wells were used to verify or update the inland extent of saltwater in 2011 (fig. 8).

Approximate Inland Extent of Saltwater in the Biscayne Aquifer

The approximate inland extent of saltwater in the Biscayne aquifer (appendix 12) was determined by using (1) salinity measurements of groundwater and surface water (chloride, total dissolved solids [TDS], or specific conductance), (2) borehole EMI data, (3) TEM data, and (4) HEM survey data collected in 2001. The word "approximate" is used because the 1995 and 2011 maps are considered to be approximations of the inland extent of saltwater. Where chloride concentration information exists from wells that fully penetrate the aquifer, the mapped line represents the approximate position of the 1,000-mg/L isochlor at the base of the Biscayne aquifer. Where constrained by EMI logs or TEM soundings, this line represents the landward limit of the occurrence of aquifer materials (including water) measured or modeled to have a bulk resistivity of less than 10 ohm-m. Resistivities between 10–15 ohm-m are considered indicative of the mixing zone at the leading edge of the saltwater front. Resistivities greater than 15 ohm-m indicate freshwater saturated materials.

Improved Spatial Coverage and Precision of the Inland Extent of Saltwater

Mapped changes of the inland extent of saltwater between 1995 and 2011 (fig. 17) are the result of improved spatial information, actual movement of the saltwater front, or a combination of both. The water-quality measurements and samples and geophysical information collected or processed during this study provided better spatial coverage than had existed in 1995 when the extent of saltwater was last mapped. This was particularly true in the Model Land area where there was insufficient information available to accurately determine the inland extent of saltwater in 1995 (Sonenshein, 1997). Estimated advances or retreats of the saltwater front are provided in areas where existing information indicates that the saltwater front has either advanced or retreated. These estimations are based on changes apparent in the monitoring data, but are relatively coarse approximations because the relation between the amount of front movement and amount of change in salinity is variable.

The precision of the estimated inland extent of the saltwater front depends on the availability of monitoring data and/or the geophysical spatial coverage. For example the Model Land area south of the Florida City Canal and east of U.S. Highway 1 had long been an area where little information was available for mapping the inland extent of saltwater. As a result, the inland extents of saltwater estimated by the maps produced in 1955 and 1995 (fig. 8) differed in this area by 1 to 4 km. Spatial coverage in the Model Land area was greatly improved during the current study through the collection of numerous TEM soundings (Fitterman and Prinos, 2011), the processing of the 2001 HEM survey (Fitterman and others, 2012), and the installation of new monitoring wells. In this area, relatively dense surface geophysical coverage was possible because of the many large open fields that were relatively free of anthropogenic interference.

Surface geophysical measurements also improved spatial coverage elsewhere in Miami-Dade County, particularly where one measurement occurred on one side of the interface and another occurred on the opposite side. Unfortunately, surface geophysical measurements could not be collected everywhere because some areas were too heavily developed to allow the collection of surface geophysical data given the transmit coil size required. In these areas, the distance between monitoring wells ranges from 0.5 to 5 km. The approximate extent of saltwater intrusion is less reliable in areas where monitoring wells are widely spaced and surface geophysical measurements could not be made.

Most of the time-series data used to evaluate movement of the saltwater front were collected by the USGS and are readily available online (U.S. Geological Survey, 2011e, 2011f, 2011g). It is not feasible to include all of these data in this report, but examples of the changes in chloride concentration that have occurred are shown in figure 18. Examples of the TSEMIL datasets are provided in the "Time-Series Electromagnetic Induction Logging" section of this report. Results of all TEM soundings used to map the location of the saltwater front are published in the companion report (Fitterman and Prinos, 2011; appendix 4).

Changes between 1995 and 2011

The saltwater front was mapped farther inland in 2011 than in 1995 (figs. 8 and 17) in eight approximated areas totaling 24.1 km^2. These eight areas are (1) a 4.5-km^2 area in northern Miami-Dade and southern Broward Counties from just south of the Biscayne Canal to the city of Hallandale Beach, (2) a 3.2-km^2 area near Interstate 95, extending from north of the Little River Canal to Interstate 195, (3) a 2.0-km^2 area from the Miami Canal to a little south of the Comfort Canal, (4) a 1.2-km^2 area between SW 8 Street (Tamiami

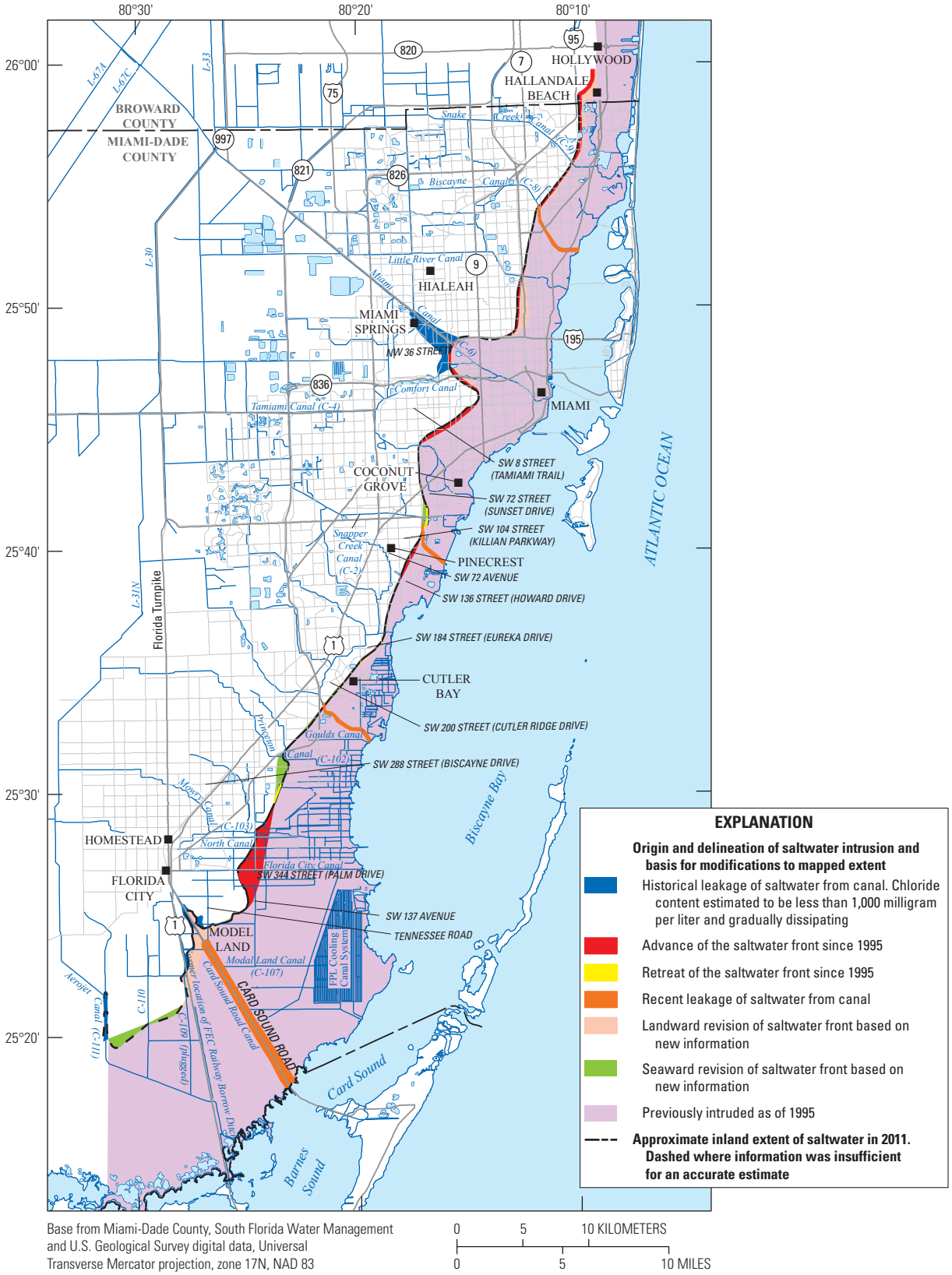

Figure 17. Origin and delineation of saltwater intrusion in the Biscayne aquifer and the basis for modifications to its mapped extent. Enlarged version of this figure available for download at *http://pubs.usgs.gov/sir/2014/5025/downloads/sir2014-5025_figure17large.pdf.*

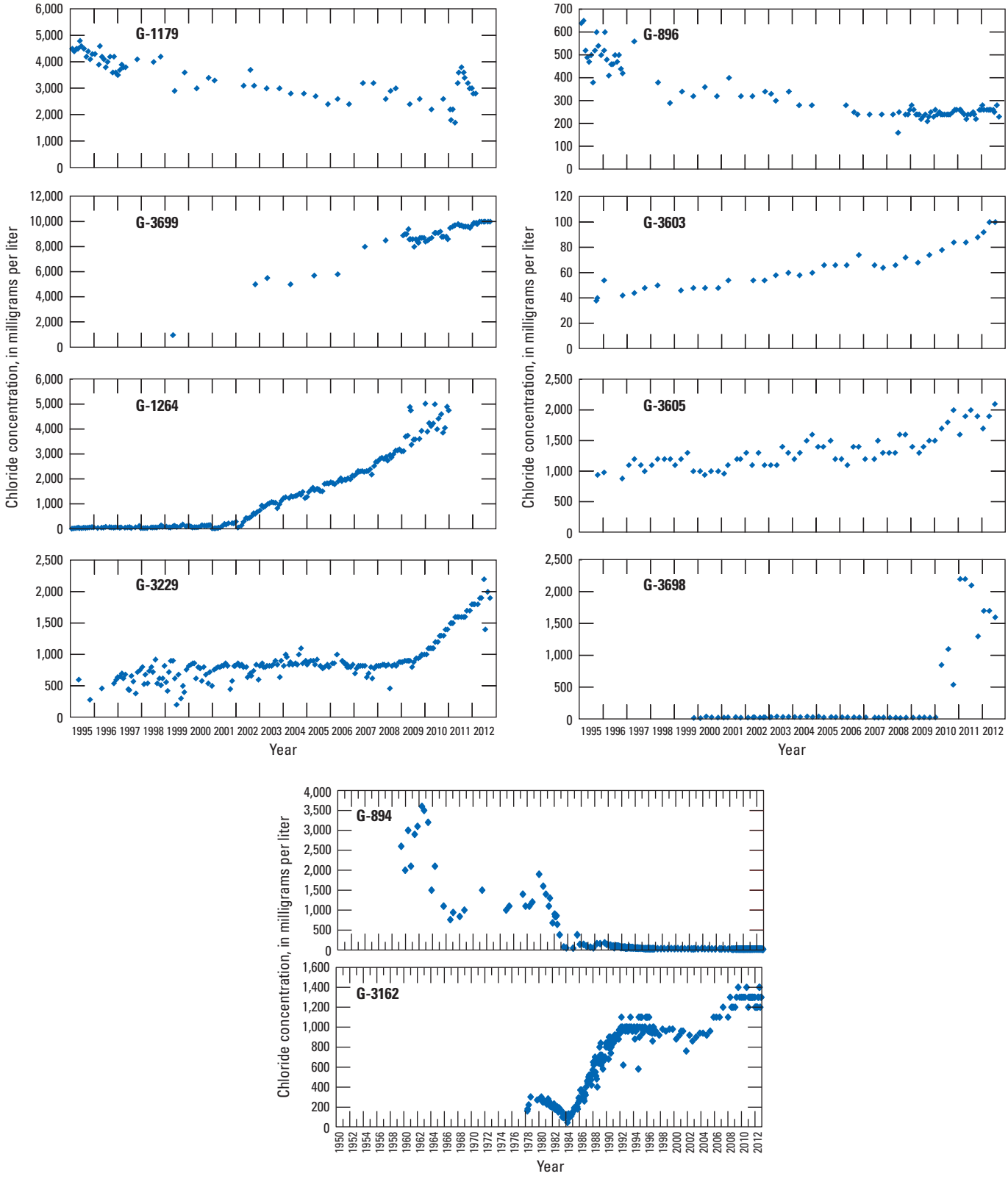

Figure 18. Chloride concentrations in water samples from long-term monitoring wells (see fig. 8 for well locations).

Trail) and the Coral Gables Canal, (5) a 0.5-km^2 area in the city of Pinecrest between SW 104 Street (Killian Parkway) and SW 136 Street (Howard Drive), (6) a 0.3-km^2 area in the city of Cutler Bay, between SW 184 Street (Eureka Drive) and SW 200 Street (Cutler Ridge Drive), (7) a 7.1-km^2 area in or near the cities of Florida City and Homestead, extending from a little south of the Military Canal to a little south of FKAA well G–1264 (fig. 8), and (8) a 5.3-km^2 area south of Florida City in the vicinity of U.S. Highway 1 and Card Sound Road. In most of these areas, the difference between mapped extent of saltwater in 1995 and 2011 is likely caused by improved spatial coverage or a combination of advances of the saltwater front and improved spatial coverage. Landward movement of the front is inferred from increases in the chloride concentration in water samples or increases in the bulk conductivity of EMI logs from monitoring wells used for this evaluation (fig. 8, appendixes 1 and 5). Examples of the increases in the chloride concentrations in samples are shown in figure 18.

In two areas, the differences between the 1995 and 2011 maps are likely caused solely by front movement. In the area between SW 8 Street and the Coral Gables Canal, analysis of water samples from well G–3229 (figs. 8 and 18) indicated an increase in chloride concentration from about 600 mg/L to 1,640 mg/L between December 1996 and September 2011 (fig. 18). The saltwater front, which had been approximately 60 m southeast of well G–3229 in 1995, had moved 230 m farther inland by 2011. Near Florida City and Homestead near SW 344 Street (Palm Drive), the saltwater front had been mapped about 0.5 km east of well G–3699 (fig. 8) in 1995. This well was installed in 1999, and the first chloride concentration sampled was 950 mg/L. The chloride concentration in samples had increased to 9,700 mg/L by 2011, and monitoring wells G–3855 and G–3856 located west of well G–3699 have become saline. Based on this information, the saltwater front was mapped to be about 1.4 km west of well G–3699 and is interpreted as having advanced by about 1.9 km between 1995 and 2011 near SW 344 Street. Water samples from wells G–1264 and G–3698 located south and north of well G–3699, respectively, also indicated increases in chloride concentration during this same period (fig. 18), and the front appears to have advanced landward in this area. The changes occurring in the vicinity of wells G–1264, G–3698, and G–3699 are described in greater detail in subsequent sections of this report.

The saltwater front was mapped closer to the coast in 2011 than it was in 1995 (figs. 8, 17) in four approximated areas totaling about 6.2 km^2. These areas are (1) a 0.7-km^2 area between the cities of Coconut Grove and Pinecrest extending from SW 72 Street (Sunset Drive) to SW 104 Street (Killian Parkway), (2) a 2.7-km^2 area south of the city of Cutler Bay extending from SW 200 Street (Cutler Ridge Drive) to a little south of SW 288 Street (Biscayne Drive), (3) a 0.1-km^2 area in the Model Land between SW 137 Avenue and Tennessee Road, and (4) a 2.7-km^2 area south of Florida City, between U.S. Highway 1 and the C–111 Canal. The changes were identified based on improvements in spatial coverage provided by the TEM soundings collected in 2008 and 2009 (Fitterman and Prinos, 2011), the HEM survey collected in the Model Land (Fitterman and others, 2012), a HEM survey in the Everglades National Park and surrounding areas (Fitterman and Deszcz-Pan, 1998, 2002), and new monitoring wells installed during this study by EAS Engineering, Inc., Florida Power and Light (FPL), Miami-Dade County, and the USGS. Decreases in the chloride concentrations in wells G–896 and G–1179 (fig. 18) indicate that some of the change in the mapped position of the front near these wells resulted from movement of the front, rather than from improved spatial coverage alone.

Characterization and Distribution of Saltwater in the Biscayne Aquifer

Water managers need to understand the origin of intruded saltwater and the temporal and spatial changes in its distribution to evaluate the potential for saltwater intrusion at coastal well fields. Saltwater that intruded early in the 20th century and is gradually dissipating may pose less of a concern, for example, than saltwater that is actively leaking from a canal near a well field. If the sources of saltwater are misidentified, the corrective measures implemented to prevent saltwater intrusion could fail to address the actual issue. Differentiating between saltwater that previously intruded the aquifer and saltwater that is actively intruding can be difficult because saltwater of various origins and ages may mix.

Water samples were analyzed to determine (1) major and trace ion geochemistry, (2) strontium isotopic ratios, (3) oxygen and hydrogen stable isotopic ratios, (4) tritium concentrations, (5) ^{3}H/^{3}He concentrations, (6) sulfur hexafluoride concentrations, and (7) dissolved gas concentrations. The concentrations of ^{3}H/^{3}He and sulfur hexafluoride were used to interpret the ages of water samples. These analyses, coupled with other types of information, were used to evaluate the prevailing climatic conditions during which saltwater intruded the Biscayne aquifer, timeframes for this intrusion, and the chemical interactions between the intruded saltwater and the aquifer.

Major and Trace Ion Geochemistry

Ions, such as chloride and bromide, are conservative indicators of freshwater and seawater mixing because these ions generally do not adsorb or interact with aquifer materials. The concentrations of many other ions, however, are affected by dissolution of aquifer materials, precipitation or reduction of chemical species, and adsorption onto or release from clay minerals, organic matter, oxyhydroxides, or fine-grained rock materials as mixing occurs, (Jones and others, 1999, p. 61). These complex chemical changes occur in a portion of the saltwater front called the ion-exchange front (fig. 9), and may include exchange of sodium in

seawater with adsorbed calcium; adsorption of potassium, boron, and lithium in seawater onto clay minerals (Jones and others, 1999, p. 66); enrichment in calcium and bicarbonate caused by dissolution of calcite and aragonite in carbonate aquifers (Richter and Kreitler, 1993, p. 107; Jones and others, 1999, p. 61); reduction of the sulfate in seawater to hydrogen sulfide under low redox conditions in the aquifer (Richter and Kreitler, 1993, p. 107; Jones and others, 1999, p. 67); and exchange of calcium adsorbed on clay minerals with magnesium in seawater (Howard and Lloyd, 1983, p. 435; Richter and Kreitler, 1993). Causes for enrichment of barium in the freshwater/seawater mixing zone include desorption of surface-bound barium from aquifer particulates by replacement with major seawater cations, and diagenetic reactions such as dissolution of authigenic barite, decomposition of barium-rich organic material, and dissolution of barium containing metal oxide phases (Shaw and others, 1998). Richter and Kreitler (1993) state: "These changes are most pronounced within the initial sea-water front that mixes with fresh water. Subsequent intrusion deviates little from sea-water composition."

The ionic exchanges that occur as seawater mixes with freshwater are indicated by deviations from the theoretical freshwater/seawater mixing line that would be created solely by mechanical mixing of freshwater and seawater (Howard and Lloyd, 1983); the seawater end member for the mixing line was taken from Turekian (1976), whereas the freshwater end member was generally the average composition of water samples collected from canals during this study. Seaward of the ion-exchange front or at depths that are well below the freshwater/saltwater interface, there may be little or no ion exchange because exchange sites of aquifer materials may be saturated and chemical equilibrium of seawater with aquifer materials may have been established. Where ion exchange is not occurring, the concentration of ions in water samples should plot on the theoretical freshwater/seawater mixing line.

A calcium to (bicarbonate + sulfate) molar ratio [$Ca/(HCO_3 + SO_4)$] greater than 1 has been used to identify the "arrival of saltwater intrusion" at a given location in the aquifer where ion exchange results from the mixing of freshwater and saltwater (Jones and others, 1999). Using this criterion, the "arrival of saltwater intrusion" is indicated at 11 sites (wells G–901, G–1264, G–3615, G–3698, G–3699, G–3704, G–3705, G–3855, G–3946D and one of each of the samples collected from wells F–279 and G–3701) (table 2–1; fig. 19). A $Ca/(HCO_3 + SO_4)$ molar ratio less than 1 and a chloride concentration of 1,000 mg/L or more (fig. 19) indicated previous saltwater intrusion at 10 sites (wells FKS4, FKS8, G–939, G–3600, G–3601, G–3602, G–3604, G–3605, G–3609, and G–3702). Some sample results may be intermediate between these conditions because the saltwater front may have passed the location, but some ion exchange sites may have remained available.

The concentrations of chloride and bromide generally plot near the theoretical freshwater/seawater mixing line because these ions are conservative indicators of freshwater and seawater mixing, and generally are not adsorbed by, or interact with, aquifer materials. As expected, the chloride and bromide concentrations in samples collected during the study all plot close to the theoretical freshwater/seawater mixing line (fig. 20). Concentrations of boron, magnesium, potassium, sodium, and sulfate were frequently depleted (figs. 21–25), whereas the concentrations of calcium were frequently enriched (fig. 26), relative to the theoretical freshwater/seawater mixing line. The extent of depletion and enrichment varied and may indicate either the arrival of the saltwater interface (sites highlighted in yellow) or the occurrence of prior intrusion (sites highlighted in blue). Unlike the evaluation of the $Ca/(HCO_3 + SO_4)$ ratios, which was based on ratios greater than or less than 1, comparisons of ion concentrations to the theoretical freshwater/seawater mixing line are somewhat more subjective.

Many of the wells from which samples had $Ca/(HCO_3 + SO_4)$ ratios greater than 1 also were among the wells most depleted in boron, magnesium, potassium, sodium, and sulfate and most enriched in calcium relative to the theoretical freshwater/seawater mixing lines. This group of wells includes G–3615, G–3698, G–3699, G–3704, and G–3855. Barium was enriched relative to the theoretical freshwater/seawater mixing line (fig. 27) in four wells (G–3699, G–3615, G–3704, and G–3855) that were more depleted in boron, sodium, sulfate, magnesium, and potassium and more enriched in calcium than most of the other wells. Similar patterns of major ion concentrations were found in well G–1264 (with the exception of boron, which was not measured), and well G–3705 (with the exception of sulfate). The described enrichments and depletions relative to the theoretical freshwater/seawater mixing lines indicate ion exchanges that are typical of the arrival of saltwater intrusion. Concentrations of major ions in wells FKS4, FKS8, G–939, G–3600, G–3601, G–3602, G–3604, and G–3605 were less depleted and generally plotted closer to the theoretical freshwater/seawater mixing lines than the concentrations of major ions in other wells, indicating that these wells are in areas where the aquifer materials are closer to equilibrium with seawater. Generally this is because the saltwater front has moved well inland of the locations of these wells, but in some areas the situation is more complex (see, for example, the Miami and Tamiami Canals section of this report).

Chloride to bromide (Cl/Br) mass ratios can be used to differentiate between rainfall (ratios of 50 to 150), shallow groundwater (ratios of 100 to 200), and sewage effluent (ratios of 300 to 800) (Davis and others, 1998). Seawater has a Cl/Br mass ratio of about 288 to 297 (Turekian, 1976; Richter and Kreitler, 1993, p. 28; Vengosh and Pankratov, 1998; Jones and others, 1999, p. 70). The Cl/Br mass ratio of most of the groundwater-well samples ranged from 178 to 305, which is close to the typical range for freshwater saturated and saltwater intruded groundwater. The Cl/Br mass ratio of most of the canal water samples ranged from 235 to 304; likely a

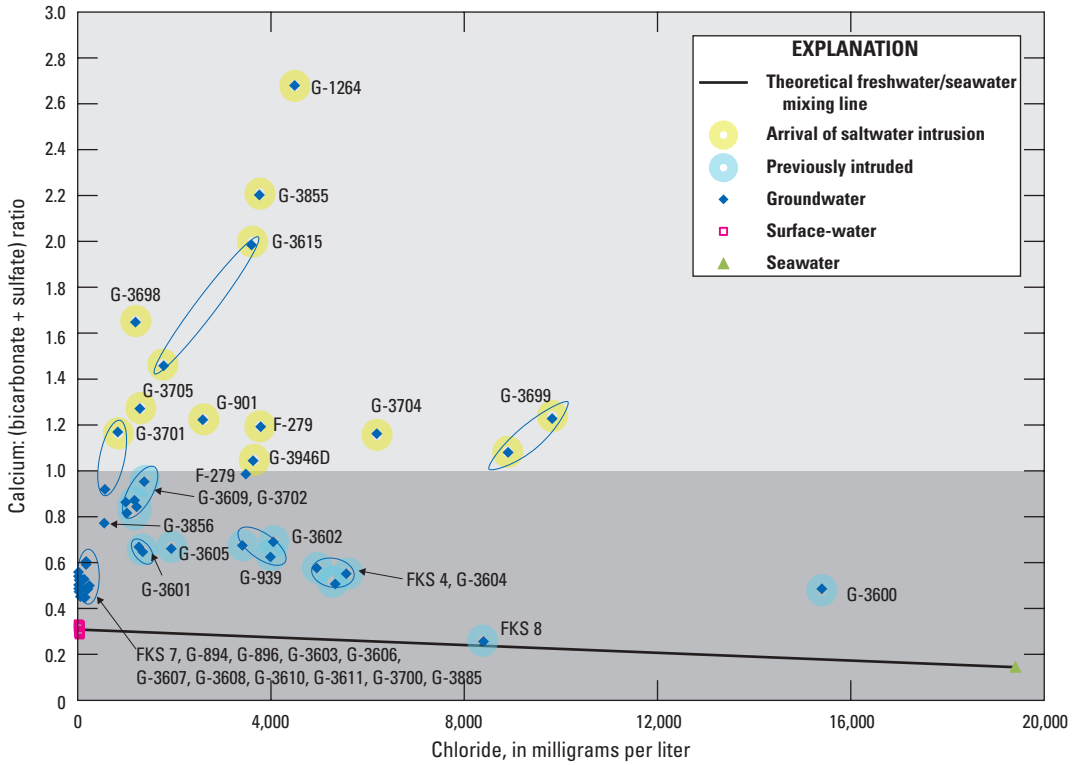

Figure 19. Calcium to (bicarbonate + sulfate) ratio and the chloride concentration in groundwater and surface-water samples collected during 2009–2010, Miami-Dade County, Florida. The composition of seawater used for this figure was described by Turekian (1976).

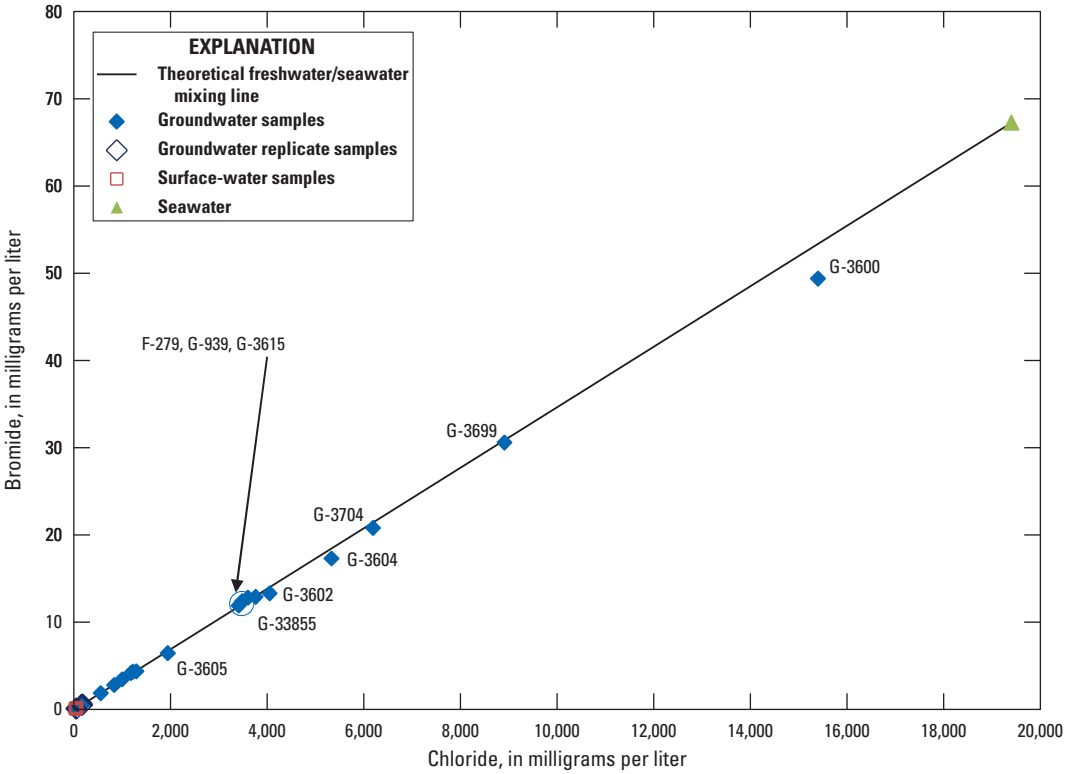

Figure 20. Bromide and chloride concentrations in groundwater and surface-water samples collected during 2009–2010, Miami-Dade County, Florida.

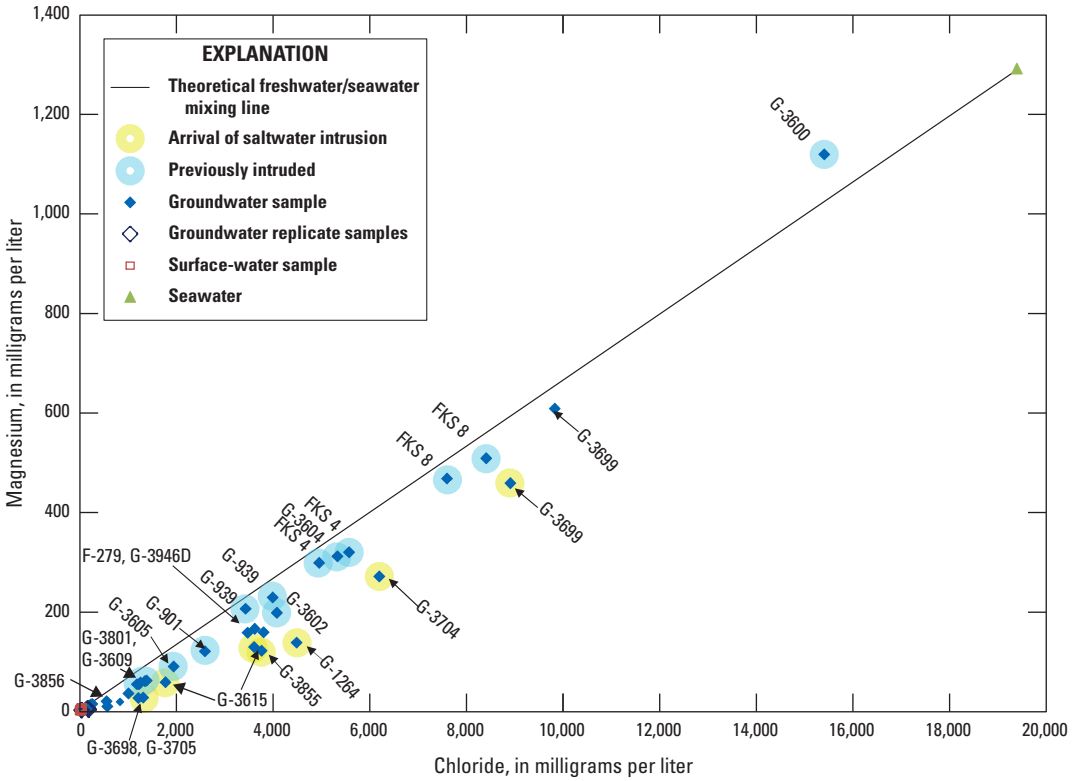

Figure 21. Magnesium and chloride concentrations in groundwater and surface-water samples collected during 2009–2010, Miami-Dade County, Florida.

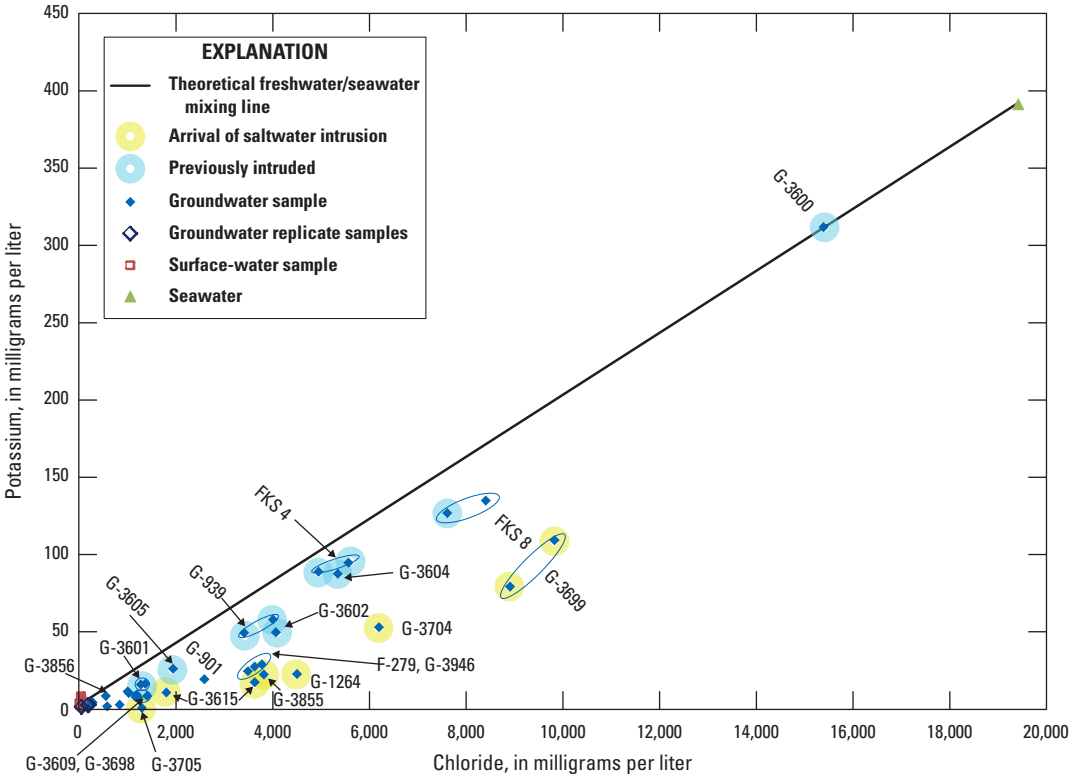

Figure 22. Potassium and chloride concentrations in groundwater and surface-water samples collected during 2009–2010, Miami-Dade County, Florida.

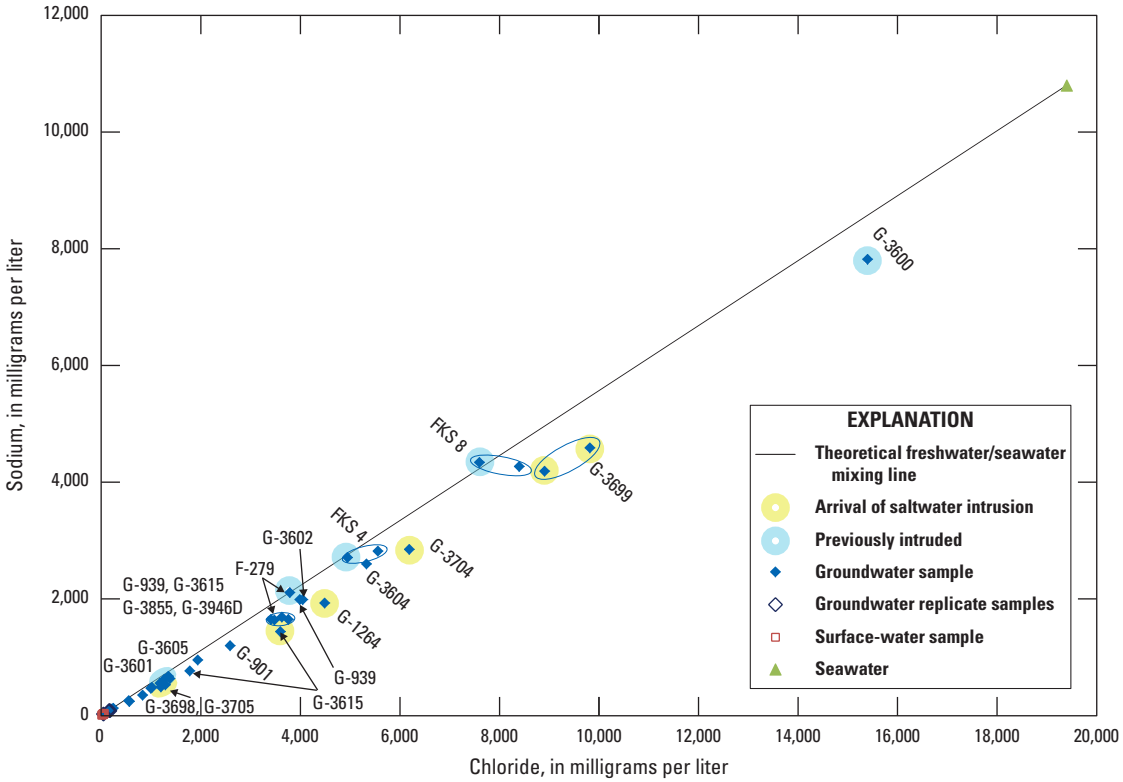

Figure 23. Sodium and chloride concentrations in groundwater and surface-water samples collected during 2009–2010, Miami-Dade County, Florida.

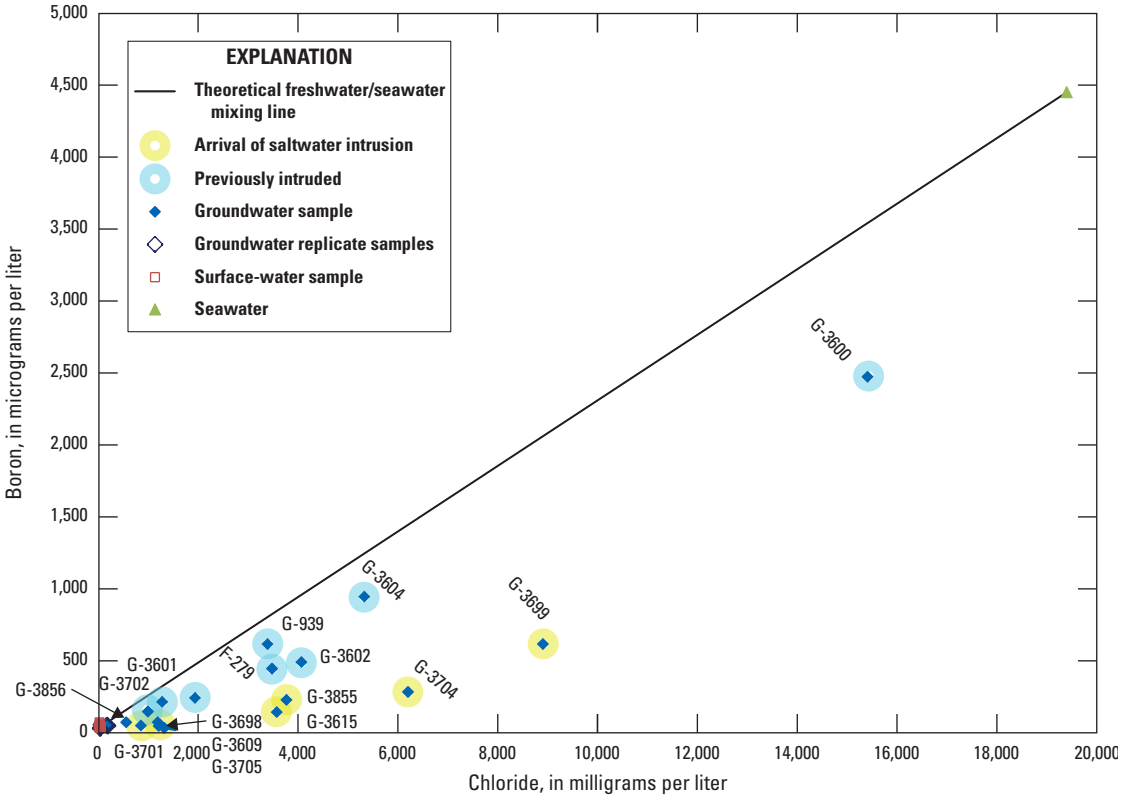

Figure 24. Boron and chloride concentrations in groundwater and surface-water samples collected during 2009–2010, Miami-Dade County, Florida.

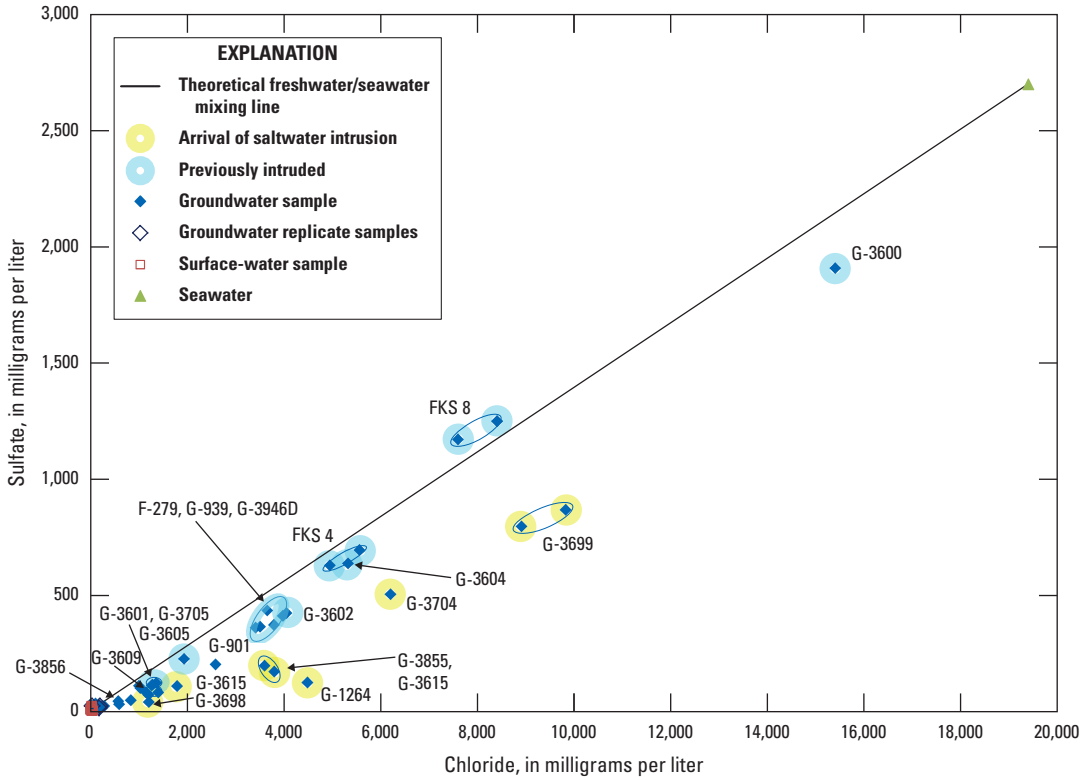

Figure 25. Sulfate and chloride concentrations in groundwater and surface-water samples collected during 2009–2010, Miami-Dade County, Florida.

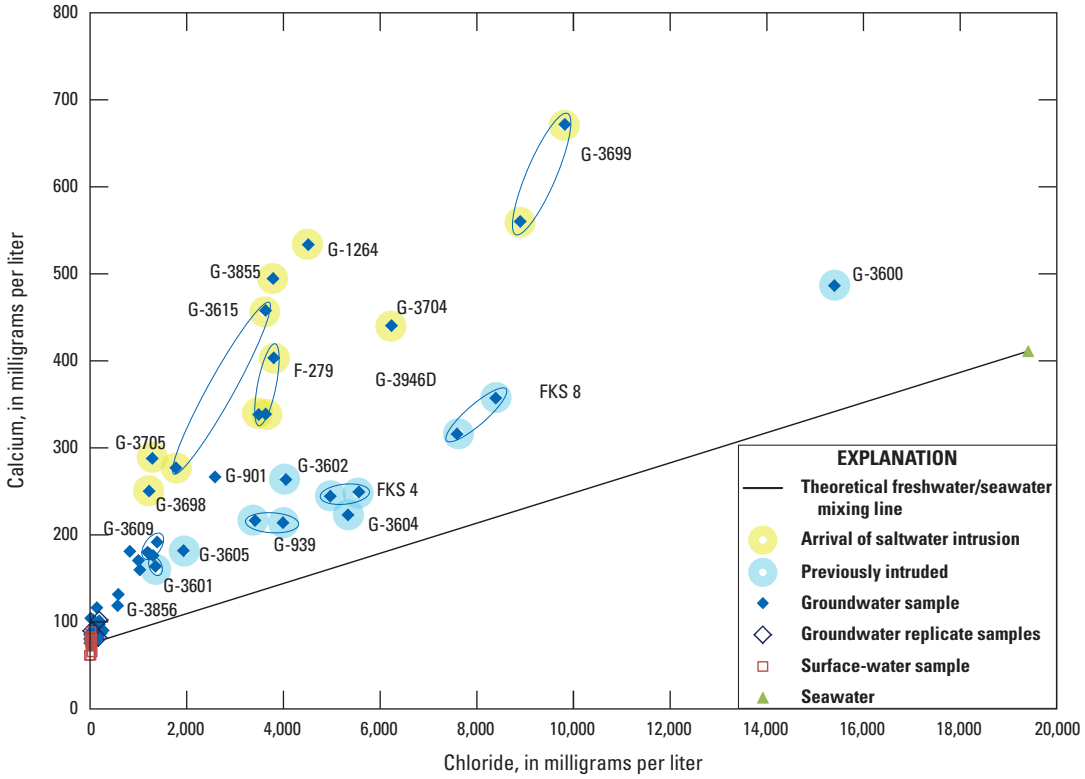

Figure 26. Calcium and chloride concentrations in groundwater and surface-water samples collected during 2009–2010, Miami-Dade County, Florida.

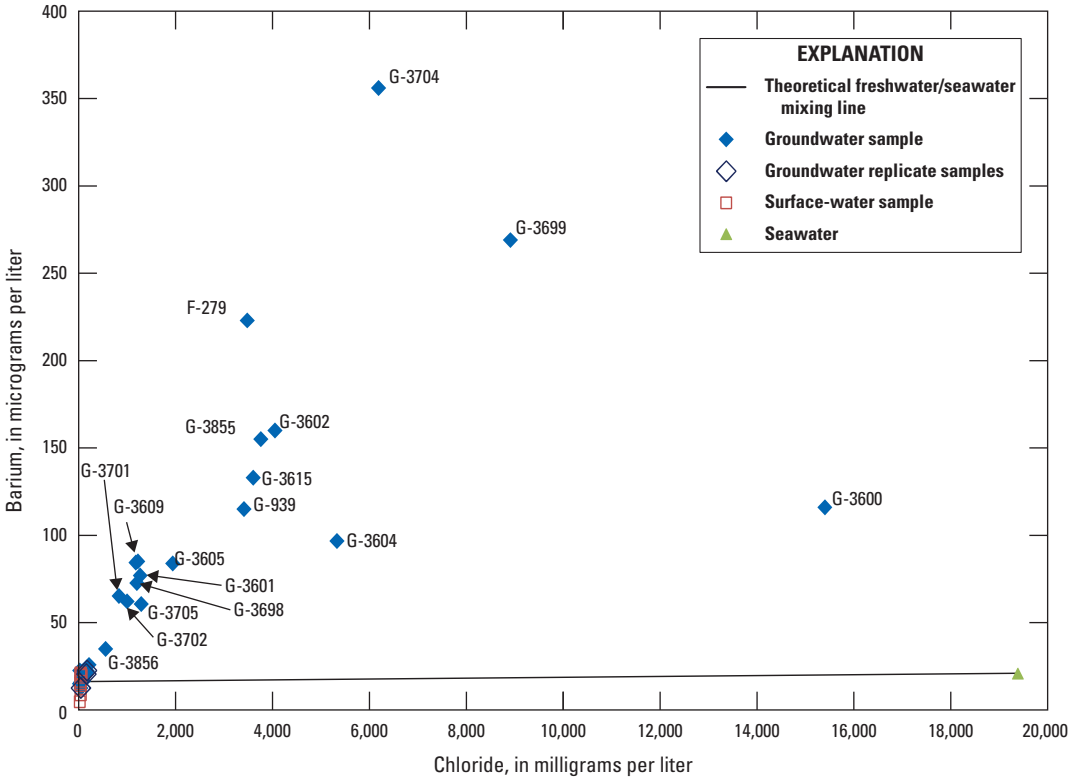

Figure 27. Barium and chloride concentrations in samples.

result of the mixing of rainfall runoff with inflow from shallow groundwater, as well as mixing of seawater in some instances. The Cl/Br mass ratios in samples from wells F–45, G3600, G–3603, G–3604, G–3607, G–3608, G–3610, G–3611 and sites Canal C100A at SW 72 Ave, Canal at G–3698, C2 Canal at G–3608, C2 Canal 150 Ft Upstream of S–22, and C5 Canal at NW 32 Ct ranged from 306 to 682, which is within the range of sewage effluent (appendix 2, table 2–1).

A triangular-shaped theoretical freshwater/seawater mixing area, within which most of the groundwater sample results occur, is defined by the maximum and minimum silica and chloride concentrations in surface water, and the concentration of these same ions in seawater (fig. 28). Silica concentrations in surface-water samples ranged from a low of 3.32 mg/L in the Card Sound Road Canal 7.7 mi Upstream from Mouth to a high of 8.81 mg/L at C9 Canal near NE 17 Ave. Silica was most enriched in groundwater samples from well G–3701 (fig. 28), which is most likely open to the Pinecrest Sand Member of the Tamiami Formation rather than to the Biscayne aquifer. The Pinecrest Sand Member typically is characterized as a fine quartz sand that has low (0.1 to 10 feet per day [ft/d]) hydraulic conductivity (Reese and Cunningham, 2000). The quartz in these sediments may have enriched the sampled water in silica relative to the water that flowed through the carbonate Biscayne aquifer. Wells G–3600, G–3601, G–3602, and G–3603, which also were enriched in silica, are the four deepest wells sampled. The lithologic descriptions from these four wells are not sufficiently detailed for stratigraphic analysis, but given their depths and locations, these wells also may be screened in the Tamiami Formation. The elevated silica concentration in samples from these four wells may have resulted from relatively long residence times of water in the quartz-sand-rich sediments of the Tamiami Formation.

Strontium Isotope Age Dating

Strontium isotopes were used to evaluate the origin of saltwater in the surficial and intermediate aquifer systems in southwest Florida (Schmerge, 2001). Strontium isotope age dating uses the relation of age and the marine strontium-87 to strontium-86 ($^{87}Sr/^{86}Sr$) ratio (Howarth and McArthur, 1997; McArthur and others, 2012). Unlike $^{3}H/^{3}He$ and SF_6 age dating, which provide estimates of the age of the water, $^{87}Sr/^{86}Sr$ ages reflect the ages of the rock with which this water has equilibrated. Most of the carbonate rocks in south Florida are marine in origin and the $^{87}Sr/^{86}Sr$ ratios in the minerals of the rock correspond to those of seawater during deposition. The $^{87}Sr/^{86}Sr$ ratios of groundwater samples, in turn, reflect those of the strata with which this water has equilibrated. This understanding can aid in determining whether the sampled water emanates from the same strata from which it was sampled, or from deeper or shallower strata. Although water with different $^{87}Sr/^{86}Sr$ ages are mixed within an aquifer, water samples that indicate older or younger $^{87}Sr/^{86}Sr$ ages than the ages of the aquifer materials may indicate upward or downward leakage of water from other aquifers (Schmerge, 2001).

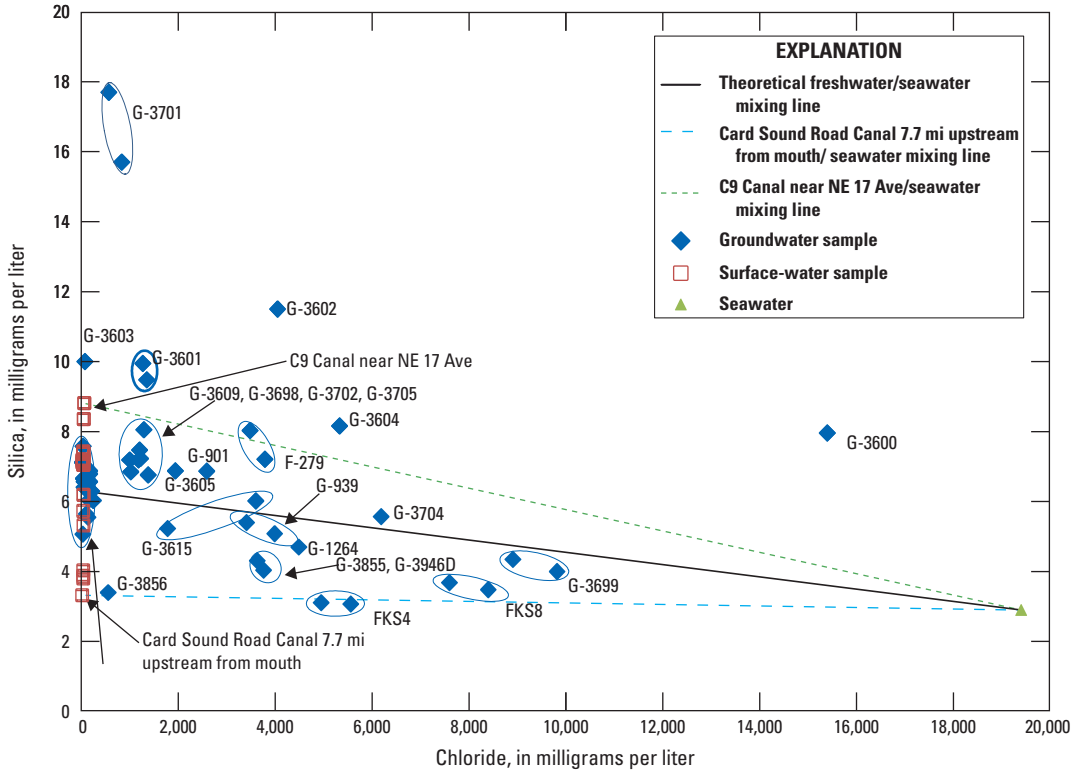

Figure 28. Silica and chloride concentrations in samples.

The $^{87}Sr/^{86}Sr$ ratios of the 14 samples collected from groundwater wells during the current study range from 0.70909 to 0.70917 (± 0.00002) (table 4), which correspond to interpolated mean $^{87}Sr/^{86}Sr$ ages of 1.87 to 0.19 million years (Ma) before present, respectively (table 4, McArthur and others, 2012). Given the precision of $^{87}Sr/^{86}Sr$ ratio analyses, the potential range in mean age is 2.51 to 0 Ma. This age range corresponds to the Pleistocene and Holocene Epochs (Walker and others, 2012) during which the strata of the Biscayne aquifer, including the Fort Thompson Formation, Key Largo Formation, Lake Flirt Marl, Miami Limestone, and Pamlico Sand, were deposited (fig. 6). The $^{87}Sr/^{86}Sr$ ages, therefore do not indicate any flow of deeper, older water into the Biscayne aquifer at these well locations.

Although the $^{87}Sr/^{86}Sr$ ages of all samples correspond to the Holocene and Plestocene Epochs, wells G–3601 and G–3701 are likely open to the upper most part of the Pinecrest Sand Member of the Tamiami Formation deposited during the Pliocene Epoch. The Pinecrest Sand Member is considered to be part of the Biscayne aquifer at the location of well G–3601. Well G–3601 is 57.9 m deep and the depth of the top of the Pinecrest Sand Member is estimated to be about 55 m in this area (Fish and Stewart, 1991). The Pinecrest Sand Member underlies the Biscayne aquifer at the location of well G–3701. Well G–3701 is 25.3 m deep, and the depth of the base of the Biscayne aquifer at this location is estimated to be 20.5 m (see the Relict Seawater from Previous Sea-Level High Stands section of this report).

The $^{87}Sr/^{86}Sr$ ages of water samples from wells G–3601 and G–3701 (1.87 and 1.66 Ma, respectively) do not coincide with the age of the Tamiami Formation; however, they are older than the ages of any other groundwater samples (table 4). These wells likely only penetrate a few meters into the Pinecrest Sand Member. There may be mixing of water between the geologic formation, therefore, which could explain the $^{87}Sr/^{86}Sr$ ages of the water samples from G–3601 and G–3701.

Oxygen and Hydrogen Stable Isotopes

The concentrations of stable isotopes of hydrogen and oxygen in water are affected by fractionation during evaporation and precipitation. Evaluations of the likely sources from which water has originated can be aided by determination of the amount of fractionation that has occurred in water samples. The oxygen and hydrogen stable isotope composition of precipitation follows a well-defined linear trend known as the global meteoric water line (GMWL) (Craig, 1961). Local evaporation causes systematic enrichment of the heavier oxygen and hydrogen stable isotopes that results in divergence of the stable isotopic composition of local surface water from the GMWL. The line showing this divergence is called the local evaporation line (LEL). The isotopic ratios of hydrogen ($^{2}H/^{1}H$) and oxygen ($^{18}O/^{16}O$) are typically expressed as delta deuterium ($\delta^{2}H$) and delta oxygen

Table 4. Determination of the strontium-87 to strontium-86 ratio in water samples collected during 2009, in Miami-Dade County, Florida.

[µg/L, micrograms per liter; –, no data]

Local identifier	USGS station number	Date	Strontium-87 to strontium-86 ratio	Strontium-87 to strontium-86 ratio rerun*	Strontium concentration, in µg/L	Interpolated mean strontium-87 to strontium-86 age in millions of years
C1 CANAL AT G -3702	253334080213600	8/6/2009	0.70910	0.70910	824	1.66
C2 CANAL 150 FT UPSTREAM OF S–22	254012080170200	8/3/2009	0.70911	–	603	1.47
C2 CANAL AT G–3608	254108080170600	7/28/2009	0.70909	–	607	1.87
C8 CANAL AT G–3601	255358080114100	8/17/2009	0.70914	–	588	0.95
F–279	255315080111501	8/2/2009	0.70914	–	3,110	0.95
FLORIDA CITY CANAL AT G–3699	252652080244300	8/20/2009	0.70919	–	807	0.00
G–894	255350080105801	8/14/2009	0.70914	–	599	0.95
G–896	254107080165201	8/4/2009	0.70912	–	801	1.29
G–939	253652080183701	8/27/2009	0.70911	–	2,940	1.47
G–3601	255358080114101	8/17/2009	0.70909	–	1,710	1.87
G–3607	254156080172101	7/17/2009	0.70916	–	978	0.47
G–3608	254108080170601	7/27/2009	0.70911	–	814	1.47
G–3609	254005080171601	7/30/2009	0.70913	–	2,450	1.12
G–3611	253710080184701	8/12/2009	0.70917	0.70917	1,130	0.19
G–3699	252652080244301	8/20/2009	0.70916	0.70915	7,320	0.47
G–3701	253214080224601	8/7/2009	0.70910	–	4,040	1.66
G–3702	253334080213601	8/6/2009	0.70916	0.70916	2,410	0.47
G–3855	252650080252701	8/18/2009	0.70913	–	5,880	1.12
G–3856	252650080252401	8/18/2009	0.70914	0.70915	1,500	0.95

* Selected samples were rerun as a quality assurance check.

18 ($\delta^{18}O$) in parts per thousand (per mil). Differences in the δ^2H and $\delta^{18}O$ composition in water samples can be evaluated graphically to differentiate between water of various sources (Richter and Kreitler, 1993, p. 28). Following the techniques similar to those applied by Schmerge (2001) in southwestern Florida, a linear regression of the results of 46 groundwater and surface-water samples with chloride concentrations less than 300 mg/L was used to infer an LEL that follows the relation:

$$\delta^2H = (5.43)\ \delta^{18}O+1.35,\ r^2 = 0.98, \quad (2)$$

The equation for this line is similar to other determinations of evaporation lines in Florida (Kendall and Coplen, 2001; Schmerge, 2001; Florea and others, 2010).

A local saltwater mixing line (LSWML) was estimated by performing a linear regression on groundwater samples that had a chloride concentration greater than 300 mg/L, with the exception of results from wells G–901, G–3601, and G–3856, which were outliers (fig. 29*A*). The resulting equation is

$$\delta^2H = (0.0013)x–10.97,\ r^2 = 0.90,\ n=32, \quad (3)$$

where x is the chloride concentration in milligrams per liter. Using the same set of sample results, an LSWML expressing δ^2H as a function of $\delta^{18}O$ is

$$\delta^2H = (5.89)\ \delta^{18}O+2.69,\ r^2 = 0.97,\ n=32, \quad (4)$$

The δ^2H and $\delta^{18}O$ in samples, as well as the GMWL, LEL, and LSWML, are presented in figure 29*B*. The δ^2H and chloride concentrations in samples and the LSWML are presented in figure 29*A*. The intersection of the LEL and the GMWL provides an estimate of the weighted mean isotopic composition of annual precipitation in the catchment (Gibson and others, 1993, p. 81). For this study area, the LEL intersects

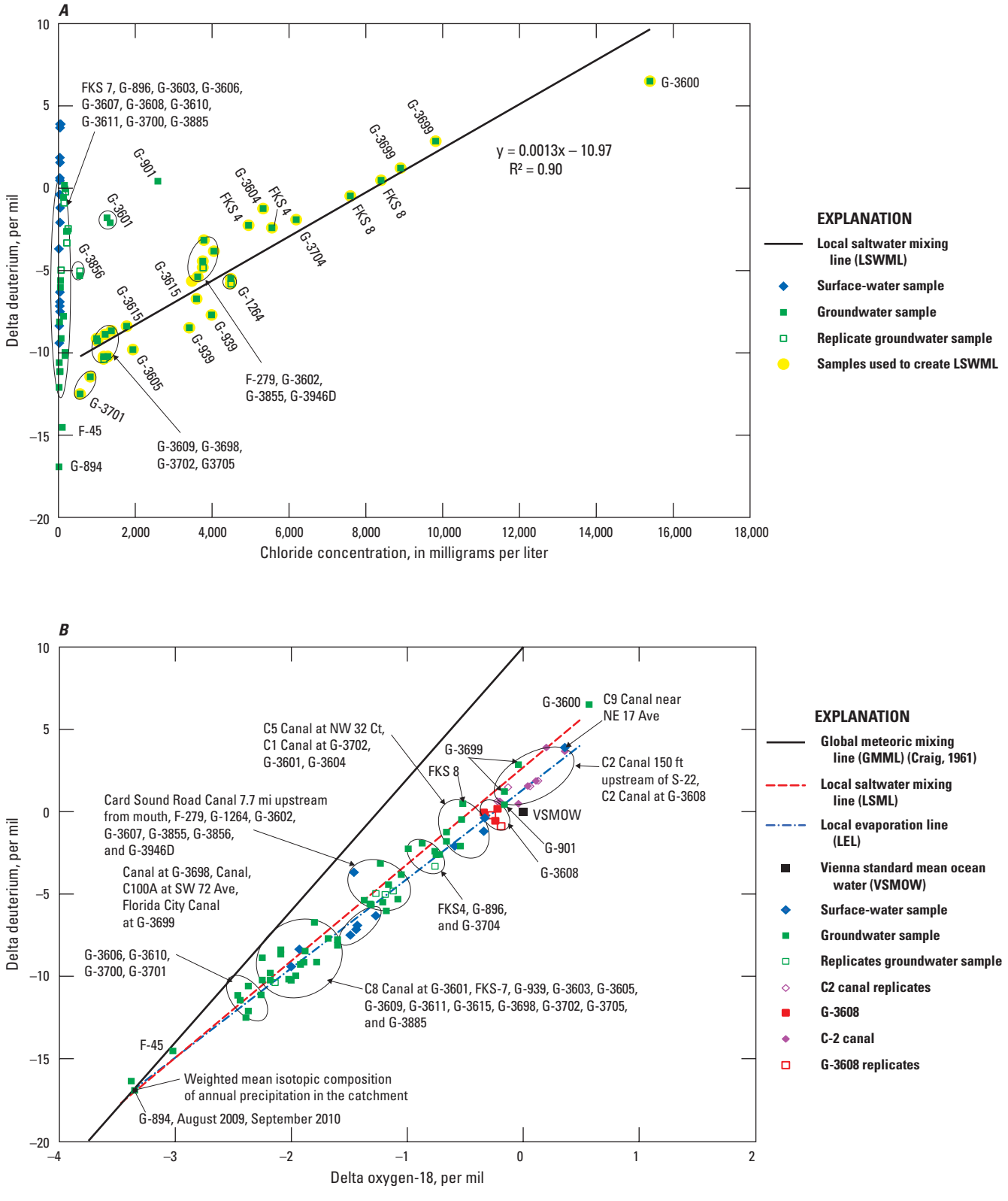

Figure 29. Relations between (*A*) chloride concentration and delta deuterium and (*B*) delta oxygen-18 and delta deuterium in groundwater and surface-water samples collected during 2009–2010, Miami-Dade County, Florida.

the GMWL at respective δ^2H and $\delta^{18}O$ values of –16.9 and –3.37, which is almost exactly where the sample results of well G–894 plot (see the Biscayne Canal section of this report).

The LSWML and LEL are similar, and it is difficult to distinguish between water that has undergone evaporation in canals or the Water Conservation Areas (WCAs) and water that has mixed with seawater. The slope of the LSWML is slightly closer to the slope of the GMWL than to the slope of the LEL. All of the samples used to determine the LSWML came from groundwater wells, but a large proportion of the samples used to create the LEL were from canals that begin at, or within, the WCAs and (or) Lake Okeechobee (fig. 1). This surface water may have undergone evaporation while it resided in the canals, WCAs, or the other surface-water features. Once the water enters an aquifer, evaporation is curtailed or ceases; therefore, the groundwater may have undergone less evaporation than the water sampled from the canals. Even so, the equations of the LEL and LSWML determined herein are similar. This similarity may be because of the considerable amount of interaction between the surface-water and groundwater systems in the study area. The δ^2H and $\delta^{18}O$ composition of some canal samples may reflect greater proportions of base flow from groundwater, whereas some well samples may reflect greater proportions of recharge to the aquifer from canals. The sample from Card Sound Road Canal 7.7 mi Upstream from Mouth (fig. 29*B*) indicates an isotopic composition that is more similar to that of many of the groundwater samples (shifted to the left of the LEL) than to the isotopic compositions of most other canal samples. The Card Sound Road Canal begins as a small ditch not far upstream from where the sample was collected, and most of the flow in the canal is sustained by base flow from groundwater.

The range of δ^2H in groundwater samples was –16.9 to 6.50 per mil, and δ^2H in surface-water samples ranged from –9.41 to 3.89 per mil. The range of $\delta^{18}O$ in groundwater samples was –3.38 to 0.57 per mil. In surface-water samples, this range was –2.00 to 0.36 per mil. The samples from well G–3600 indicated greater δ^2H and $\delta^{18}O$ values than any of the other samples (fig. 29*B*). This finding may stem from a combination of a greater extent of evaporation, and a greater proportion of seawater in the samples from this well than in other samples. Water samples from C2 Canal at G–3608 and C2 Canal 150 ft Upstream of S–22 on the Snapper Creek Canal and C9 Canal near NE 17 Ave on the Snake Creek Canal appear to have undergone more evaporation relative to the other canal samples (fig. 29*B*). Wells G–3608 and G–901, which are near the Snapper Creek Canal, also have sample results that plot close to those from the Snapper Creek Canal (fig. 29*B*). This finding may indicate that surface water within the Snapper Creek Canal has contributed a large proportion of the water sampled in these wells (see the Snapper Creek Canal section of this report).

The water samples collected from wells FKS8 and G–3699 had greater δ^2H and $\delta^{18}O$ values than did the samples from the canals adjacent to these wells, which are the Card Sound Road and the Florida City Canals, respectively. These wells also have chloride concentrations ranging between 7,600 and 9,820 mg/L. The relative enrichment in heavier isotopes of the samples from these wells therefore is likely a result of mixing with encroaching seawater (see the Saltwater Encroachment section of this report).

Tritium and Uranium Concentration

Tritium concentration in samples in the study area averaged 1.3 TU, and had a standard deviation of 0.8 TU, with the exception of the samples from Card Sound Road Canal 7.7 mi Upstream from Mouth, wells G–1264, G–3698, G–3699, G–3855, and G–3856, and in one of the two samples from well FKS4, which had tritium concentrations ranging from 4.1 to 53.3 TU and averaging 12.4 TU. These sites are all located within 8.5 km of the Turkey Point Nuclear Power Plant Cooling Canal System (CCS) (see the Turkey Point Nuclear Power Plant Cooling Canal System section of this report).

Dissolved uranium ranged from 0.852 to 8.83 micrograms per liter (µg/L) in samples from the surface-water sites C1 Canal at G–3702, Canal at G–3698, and Florida City Canal at G–3699 and in samples from wells G–3615, G–3698, G–3699, G–3700, G–3701, G–3702, G–3855, and G–3856 (appendix 2, table 2–1), which are located in a 6.1-km^2 area in southeastern Miami-Dade County near the CCS. The greatest dissolved uranium concentrations were 8.83 and 6.25 µg/L in wells G–3699 and G–3701, respectively (appendix 2, table 2–1). All samples from surface-water sites or wells located outside of the 6.1-km^2 area had dissolved uranium concentrations less than 0.656 µg/L; the average concentration was 0.181 µg/L ± 0.216 µg/L. Samples from many of the sites in the 6.1-km^2 area also indicate tritium concentrations ranging from 4.1 to 53.3 TU. The site Card Sound Road Canal 7.7 mi Upstream from Mouth and wells FKS4 and G–1264 had elevated tritium concentrations, but were not sampled for uranium.

Tritium/Helium-3 Age Dating

$^3H/^3He$ age dating can be used to date water younger than about 40 years. Generally tritium and helium are non-reactive and are unaffected by groundwater chemistry or by anthropogenic contamination. $^3H/^3He$ age dating uses the known half-life of tritium and the $^3H/^3He$ ratio measured in water samples to estimate an age of the water. Although some mixing of younger and older water may occur as water flows through the ground, the "simplest and most common transport assumption in ground-water age dating is to assume piston flow, which assumes that the constituent concentration was not altered by transport processes (such as mixing or dispersion) from the point of entry to the measurement point in the aquifer" (Rupert and Plummer, 2004, p. 9). Within the study area, however, intruding saltwater has almost certainly mixed with freshwater in the aquifer and/or canals. Saltwater from recent intrusion events may have mixed with saltwater from previous intrusion events. Therefore, although the piston-flow

ages are provided, the age likely represents a mixture of water of various ages.

After corrections were applied (appendix 10), the analytical ages of water in the study area ranged from 6 ± 0.5 to 46 ± 2.3 years (table 5). Actual ages of water are likely less precise than the analytical ages provided (table 5) because of uncertainties in the $^{3}He/^{4}He$ ratio, recharge temperature, and the amount gas fractionation. Therefore, interpreted piston-flow ages are provided (table 5) that consider these factors. Many of the wells sampled have water younger than 1970, which could be caused by saltwater intrusion events occurring after 1970 or mixing of younger freshwater with older saltwater. The interpreted piston-flow ages of water samples that had a chloride concentration of about 1,000 mg/L or greater were generally older than those samples with a chloride concentration of less than about 1,000 mg/L. The ages of water samples that had a chloride concentration of about 1,000 mg/L or greater correspond to a period during which droughts were more frequent and of longer duration (fig. 30). The relation between the ages of saltwater samples and drought periods (fig. 30) concurs with historical observations that the greatest extents of saltwater intrusion generally occurred during droughts, when fresh groundwater heads are low and saltwater may encroach along the base of the aquifer or flow inland in canals, rivers, or tidal marshes (see Relation of Urban Development to Saltwater Intrusion section of this report).

Sulfur Hexafluoride Age Dating

Sulfur hexafluoride (SF_6) can be used to date groundwater that is younger than 30 years (Busenberg and Plummer, 2000). SF_6 concentrations in 40 samples ranged from 0.33 to 136 parts per thousand total volume (pptv) (appendix 2, table 2–4). Ages could not be determined for most of these samples, however, because the samples contained greater amounts of SF_6 than would result from equilibrium with the expected atmospheric concentration. Samples containing the highest concentrations of SF_6 generally were from surface-water monitoring sites or monitoring wells near electrical power distribution facilities. These sites include C2 Canal 150 FT Upstream of S–22, Florida City Canal at G–3699, C2 Canal at G–3608, and Canal at G–3698 and wells F–45 and G–3700 (appendix 2, table 2–4). Leakage of SF_6 from electrical power generation facilities in southeast Florida has been noted previously (U.S. Environmental Protection Agency, 2000) and may account for the excess SF_6 found in at least some of the samples.

Even where SF_6 concentrations were low enough to allow an estimation of age, the SF_6 ages typically disagreed with the $^{3}H/^{3}He$ ages (table 6). Only the near absence of SF_6 in some samples indicates that water at these locations may be older than elsewhere. Samples from wells G–3600, G–3601, G–3603, G–3609, and G–3701 had the least amounts of SF_6 (0.33 to 1.21 pptv; appendix 2, table 2–4). Samples from wells G–3600, G–3601, and G–3701 also had too little tritium for $^{3}H/^{3}He$ age dating.

Estimates of Recharge Temperature Based on Dissolved Gases

Recharge temperature is the temperature of groundwater after it is isolated from the soil atmosphere (Plummer and others, 2003). Recharge temperatures are determined using the assumptions that the gases dissolved in the groundwater originate from air-water solubility as described by Henry's Law and that excess air is introduced into the aquifer during recharge from air-bubble entrainment as a result of a rise in the water table (Hinkle and others, 2010, Aeschbach-Hertig and others, 1999, 2000). Dissolved nitrogen (N_2) and argon (Ar) concentrations are used to evaluate recharge temperatures (Aeschbach-Hertig and others, 1999; 2000; Busenberg and others, 1993; Heaton, 1981; and Heaton and Vogel, 1981). The accuracy of this method is typically ± 0.5 °C using laboratory standards (Plummer and others, 2003). Uncertainty in the nitrogen/argon (N_2/Ar) recharge temperatures can result from uncertainties in recharge elevation, presence of excess N_2 from denitrification of NO_3^- (degassing), and the presence of excess air in samples. In Miami-Dade County near the coast, where samples were collected, the water table generally varies seasonally and geographically by only a few feet (Lietz and others, 2002), so uncertainty in recharge elevation is negligible. Denitrification can affect the determination of recharge temperatures and excess air in samples. The amount of excess N_2 from denitrification was estimated from the solubility of Ar using an iterative procedure.

The dissolved gas concentrations of argon, carbon dioxide, methane, nitrogen, and oxygen, were determined for 23 samples from selected sites (appendix 2, table 2–2; U.S. Geological Survey, 2011i) to determine the recharge temperatures of individual samples. Sample results indicate a relation between, N_2/Ar recharge temperature, seasonal changes in air temperature and water level, and the salinity of samples (figs. 31*A* and 31*B*, table 7). The recharge temperatures of most of the samples with chloride concentrations greater than or equal to about 1,000 mg/L (samples from the seaward side of the saltwater interface) indicated a range in the N_2/Ar recharge temperature of 23.8 – 25.4 °C, which is similar to the air temperatures that occur when aquifer water levels are at minimum levels, and the potential for saltwater intrusion is greatest (The Weather Channel, 2013; figs. 31*A* and 31*B*, table 7).

The recharge temperatures of samples with chloride concentrations less than about 1,000 mg/L (the freshwater side of the saltwater interface) generally indicated warmer recharge temperatures and, with one exception, had recharge temperatures between 25.5 – 26.8 °C. This range of temperatures corresponds to average air temperatures in the second half of May when rainfall and water levels in the aquifer typically begin to increase (figs. 31*A* and 31*B*). The samples from wells G–3609 and G–3855 were exceptions to these general relations.

Water samples that have N_2/Ar recharge temperatures indicative of the end of the dry season when aquifer water levels are low, also have interpreted $^{3}H/^{3}He$ piston-flow ages that correspond to a period of frequent droughts (see the

Table 5. Results of tritium/helium-3 age dating of water samples collected during 2009–2010 in Miami-Dade County, Florida.

[?, could not be determined; σ, standard deviation; TU, tritium unit; %, percent; <, less than; ~, about; –, no data]

Local identifier	USGS station number	Sample date	Tritium		Δ^4He	ΔNe	Δ^4He/ΔNe Ratio[1]	Terrigenic He[2]	Analytical age, uncorrected for terrignic helium[3]		Analytical age, corrected for terrignic helium		Interpreted piston-flow age[4]	Comments
			TU	±1σ (TU)				%	years	±1σ (years)	years	±1σ (years)	year	
C2 CANAL AT G–3608	254108080170600	7/28/2009	2.08	0.13	2.6	4.8	0.5	–2.95	1	0.1	–	–	–	Result not used because of gas fractionation and direct exposure to air.
F–279	255315080111501	8/21/2009	0.67	0.12	31.5	7.5	4.2	17.39	–	–	45	3.0	< 1970	Result corrected for terrigenic helium.
G–3600	255626080093201	8/12/2010	0.25	0.04	13.6	–7.7	–1.8	19.87	–	–	–	–	–	Negative ΔNe indicates gas fractionation, age is questionable.
G–3601	255358080114101	8/17/2009	–0.05	0.1	32.3	9.7	3.3	15.89	–	–	–	–	–	Too little tritium to age date.
G–3607	254156080172101	7/17/2009	1.68	0.09	19.5	17.4	1.1	–0.64	16	0.6	–	–	~ 1993	Result without terrigenic helium correction.
G–3608	254108080170601	7/27/2009	1.66	0.1	5.8	8.6	0.7	–3.95	12	0.5	–	–	~ 1997	Result without terrigenic helium correction. Possible gas fractionation.
G–3609	254005080171601	7/30/2009	0.74	0.08	43.6	19.1	2.3	14.97	–	–	34	1.8	1970s	Result corrected for terrigenic helium, age uncertain because of very low tritium.
G–3611	253710080184701	8/12/2009	1.55	0.11	26.1	24.3	1.1	–1.68	29	1.1	–	–	late 1970s early 1980s	Result without terrigenic helium correction, age uncertain because of very low tritium.
G–3698	252814080244101	7/20/2010	5.73	0.11	34.6	9.2	3.8	17.73	–	–	24	0.3	~ 1986	Result corrected for terrigenic helium.
G–3699	252652080244301	8/20/2009	45.8	0.91	24.3	4.6	5.3	15.3	–	–	28	0.3	~ 1981	Result corrected for terrigenic helium.
G–3701	253214080224601	8/7/2009	0	0.11	33.1	18	1.8	9.17	–	–	–	–	–	Too little tritium to age date.
G–3702	253334080213601	8/6/2009	0.74	0.1	31.7	20.4	1.6	6.02	–	–	46	2.3	< 1970	Result corrected for terrigenic helium.
G–3704	254822080125501	7/21/2010	0.54	0.04	71.7	11.4	6.3	33.85	–	–	29	1.2	late 1970s early 1980s	Result corrected for terrigenic helium age uncertain because of low very low tritium.
G–3705	255625080094901	8/12/2010	1.49	0.05	15.4	4.2	3.7	9.13	–	–	30	0.5	~ 1980	Result corrected for terrigenic helium.
G–3855 (Trigger)	252650080252701	8/18/2009	17.8	0.36	20.3	8.1	2.5	9.01	–	–	26	0.3	~ 1983	Result corrected for terrigenic helium.
G–3856 (Sentinel)	252650080252401	8/18/2009	4.59	0.13	5.4	4.9	1.1	-0.26	17	0.3	–	–	~ 1992	Result without terrigenic helium correction.
G–894	255350080105801	8/14/2009	1.43	0.15	10	13	0.8	–4.62	6	0.5	–	–	~ 2003	Result without terrigenic helium correction. Possible gas fractionation.
G–896	254107080165201	8/4/2009	1.68	0.06	9.8	13.4	0.7	-5.24	11	0.3	–	–	~1998	Result without terrigenic helium correction. Possible gas fractionation.
G–939	253652080183701	8/27/2009	1.08	0.12	18.6	10.5	1.8	5.47	–	–	26	1.7	~1983	Result corrected for terrigenic helium.z

[1]Samples indicating a Δ4He/ΔNe ratio of less than 1 may have been affected by gas fractionation.

[2]Corrections for terrigenic helium were applied to samples that indicated that terrigenic helium was greater than 5 percent.

[3]Analytical age is based on precision of analysis but this precision does not consider other factors such as uncertainties in the recharge temperature, 3He/4He ratio, and gas fractionation.

[4]Interpreted piston-flow age considers some uncertainties in the analysis, but does not consider the mixing which likely occurred as saltwater intruded the aquifer.

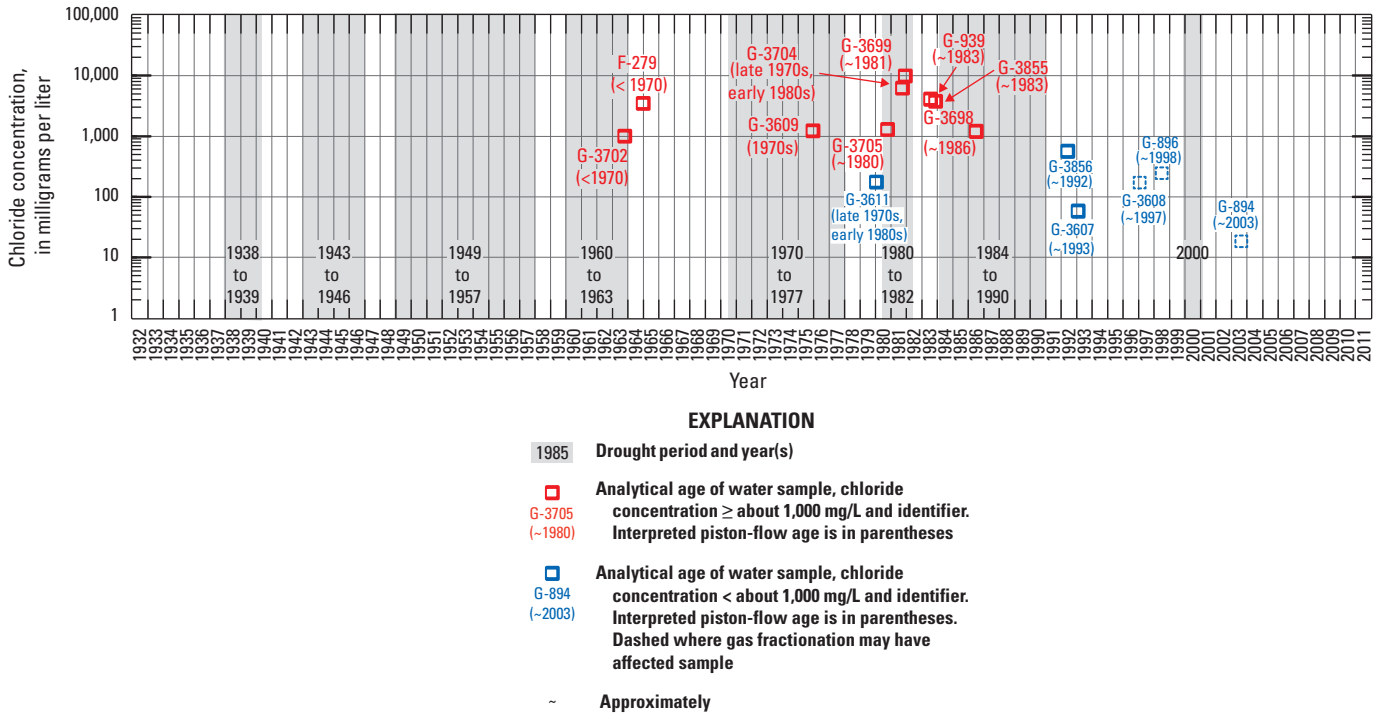

EXPLANATION

1985 — Drought period and year(s)

G-3705 (~1980) — Analytical age of water sample, chloride concentration ≥ about 1,000 mg/L and identifier. Interpreted piston-flow age is in parentheses

G-894 (~2003) — Analytical age of water sample, chloride concentration < about 1,000 mg/L and identifier. Interpreted piston-flow age is in parentheses. Dashed where gas fractionation may have affected sample

~ — Approximately

Figure 30. $^{3}H/^{3}He$ interpreted piston-flow ages of water samples collected during 2009–2010 in the Miami-Dade County area and dates of documented droughts in south Florida. [mg/L, milligrams per liter]

Tritium/Helium-3 Age Dating section of this report), whereas those that have warmer recharge temperatures generally have younger ages that correspond to a period during which droughts were infrequent (fig. 30). Previous research has shown that saltwater usually intrudes when water levels in the aquifer and in canals are at minimum levels, particularly during droughts (Cross and Love, 1942, p. 501). Minimum water levels are usually reached near the end of the dry season from April to early May, so the observed relation between recharge temperatures, water levels in the aquifer, and salinity of samples is not surprising. This relation assumes piston flow, however, which may not be the best assumption since saltwater and freshwater likely mixed in the aquifer.

Sources of Saltwater in the Biscayne Aquifer

The Biscayne aquifer has several potential sources of saltwater or pathways through which saltwater can intrude. It is important to differentiate between these sources or pathways because if they are misconstrued, the corrective measures implemented to prevent saltwater intrusion in affected areas could fail to address the actual causes. Geochemistry, TSEMIL datasets, TEM soundings, long-term chloride concentration data, and the 2001 HEM survey were used to identify the probable sources and ages of saltwater in the aquifer at various locations within the study area.

Relict Seawater from Previous Sea-Level High Stands

Results of this study indicate that saltwater sampled in the Biscayne aquifer in eastern and southern Miami-Dade County is not relict seawater from previous sea-level high stands. Most of the interpreted piston-flow ages indicate that the water sampled was too young to be considered relict seawater. Recent changes in the bulk conductivity of EMI logs and the chloride concentrations in samples collected from these wells indicate that the water in these wells is probably not relict seawater. The chloride concentrations in water sampled from these wells has varied by between 325 mg/L and 2,732 mg/L during the few decades that the wells have been monitored. Changes in salinity occurring during such short periods of time indicate that the transmissivity of the aquifer at these locations is likely sufficient to have allowed freshwater to replace any relict saltwater during the last Pleistocene low stand.

The changes in chloride and bulk resistivity at monitoring wells G–3601 and G–3701, open to the Pinecrest Sand Member of the Tamiami Formation, are likely too large to be due to relict seawater, even though the transmissivity of this geologic unit is very low relative to transmissivities of most of the geologic units in the Biscayne aquifer. The chloride concentration in well G–3601 (fig. 32*B*) increased from 660 to 1,400 mg/L during 1999 to 2011. The bulk conductivity of EMI logs from well G–3601 (figs. 32*A* and 32*B*) gradually increased from about 42 to 87 mS/m during 1996 to

Table 6. Differences between ages determined using SF_6 and tritium/helium-3 age dating for samples collected in Miami-Dade County, Florida, during 2009–2010.

[/, denotes ratio; C, contaminated with excess SF_6; --, no data]

Local identifier	USGS station number	Sample date	Average piston-flow model SF_6 recharge age, in years [1]	Analytical tritium/ helium-3 piston flow age, in years[2]	Difference between analytical tritium/ helium-3 age and SF_6 age, in years	Comments
C2 CANAL AT G–3608	254108080170600	7/28/2009	C	1	--	Tritium/helium-3 age not used because of gas fractionation and exposure to air
F–279	255315080111501	8/21/2009	23.6	45	21	--
G–3600	255626080093201	8/12/2010	27.6	--	--	Tritium/helium age likely affected by gas fractionation
G–3601	255358080114101	8/17/2009	36.4	--	--	Tritium content too low for tritium/ helium-3 age dating
G–3607	254156080172101	7/17/2009	C	16	--	--
G–3608	254108080170601	7/27/2009	C	12	--	--
G–3609	254005080171601	7/30/2009	29.8	34	4	--
G–3611	253710080184701	8/12/2009	14.9	29	15	--
G–3698	252814080244101	7/20/2010	C	24	--	--
G–3699	252652080244301	8/20/2009	C	28	--	--
G–3701	253214080224601	8/7/2009	32.6	--	--	Tritium content too low for tritium/ helium-3 age dating
G–3702	253334080213601	8/6/2009	4.10	46	42	--
G–3704	254822080125501	7/12/2010	24.3	29	5	--
G–3705	255625080094901	8/12/2010	23.1	30	7	--
G–3855	252650080252701	8/18/2009	2.90	26	23	--
G–3856	252650080252401	8/18/2009	C	17	--	--
G–894	255350080105801	8/14/2009	5.90	6	0	--
G–896	254107080165201	8/4/2009	C	11	--	--
G–939	253652080183701	8/27/2009	17.9	26	8	--

[1]Because so many of the samples were contaminated with excess amounts of SF_6, and because the ages determined even for those samples with "dateable" amounts of SF_6 were younger in every instance than the ages determined using tritium-helium-3 age dating, the SF_6 ages are not reliable and should not be used.

[2]Analytical age is based on precision of analysis but this precision does not consider other factors such as uncertainties in the recharge temperature, $^3He/^4He$ ratio, and gas fractionation.

2011. If changes of this magnitude occurred in a little more than one decade, then the freshwater flow during the last sea-level low stand should have been sufficient to remove any relict saltwater in this part of the aquifer. EMI logs from well G–3701 show changes in bulk conductivity within the Biscayne aquifer, and below it, in the Pinecrest Sand Member (fig. 33*A* and 33*B*). The open interval of this well begins 3.3 m below the base of the Biscayne aquifer. Changes in bulk resistivity in the Biscayne aquifer at well G–3701 are much greater than those in the Pinecrest Sand Member. Nonetheless, during 2002 to 2011, the chloride concentration of water samples from well G–3701 (fig. 33*B*) varied from 355 to 680 mg/L, which is likely sufficient variation to indicate that freshwater replaced any relict saltwater within the Pinecrest Sand Member.

The SF_6 concentrations in samples from wells G–3601, G–3602, G–3604, G–3605, and G–3701 (0.33 to 5.92 pptv) (appendix 2, table 2–4) indicate that the interpreted piston-flow age of water in these wells is more recent than 1952, but potential contamination by excess SF_6 (table 6) renders the result inconclusive.

Historical Leakage of Saltwater from Canals

Some of the existing saltwater in the Biscayne aquifer near primary drainage canals such as the Biscayne, Miami, Tamiami, and Card Sound Road Canals may have been caused by the flow of saltwater inland prior to the installation of salinity control structures. Between May and July 1945,

Table 7. Average recharge temperature and chloride concentration of surface-water and groundwater samples collected in Miami-Dade County, Florida during 2009–2010.

[°C, degrees Celsius; mg/L, milligrams per liter]

Local identifier	USGS station number	Sample date	Average recharge temperature (°C)	Chloride water, filtered * (mg/L)
C2 CANAL 150 FT UPSTREAM OF S–22	254012080170200	12/15/2009	26.6	44.7
C2 CANAL AT G–3608	254108080170600	12/14/2009	26.8	42.5
C2 CANAL AT G–3608	254108080170600	7/28/2009	29.6	41.2
F–279	255315080111501	8/21/2009	25.3	3,480
G–3601	255358080114101	8/17/2009	24.7	1,270
G–3607	254156080172101	7/17/2009	25.9	58.2
G–3608	254108080170601	12/15/2009	26.5	158
G–3608	254108080170601	7/27/2009	26.5	173
G–3609	254005080171601	12/17/2009	25.4	1,220
G–3609	254005080171601	7/30/2009	26.4	1,180
G–3611	253710080184701	8/12/2009	26.6	175
G–3615	253024080231001	12/16/2009	24.6	3,600
G–3698	252814080244101	7/20/2010	24.7	1,200
G–3699	252652080244301	8/20/2009	24.5	8,910
G–3700	253027080234701	12/16/2009	25.7	23.2
G–3701	253214080224601	8/7/2009	25.9	832
G–3702	253334080213601	8/6/2009	25.1	997
G–3704	254822080125501	7/21/2010	24.8	6,190
G–3855	252650080252701	8/18/2009	26.8	3,760
G–3856	252650080252401	8/18/2009	25.7	553
G–894	255350080105801	8/14/2009	25.8	18.0
G–896	254107080165201	8/4/2009	25.5	211
G–939	253652080183701	8/27/2009	23.8	3,410

* Samples with a chloride concentration of about 1,000 mg/L or greater are highlighted in pink.

saltwater with chloride concentrations ranging from 1,100 to 26,000 ppm was sampled at distances ranging from 4.7 to 20 km inland in most of the primary canals in Miami-Dade County (Parker and others, 1955, p. 633 and 680). Samples from wells and geophysical measurements made near these canals in the present study indicate elevated chloride concentrations and bulk conductivities and lower than normal resistivity in these areas.

The Card Sound Road Canal and FEC Railway Borrow Ditches

Historical saltwater intrusion near the Card Sound Road Canal and Florida East Coast (FEC) railway borrow ditches likely contributed to the saltwater detected by the 2001 HEM survey (Fitterman and others, 2012). Fitterman and others (2012) identified saltwater at the base of the Biscayne aquifer, extending about 15 km inland, beneath the Card Sound Road Canal. This saltwater extends farther inland in the area between U.S. Highway 1 and the Card Sound Road Canal than it does to the west. Fitterman and others (2012) concluded that this saltwater likely leaked from the Card Sound Road Canal and FEC borrow ditches. During the drought of 1943–46 (fig. 4), saltwater with a chloride concentration of 26,000 ppm was sampled in the Card Sound Road Canal as far inland as 20.0 km (Parker and others, 1955, p. 680, fig. 188). In June or July 1945, the FEC railway borrow ditches were "strongly contaminated [with saltwater] to a distance less than 6 mi from Florida City," and it was considered possible that "ground-water contamination continued even farther inland" (Parker and others, 1955, p. 682). A 1955 map shows saltwater in the Biscayne aquifer extending about 18–19 km inland beneath the Card Sound Road Canal and the FEC railway

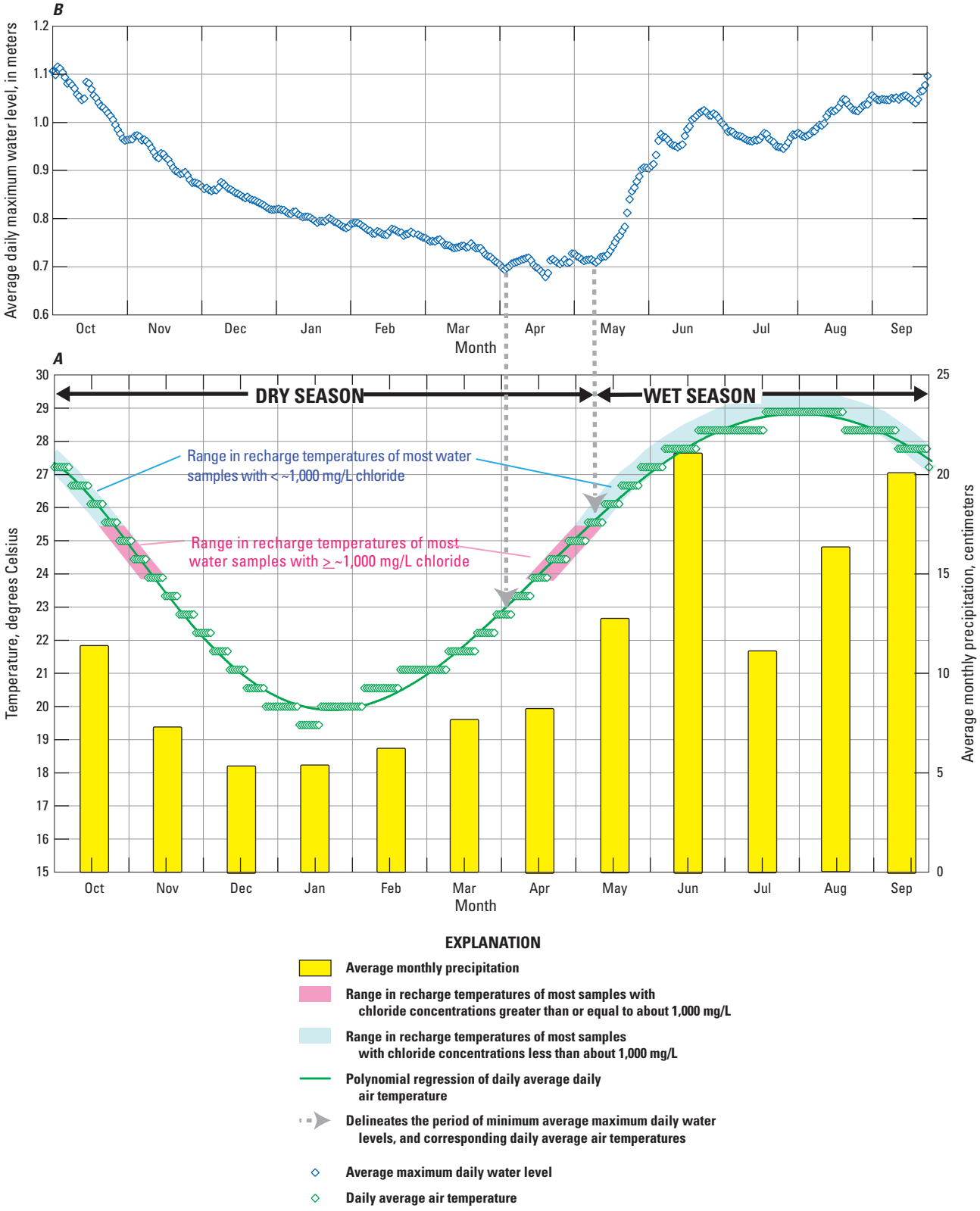

Figure 31. (*A*) Average monthly precipitation, daily average air temperature in Miami, Florida, and the range of recharge temperatures of water samples collected from the Biscayne aquifer in Miami-Dade County, Florida, and (*B*) average of daily maximum water levels in selected wells open to the Biscayne aquifer during October 1, 1974, to September 30, 2009. [<, less than; mg/L, milligrams per liter; ≥, greater than or equal to]

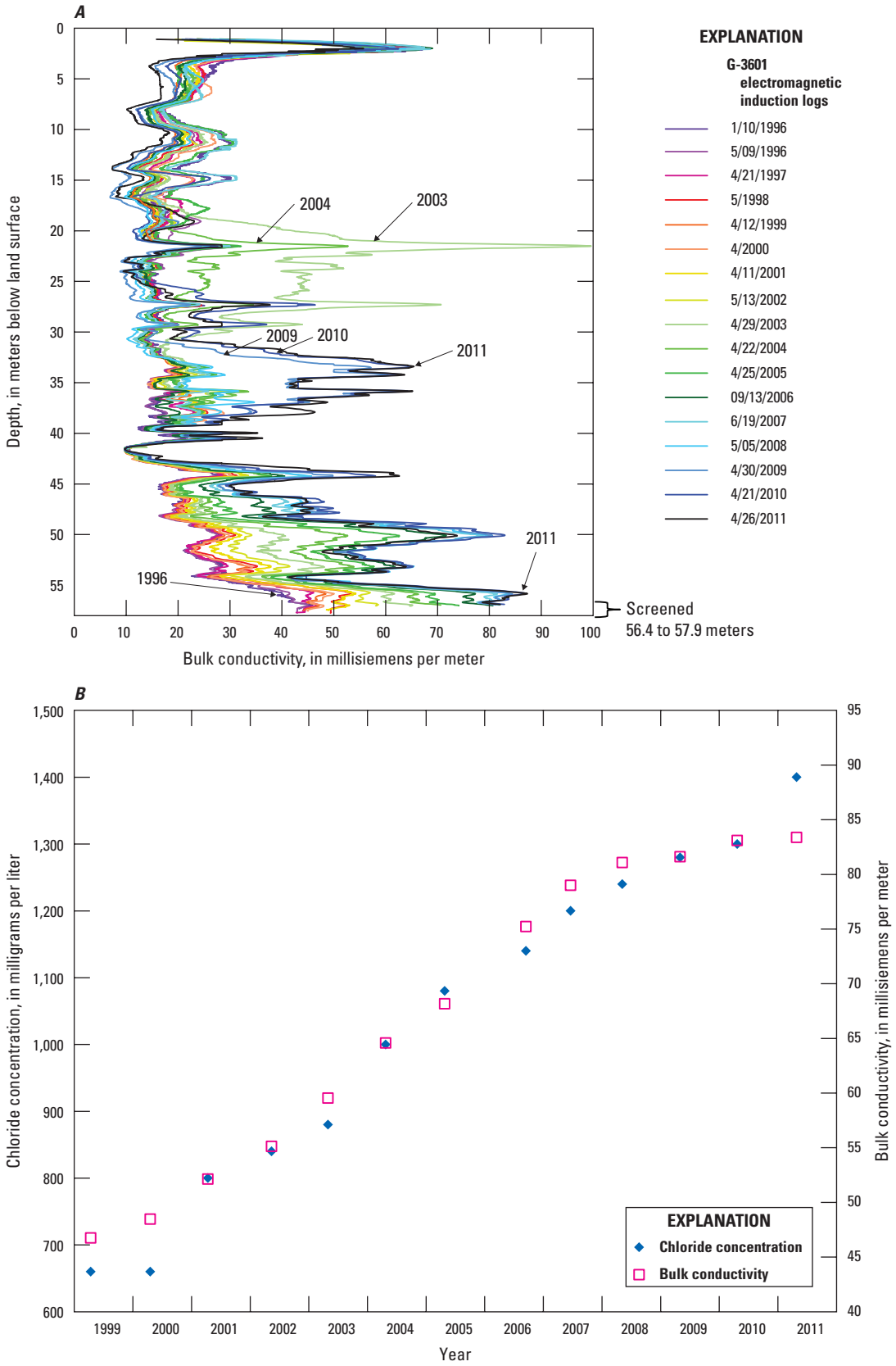

Figure 32. (*A*) Time-series electromagnetic induction log (TSEMIL) dataset and (*B*) chloride concentrations in samples from monitoring well G–3601 and bulk conductivity measured at a depth of 56.1 meters, Biscayne aquifer, Miami-Dade County, Florida.

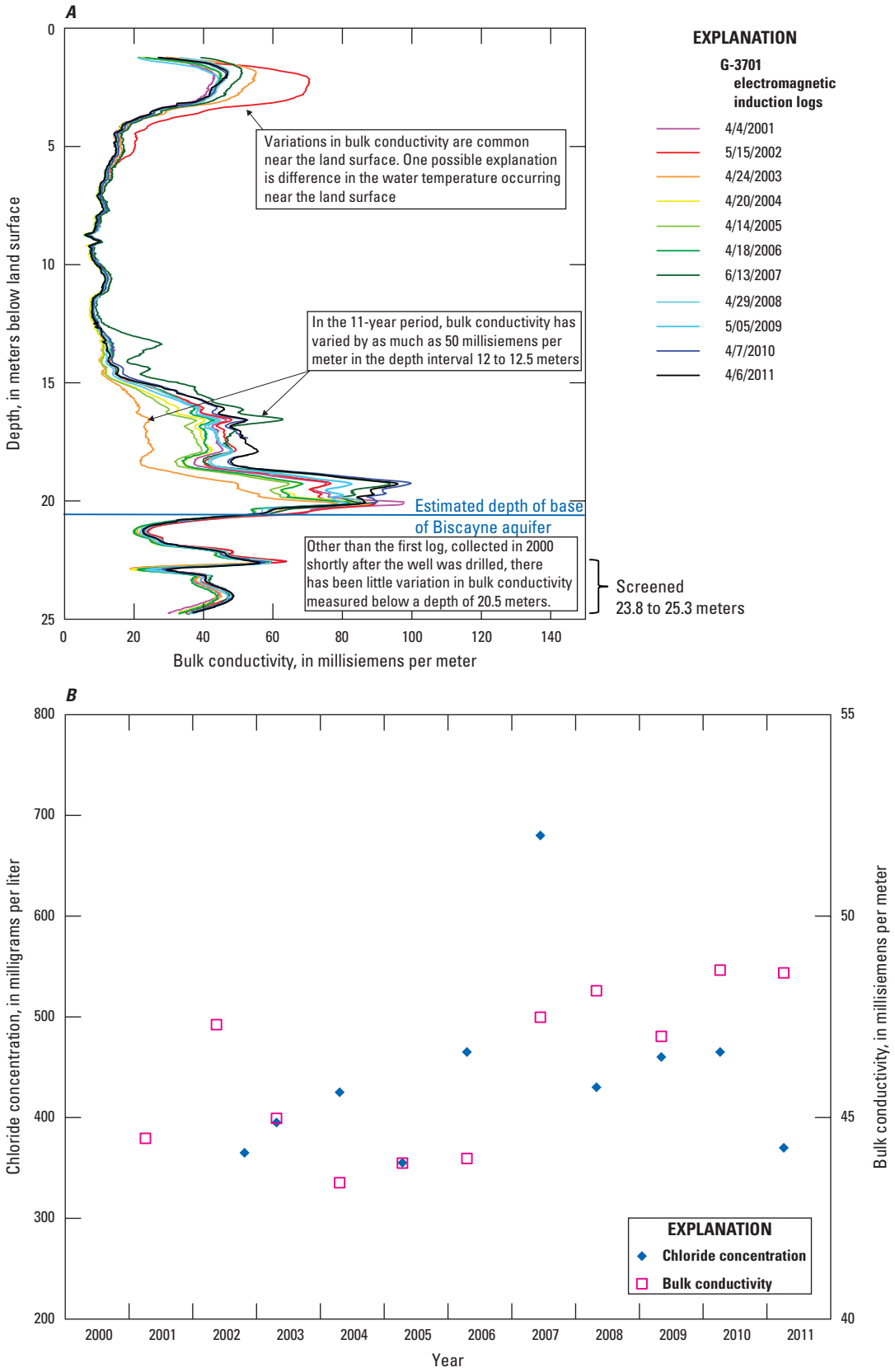

Figure 33. (*A*) Time-series electromagnetic induction log (TSEMIL) dataset; and (*B*) chloride concentrations in samples from monitoring well G–3701 and bulk conductivity measured at a depth of 24.0 meters, Biscayne aquifer, Miami-Dade County, Florida.

borrow ditches (Parker and others, 1955, p. 709, fig. 200). The inland extent of the saltwater described by Fitterman and others (2012) is about 1.5 km less than the extent mapped in the Biscayne aquifer by Parker and others (1955, p. 709, fig. 200), but is about 6 and 3 km inland of wells FKS4 and FKS8, respectively. The ion exchange front is, therefore, well inland of these wells. This mapped extent of saltwater helps to explain why the $Ca/(HCO_3 + SO_4)$ molar ratio in water, sampled from these wells, is less than 1 and concentrations of major ions typically plot near the theoretical freshwater/seawater mixing line (figs. 19, 21, 23, 25, 26). Results indicate that little or no ion exchange is taking place at these locations.

Miami and Tamiami Canals

Surface water in the Miami Canal at USGS monitoring station Miami Canal at Water Plant (appendix 1) (U.S. Geological Survey, 2011f), 4 km upstream of salinity control structure S–26, had become saline (335 mg/L chloride concentration) during the drought of 1970 to 1977, and the chloride concentration of water in wells adjacent to this canal had increased (fig. 13). The subsequent decrease in chloride concentrations in wells near the Miami Canal and west of salinity control structure S–26 (fig. 13) may be the result of the dissipation of saltwater that had leaked from the canal. The area of probable historical canal leakage is indicated in figure 17. A $^3H/^3He$ age-dating sample could not be obtained from well G–1351 to determine if the saltwater entered the aquifer during the 1970 to 1977 drought. The major and trace ion geochemistry of samples from wells G–3604 and G–3605 near the Miami and Tamiami Canals (fig. 8) indicate little or no ion exchange. The episodes of saltwater intrusion during the droughts of 1938–1939 and 1970–1977 (figs. 4 and 13) may have filled the ion-exchange sites of the rocks and sediments in the aquifer at these locations. The extent of saltwater intrusion in 1955 (fig. 8), 1969 (Renken and others, 2005a), and 1984 (Klein and Waller, 1985) was inland of both of these wells, particularly well G–3604.

C–111 Canal

A narrow finger of conductive groundwater extends at least 2.7 km inland along the C–111 Canal (fig. 8) (Fitterman and Deszcz-Pan, 1998, 2002). This finger is likely related to the leakage of saltwater from the C–111 Canal occurring between 1965 when the canal was installed and 1969 when salinity control structure S–197 was installed. Leakage of saltwater from the C–111 Canal peaked in 1965 when tidal inundation from Hurricane Betsy caused saltwater with a chloride concentration of 10,000 mg/L to flow as far inland as about 3 km upstream from salinity control structure S–18C (Meyer, 1974, p. 28). Meyer (1974, p. 30a) also reported the occurrence of saltwater between 1970 and 1971 in the C–109 and C–110 Canals about 3 to 4 km north of the C–111 Canal.

Turkey Point Nuclear Power Plant Cooling Canal System

The cooling canal system (CCS) of the Turkey Point Nuclear Power Plant east of Florida City (fig. 8) was constructed during the early 1970s and contains hypersaline water (Janzen and Krupa, 2011). This hypersaline water may be contributing to saltwater encroachment in this area (Hughes and others, 2010). Water in the cooling canals is reported to have tritium "concentrations at least two orders of magnitude above surrounding surface and groundwater and [tritium] therefore [is] considered a potential tracer of waters from the CCS" (Janzen and Krupa, 2011, section 2, p. 8). The tritium concentration of samples collected from sites located within 8.5 km of the CCS ranged from 4.1 to 53.3 TU and averaged 12.4 TU, whereas the tritium concentration of samples collected farther away from the CCS averaged 1.3 TU (appendix 2, table 2–3) (see the Tritium and Uranium Concentration section of this report). Saltwater intrusion is a recent occurrence at most of the groundwater monitoring wells (figs. 18, 19, 21–26) within 8.5 km of the CCS, except at wells FKS4 and FKS8 near the Card Sound Road Canal (see the Card Sound Road Canal section of this report). No samples were collected from the CCS or wells within it as part of the current study to detect any possible influxes of CCS water into the aquifer; however, monitoring wells were installed in 2010 adjacent to the CCS for other studies and these wells are being monitored using electromagnetic induction logging.

Recent Leakage from Canals

Although salinity control structures have been installed in most of the tidal canals, the leakage of saltwater through the porous rock of the Biscayne aquifer and around existing salinity control structures is documented (Parker and others, 1955; Kohout and Leach, 1964; Leach and Grantham, 1966). Kohout and Leach (1964) reported that any saltwater upstream of the salinity control structures could be driven into the aquifer when freshwater heads in the canals upstream of these structures increased. Monthly measurements of salinity collected by the Miami-Dade County Permitting, Environmental, and Regulatory Affairs (M-D PERA) during 1988 to 2010 (appendix 11) show influxes of saltwater in many of the canals upstream of the salinity control structures. These measurements at stations BL03, BS04, CD02, GL03, LR06, PR03, MI03, MW04, and SP04, located in the Black Creek, Biscayne, Cutler Drain, Goulds Canal, Little River, Princeton, Military, Mowry, and Snapper Creek Canals, respectively (fig. 8), have detected influxes of saltwater upstream of the water control structures in these canals. The occurrences have ranged from rare influxes of water with salinity between 0.5 and 1.4 PSU at station SP04 in the Snapper Creek Canal, to frequent influxes of water with a salinity of between 15 and 32 PSU at station BS04 in the Biscayne Canal (appendix 11). This saltwater may be leaking into the aquifer in some areas. Moreover, many existing

monitoring-network wells are in the right-of-way of local canals. A landward bias may exist in the assessment of the inland extent of saltwater in the Biscayne aquifer if (1) these canals are leaking saltwater, (2) there are insufficient data to define the inland extent of saltwater in areas away from these canals, and (3) the occurrence of saltwater at these locations is misconstrued as originating from movement of the saltwater front rather than canal leakage.

Card Sound Road Canal

Prior to May 2010 the Card Sound Road Canal (fig. 1) was one of the few canals in Miami-Dade County that lacked a salinity control structure. To evaluate the potential for landward flow of saline surface water in the Card Sound Road Canal, salinity profiles were collected at 11 and 12 sites, respectively, on December 5, 2008, and May 18, 2009. The 11 salinity profiles collected on December 5, 2008, indicated that salinity in the canal gradually increased from 0.27 ppt at a distance of 9.5 km from the mouth of the canal, to 4.24 ppt at a distance of 0.64 km from the mouth of the canal (appendix 3). As water levels in the Biscayne aquifer declined to near record low altitudes by May 16, 2009, the flow in the Card Sound Road Canal reversed, and saltwater from the Florida Bay flowed inland. On May 18, 2009, water at nine sites ranging from 0.64 to 11.6 km inland from the mouth was hypersaline, and salinity ranged from 43.7 to 42.3 ppt. At monitoring well FKS8, which is approximately 5 m from the Card Sound Road Canal and 12.4 km from its mouth, the average salinity of canal water was 38.6 ppt. Farther inland, at distances of 13.5 and 15.9 km from the mouth of the Card Sound Road Canal, the salinity of canal water was 0.27 and 0.18 ppt, respectively.

The influx of saltwater upstream in the Card Sound Road Canal was identified in groundwater samples from well FKS8. During February 24, 2004, to March 31, 2009, the chloride concentrations in samples from a depth of 23 m in well FKS8 ranged from 4,680 to 9,480 mg/L and averaged 8,660 mg/L, but on May 4, 2009, and May 18, 2009, chloride concentrations from this depth were 14,750 and 11,575 mg/L, respectively (Jolynn Reynolds, Florida Keys Aqueduct Authority, written commun., 2009). Increases in chloride concentrations in water samples from well FKS8 also occurred in samples from the depths 11 and 17 m. By June 29, 2009, the chloride concentrations in samples from the depth 23 m had returned to near average, but the chloride concentrations in samples from the depth intervals of 11 and 17 m were still greater than the maximums recorded at these depths prior to the influx of saltwater up the Card Sound Road Canal (Jolynn Reynolds, Florida Keys Aqueduct Authority, written commun., 2009).

On May 18, 2009, saltwater in the Card Sound Road Canal was not as far inland as the apparent extent of saltwater in the Biscayne aquifer determined in the 2001 HEM survey or mapped by Parker and others (1955, p. 709). Saltwater traveled farther inland up the Card Sound Road Canal during the previous droughts than it did in 2009. For example, in 1945, saltwater had been detected near the northern end of the Card Sound Road Canal (Parker and others, 1955, p. 680) about 5 km farther inland than in 2009. Canal levels in the area were lower during previous droughts than in 2009. For example during the drought of 1971, groundwater levels in this area declined to about 0.3 m below sea level (Meyer, 1974, p. 24). During the 1971 drought, water levels measured in wells S–196A and G–613 near Homestead and Florida City declined to levels that were 0.5 to 0.9 m lower, respectively, than in 2009 (U.S. Geological Survey, 2011f). Other factors such as tide magnitudes, storm surge from hurricanes, and encroachment along the base of the aquifer also may have contributed to the inland extent of saltwater in the Biscayne aquifer near the Card Sound Road Canal.

A salinity control structure was installed in the Card Sound Road Canal just above its junction with Canal L–31E in May 2010. This structure likely will reduce the flow of saltwater up the Card Sound Road Canal and also may increase freshwater head in the Biscayne aquifer in the area. In time, it may reduce the landward extent of saltwater in this area, but the gradual declines in chloride concentration near the Miami Canal (fig. 13) indicate that it may take a long time for intruded water near the Card Sound Road Canal to dissipate.

Biscayne Canal

Salinity control structure S–28 was installed in 1960 (table 1) about 1 km west of U.S. Highway 1 to prevent incursions of saltwater up this canal; however, water with a salinity of 20 PSU or greater has frequently been detected at station BS04 upstream of the salinity control structure (fig. 10). This saltwater could be leaking into the Biscayne aquifer, but it is unknown how far upstream of this station the saltwater travels. Monitoring well G–3601 is on the eastern bank of the Biscayne Canal about 5.6 km from the mouth of the canal and about 3.8 km upstream of structure S–28. The TSEMIL dataset from well G–3601 (fig. 32*A*) indicates little if any change in bulk conductivity occurring in the depth interval 41 to 42 m, but there are changes occurring in shallower and deeper intervals than this interval that do not appear to be related. Below this depth interval, gradual increases in bulk conductivity indicate that the saltwater interface is gradually encroaching landward. Shallower than this depth interval, there have been two short-term influxes of conductive water: the first occurring during 2003 through 2004 in the depth interval 18 to 32 m, and the second occurring during 2009 through 2011 in the depth interval 30 to 39 m. One possible source of these relatively shallow influxes could be leakage of saltwater from the adjacent canal.

An alternative possibility is that these influxes are associated with the saltwater front. Monitoring well G–894 is about 1.3 km east of well G–3601. Well G–894 is open to the depth interval (22.7 to 23.2 m) that coincides closely with the depth of the maximum bulk conductivity measured in 2003 in well G–3601. Between 1959 and 1981, the chloride concentrations in samples from well G–894 ranged from 680 to 3,600 mg/L (fig. 18). The maximum concentration

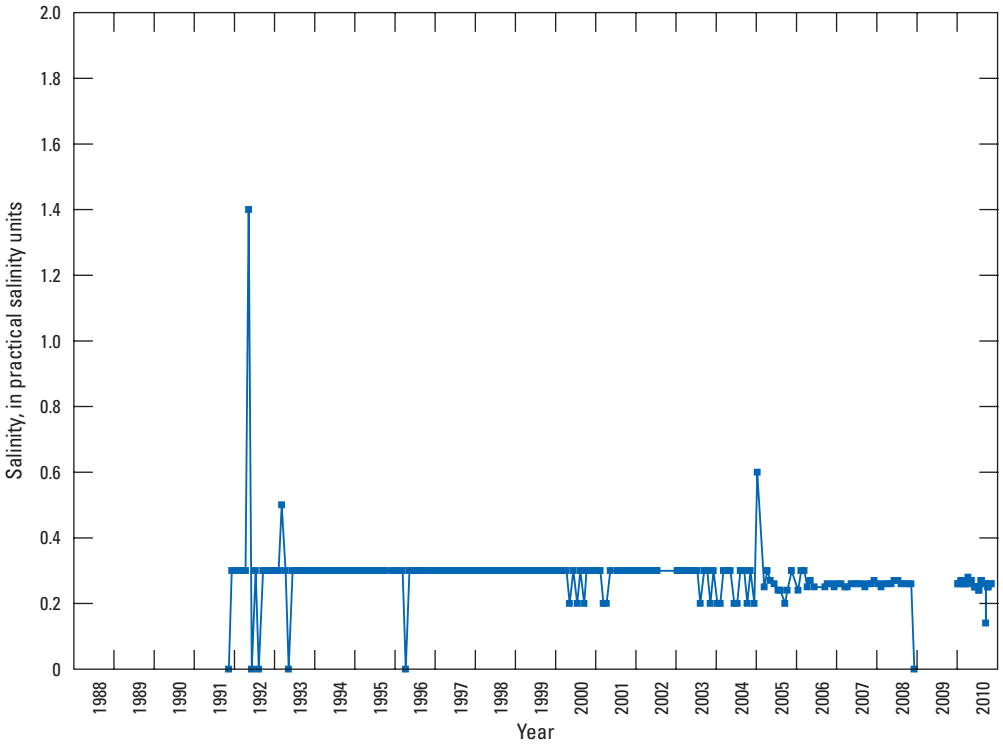

Figure 34. Salinity of the Snapper Creek Canal at station SP04, 1991–2010, Miami-Dade County, Florida.

occurred on June 4, 1962, during the drought of the early 1960s (Waller, 1985; Bridges and others, 1991). Since 1995, none of the samples from well G–894 have had a chloride concentration greater than 50 mg/L. The current chemistry of samples from well G–894, appears to be dominated by recharge from precipitation rather than encroaching saltwater because the δ^2H and $\delta^{18}O$ of samples from this well are about the same as the estimated weighted mean isotopic composition of annual precipitation in the catchment (see the Oxygen and Hydrogen Stable Isotopes section of this report). The most likely source of saltwater contributing to shallow saline influxes at well G–3601, therefore, is the Biscayne Canal rather than saltwater encroaching from the direction of well G–894. This likely source could be further evaluated by monitoring salinity in the canal adjacent to the well.

Snapper Creek Canal

Saltwater in the Snapper Creek Canal has leaked around salinity control structure S–22 through the highly permeable Biscayne aquifer and has flowed inland (Sherwood and Leach, 1962). USGS water-quality monitoring during 1966 to 1992 at station Snapper Creek Canal at S–22 Near South Miami, Fl (USGS ID 02290700), about 60 m upstream of S–22, detected brackish water in September 1974, December 1975, January 1976, and February, March, and June 1977. Chloride concentrations ranged from 254 to 638 mg/L, and specific conductance ranged from 1,000 to 2,500 µS/cm during the period (U.S. Geological Survey, 2011f). Monthly salinity monitoring during 1988 to 2010 at station SP04, 0.5 km upstream of water control structure S–22 (figs. 8 and 34), detected only a few influxes of saltwater in the Snapper Creek Canal (Maria Idia Macfarlane, Miami-Dade County Water and Sewer Department, written commun., March 7, 2011; Craig Grossenbacher, Miami-Dade County Permitting, Environmental, and Regulatory Affairs, written commun., July 7, 2010). These influxes included (1) a salinity of 1.4 PSU measured in May 1992, (2) a salinity of 0.5 PSU measured in March 1993, and (3) a salinity of 0.6 PSU measured in January 2005. Although much lower than those measured in some of the other canals, these salinities are equivalent to chloride concentrations of about 260 mg/L to 760 mg/L.

The TSEMIL dataset from well G–3608 indicated a shallow increase in bulk conductivity that may have resulted from leakage of saltwater or brackish water from the adjacent Snapper Creek Canal (fig. 35*A*). Well G–3608 is on the west bank of Snapper Creek Canal, 3.8 km upstream of its mouth and 1.7 km upstream of salinity control structure S–22. Well G–3608 is open to the Biscayne aquifer in the depth interval 29.0 to 30.5 m. The TSEMIL dataset indicated an increase in bulk conductivity in the depth interval 16 to 26 m of the log collected April 30, 2003. The bulk conductivity gradually diminished in subsequent logs until it was no longer evident in the TSEMIL dataset. Below a depth of 26 m, the bulk conductivity of logs collected from G–3608 increased between April 2003 and April 2006 (fig. 35*A*). During this period, the chloride concentrations in samples increased from 72 to 230 mg/L (fig. 35*B*). Between 2006 and 2011 the chloride concentrations in samples and the bulk conductivity of logs from this well decreased to levels near those occurring prior to the influx of conductive water. This pattern could be caused by the leakage of saltwater or brackish water from the Snapper Creek Canal, some of which gradually sank to the base of the aquifer where it gradually dissipated.

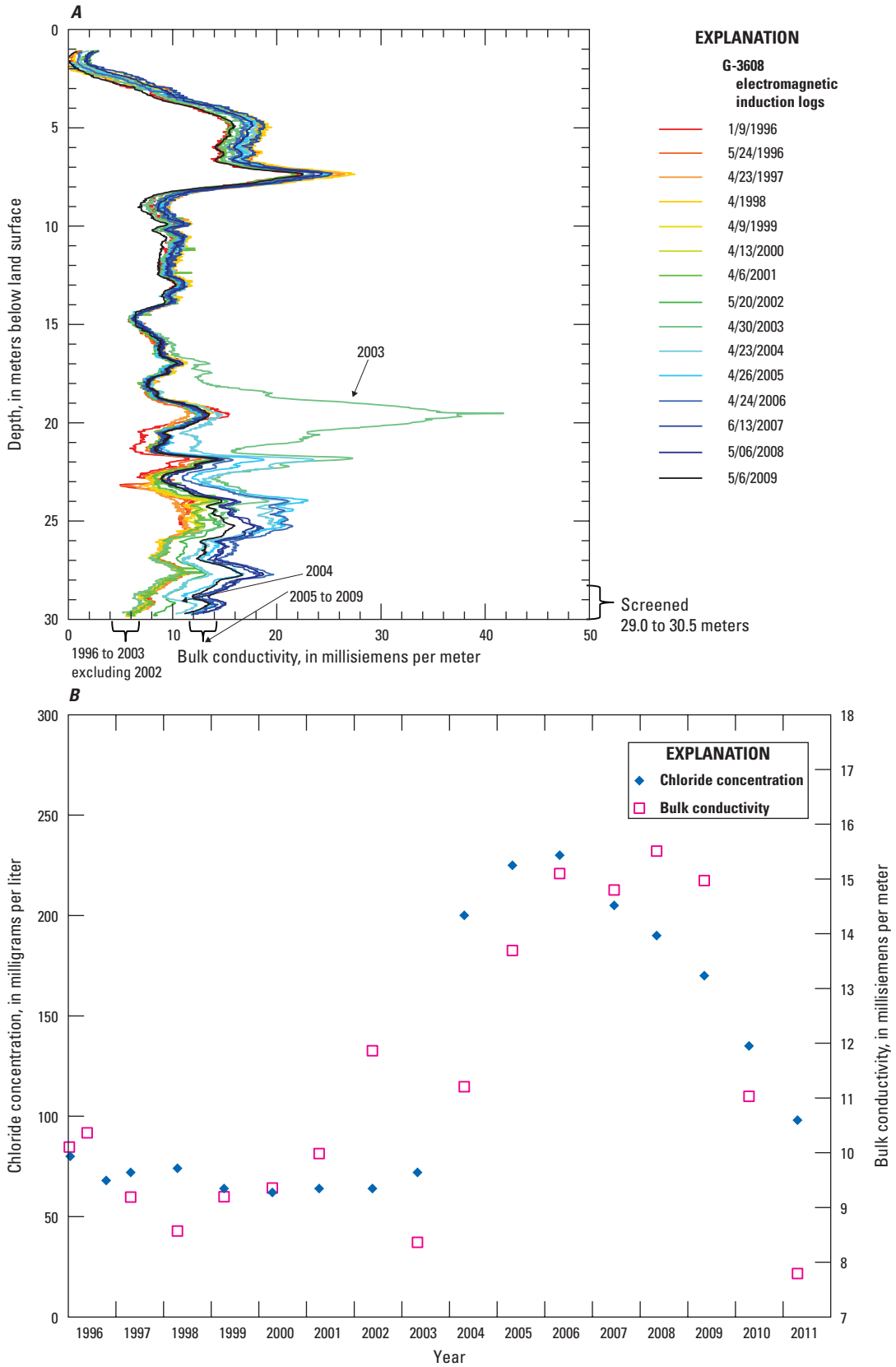

Figure 35. (*A*) Time-series electromagnetic induction log (TSEMIL) dataset; and (*B*) chloride concentrations in samples collected from well G–3608 and bulk conductivity measured at a depth of 28.9 meters, Biscayne aquifer, Miami-Dade County, Florida.

The following information supports the interpretation that the conductive water detected in well G–3608 and G–896 emanated from the Snapper Creek Canal.

- The oxygen and hydrogen stable isotope compositions in samples from well G–3608 consistently plotted closely to those of samples from the C–2 (Snapper Creek) Canal (fig. 29B), but the stable isotope compositions of samples of well G–3609, located 1.8 km south-southeast of well G–3608, and well G–3607, located 1.7 km north of well G–3608, consistently plotted closer to the intersection of the LSWML with the GMWL (fig. 29B). Well G–3609 is on the saltwater side of the saltwater front and is open to the encroaching saltwater front.

- The interpreted piston-flow ages of water samples from wells G–896 and G–3608 are relatively young compared to those of samples from wells G–3607 and G–3609 (table 5).

- Water from the Snapper Creek Canal near well G–3608 had SF_6 concentrations ranging from 9.39 pptv in December 2009 to 37.0 pptv in July 2009 (appendix 2, table 2–4). The SF_6 concentrations in samples from wells G–896 and G–3608 were within this range. Conversely samples from nearby well G–3609, which is open below the saltwater interface, contained only 0.79 to 0.93 pptv SF_6, which is about an order of magnitude less than that of samples from wells G–896 and G–3608.

None of the influxes of saltwater in the Snapper Creek Canal correspond to the interpreted piston-flow age determined for water sampled from well G–3608 (table 5), but monthly measurements may have failed to capture a short-term influx of saltwater in this canal upstream of S–22, and the water sampled at G–3608 is likely a mixture of water of different ages, including a relatively young component. Another potential explanation for the occurrence of saltwater at well G–3608 is encroachment of saltwater through a shallow preferential flow zone occurring in the aquifer. If the saltwater front in this area were moving westward, the westward movement likely would be evident in samples from the 18.3- to 22.6-m depth interval of well G–896, 438 m northeast of well G–3608 and 377 m east of the Snapper Creek Canal (fig. 8). The chloride concentrations in samples from well G–896 increased to a maximum of 1,500 mg/L in June 1992; however, by April 1998, the chloride concentration of water in well G–896 had declined to 380 mg/L, and between April 1998 and May 2012, it gradually declined to 260 mg/L (fig. 36). The influx of saltwater detected in April 2003 at well G–3608 occurred approximately 11 years after the chloride concentrations in water samples from well G–896 began declining. If the saltwater in well G–896 was associated with the saltwater front, it seems unlikely that the saltwater front could have advanced to the location of well G–3608 in 2003 when the samples from well G–896 indicate that the saltwater front was probably retreating.

Water levels at well G–3608 are generally 0.09 to 0.14 m higher on average than at well G–896 (fig. 37). Even if density differences resulting from changes in salinity are considered, this head differential indicates that groundwater flow would generally be towards the east from well G–3608 to well G–896, rather than in the other direction. If saltwater leaked from the Snapper Creek Canal at well G–3608, the prevailing groundwater-flow direction potentially could move saltwater toward well G–896. This movement would account for (1) the occasional influxes of saltwater observed at well G–896; (2) the similarity in interpreted piston-flow ages of samples from wells G–896 and G–3608; (3) the elevated concentrations of SF_6 in samples from wells G–896 and G–3608, relative to those of samples from G–3609; and (4) the oxygen and hydrogen stable isotope compositions of the samples from well G–896, which plot closer to those of the surface water samples from the Snapper Creek Canal than to those of the groundwater samples from wells G–3607 and G–3609.

Black Creek Canal

The TSEMIL dataset collected from well G–3702 (fig. 38*A*), located on the western bank of the Black Creek Canal 3.9 km upstream from water control structure S–21 (fig. 8), identified a shallow influx of conductive water that may have been caused by the leakage of saltwater from this canal. In the June 13, 2007, log of the TSEMIL dataset, in the depth interval 9.8 to 17 m, there was an abrupt increase in bulk conductivity. This increase may correspond to an influx of water in the Black Creek Canal at station BL03 on May 9, 2007, with a salinity of 14.5 PSU (fig. 39; Maria Idia Macfarlane, Miami-Dade County Water and Sewer Department, written commun., March 7, 2011; Craig Grossenbacher, Miami-Dade County Permitting, Environmental, and Regulatory Affairs, written commun., July 7, 2010) 1.9 km upstream of water control structure S–21 and 1.9 km downstream from well G–3702. A salinity of 14.5 PSU corresponds to a chloride concentration of approximately 8,000 mg/L. The salinity of the water in the canal on May 9, 2007, was one of the greatest measured at this site to date and was exceeded only by another influx of water with a salinity of 19.6 PSU on October 3, 2007.

The EMI log collected in well G–3702 on May 6, 2008, indicated that the conductive water detected previously in the 9.8- to 16.8-m depth interval had almost completely dissipated. If any of this conductive water sank to the base of the aquifer, it does not appear to have had a lasting effect on the water chemistry and salinity at this location because of the following:

- Near the bottom of well G–3702 in the depth interval 20 to 25 m, the TSEMIL dataset indicates a conductive layer. There was a small increase in bulk conductivity in the depth interval 17 to 20 m, but below this depth, the bulk conductivity of subsequent EMI logs decreased slightly (fig. 38*A*).

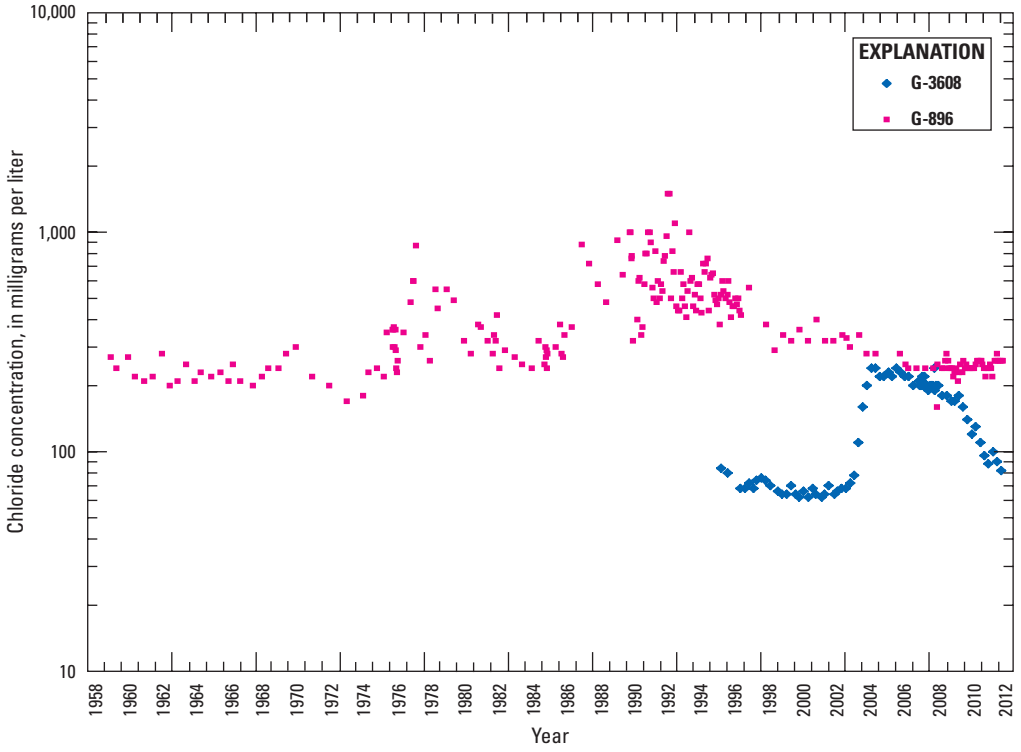

Figure 36. Chloride concentrations in water samples from wells G–896 and G–3608, Miami-Dade County, Florida.

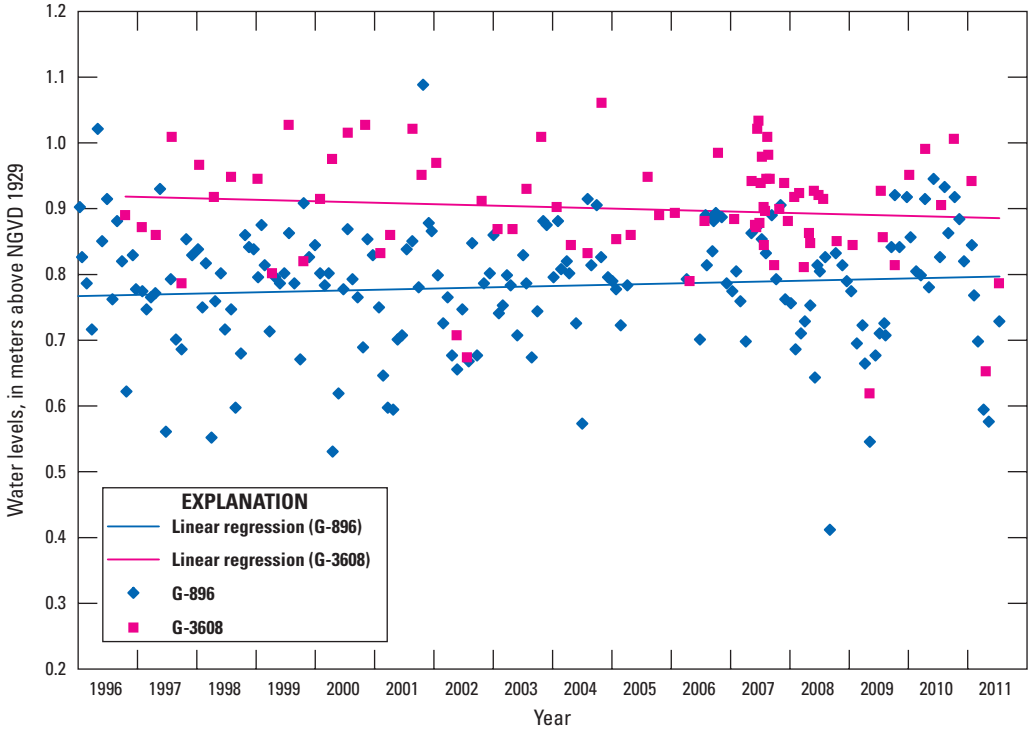

Figure 37. Water levels in wells G–896 and G–3608, 1996–2011, Miami-Dade County, Florida.

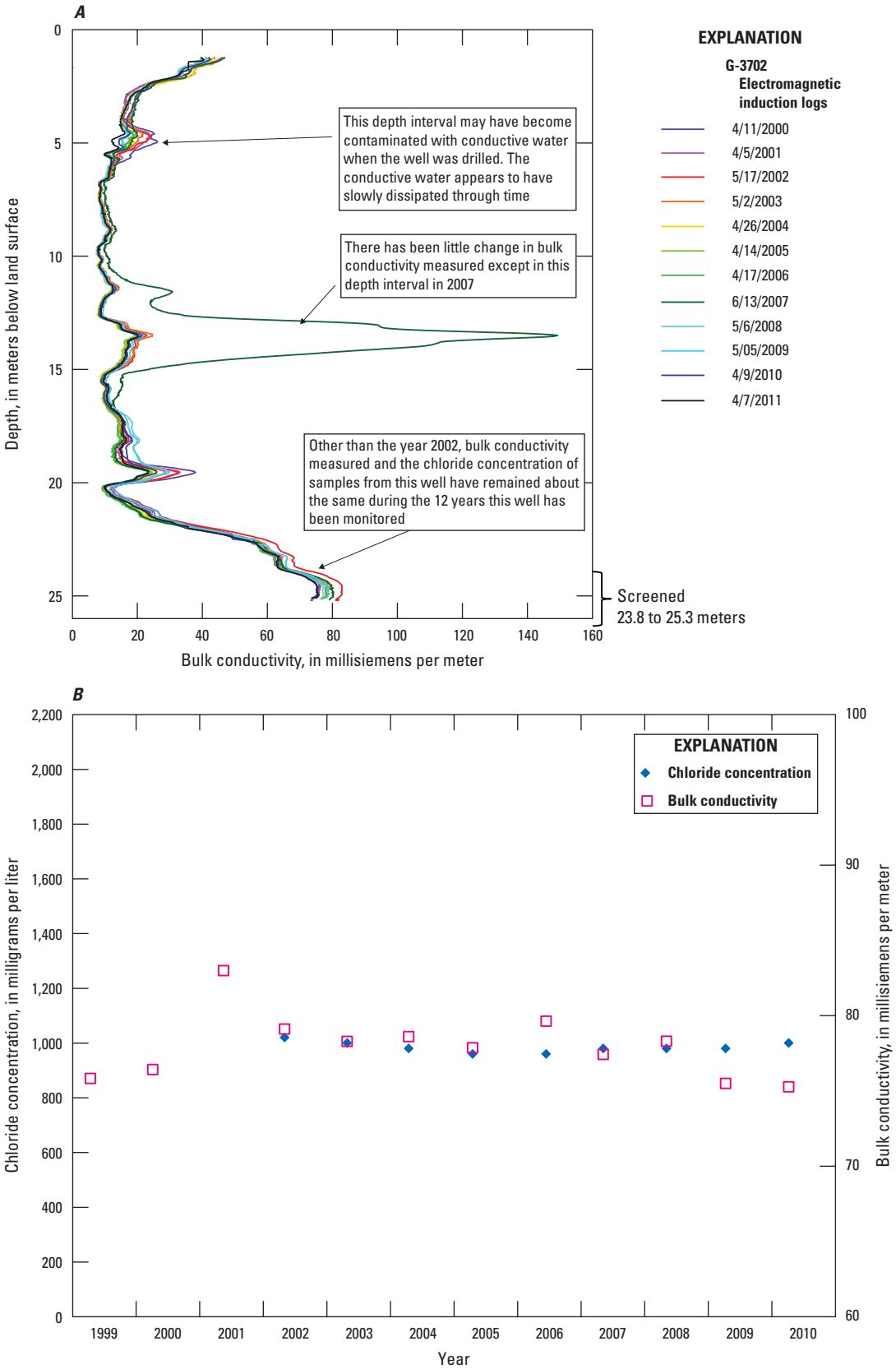

Figure 38. (*A*) Time-series electromagnetic induction log (TSEMIL) dataset; and (*B*) chloride concentrations in water samples from well G–3702 and bulk conductivity measured at a depth of 24.6 meters, Biscayne aquifer, Miami-Dade County, Florida.

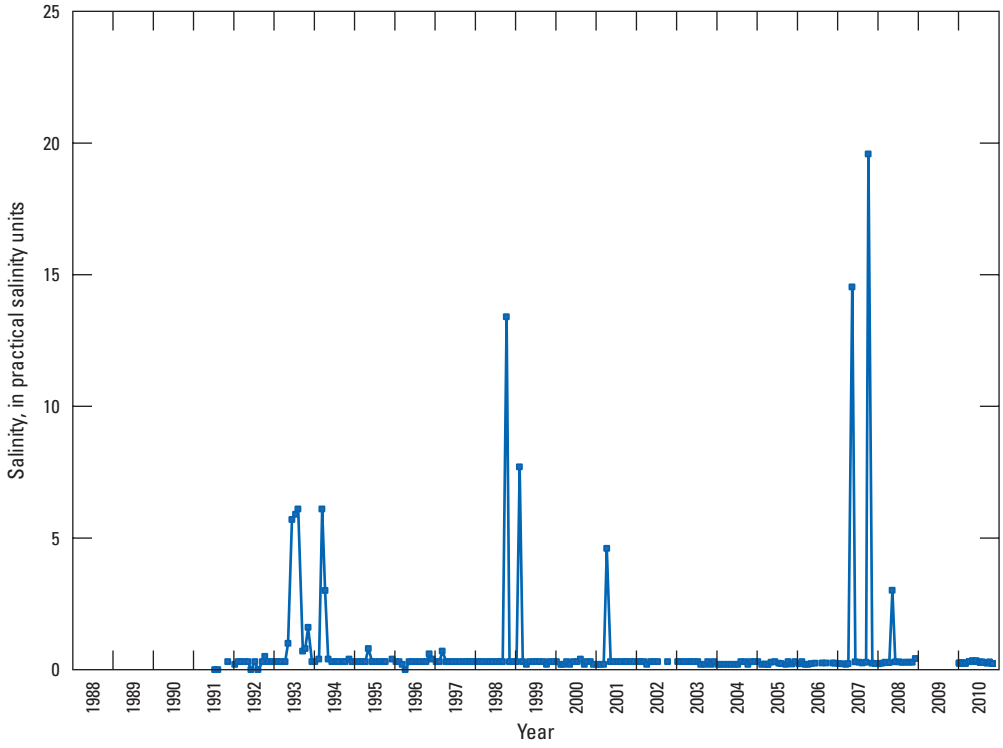

Figure 39. Salinity of the Black Creek Canal at station BL03, 1991–2008 and 2010, Miami-Dade County, Florida.

- Well G–3702 is open to the aquifer in depth interval 23.8 to 25.3 m. Water samples from this well indicate that the chloride concentration has been fairly constant at about 940 to 1,000 mg/L (fig. 38*B*) since salinity sampling began in 2002. Between June 2007 and April 2011, chloride concentrations in this well increased by only 40 mg/L.
- The oxygen and hydrogen stable isotopic compositions of water from well G–3702 and the site C1 Canal at G–3702 do not plot close to each other (fig. 29*B*).
- The SF_6 concentrations in water samples from well G–3702 are 5.82 and 9.77 pptv, which are less than the SF_6 concentration of 18.2 pptv in a sample from the canal (appendix table 2–4).

$^3H/^3He$ age-dating of the sample from well G–3702 indicated an apparent (piston flow) age of < 1970 (table 5). During the drought of 1960–63 water levels in long-term monitoring well S–182A, (USGS ID 253549080214101) located 4.2 km north of well G–3702, declined to 0.20 m (U.S. Geological Survey, 2011f). This water level was the 4th lowest water level recorded in this well. During the 1943–57 drought, Black Creek was a stream that extended from the coast to a little north of the location of well G–3702. The Black Creek Canal was dredged between April 1960 and December 1963 (Renken and others, 2005a). These events may have allowed saltwater to leak from the canal as it was being dredged, or it may have encroached into the Biscayne aquifer during the drought of 1960–63.

Princeton Canal

Samples from monitoring well G–3162 (USGS ID 253202080232601) in the right of way of the Princeton Canal (fig. 8) indicate that chloride concentrations increased from 160 to 1,300 mg/L between April 1978 and December 2011 (fig. 18) (U.S. Geological Survey, 2011f). Well G–3162 was not sampled during the present study because well construction did not accommodate the types of geochemical samples needed, but some of the information collected during this study indicates that the saltwater sampled in this canal may have leaked from the canal, or encroached farther inland beneath the canal than on either side of the canal. USGS monitoring of the Princeton Canal between 1975 and 1978 at station Canal 102 at SW 107 Ave near Homestead, FL (USGS ID 253108080215200) 1.8 km west of water control structure S–21A and 2.6 km east of well G–3162, indicated two influxes of saltwater in the canal: (1) between April and June 1975 with a maximum chloride concentration of 1,300 mg/L, and (2) in March 1977 with a chloride concentration of 2,080 mg/L (U.S. Geological Survey, 2011f). There is a gap of 13 years between the end of USGS monitoring and the beginning of the salinity information provided by the M-D PERA (Maria Idia Macfarlane, Miami-Dade County Water and Sewer Department, written commun., March 7, 2011; Craig Grossenbacher, Miami-Dade County Permitting, Environmental, and Regulatory Affairs, written commun., July 7, 2010). In November 1993,

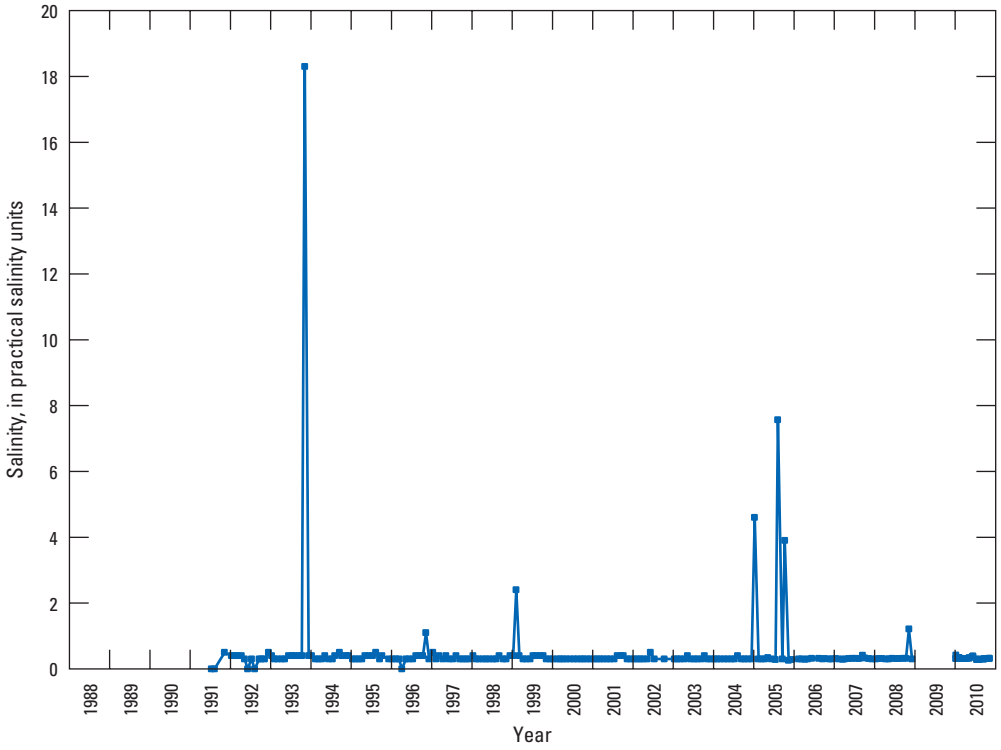

Figure 40. Salinity of the Princeton Canal at station PR03, 1991–2008 and 2010, Miami-Dade County, Florida.

a salinity of 18.3 PSU (fig. 40) was measured by the M-D PERA at station PR03 (fig. 8) near the same location where the USGS collected samples. This salinity is equivalent to a chloride concentration of approximately 10,000 mg/L. Salinities of 1.1, 2.4, 4.6, 7.6, 3.9, and 1.2 were measured in November 1996, February 1999, January 2005, August 2005, October 2005, and November 2008, respectively (fig. 40). These influxes of saltwater in the canal could account for an increase in salinity in the Biscayne aquifer adjacent to the canal.

TEM soundings MIA136 and MIA137 (fig. 8) collected 0.20 and 0.38 km south of the Princeton Canal, respectively, did not detect saltwater (appendix 4). Sounding MIA137 was collected 0.26 km east of the location of well G–3162. The saltwater front is, therefore, at least 0.26 km farther inland at the location of well G–3162 adjacent to the canal, than it is 0.38 km south of the canal (fig. 8). This difference in the inland extent of saltwater near the canal versus farther away from the canal could potentially be caused by leakage of saltwater from the Princeton Canal or encroachment under the canal potentially caused by low freshwater levels caused by canal drainage.

EMI logs could not be collected from well G–3162; therefore, the same kinds of observations made at wells FKS8, G–3601, G–3608, and G–3702 could not be made for this location. Also, it was not possible to collect a sample for evaluation of the $^{3}H/^{3}He$ age. More information is needed to determine the source of the saltwater detected at well G–3162.

Saltwater Encroachment

The piston-flow ages and the recharge temperatures of samples with a chloride concentration greater than or equal to about 1,000 mg/L generally correspond closely to a period with frequent droughts and the air temperatures that are typical of the end of the dry season (figs. 30 and 31*A*), when water levels in the aquifer reach a minimum (fig. 31*B*) and saltwater encroachment along the base of the aquifer or saltwater leakage from canals is most likely to be at a maximum. Whether this saltwater encroached from the ocean or bays, or leaked from canals, cannot be evaluated by using these two geochemical relations alone. Differentiation of the source potentially can be made by using (1) results of the 2001 HEM survey, (2) TSEMIL datasets, (3) results of long-term monitoring of chloride concentrations (figs. 18 and 47) (U.S. Geological Survey, 2011f), and (4) information about other geochemical relations.

Resistivity data collected from each flight line of the 2001 HEM survey (Fitterman and others, 2012) were used to create differential resistivity and inverted resistivity profiles. Many of these profiles intersected the saltwater front and generally indicated a wedge-shaped mass of saltwater that extended about 9 to 15 km inland from the coast in the Biscayne aquifer. This wedge shape is typical of encroached seawater (Brown and Parker, 1945). The wedge-like shape of encroaching saltwater is most evident in the eastern part of the HEM survey area (Fitterman and others, 2012). In the parts of the HEM survey area adjacent to the Card Sound Road Canal

and U.S. Highway 1, however, the slope of the intruded saltwater is almost vertical in some areas (Fitterman and others, 2012). As discussed in the section "Card Sound Road Canal," this is an area where saltwater has been interpreted to have leaked from the canal and the old railway borrow ditch.

TSEMIL datasets can be used to evaluate the depth intervals in which changes in the electrical conductivity of water are occurring. If a wedge-shaped body of saltwater encroaches along the base of the aquifer, the first indication of encroachment at a given monitoring well is generally an increase in bulk conductivity and chloride concentration near the base of the aquifer. As saltwater continues to encroach, bulk conductivity and chloride concentration near the base of the aquifer would increase, and the depth to the top of the saltwater interface would decrease. Such changes are evident in the TSEMIL datasets from 12 wells: G–3604 (fig. 41*A*), G–3605 (U.S. Geological Survey, 2011g), G–3609 (fig. 42*A*), G–3615 (U.S. Geological Survey, 2011g), G–3698 (fig. 43*A*), G–3699 (fig. 44*A*), G–3704 (U.S. Geological Survey, 2011g), G–3705 (U.S. Geological Survey, 2011g), G–3855 (fig. 46*A*), G–3856 (fig. 46*B*), and the deeper parts of wells G–3601 (fig. 32*A*) and G–3602 (fig. 45*A*). Long-term sampling of wells G–3601 (fig. 32*B*), G–3602 (fig. 45*B*), G–3604 (fig. 41*B*), G–3605 (fig. 18), G–3609 (fig. 42*B*), G–3615 (fig. 47), G–3698 (fig. 43*B*), G–3699 (fig. 44*B*), G–3704 (fig. 47), and G–3705 (fig. 47) indicates that the chloride concentration has increased in water samples from these wells.

Long-term chloride sampling and/or TSEMIL datasets indicated that saltwater was actively encroaching near the base of the Biscayne aquifer in 12 wells (figs. 19, 21–26). Geochemical sampling indicated the recent onset of saltwater intrusion in six of the wells (G–3615, G–3698, G–3699, G–3704, G–3705, and G–3855) and ongoing saltwater encroachment in four of the wells (G–3601, G–3602, G–3604, and G–3605). Results were inconclusive in two wells (G–3856 and G–3609).). The recent onset of saltwater intrusion near wells G–1264 (fig. 18), G–3615 (fig. 47), G–3698 (fig. 43B), G–3699 (fig. 44B), and G–3705 (fig. 47) was confirmed by long-term monitoring, indicating that the chloride concentrations in samples increased from less than 1,000 mg/L to greater than 1,000 mg/L sometime during or after 1994. The chloride concentration in well G–3704 (fig. 47) increased from 3,400 to 6,800 mg/L during April 2006 to April 2011. It is uncertain when the saltwater front passed this well, but it may have occurred fairly recently based on the rate at which salinity in this well increased.

TSEMIL datasets were not collected from wells F–279, G–901, and G–1264. Each of these wells is shallower than the base of the Biscayne aquifer, but the evaluation of trace and major ions in the wells indicated that saltwater had recently intruded the aquifer at the sampling depths of these three locations (figs. 19, 21–26). Long-term monitoring indicates that the chloride concentration of sampled water increased to greater than 1,000 mg/L in 1959 at well F–279 (fig. 47), in 1994 at well G–901 (fig. 47), and in 2003 at well G–1264 (fig. 18).

Although the TSEMIL datasets indicated that saltwater is also encroaching near wells G–3601, G–3602, G–3604, and G–3605, the water samples from these wells did not indicate the extent of ion depletion or enrichment observed in the other wells (figs. 19, 21–26). The lack of enrichment or depletion is typical of areas of preexisting saltwater intrusion. Wells G–3604 and G–3605 are just south of the Tamiami and Miami Canals where historical saltwater intrusion had occurred (Parker and others, 1955); therefore, many of the ion exchange sites in this portion of the aquifer may have been filled when saltwater previously intruded this area. Historical saltwater intrusion also has been documented (Parker and others, 1955) in the aquifer near wells G–3601 and G–3602, which are close to the Biscayne and Little River Canals, respectively.

The increases in measured bulk conductivity and chloride concentration in well G–3698 may have resulted from saltwater encroachment, or they may be the direct or indirect results of leakage of saltwater from a canal. Well G–3698 is a few meters from a small canal that leads to the Mowry Canal. The sudden increase in bulk conductivity observed in the TSEMIL dataset from this well throughout a 12-m-thick portion of the aquifer (fig. 43*A*) and the sudden increase and subsequent decrease in the chloride concentration in samples collected from this well (fig. 18) are unusual. The changes at well G–3698 are similar in some ways to the shallow and short-term influxes of conductive water detected in the TSEMIL datasets from wells G–3601 (fig. 32*A*), G–3608 (fig. 35*A*), and G–3702 (fig. 38*A*), where canal leakage is a likely factor. Saltwater has been detected in the past in the Mowry Canal at structure S–179 near well G–3698. Eighteen percent of samples from the Mowry Canal on the downstream side of structure S–179 during 1972 to 1979 indicated chloride concentrations ranging from 740 to 7,200 mg/L (4 to 40 PSU) (U.S. Geological Survey, 2011f). USGS sampling of the site was discontinued in November 1979. Monthly measurements of salinity during July 1991 to December 2008 and January 2010 to November 2010 at the bottom of the Mowry Canal at site MW04 (fig. 48), 3.3 km upstream of water control structure S–20F and 3.5 km downstream of S–179, indicate that about 12 percent of the measurements had a salinity of 4.3 to 23 PSU. At least some of the saltwater may have leaked from this canal. Whether the saltwater detected at well G–3698 leaked from the canal or encroached along the base of the aquifer, or both, is uncertain given existing geochemical evidence. The interpreted piston-flow age of the sample from well G–3698 is about 1986 (table 5), which corresponds to a period with frequent droughts.

Limitations

The accuracy of the map showing the inland extent of saltwater in the Biscayne aquifer in 2011 (figs. 8, 17) can be evaluated by considering the spatial coverage of monitoring wells and TEM soundings used to create the map (fig. 8). The TEM soundings MIA105 and MIA106 (fig. 8), for

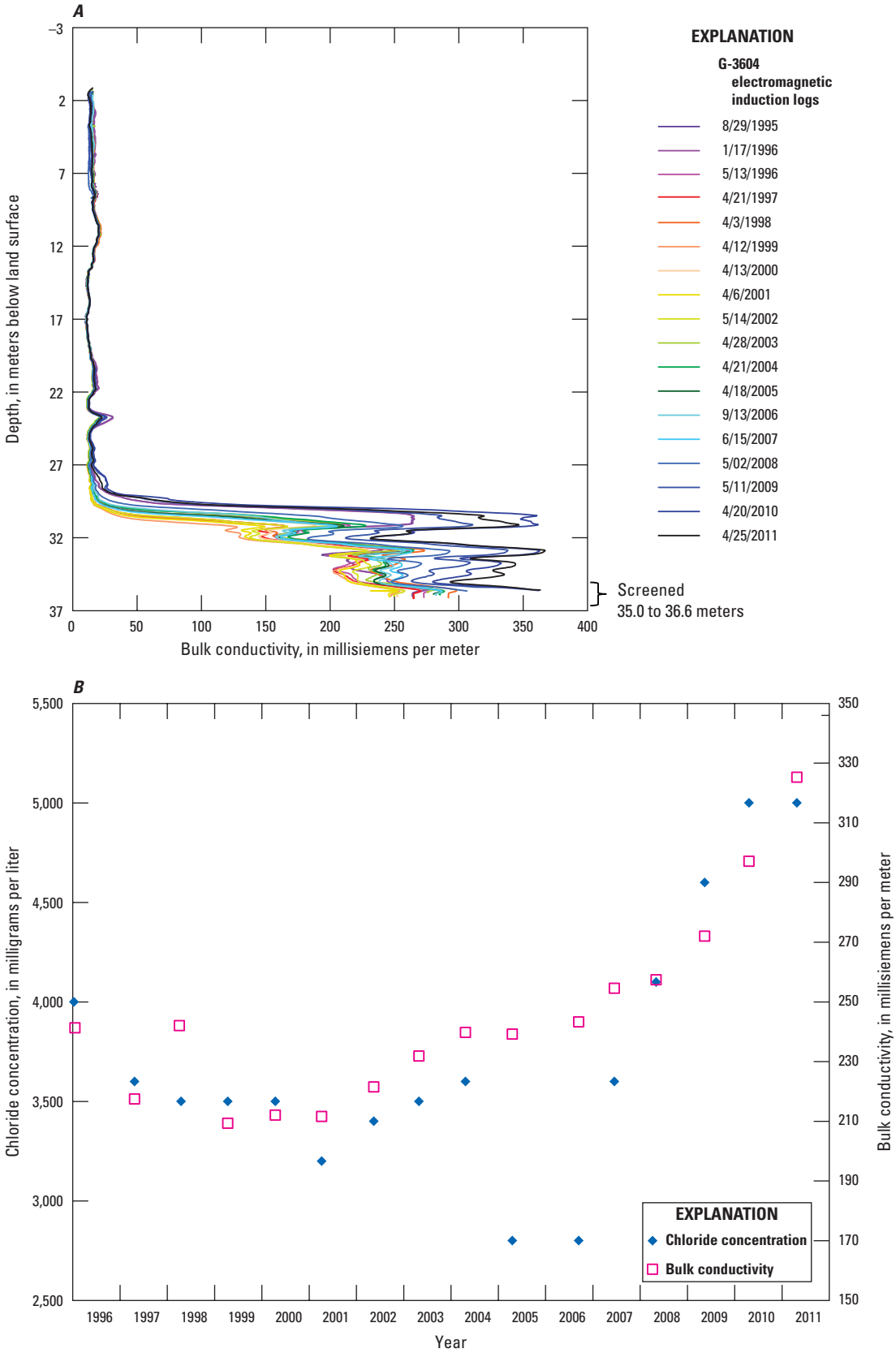

Figure 41. (*A*) Time-series electromagnetic induction log (TSEMIL) dataset; and (*B*) chloride concentrations in samples from monitoring well G–3604 and bulk conductivity measured at a depth of 34.7 meters, Biscayne aquifer, Miami-Dade County, Florida.

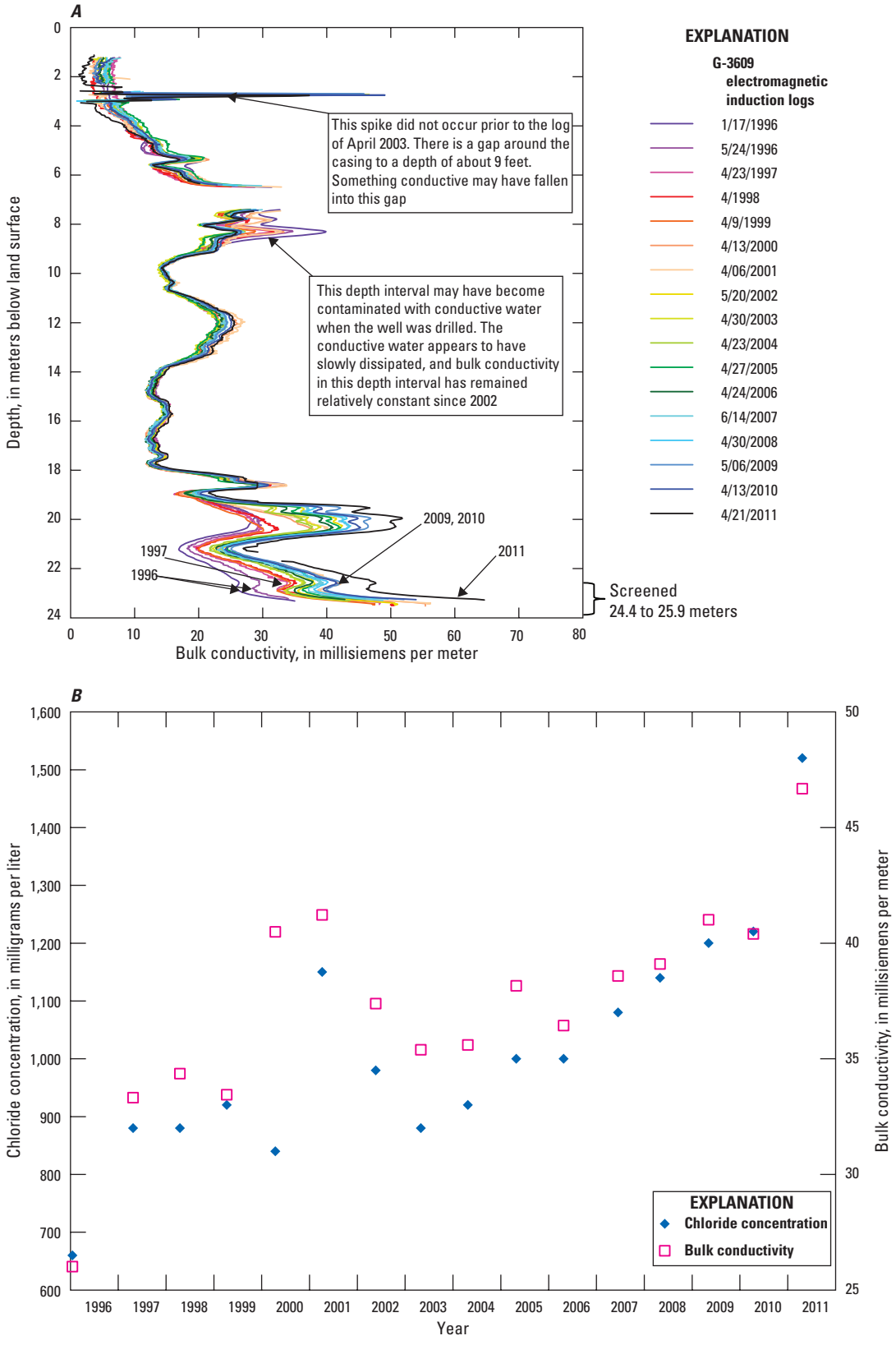

Figure 42. (*A*) Time-series electromagnetic induction log (TSEMIL) dataset; and (*B*) chloride concentrations in water samples from monitoring well G–3609 and bulk conductivity measured at a depth of 22.7 meters, Biscayne aquifer, Miami-Dade County, Florida.

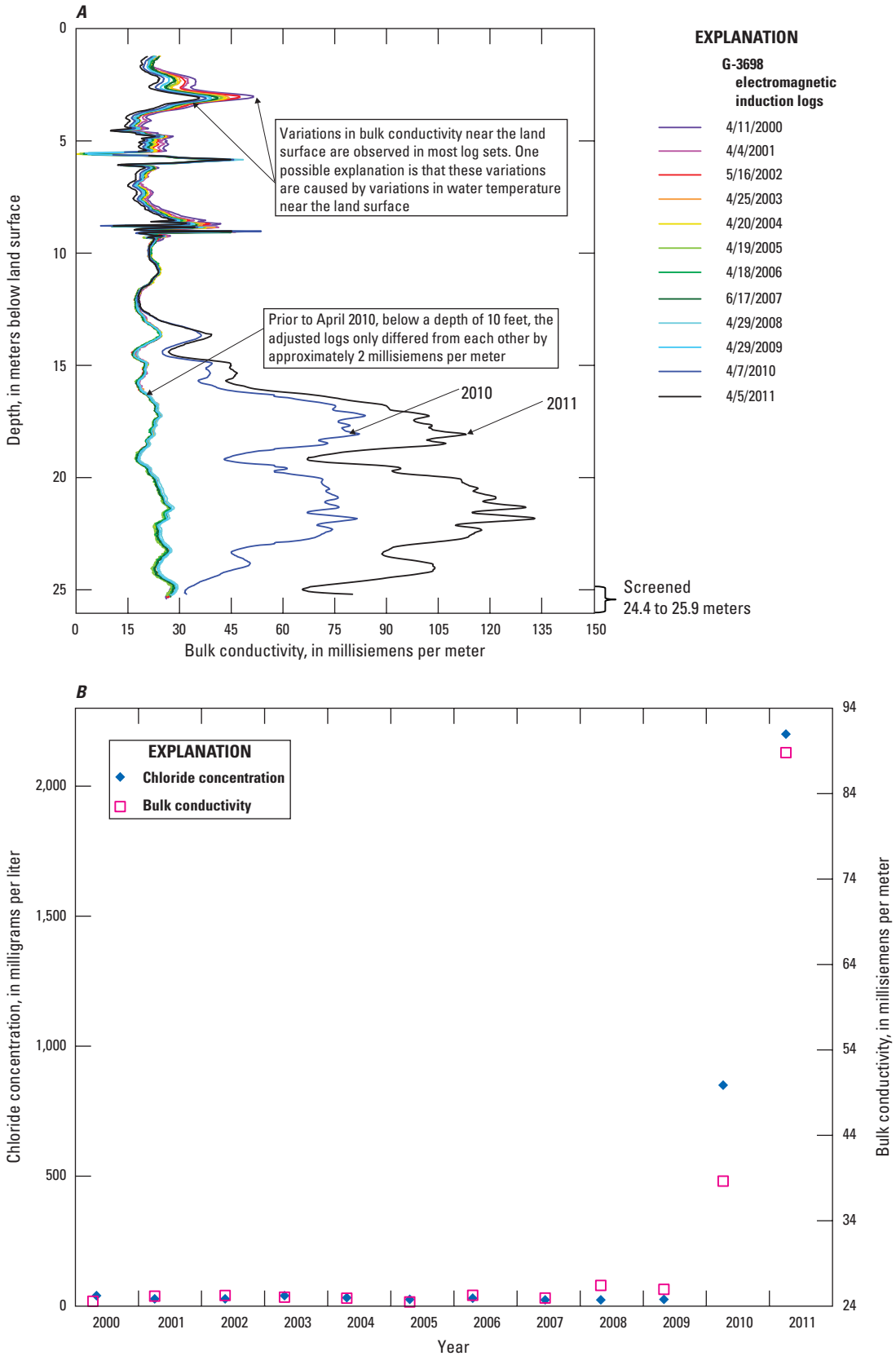

Figure 43. (*A*) Time-series electromagnetic induction log (TSEMIL) dataset; and (*B*) chloride concentrations in water samples from monitoring well G–3698 and bulk conductivity measured at a depth of 24.5 meters, Biscayne aquifer, Miami-Dade County, Florida.

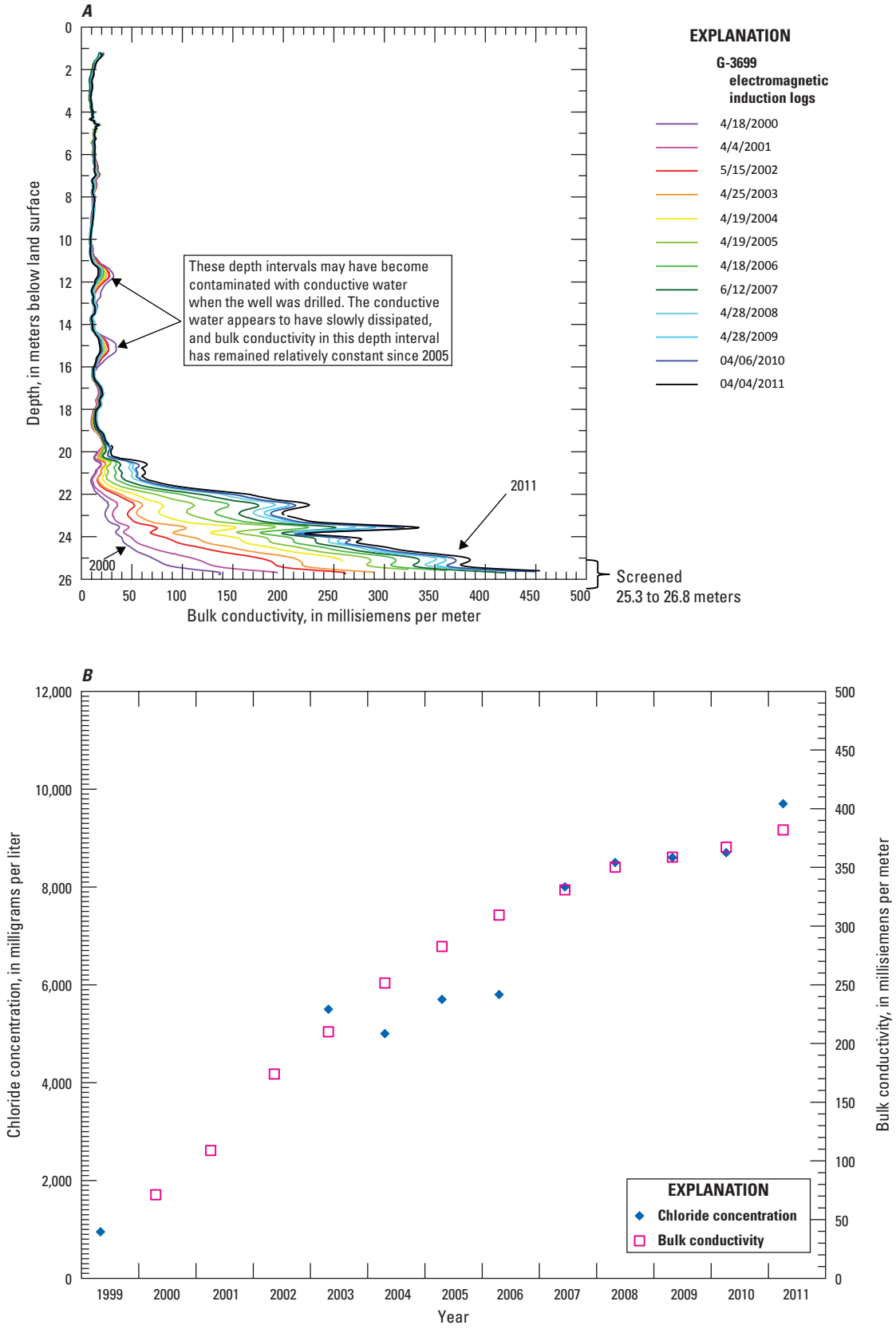

Figure 44. (*A*) Time-series electromagnetic induction log (TSEMIL) dataset; and (*B*) chloride concentrations in water samples from monitoring well G–3699 and bulk conductivity measured at a depth of 25.3 meters, Biscayne aquifer, Miami-Dade County, Florida.

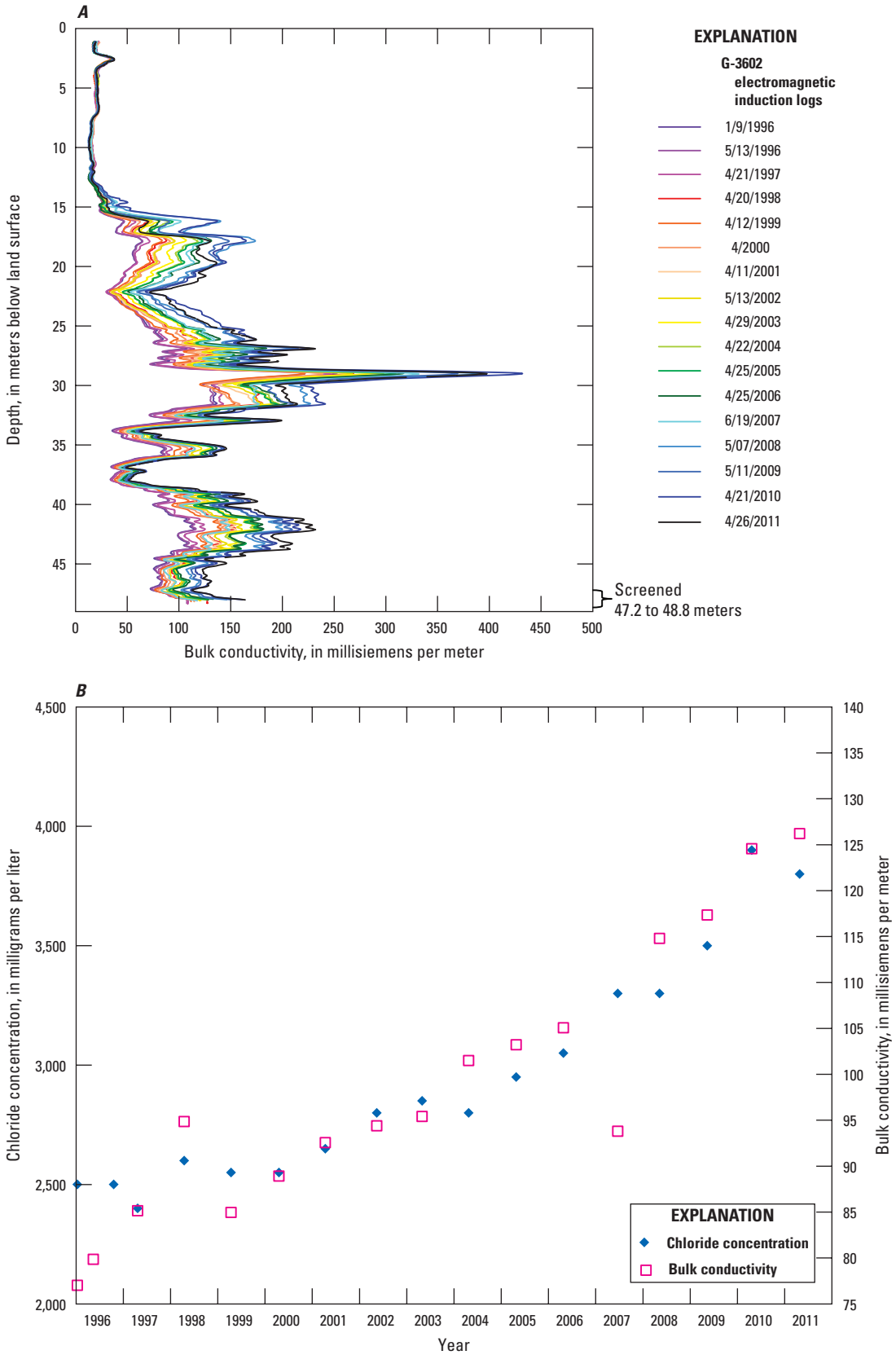

Figure 45. (*A*) Time-series electromagnetic induction log (TSEMIL) dataset; and (*B*) chloride concentrations in water samples from monitoring well G–3602 and bulk conductivity measured at a depth of 46.9 meters, Biscayne aquifer, Miami-Dade County, Florida.

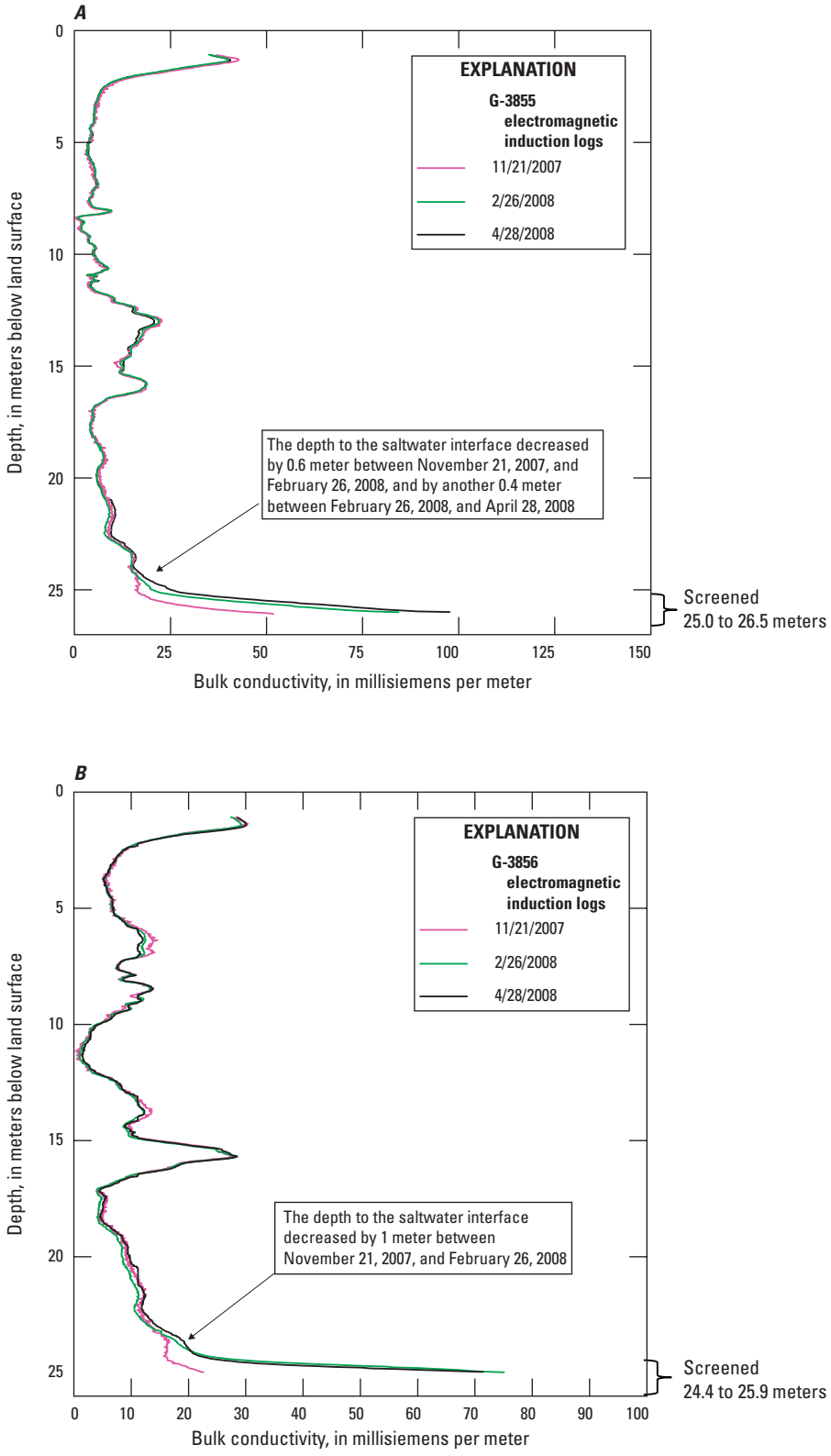

Figure 46. Time-series electromagnetic induction log (TSEMIL) datasets from monitoring wells (*A*) G–3855 and (*B*) G–3856 for November 2007 to April 2008, Biscayne aquifer, Miami-Dade County, Florida

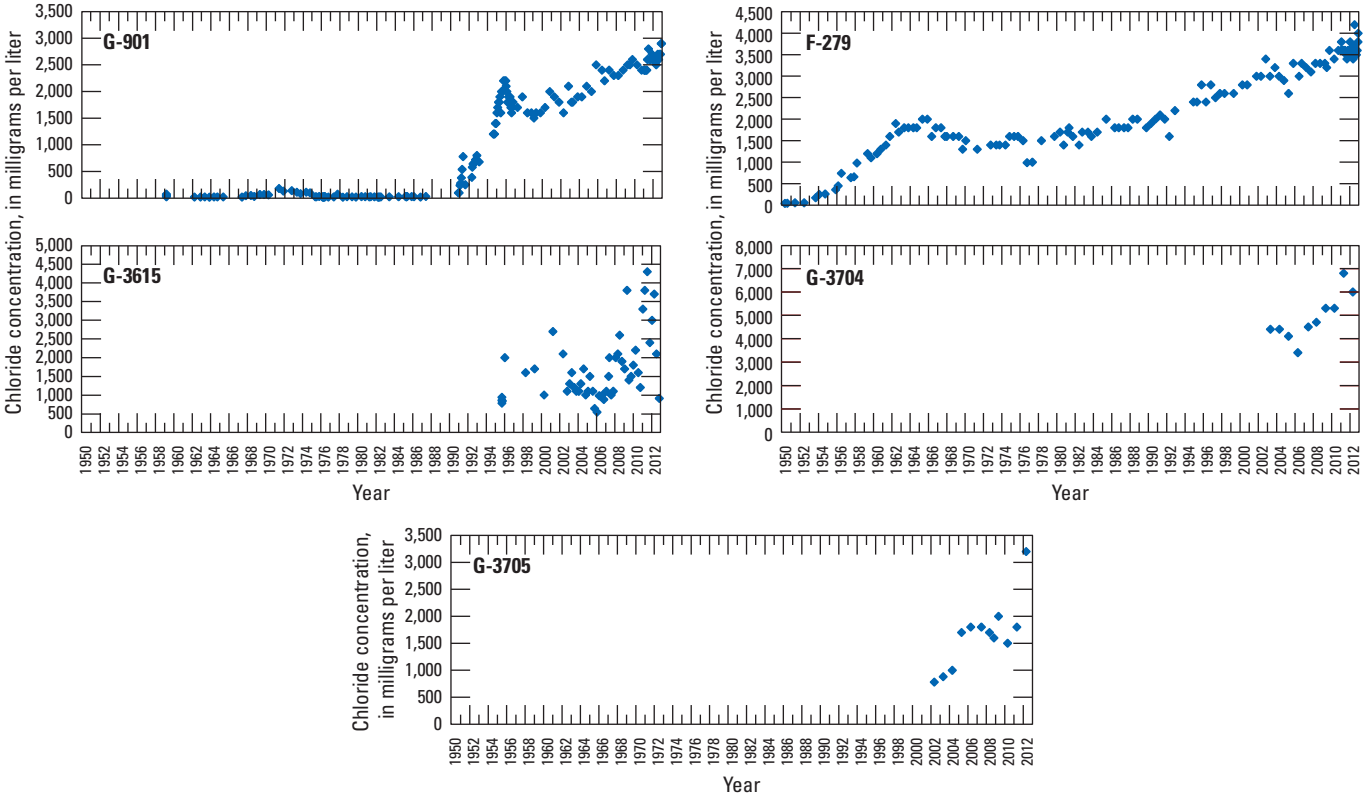

Figure 47. Chloride concentrations in samples from monitoring wells, Miami-Dade County, Florida.

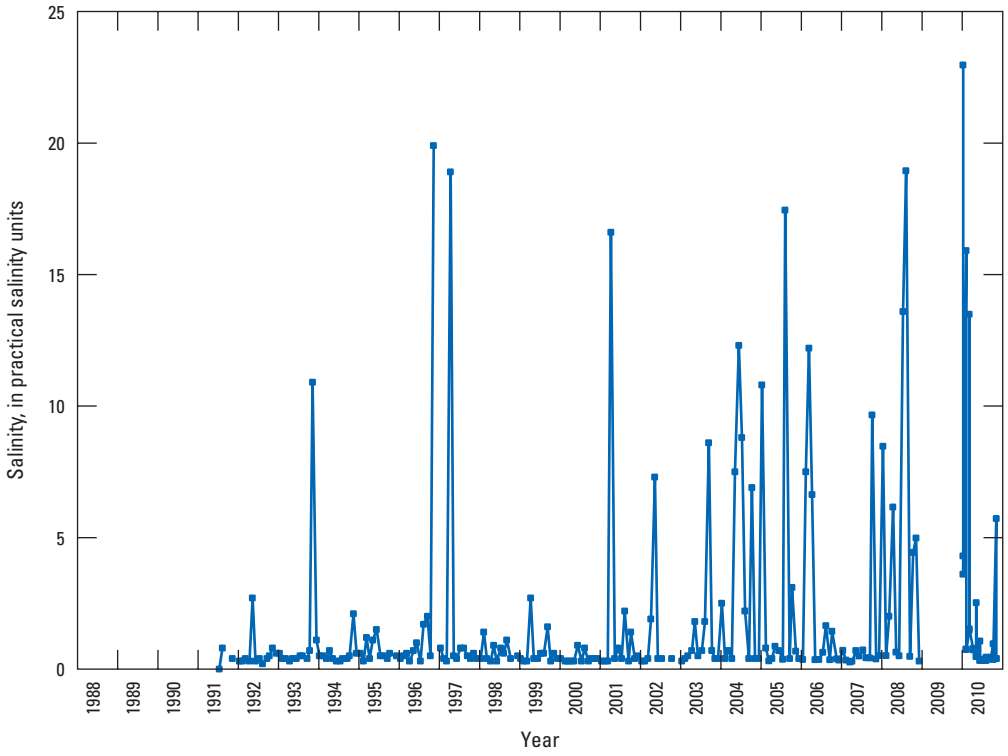

Figure 48. Salinity of the Mowry Canal at station MW04, 1991–2009 and 2010, Miami-Dade County, Florida.

example, are only 120 m apart; therefore, the inland extent of saltwater was narrowly constrained at this location. TEM sounding MIA106 indicated freshwater in the Biscayne aquifer, whereas MIA105 indicated saltwater in the aquifer (appendix 4). In general, however, the map was not this narrowly constrained. Near monitoring wells G–3229 and G–3888 (fig. 8), no other actively monitored wells are on the western side of the saltwater front to constrain the determination of its inland extent. The saltwater front (1,000 mg/L isochlor) had passed the location of well G–3229 between October 13, 2009, and December 15, 2009 (fig. 18). By February 2011, the chloride concentration in samples from G–3229 had increased to 1,500 mg/L (fig. 18). Generally, the precision and accuracy of the map showing the inland extent of saltwater in the Biscayne aquifer ranged from about ±50 m to ± 1 km, and the line showing the inland extent of saltwater in the Biscayne aquifer is referred to as "approximate" whenever referenced in a map. Some active monitoring wells, such as well G–1351 (fig. 8 and appendix 1) were too shallow to fully evaluate the extent of saltwater within the Biscayne aquifer. A few active monitoring wells, such as wells F–279 and G–3313C (fig. 8 and appendix 1) have long open intervals that may be susceptible to ambient borehole flow, which may reduce the quality of salinity measurements in the aquifer at these locations.

Most of the active monitoring wells and the TEM measurements were near the leading edge of the saltwater front. The thickness of the saltwater front throughout the aquifer cannot be fully evaluated by using active monitoring or TEM measurements. Additional monitoring, including TEM soundings and TSEMIL datasets, could allow mapping of the saltwater interface in three dimensions if collected between the leading edge of the saltwater front and the ocean. The HEM survey data collected in 2001 (figs. 1 and 16) provided detailed three-dimensional information (Fitterman and others, 2012) concerning the distribution of saltwater, but the survey was limited to a small part of the county.

Many of the monitoring wells do not extend beyond the base of the Biscayne aquifer, so the depth or occurrence of saltwater intrusion may be uncertain. Some of the TEM soundings detected saltwater in the surficial aquifer below the base of the Biscayne aquifer (Fitterman and Prinos, 2011), and some indicated freshwater throughout the surficial aquifer. The eight new monitoring wells extend below the base of the Biscayne aquifer to monitor saltwater within part of the surficial aquifer system, but the spatial coverage of wells and soundings that can evaluate salinity below the base of the Biscayne aquifer is limited.

Additional monitoring in and near canals is needed to better understand the potential effects of saltwater leakage from canals. Continuous salinity monitoring in canals, and in wells adjacent to the canals, could help quantify the amount of saltwater leaking from these canals upstream of the salinity control structures. Additional TEM soundings, resistivity surveys, or monitoring wells could be used to better delineate the inland extent of saltwater near canals.

Movement of the saltwater front is an ongoing phenomenon. The data collected for this study spanned 4 years, and during that time, many of the wells were actively monitored; as a result, the most recent information was used to produce the maps of the inland extent of saltwater in 2008 and 2011. TEM soundings were completed during a 2-year period, however, and provided spatial coverage where there were no existing data; therefore, in some locations, the extent of the saltwater front may have already changed by the time the 2011 map (fig. 8) was created. In addition, the HEM survey that was calibrated and published in 2012 (Fitterman and others) had been collected in 2001. If a new HEM survey had been collected during this study, it potentially could have been calibrated using the TEM soundings collected in 2009, which would have provided a direct comparison of the 2001 survey with a more recent survey.

Additional samples for $^{3}H/^{3}He$ age dating could increase the understanding of the sources of saltwater and the movement of saltwater and freshwater in the aquifer. SF_6 data could potentially have provided spatially distributed age dating information, but excess SF_6 in the aquifer prevented the use of this method. Analyses of the ages of samples were based on the assumption of piston flow because there was insufficient information to evaluate the potential mixing of younger and older water at each location. The piston-flow assumption may not be valid because most of the samples were collected from near the freshwater/saltwater interface where mixing likely occurred. This mixing may have affected the ages determined for some samples; however, if old tritium-free water were mixed with young water, the age determined could still be accurate because tritium/helium age dating is based on an isotopic ratio (Plummer and others, 2003).

Summary and Conclusions

In Miami-Dade County, the principal source of drinking water is the Biscayne aquifer. Prior to development, the estimated level of freshwater (3 to 4.3 m) in the Everglades near Miami was likely sufficient to prevent saltwater encroachment in the Biscayne aquifer in this area. The head differential between the Everglades and the coast was evidenced by numerous freshwater springs that flowed near the coast line and boiled up in Biscayne Bay. Beginning in 1845, drainage canals effectively drained the Everglades and resulted in an estimated 2.9-m permanent reduction in Biscayne aquifer water levels in east-central Miami-Dade County, which allowed saltwater to encroach landward along the base of the Biscayne aquifer. Landward encroachment was exacerbated during drought periods when water levels in the aquifer fell to or below sea level. Saltwater also flowed inland up the canals and into the Biscayne aquifer. Water control structures on most of the major drainage canals in Miami-Dade County reduced, but did not completely eliminate, the ability of saltwater to flow inland through these canals during drought periods. The various pathways of seawater into the highly permeable Biscayne aquifer have combined to intrude approximately 1,200 km^2 of this aquifer with saltwater.

To map the inland extent of saltwater in the Biscayne aquifer, the following data were compiled and analyzed: (1) all available salinity information, (2) TSEMIL datasets from 35 wells that were processed using a newly developed method, (3) TEM soundings collected at 79 locations in 2008 and 2009 and used to evaluate the depth to saltwater (if present) and the depth to the base of the Biscayne aquifer, (4) a HEM survey collected in 2001 that was processed and interpreted during this study, (5) cores and geophysical logs collected from 8 sites for stratigraphic analysis, (6) analyses of samples from 8 new single or multi-depth monitoring wells installed in these core holes, and (7) analyses of 69 geochemical samples. These data were evaluated, and GIS software was used to map the inland extent of saltwater in the Biscayne aquifer in 2008 and in 2011.

The saltwater front was mapped farther inland than it was in 1995 in eight approximated areas totaling 24.1 km^2, most notably near the Florida City Canal where the front had advanced by as much as 1.9 km between 1995 and 2011. The saltwater interface was mapped closer to the coast than it was in 1995 in four approximated areas totaling 6.2 km^2. The saltwater interface was mapped closer to the coast near the Snapper Creek Canal than it had been in 1995. Some revisions to the saltwater interface were the result of the improved spatial coverage provided by additional wells, TEM soundings, and the HEM survey. One area with extensive revisions resulting primarily from improved spatial coverage was near the Card Sound Road Canal and U.S. Highway 1.

The sources and changes in the distribution of saltwater in the Biscayne aquifer were evaluated by using (1) geochemical sampling, (2) salinity measurements collected in canals, and (3) TSEMIL datasets. A total of 69 geochemical water samples were collected from 44 sites. Analyses included (1) major ion chemistry and trace ion chemistry, (2) strontium isotope ratios, (3) oxygen and hydrogen isotope ratios, (4) tritium concentration, (5) tritium/helium-3 ($^3H/^3He$) age dating, (6) sulfur hexafluoride (SF_6) age dating, and (7) dissolved gas composition.

The results of geochemical analyses indicate that saltwater intrusion has recently arrived at wells G–1264, G–3615, G–3698, G–3699, G–3704, G–3705, and G–3855. Long-term records of chloride concentration confirm that the saltwater interface (1,000 mg/L) first became evident at most of these locations during or after 1994. Geochemical analyses at wells FKS4, FKS8, G–939, G–3600, G–3601, G–3602, G–3604, and G–3605 generally indicate preexisting saltwater intrusion as reported by previous researchers.

Droughts and intruded saltwater are closely connected. The piston-flow ages determined from $^3H/^3He$ age samples of saltwater with a chloride concentration of about 1,000 mg/L or greater generally correspond to a period of frequent droughts. Recharge temperatures of water samples determined by using dissolved-gas analyses are consistent with air temperatures that occur in April or early May, when water levels are typically at their lowest. Conversely, most of the samples of water with chloride concentrations less than about 1,000 mg/L indicate recharge temperatures corresponding to air temperatures in mid to late May when water levels in the aquifer begin to increase, and the piston-flow age determinations correspond to wet years. The piston-flow ages of freshwater samples were generally younger than ages determined for saltwater.

The silica concentrations in samples from well G–3701 indicate that this well is screened in the Pinecrest Sand Member of the Tamiami Formation below the base of the Biscayne aquifer. Samples from the wells G–3600 and G–3601, which are screened in a part of the Biscayne aquifer that includes the Tamiami Formation, also indicated silica concentrations that were elevated relative to samples from most other wells.

The strontium ($^{87}Sr/^{86}Sr$) isotope ratio in samples was used to evaluate the origin of saltwater in the Biscayne aquifer, but the method did not prove useful because the standard error was too large relative to the range of the $^{87}Sr/^{86}Sr$ isotope ratios in the study area. Most of the $^{87}Sr/^{86}Sr$ isotope ratios determined from samples corresponded with the Pleistocene age of most sediments in the Biscayne aquifer. Two of the lowest ratios were observed for samples from wells G–3701 and G–3601. These wells likely are open to materials that are of Pliocene age.

Oxygen and hydrogen isotopes indicated that water from well G–3608 was similar in isotopic composition to water from the adjacent Snapper Creek Canal. The relatively shallow increase in bulk conductivity evident in the TSEMIL dataset from G–3608, the interpreted piston-flow age of water from this well, and the local hydraulic gradient indicated that the saltwater at this location likely emanated from seawater that had flowed up the Snapper Creek Canal and leaked into the aquifer.

Geochemical analyses had indicated preexisting saltwater intrusion at wells G–3600, G–3601, G–3602, G–3604, and G–3605. The highest tritium concentrations (3.2 to 53.3 TU) measured during the study were measured in water from wells FKS4, FKS7, G–1264, G–3698, G–3699, G–3855, and G–3856. These seven wells are within 10 km of the Turkey Point Nuclear Power Plant, and hypersaline water with high tritium concentrations from the cooling canals may be contributing to saltwater encroachment near the wells. Geochemical analyses and long-term monitoring data from wells G–1264, G–3698, G–3699, G–3855, and G–3856 confirmed the recent arrival of saltwater intrusion.

$^3H/^3He$ age dating indicated that the water sampled from wells G–3601 and G–3701 contained too little tritium to be evaluated using this method. The sample from well G–3600 showed the characteristics of gas fractionation and could not be dated using $^3H/^3He$ age dating. Water samples from wells G–3600, G–3601, G–3602, G–3604, and G–3701 also indicated silica concentrations that were greater than the theoretical mixing of freshwater and saltwater in the area would produce. These elevated silica concentrations could be caused by relatively longer residence times within a quartz-sand-rich formation.

SF_6 age dating could not be used effectively in the study area principally because there was excess SF_6 in most samples that may have been caused by leakage of SF_6 from electrical switching facilities. Moreover, SF_6-interpreted piston-flow ages are generally younger than $^3H/^3He$ ages. The lowest SF_6 concentrations determined were for water sampled from wells G–3601 and G–3701. These samples also contained no tritium.

Evaluations of long-term chloride monitoring and the geochemistry of water samples indicated that the saltwater sampled in the Biscayne aquifer is likely not relict seawater of Pleistocene or Pliocene ages. Some saltwater likely leaked from canals prior to the installation of water control structures. Near the Miami Canal northwest of the water control structure S–26, this saltwater is gradually mixing with the groundwater, and salinity is gradually decreasing. Modern leakage of saltwater likely is occurring along the Card Sound Road Canal and upstream of salinity control structures in the Biscayne, Black Creek, and Snapper Creek Canals. Saltwater also may have leaked from the Princeton Canal and the canal adjacent to well G–3698, although this leakage could not be confirmed or refuted with available information.

Additional information, such as TEM soundings or resistivity surveys collected from the canals and monitoring wells adjacent to these canals, could be used to evaluate the effect that saltwater leakage around or through existing structures has on the inland extent of saltwater in the Biscayne aquifer. Influxes of saltwater in canals may be undetected because the interval between samples is too long. Continuous salinity monitoring in canals could be useful in the detection of any future influxes of saltwater upstream of existing water control structures.

Selected References

Aeschbach-Hertig, W., Peeters, F., Beyerle, U., and Kipfer, R., 1999, Interpretation of dissolved atmospheric noble gases in natural waters: Water Resources Research, v. 35, p. 2779–2792.

Aeschbach-Hertig, W., Peeters, F., Beyerle, U., and Kipfer, R., 2000, Paleotemperature reconstruction from noble gases in ground water taking into account equilibration with entrapped air: Nature, v. 405, p. 1040–1044.

Anderson, P.F., Mercer, J.W., and White, H.O., 1988, Numerical modeling of salt-water intrusion at Hallandale, Florida: Ground Water, v. 26, no. 5, p. 619–633.

ASTM International, 2007, Standard guide for conducting borehole geophysical logging—electromagnetic induction: ASTM International D 6726–01 (reapproved 2007), 8 p.

Barlow, P.M., 2003, Ground water in freshwater-saltwater environments of the Atlantic Coast: U.S. Geological Survey Circular 1262, 113 p.

Bearden, H.W., 1974, Groundwater resources of the Hollywood area, Florida: State of Florida, Department of Natural Resources, Division of Interior Resources, Bureau of Geology, Report of Investigations no. 77, 35 p.

Begemann, Friedrich, and Friedman, Irving, 1959, Tritium and deuterium content of atmospheric hydrogen: Zeitschrift für Naturforschung, v. 14a, p. 1024.

Benson, M.A., and Gardner, R.A., 1974, The 1971 drought in South Florida and its effect on the hydrologic system: U.S. Geological Survey Water-Resources Investigations Report 74–12, p. 35–37.

Bridges, W.B., Franklin, M.A., and Fleeson, T.A., 1991, Florida floods and droughts in Paulson, R.W., and others, eds., National Water Summary 1988–89—Hydrologic events and floods and droughts: U.S. Geological Survey Water-Supply Paper 2375, p. 231–238.

Brown, J.S., 1925, A study of coastal ground water, with special reference to Connecticut: U.S. Geological Survey Water-Supply Paper 537, p. 16–17.

Brown, R.H., and Parker, G.G., 1945, Salt water encroachment in limestone at Silver Bluff, Miami, Florida: Economic Geology, v. 60, no. 4, p. 235–262.

Busenberg, Eurybiades, and Plummer, L.N., 2000, Dating young groundwater with sulfur hexafluoride: Natural and anthropogenic sources of sulfur hexafluoride: Water Resources Research, v. 36, p. 3011–3030.

Busenberg, Eurybiades, Plummer, L.N., Doughten, M.W., Widman, P.K., and Bartholomay, R.C., 2000, Chemical and isotopic composition and gas concentrations of ground water and surface water from selected sites at and near the Idaho National Engineering and Environmental Laboratory, Idaho, 1994–97: U.S. Geological Survey Open-File Report 00–81, 51 p.

Busenberg, Eurybiades, Weeks, E.P., Plummer, L.N., and Bartholemay, R.C., 1993, Age dating ground water by use of chlorofluorocarbons (CC13F and CC12F2), and distribution of chlorofluorocarbons in the unsaturated zone, Snake River Plain aquifer, Idaho National Engineering laboratory, Idaho: U.S. Geological Survey Water-Resources Investigations Report 93–4054, 47 p.

Causaras, C.R., 1987, Geology of the surficial aquifer system, Dade County, Florida: U.S. Geological Survey Water-Resources Investigations Report 86–4126, 240 p., 2 sheets.

Clesceri, L.S., Greenburg, A.E., and Eaton, A.D., eds., 1998, Standard methods for the examination of water and wastewater (20th ed.): Washington, D.C., American Public Health Association, American Water Works Association, and Water Environment Federation, p. 3–37 to 3–43.

Craig, Harmon, 1961, Standard for reporting concentrations of deuterium and oxygen-18 in natural waters: Science, v. 133, p. 1833–1834.

Cross, W.P., and Love, S.K., 1942, Groundwater in southeastern Florida: Journal of the American Water Works Association, v. 34, no. 4, p. 490–504.

Cunningham, K.J., Bukry, D., Sato, T., Barron, J.A., Guertin, L.A., and Reese, R.S., 2001, Sequence stratigraphy of a south Florida carbonate ramp and bounding siliciclastics (late Miocene-Pliocene), *in* Missimer, T.M., and Scott, T.M., eds., Geology and hydrology of Lee County: Florida Geological Survey Special Publication 49, p. 35–66.

Cunningham, K.J., Carlson, J.L., Wingard, G.L., Robinson, Edward, and Wacker, M.A., 2004, Characterization of aquifer heterogeneity using cyclostratigraphy and geophysical methods in the upper part of the karstic Biscayne aquifer, southeastern Florida: U.S. Geological Survey Water-Resources Investigations Report 03–4208, 46 p.

Cunningham, K.J., Locker, S.D., Hine, A.C., Bukry, D., Barron, J.A., and Guertin, L.A., 2003, Interplay of late Cenozoic siliciclastic supply and carbonate response on the southeast Florida Platform: Journal of Sedimentary Research, v. 73, no. 1, p. 31–46.

Cunningham, K.J., McNeill, D.F., Guertin, L.A., Ciesielski, P.F., Scott, T.M., and de Verteuil, L., 1998, New Tertiary stratigraphy for the Florida Keys and southern peninsula of Florida: Geological Society of America Bulletin, v. 110, no. 2, p. 231–258.

Cunningham, K.J., Renken, R.A., Wacker, M.A., Zygnerski, M.R., Robinson, E., Shapiro, A.M., and Wingard, G.L., 2006a, Application of carbonate cyclostratigraphy and borehole geophysics to delineate porosity and preferential flow in the karst limestone of the Biscayne aquifer, SE Florida, *in* Harmon, R.S., and Wicks, C., eds., Perspectives on karst geomorphology, hydrology, and geochemistry—A tribute volume to Derek C. Ford and William B. White: Geological Society of America Special Paper 404, p. 191–208.

Cunningham K.J., Sukop, M.C., Huang, H., Alvarez, P.F., Curran, H.A., Renken, R.A., and Dixon, J.F, 2009a, Prominence of ichnologically influenced macroporosity in the karst Biscayne aquifer—Stratiform “super K” zones: GSA Bulletin, v. 121, no. 1/2, p. 164–180.

Cunningham, K.J., and Wacker, C., 2009, Seismic-sag structural systems in Tertiary carbonate rocks beneath southeastern Florida, USA—Evidence for hypogenic speleogenesis? *in* Klimchouk, A.B., and Ford, D.C., eds., Hypogene speleogenesis and karst hydrogeology of artesian basins: Simferopol, Ukraine, Ukrainian Institute of Speleology and Karstology, Special Paper no. 1, p. 151–158.

Cunningham, K.J., Wacker, M.A., Robinson, Edward, Dixon, J.F., and Wingard, G.L., 2006b, A cyclostratigraphic and borehole geophysical approach to development of a three-dimensional conceptual hydrogeologic model of the karstic Biscayne aquifer, southeastern Florida: U.S. Geological Survey Scientific Investigations Report 2005–5235, 75 p., 4 sheets.

Davis, S.N., Whittemore, D.O., and Fabryka-Martin, June, 1998, Uses of chloride/bromide ratios in studies of potable water: Ground Water, v. 36, no. 2, p. 338–350.

Federal Register Notice, 1979, October 11, 1979, v. 44, no. 198.

Fish, J.E., 1988, Hydrogeology, aquifer characteristics, and groundwater flow of the surficial aquifer system, Broward County, Florida: U.S. Geological Survey Water-Resources Investigations Report 87–4034, 80 p.

Fish, J.E., and Stewart Mark, 1991, Hydrogeology of the surficial aquifer system, Dade County, Florida: U.S. Geological Survey Water-Resources Investigations Report 90–4108, 50 p., 11 sheets.

Fishman, M.J., ed., 1993, Methods of analysis by the U.S. Geological Survey National Water Quality Laboratory—Determination of inorganic and organic constituents in water and fluvial sediments: U.S. Geological Survey Open-File Report 93–125, 217 p.

Fishman, M.J., and Friedman, L.C., 1989, Methods for determination of inorganic substances in water and fluvial sediments: U.S. Geological Survey Techniques of Water-Resources Investigations, book 5, chap. A1, 545 p.

Fitterman, D.V., 1989, Detectability levels for central induction transient soundings: Geophysics, v. 54, p. 127–129.

Fitterman, D.V., and Deszcz-Pan, Maria, 1998, Helicopter EM mapping of saltwater intrusion in Everglades National Park: Florida Exploration Geophysics, v. 29, p. 240–243.

Fitterman, D.V., and Deszcz-Pan, Maria, 2002, Helicopter electromagnetic data from Everglades National Park and surrounding areas, Florida—Collected 9–14 December 1994: U.S. Geological Survey Open-File Report 2002–101, 1 CD-ROM.

Fitterman, D.V., Deszcz-Pan, Maria, and Prinos, S.T., 2012, Helicopter electromagnetic survey of the Model Land Area, southeastern Miami-Dade County, Florida: U.S. Geological Survey Open-File Report 2012–1176, 75 p., 1 app.

Fitterman, D.V., Deszcz-Pan, Maria, and Stoddard, C.E., 1999, Results of time-domain electromagnetic soundings in Everglades National Park, Florida (on CD–ROM): U.S. Geological Survey Open-File Report 99–426, 152 p.

Fitterman, D., and Labson, V.F., 2005, Electromagnetic induction methods for environmental problems, *in* Butler, D.K., ed., Near-surface geophysics, part 1—Concepts and fundamentals: Tulsa, Society of Exploration Geophysicists, p. 295–349.

Fitterman, D.V., and Prinos, S.T., 2011, Results of time-domain electromagnetic soundings in Miami-Dade and southern Broward Counties, Florida: U.S. Geological Survey Open-File Report 2011–1299, 289 p.

Fitterman, D.V., and Stewart, M.T., 1986, Transient electromagnetic sounding for groundwater: Geophysics, v. 51, p. 995–1005.

Fletcher, D.U., 1911, Everglades of Florida—Acts, reports and other papers State and National, relating to the Everglades of the State of Florida and their reclamation: Washington, Government Printing Office, 193 p.

Florea, L.J., McGee, D.K., and Wynn, J.G., 2010, Stable isotopic and geochemical variability within shallow groundwater beneath a hardwood hammock and surface water in an adjoining slough (Everglades National Park, FL): Proceedings of the 14th Symposium on the Geology of the Bahamas and other Carbonate Regions, 15 p., accessed October 31, 2012, at *http://digitalcommons.wku.edu/geog_fac_pub/14*.

Florida Department of Environmental Protection, 2001, Southeast district assessment and monitoring program, ecosummary, Miami River, Miami-Dade County, accessed January 31, 2011, at *http://www.dep.state.fl.us/southeast/ecosum/ecosums/Miami_River.pdf*.

Florida Department of Health, 2005, Chemicals in private drinking water wells—Fact sheet—Sodium: Florida Department of Health, 2 p.

Florida Division of Emergency Management, 2009, Miami-Dade County 2 ft contour lines: Tallahassee, FL, Florida Division of Emergency Management, Shapefile, accessed February 10, 2011, at *http://www.floridadisaster.org/gis/index.asp*.

Fuller, M.L., 1904, Contributions to the hydrology of eastern United States: U.S. Geological Survey Water-Supply Paper 102.

Galli, Gianni, 1991, Mangrove-generated structures and depositional model of the Fort Thompson Formation (Florida Plateau): Facies, v. 25, p. 297–314.

Garbarino, J.R., 1999, Methods of analysis by the U.S. Geological Survey National Water Quality Laboratory—Determination of dissolved arsenic, boron, lithium, selenium, strontium, thallium, and vanadium using inductively coupled plasma-mass spectrometry: U.S. Geological Survey Open-File Report 99–093, 31 p.

Garbarino, J.R., Kanagy, L.K., and Cree, M.E., 2006, Determination of elements in natural-water, biota, sediment, and soil samples using collision/reaction cell inductively coupled plasma-mass spectrometry: U.S. Geological Survey Techniques and Methods, book 5, sec. B, chap. 1, 88 p.

Geonics Limited, 2006, Protem 47D operating manual for 20/30 gate model: Geonics Limited, 80 p.

Guertin, L.A., 1998, A late Cenozoic mixed carbonate/siliciclastic system, south Florida—Lithostratigraphy, chronostratigraphy, and sea-level record: Miami, University of Miami, Ph.D. dissertation, 335 p.

Ghyben, W.B., 1889, Nota in verband met de voorgenomen putboring nabij Amsterdam; K. Inst Ing. Tijdschr, 1888–89, p. 21.

Gibson, J.J., Edwards, T.W.D., Bursey, G.G., and Prowse, T.D., 1993, Estimating evaporation using stable isotopes: Quantitative results and sensitivity analysis for two catchments in northern Canada: Nordic Hydrology, no. 24, p. 79–94.

Godfrey, M.C., 2006, River of interests—Water management in south Florida and the Everglades, 1948–2000: U.S. Army Corps of Engineers, 460 p.

Goldman, M., Gilad, D., Ronen, A., and Melloul, A., 1991, Mapping seawater intrusion into the coastal aquifer of Israel by the time domain electromagnetic method: Geoexploration, v. 28, p. 153–174.

Hagemeyer, Bart, 2012, ENSO's relation with Florida's climate and predictability—Florida dry season forecast and El Niño-Southern Oscillation (EÑSO): National Aeronautical and Atmospheric Administration, National Weather Service Forecast Office, Melbourne Florida, accessed January 23, 2012, at *http://www.srh.noaa.gov/mlb/?n=enso_florida_climate_forecast*.

Harvey, J.W., Krupa, S.L., Gefvert, Cynthia, Mooney, R.H., Choi, Jungyill, King, S.A., and Giddings, J.B., 2002, Interactions between surface water and ground water and the effects of mercury transport in the north-central Everglades: U.S. Geological Survey Water-Resources Investigations Report 02–4050, 82 p.

Heaton, T.H.E., 1981, Dissolved Gases: Some Applications to Groundwater Research: Transactions of the Geological Society of South Africa, v. 84, p. 91–97.

Heaton, T.H.E., and Vogel, J.C., 1981, "Excess air" in groundwater: Journal of Hydrology, v. 50, p. 201–216.

Herzberg, A., 1901, Die Wasserversorgung einiger Nordseebader [The water supply on parts of the North Sea coast]: Munich, Jour. Gasbeleuchtung und Wasser versorgung, v. 44, p. 815–819, 842–844.

Hickey, T.D., Hine, H.C., Shinn, E.A., Kruse, S.E., and Poore, R.Z., 2010, Pleistocene carbonate stratigraphy of south Florida—Evidence for high-frequency sea-level cyclicity: Journal of Coastal Research, v. 26, no. 4, p. 605–614.

Hinkle, S.R., Shapiro, S.D., Plummer, L.N., Busenberg, Eurybiades, Widman, P.K., Casile, G.C., and Wayland, J.E., 2010, Estimates of tracer-based piston-flow ages of groundwater from selected sites—National Water-Quality Assessment Program, 1992–2005: U.S. Geological Survey Scientific Investigations Report 2010–5229, 90 p.

Hittle, C.D., 1999, Delineation of saltwater intrusion in the surficial aquifer system in eastern Palm Beach, Martin, and St. Lucie Counties, Florida, 1997–98: U.S. Geological Survey Water-Resources Investigations Report 99–4214, 1 sheet.

Hoffmeister, J.E., Stockman, K.W., and Multer, H.G., 1967, Miami limestone and its recent Bahamian counterpart: Geological Society of America Bulletin v. 78, p. 175–190.

Howard, K.W.F., and Lloyd, J.W., 1983, Major ion characterization of coastal saline ground waters: Groundwater, v. 21, no. 4, p. 429–437.

Howarth, R.J., and McArthur, J.M., 1997, Statistics for strontium isotope stratigraphy; a robust LOWESS fit to the marine Sr-isotope curve for 0 to 206 Ma with look-up table for derivation of numeric age: The Journal of Geology, v. 105, no. 4, p. 441–456.

Hoy, N.D., 1952, Two maps of Dade County, Florida, showing approximate position of the 1,000-ppm isochlor as of 1951 and approximate area of potential salt-water penetration under 1945 conditions: U.S. Geological Survey Open-File Report 52–78.

Hoy, N.D., and others, 1951, Six cross sections and an index map of the Miami area, Florida, showing changes in the position of the salt front in the Biscayne aquifer from 1946 to 1950: U.S. Geological Survey Open-File Report 51–119.

Hughes, J.D., Langevin, C.D., and Brakefield-Goswami, Linzy, 2010, Effect of hypersaline cooling canals on aquifer salinization: Hydrogeology Journal, v. 18, p. 25–38.

Janzen, J.H., and Krupa, Steven, 2011, Water quality characterization of southern Miami-Dade County and nearby FPL Turkey Point Power Plant, Miami-Dade County, Florida: South Florida Water Management District Technical Publication WS–31, 5 sections, 171 p., 6 appendixes.

Jennings, W.S., 1909, Letter in annual report of Trustees of the Internal Improvement Fund, State of Florida, p. 122.

Jones, B.F., Vengosh, A., Rosenthal, E., and Yechieli, Y., 1999, Geochemical Investigations, in Bear, Jacob, Cheng, A.H.D., Sorek, Shaul, Ouazar, Driss, and Herrera, Ismael, eds., Seawater intrusion in coastal aquifers—Concepts, methods, and practices: Dordrecht, Netherlands, Kluwer Academic Publishers, 625 p.

Katz, B.G., and Bullen, T.D., 1996, The combined use of $^{87}Sr/^{86}Sr$ and carbon and water isotopes to study the hydrochemical interaction between groundwater and lakewater in mantled karst: Geochimica et Cosmochimica Acta, v. 60, no. 24, p. 5075–5087.

Kaufman, A.A., and Keller, G.V., 1983, Frequency and transient sounding: Amsterdam, Elsevier, 685 p.

Keller, G.V., and Frischknecht, F.C., 1966, Electrical methods in geophysical prospecting: International Series of Monographs in Electromagnetic Waves: Oxford, Pergamon Press, 519 p.

Kendall, C., and Coplen, T.B., 2001, Distribution of oxygen-18 and deuterium in river waters across the United States: Hydrological Processes, v. 15, p. 1363–1393.

Klein, Howard, 1957, Salt-water encroachment in Dade County, Florida: Florida Geological Survey Information Circular 9, 5 p.

Klein, Howard, 1965, Probable effect of Canal 111 on salt-water encroachment, southern Dade County Florida: U.S. Geological Survey Open-File Report 65–86, 26 p.

Klein, Howard, and Hull, J.E., 1978, Biscayne Aquifer, Southeast Florida: U.S. Geological Survey Water-Resources Investigations Report 78–107, p. 22–27.

Klein, Howard, and Ratzlaff, K.W., 1989, Changes in salt-water intrusion in the Biscayne aquifer, Hialeah-Miami Springs area, Dade County, Florida: U.S. Geological Survey Water-Resources Investigations Report 87–4249, 1 sheet.

Klein, Howard, and Waller, B.G., 1985, Synopsis of salt-water intrusion in Dade County, Florida, through 1984: U.S. Geological Survey Water-Resources Investigations Report 85–4101, 1 sheet.

Kohout, F.A., 1964, The flow of fresh water and salt water in the Biscayne aquifer of the Miami area, Florida, *in* Cooper, H.H., Jr., Kohout, F.A., Henry, H.R., and Glover, R.E., Sea water in coastal aquifers: U.S. Geological Survey Water-Supply Paper 1613–C, p. C12–C32.

Kohout, F.A., and Hoy, N.D., 1963, Some aspects of sampling salty ground water in coastal aquifers: Ground Water, v. 1, no. 1, p. 28–32.

Kohout, F.A., and Leach, S.D., 1964, Saltwater movement caused by control-dam operation in the Snake Creek Canal, Miami, Florida: State of Florida, State Board of Conservation, Division of Geology, Florida Geological Survey, Report of Investigations, no. 24, part IV, 49 p.

Koszalka, E.J., 1995, Delineation of saltwater intrusion in the Biscayne aquifer, eastern Broward County Florida, 1990: U.S. Geological Survey Water-Resources Investigations Report 93–4164, 1 sheet.

Lane, S.L., Flanagan, Sarah, and Wilde, F.D., 2003, Selection of equipment for water sampling (ver. 2.0): U.S. Geological Survey Techniques of Water-Resources Investigations, book 9, chap. A2, March 2003, accessed June 25, 2013, at *http://pubs.water.usgs.gov/twri9A2/*.

Leach, S.D., and Grantham, R.G., 1966, Salt-water study of the Miami River and its tributaries, Dade County, Florida: Florida Geological Survey Report of Investigations no. 45, 35 p.

Leach, S.D., Klein, Howard, and Hampton, E.R., 1972, Hydrologic effects of water control and management of southeastern Florida: Florida Bureau of Geology, Report of Investigations no. 60, 115 p.

Lietz, A.C., 1999, Methodology for estimating nutrient loads discharged from the east coast canals to Biscayne Bay, Miami-Dade County, Florida: U.S. Geological Survey Water-Resources Investigations Report 99–4094, 36 p.

Lietz, A.C., Dixon, Joann, and Byrne, Michael, 2002, Average altitude of the water table (1990–99) and frequency analysis of water levels (1974–99) in the Biscayne aquifer, Miami-Dade County, Florida: U.S. Geological Survey Open-File Report 02–91, 7 sheets.

Ludin, A.I., Weppernig, Ralf, Bonisch, G., and Schlosser, Peter, 1997, Mass spectrometric measurement of helium isotopes and tritium in water samples: Lamont-Doherty Earth Observatory of Columbia University, Technical Report 98.6, accessed May 12, 2011, at *http://www.ldeo.columbia.edu/~etg/ms_ms/Ludin_et_al_MS_Paper.html*.

Marella, R.L., 1993, Public-supply water use in Florida, 1990: U.S. Geological Survey Open-File Report 93–134, 46 p.

Marella, R.L., 1999, Water withdrawals, use, discharge, and trends in Florida, 1995: U.S. Geological Survey Water-Resources Investigations Report 99–4002, 90 p.

Marella, R.L., 2004, Water withdrawals, use, discharge, and trends in Florida, 2000: U.S. Geological Survey Scientific Investigations Report 2004–5151, 50 p.

Marella, R.L., 2009, Water withdrawals, use, and trends in Florida, 2005: U.S. Geological Survey Scientific Investigations Report 2009–5125, p. 11.

Matson, G.C., and Sanford, S., 1913, Geology and ground waters of Florida: U.S. Geological Survey Water-Supply Paper 319, 445 p.

McArthur, J.M., Howarth, R.J., and Shields, G.A., 2012, Strontium Isotope Geochronology in The Geologic Time Scale, Gradstein, F.M., Ogg, J.G., Schmitz, M.D., Ogg, G.M., eds., Elsevier Amsterdam, 1040 p., 3 appendixes.

McNeill, J.D., 1986, Geonics EM39 borehole conductivity meter theory of operation: Geonics Limited, Technical Note TN–20, 9 p., 1 addendum.

McNeill, J.D., 1990, Use of electromagnetic methods for groundwater studies, *in* Ward, S.H., ed., Geotechnical and environmental geophysics: Tulsa, Society of Exploration Geophysicists, p. 191–218.

McNeill, J.D., Bosnar, M., and Snelgrove, F.B., 1990, Resolution of an electromagnetic borehole conductivity logger for geotechnical and ground water applications: Geonics Technical Note TN–25, 28 p.

Meinzer, O.E., Wenzel, L.K., and others, 1940, Water levels and artesian pressure in observation wells in the United States in 1939: U.S. Geological Survey Water-Supply Paper 886.

Meyer, F.W., 1974, Availability of ground water for the U.S. Navy well field near Florida City, Dade County, Florida: U.S. Geological Survey Open-File Report 74–1072, 50 p.

Miller, J.A., 1986, Hydrogeologic framework of the Floridan aquifer system in Florida and in parts of Georgia, South Carolina, and Alabama: U.S. Geological Survey Professional Paper 1403–B, 91 p.

Miller, J.A., 1990, Ground water atlas of the United States; Alabama, Segment 6; Alabama, Florida, Georgia, and South Carolina: U.S. Geological Survey Hydrologic Investigations Atlas 730–G, 28 p.

Mount Sopris Instrument Co., Inc., 2002, 2PIA–1000 Poly induction probe, 2EMA–1000 conductivity probe (2 EMB–1000 and 2ECM–1000) EMP–2493 and EMP–4493: Golden CO, Mount Sopris, 19 p.

Munroe, R.M., and Gilpin, Vincent, 1930, The Commodore's story, the early days on Biscayne Bay, reprinted, Historical Association of Southern Florida, 1966, 384 p.

National Climatic Data Center, 2012, Normal daily mean temperature, degrees Fahrenheit: National Aeronautical and Atmospheric Administration, National Climatic Data Center, accessed January 23, 2012, at *http://lwf.ncdc.noaa.gov/oa/climate/online/ccd/meantemp.html*.

National Oceanic and Atmospheric Administration, 2012, Sea levels online: National Oceanic and Atmospheric Administration, accessed November 30, 2012, at *http://tidesandcurrents.noaa.gov/sltrends/sltrends.shtml*.

Northwest Dade County Freshwater Lake Belt Plan, 1997, Making a whole not just a hole: South Florida Water Management District, 30 p.

Oki, D.S., and Presley T.K., 2008, Causes of borehole flow and effects on vertical salinity profiles in coastal aquifers: Conference program and proceedings, Program and proceedings book, 20th Salt Water Intrusion Meeting, June 23–27, 2008, p. 170–173, accessed June 14, 2013, at *http://conference.ifas.ufl.edu/swim/papers.pdf*.

Oldenburg, D.W., and Li, Y., 2005, Inversion for applied geophysics—A tutorial, *in* Butler, D.K., ed., Near surface geophysics, Part 1—Concepts and fundamentals: Tulsa, Society of Exploration Geophysicists, p. 89–150.

Paige, J.C., 1986, Historic resource study for Everglades National Park, U.S. Department of the Interior, National Park Service: Department of Commerce, National Technical Information Service, PB87199097, p. 138–143.

Parker, G.G., 1945, Salt water encroachment in southern Florida: Journal of the American Water Works Association, v. 37, no. 6, p. 526–542.

Parker, G.G., and Cooke, C.W., 1944, Late Cenozoic geology of southern Florida, with a discussion of the groundwater: Florida Geological Survey, Geological Bulletin no. 27, 3 pls.

Parker, G.G., Ferguson, G.E., Love, S.K., and others, 1955, Water resources of southeastern Florida, with special reference to the geology and ground water of the Miami area: U.S. Geological Survey Water-Supply Paper 1255, 965 p.

Parks, A.M., 1987, Miami memoirs, John Sewell—A new pictorial addition: Miami, Arva Parks & Co., 267 p.

Perkins, R.D., 1977, Depositional framework of Pleistocene rocks in south Florida, *in* Enos, Paul, and Perkins, R.D., eds., Quaternary sedimentation in south Florida: Geological Society of America Memoir 147, p. 131–198.

Plummer, L.N., Böhkle, J.K., and Busenberg, Eurybiades, 2003, Approaches for ground-water dating, *in* Lindsey, B.D., Phillips, S.W., Donnelly, C.A., Speiran, G.K., Plummer, L.N., Böhlke, J.K., Focazio, M.J., Burton, W.C., and Busenberg, Eurybiades, Residence times and nitrate transport in groundwater discharging to streams in the Chesapeake Bay Watershed: U.S. Geological Survey Water-Resources Investigations Report 03–4035, p. 12–24.

Prinos, S.T., 2005, Correlation analysis of a ground-water level monitoring network, Miami-Dade County, Florida: U.S. Geological Survey Open-File Report 2004–1412. (Also available at *http://pubs.usgs.gov/of/2004/1412/index.html*.)

Prinos, S.T., Lietz, A.C., and Irvin, R.B., 2002, Design of a real-time ground-water level monitoring network and portrayal of hydrologic data in southern Florida: U.S. Geological Survey Water-Resources Investigation Report 01–4275, 108 p.

Raymer, L.L., Hunt, E.R., and Gardner, J.S., 1980, An improved sonic transit time-to-porosity transform, paper P, *in* 21st Annual Logging Symposium Transactions: Society of Professional Well Log Analysts, 12 p.

Reese, R.S., 1994, Hydrogeology and the distribution and origin of salinity in the Floridan aquifer system, southeastern Florida: U.S. Geological Survey Water-Resources Investigations Report 94–4010, 56 p.

Reese, R.S., and Cunningham, K.J., 2000, Hydrogeology of the gray limestone aquifer in southern Florida: U.S. Geological Survey Water-Resources Investigations Report 99–4213, 244 p.

Reese, R.S., and Richardson, E., 2008, Synthesis of the hydrogeologic framework of the Floridan aquifer system and delineation of a major Avon Park permeable zone in central and southern Florida: U.S. Geological Survey Scientific Investigations Report 2007–5207, 60 p.

Reese, R.S., and Wacker, M.A., 2009, Hydrogeologic and hydraulic characterization of the surficial aquifer system, and origin of high salinity groundwater, Palm Beach County Florida: U.S. Geological Survey Scientific Investigations Report 2009–5113, 42 p., 2 appendixes.

Renken, R.A., Cunningham, K.J., Shapiro, A.M., Harvey, R.W., Zygnerski, M.R., Metge, D.W., and Wacker, M.A., 2009, Pathogen and chemical transport in the karst limestone of the Biscayne aquifer—1. Revised conceptualization of groundwater flow: Water Resources Research, v. 44, W08429, doi:10.1029/2007WR006058.

Renken, R.A., Dixon, Joann, Koehmstedt, John, Ishman, Scott, Lietz, A.C., Marella, R.L., Telis, Pamela, Rodgers, Jeff, and Memberg, Steven, 2005a, Impact of anthropogenic development on coastal ground-water hydrology in southeastern Florida, 1900–2000: U.S. Geological Survey Circular 1275, 77 p.

Renken, R.A., Shapiro, A.M., Cunningham, K.J., Harvey, R.W., Metge, D.W., Zygnerski, M.R., Osborn, C.L., Wacker, M.A., and Ryan, J.N., 2005b, Assessing the vulnerability of a municipal well field to contamination in a karst aquifer: Environmental and Engineering Geoscience, v. 11, no. 4, p. 341–354.

Révész, Kinga, and Coplen, T.B., 2008a, Determination of the $\delta(^2H/^1H)$ of water: RSIL lab code 1574, chap. C1 of Révész, Kinga, and Coplen, T.B., eds., Methods of the Reston Stable Isotope Laboratory: U.S. Geological Survey Techniques and Methods 10–C1, 27 p.

Révész, Kinga, and Coplen, T.B., 2008b, Determination of the $\delta(180/160)$ of water: RSIL lab code 489, chap. C2 of Révész, Kinga, and Coplen, T.B., eds., Methods of the Reston Stable Isotope Laboratory: U.S. Geological Survey Techniques and Methods, 10–C2, 28 p.

Richter, B.C., and Kreitler, C.W., 1993, Geochemical techniques for identifying sources of ground-water salinization: Boca Raton, FL, CRC Press, 258 p.

Rupert, M.G., and Plummer, L.N., 2004, Ground-water flow direction, water quality, recharge sources, and age, Great Sand Dunes National Monument, south-central Colorado, 2000–2001: U.S. Geological Survey Scientific Investigations Report 2004–5027, 28 p.

Schlosser, Peter, Stute, Martin, Dorr, Helmut, Sonntag, Christian, and Munnich, K.O., 1988, Tritium/3He dating of shallow groundwater: Earth and Planetary Science Letters, v. 89, p. 353–362.

Schlosser, Peter, Stute, Martin, Sonntag, Christian, and Munnich, K.O., 1989, Tritiogenic 3He in shallow groundwater: Earth and Planetary Science Letters, v. 94, p. 245–256.

Schmerge, D.L., 2001, Distribution and origin of salinity in the surficial and intermediate aquifer systems, southwestern Florida: U.S. Geological Survey Water-Resources Investigations Report 2001–4159, 41 p.

Schroeder, M.C., and Klein, Howard, 1954, Geology of the western Everglades Area, southern Florida: Florida Geological Survey, Geologic Survey Circular 314, 26 p.

Schroeder, M.C., Klein, Howard, and Hoy, N.D., 1958, Biscayne aquifer of Dade and Broward Counties, Florida: Florida Geological Survey Report of Investigations no. 17, 56 p.

Shaler, N.S., 1890, The topography of Florida: Bulletin of the Museum of Comparative Zoology at Harvard College, v. 16, no. 7, p. 139–156.

Shalev, Eyal, Lazar, Ariel, Wollam, Stuart, Kington, Shushanna, Yechieli, Yoseph, and Gvirtzman, Haim, 2009, Biased monitoring of freshwater-salt water mixing zone in coastal aquifers: Ground Water, v. 47, no. 1, p. 49–46.

Shapiro, A.M., Renken, R.A., Harvey, R.W., Zygnerski, M.R., and Metge, D.W., 2008, Pathogen and chemical transport in the karst limestone of the Biscayne aquifer—2. Chemical retention from diffusion and slow advection: Water Resources Research, v. 44, W08430, doi:10.1029/2007WR006059.

Shaw, T.J., Moore, W.S., Kloepfer, Jeremiah, and Sochaski, M.A., 1998, The flux of barium to the coastal waters of the southeastern USA—The importance of submarine groundwater discharge: Geochimica et Cosmochimica Acta, v. 62, no. 18, p. 3047–3054.

Sherwood, C.B., and Klein, Howard, 1963, Surface- and ground-water relation in a highly permeable environment: Berkeley, International Association of Scientific Hydrology, publication no. 63, p. 454–463.

Sherwood, C.B., and Leach, S.D., 1962, Hydrologic studies in the Snapper Creek Canal area, Dade County, Florida: Florida Geological Survey, Report of Investigations no. 24, Part II, 32 p.

Smith, R.S., 1909, The reclamation of the Florida Everglades, Miami, Florida, p. 16b.

Sonenshein, R.S., 1997, Delineation and extent of saltwater intrusion in the Biscayne aquifer, eastern Dade County, Florida, 1995: U.S. Geological Survey Water-Resources Investigations Report 96–4285, 1 sheet.

Sonenshein, R.S., and Koszalka, E.J., 1996, Trends in water-table altitude (1984–1993) and saltwater intrusion (1974–1993) in the Biscayne aquifer, Dade County, Florida: U.S. Geological Survey Open-File Report 95–705, 2 sheets.

Southeastern Geological Society Ad Hoc Committee on Florida Hydrostratigraphic Unit Definition, 1986, Hydrogeological units of Florida: Florida Department of Natural Resources, Bureau of Geology, Special Publication 28, 9 p.

South Florida Water Management District, 1985, Interim drought management report: South Florida Water Management District May 9, 1985, Update, 112 p.

South Florida Water Management District, 2010, Water use permit no. re-issue 13–00017–W, non-assignable, South Water Management District, 31 p., 37 app., Exhibit 5A, accessed January 12, 2012, at *http://www.miamidade.gov/wasd/wup.asp*.

Stalker, J.C., McFarlane, Andrew, and Price, R.M., 2010, Geochemical investigation of the surface water and groundwater in the immediate vicinity of Florida Power and Light, Turkey Point Cooling Canals: Florida International University, 43 p.

Stewart, M.A., Bhatt, T.N., Fennema, R.J., and Fitterman, D.V., 2002, The road to flamingo—An evaluation of flow pattern alterations and salinity intrusion in the Lower Glades, Everglades National Park: U.S. Geological Survey Open-File Report 2002–59, 36 p.

Stoneman-Douglas, Marjory, 1947, The Everglades—River of grass: Sarasota, Florida, Pineapple Press, Inc., 50th Anniversary Edition, 1997, 455 p.

Swayze, L.J., 1980, Water-level contour and salt front map, Hialeah-Miami Springs well field area, Dade County, Florida, October 13, 1978: U.S. Geological Survey Open-File Report 80–8, 1 sheet.

Taylor, K.C., Hess, J.W., and Mazzela, Aldo, 1989, Field evaluation of slim-hole borehole induction tool: Groundwater Monitoring & Remediation, v. 9, issue 1, p. 100–104.

The Weather Channel, 2013, Monthly and daily averages for Miami, Florida, accessed January 3, 2011, at *http://www.weather.com/weather/wxclimatology/monthly/graph/USFL0316*.

Trimble, P.J., Marban, J.A., Molian, Medardo, and Scully, S.P., 1990, Analysis of the 1989–1990 drought: South Florida Water Management District Special Report DRE 286, 80 p.

Turekian, K.K., 1976, Oceans (2d ed.): Prentice-Hall, 149 p.

U.S. Census Bureau, 2010, State and county quick facts, Miami-Dade County, Florida, accessed September 9, 2011, at *http://quickfacts.census.gov/qfd/states/12/12086.html*.

U.S. Census Bureau, 2013, Population estimates, counties, accessed March 15, 2013, at *http://www.census.gov/popest/data/historical/index.html*.

U.S. Congress, 1850, Index to Executive Documents printed by order of the United States during the first session of the thirty-first congress 1849–50, Washington: Wm. M. Belt, 98 p.

U.S. Environmental Protection Agency, 2000, SF_6 Emissions reduction partnership for electronic power systems, annual report, 2000: U.S. Environmental Protection Agency, 9 p., accessed May 17, 2001, at *http://www.epa.gov/electricpower-sf6/documents/sf6_emiss_rep.pdf*.

U.S. Environmental Protection Agency, 2011a, Secondary drinking water regulations; guidance for nuisance chemicals: U.S. Environmental Protection Agency Report 816–f–10–079, accessed January 26, 2011, at *http://water.epa.gov/drink/contaminants/secondarystandards.cfm*.

U.S. Environmental Protection Agency, 2011b, Drinking water contaminants—National primary drinking water standards, accessed February 23, 2011, at *http://water.epa.gov/drink/contaminants/index.cfm*.

U.S. Geological Survey, variously dated, National field manual for the collection of water-quality data: U.S. Geological Survey Techniques of Water-Resources Investigations, book 9, chaps. A1–A9, available online at *http://pubs.water.usgs.gov/twri9A*.

U.S. Geological Survey, 2011a, Reston Chlorofluorocarbon Laboratory—SF_6 sampling: U.S. Geological Survey, accessed April 29, 2011, at *http://water.usgs.gov/lab/sf6/sampling/*.

U.S. Geological Survey, 2011b, Reston Chlorofluorocarbon Laboratory—Dissolved Gas N_2 / Ar and 4He Sampling: U.S. Geological Survey, accessed June 25, 2013, at *http://water.usgs.gov/lab/dissolved-gas/sampling/*.

U.S. Geological Survey, 2011c, Reston Chlorofluorocarbon Laboratory—$^3H/^3He$ sampling: U.S. Geological Survey, accessed April 26, 2011, at *http://water.usgs.gov/lab/3h3he/sampling/*.

U.S. Geological Survey, 2011d, Reston Chlorofluorocarbon Laboratory—Analytical procedures for SF_6: U.S. Geological Survey, accessed April 26, 2011, at *http://water.usgs.gov/lab/sf6/lab/analytical_procedures/*.

U.S. Geological Survey, 2011e, Annual Water Data Reports: U.S. Geological Survey, accessed June 18, 2013, at *http://wdr.water.usgs.gov/*.

U.S. Geological Survey, 2011f, National Water Information System—Web interface—Water Data for the Nation: U.S. Geological Survey, accessed October 5, 2011, at *http://nwis.waterdata.usgs.gov/usa/nwis/*.

U.S. Geological Survey, 2011g, Saline intrusion monitoring, Miami-Dade County, Florida: U.S. Geological Survey, accessed October 10, 2011, at *http://www.envirobase.usgs.gov/FLIMS/*.

U.S. Geological Survey, 2011h, Groundwater conditions in southern Florida: U.S. Geological Survey, accessed October 5, 2011, at *http://www.sflorida.er.usgs.gov/edl_data/index_ndt.html*.

U.S. Geological Survey, 2011i, Reston Chlorofluorocarbon Laboratory—Analytical procedures for dissolved gasses N_2 / Ar: U.S. Geological Survey, accessed April 26, 2011, at *http://water.usgs.gov/lab/dissolved-gas/lab/analytical_procedures/*.

Van Wagoner, J.C., 1985, Reservoir facies distribution as controlled by sea-level change: Abstract and Poster Session, Society of Economic Paleontologists and Mineralogists Mid-Year Meeting, Golden, Colorado, p. 91–92.

Vengosh, Avner, and Pankratov, Irena, 1998, Chloride/bromide and chloride/fluoride ratios of domestic sewage effluents and associated contaminated ground water: Ground Water, v. 36, no. 5, p. 815–824.

Verdi, R.J., Tomlinson, S.A., and Marella, R.L., 2006, The drought of 1998–2002—Impacts on Florida's Hydrology and Landscape: U.S. Geological Survey Circular 1295, 34 p.

Wacker, M.A., 2010, Tools and data acquisition of borehole geophysical logging for the Florida Power and Lights Company Turkey Point Power Plant in support of a groundwater, surface-water, and ecological monitoring plan, Miami-Dade County, Florida: U.S. Geological Survey Open-File Report 2010–1260, 5 p., appendixes.

Wacker, M.A., and Cunningham, K.J., 2008, Borehole geophysical logging program—Incorporating new and existing techniques in hydrologic studies: U.S. Geological Survey Fact Sheet 2008–3098, 4 p.

Waller, B.G., 1985, Drought of 1980–82 in southeast Florida with comparison to the 1961–62 and 1970–71 droughts: U.S. Geological Survey Water-Resources Investigations Report 85–4152, p. 24–28.

Wright, J.O., 1912, The Everglades of Florida—Their adaptability for the growth of sugar cane: Tallahassee, FL, 81 p.

Appendixes 1–12

Appendix 1. Site Location and Construction Information

Appendix 1 provides site location and construction information for sites used to evaluate the inland extent of saltwater or the causes of saltwater intrusion in the Biscayne aquifer. Monitoring results from these sites are available from the USGS Annual Water Data Reports and National Water Information System—Web interface—Water quality samples for the Nation websites (U.S. Geological Survey, 2011a, b) or from the organizations listed in this appendix. This information is provided in a supplementary Microsoft Excel™ file. The latitude and longitude of each site are provided in a decimal degree format that has been adjusted to the NAD83 datum. This can be used to import this file into a GIS.

See supplemental file *http://pubs.usgs.gov/sir/2014/5025/appendix/sir2014-5025_appendix_01.xlsx*.

References

U.S. Geological Survey, 2011a, Annual Water Data Reports: U.S. Geological Survey, accessed June 18, 2013, at *http://wdr.water.usgs.gov/*.

U.S. Geological Survey, 2011b, National Water Information System—Web interface—Water Data for the Nation: U.S. Geological Survey, accessed October 5, 2011, at *http://nwis.waterdata.usgs.gov/usa/nwis/*.

Appendix 2. Results of Geochemical Sampling

Appendix 2 provides the results of 69 geochemical samples and 3 replicate samples from 44 sites. This information is available in 7 supplementary Microsoft Excel™ files.

See supplemental files:

Appendix_02_Table1.xlsx
Appendix_02_Table2.xlsx
Appendix_02_Table3.xlsx
Appendix_02_Table4.xlsx
Appendix_02_Table5.xlsx
Appendix_02_Table6.xlsx
Appendix_02_Table7.xlsx

available at *http://pubs.usgs.gov/sir/2014/5025/appendix/sir2014-5025_appendix_02*.

Appendix 3. Salinity Profiles Collected from the Card Sound Road Canal

Salinity profiles were collected in the Card Sound Road Canal to evaluate the extent to which saltwater can flow inland along this canal (appendix 3). The latitude and longitude of each site are provided in a decimal degree format that has been adjusted to the NAD83 datum. This can be used to import this file into a GIS.

See supplemental file *http://pubs.usgs.gov/sir/2014/5025/appendix/sir2014-5025_appendix_03.xlsx*.

Appendix 4. Results of Time-Domain Electromagnetic Soundings

Appendix 4 provides a summary of information concerning 79 TEM soundings that were made during 2008 and 2009. This summary is provided in a supplementary Microsoft Excel™ file. Soundings MIA101–MIA137 were collected between April 28, 2008, and May 8, 2008. Soundings MIA201–MIA242 were collected between February 23, 2009, and March 9, 2009. The 2008 field season focused on gathering information from the Broward County line south to Florida City in southern Miami-Dade County to fill gaps in the spatial coverage of existing monitoring wells and to determine if the extent of saltwater encroachment had changed since the work of Sonenshein (1997). The 2009 field season was focused primarily in southeast Miami-Dade County in the Model Land, but also includes a number of soundings in southern Broward County, which helped to establish the location of the saltwater front in northern Miami-Dade County. The soundings collected in the Model Land were located to help interpret the HEM survey flown in 2001 to map saltwater encroachment. The locations of the TEM soundings were determined by global positioning system (GPS) measurements. Horizontal coordinates are in UTM Zone 17R, in meters, referenced to NAD 83. Positioning errors are 4 to 5 m. Detailed information concerning these measurements is provided in Fitterman and Prinos (2011).

See supplemental file *http://pubs.usgs.gov/sir/2014/5025/appendix/sir2014-5025_appendix_04.xlsx*.

References

Fitterman, D.V., and Prinos, S.T., 2011, Results of time-domain electromagnetic soundings in Miami-Dade and southern Broward Counties, Florida: U.S. Geological Survey Open-File Report 2011–1299, 289 p.

Sonenshein, R.S., 1997, Delineation and extent of saltwater intrusion in the Biscayne aquifer, eastern Dade County, Florida, 1995: U.S. Geological Survey Water-Resources Investigations Report 96–4285, 1 sheet.

Appendix 5. Time-Series Electromagnetic Induction Log (TSEMIL) Dataset Calibration and Processing

The following is a synopsis of induction log calibration procedures and TSEMIL dataset processing.

Calibration Procedures

Prior to the collection of individual induction logs, factory-prescribed procedures (Mount Sopris Instrument Co., Inc., 2002, p. 7–11, 15) that adhere to ASTM International guidelines (ASTM International, 2007) are used to calibrate the logging probe. Given the variety of equipment used through time, differences in temperature and humidity during calibrations, and variations in instrument sensitivity and drift, the only actual constants existing in the calibration process are the calibration coils themselves. Each calibration performed is an attempt to align the data with these constants. The probe readings in counts per second (cps) are converted to values of bulk conductivity by using the equation of a straight line that is determined by a two-point calibration process. Calibration is accomplished by using a factory-manufactured calibration coil. The coil is designed to provide known bulk conductivity values that can be selected by using a switch on the coil. Available settings are 0, 91, 460, and 1,704 mS/m. The settings selected depend on the desired range, which can be 0 to 100, 0 to 1,000, or 0 to 10,000 mS/m. During the calibration process, a coil setting of zero is selected for the first calibration point. The second calibration point is obtained by selecting the coil setting that is most appropriate for the selected range. The range used for this effort was 0 to 1,000 mS/m because many of the wells used already yielded saltwater.

Several different calibration settings and methods were used during this effort. An older calibration coil used for this study had settings of 0, 81, 345, and 1,301 mS/m. This coil was used to calibrate the logs collected from 1996 to 2007. This coil is discussed in greater detail in subsequent sections of this appendix. The logs collected in 1995 were calibrated by using an alternate procedure described by Mount Sopris Instrument Co., Inc., (2002, p. 7) that uses free air for the zero setting and a value for the second calibration point that consists of the frequency of pulses from the tool at the zero point plus 5,000. Most of the logs collected during 1996 to 2001, excluding 1998, were calibrated by using a setting of 1,301 on the calibration coil for the second calibration point. Most of the logs collected in 1998 and during 2002 to 2007 were calibrated by using the 345-mS/m setting for the second point. All of the logs collected since 2008 have been calibrated by using the newer coil and a setting of 460 for the second point.

During calibration, metal objects also are kept as far from the probe as possible. Care is taken to avoid calibrating the probe near an area with the potential for electromagnetic interference. When there is a significant difference between the temperature of the induction probe and the temperature of water in the borehole, there can be a shift in the observed log (Mount Sopris Instrument Co., Inc., 2002, p. 15), so prior to calibration, the probe is allowed to equilibrate with the water in the well at a depth of about 6 m until the readings stabilize. Once readings are stable, the probe is removed from the well, and the calibration is performed as quickly as possible to reduce temperature-induced variations. Following calibration, the probe is returned to the well at a depth of about 6 m and is again allowed to equilibrate with the water in the well until readings are constant. Once readings have stabilized, the probe is raised until a selected reference point on the probe aligns with a reference point near the top of the well. The down-hole log is then collected. Logs are generally collected in both a down-hole and an up-hole direction. These two logs are compared to evaluate the quality of each log. In tight wells, the probe may become temporarily stuck in the well even as additional cable is played out by the winch. This can cause a temporary discontinuity between the actual depth of the probe and the depth recorded by the winch. To ensure data quality, therefore, the up-hole log is generally used because this allows the maximum amount of time for the probe temperature to achieve equilibrium with the water in the borehole and because the cable connected to the probe is under constant tension, which reduces the potential for inaccurate depth measurements.

The induction logging systems and software used for collection of the logs presented in this report have changed a number of times during the 17 years that data have been collected. Between 1995 and 1997, the equipment used was a Mount Sopris Instrument Co., Inc. MGX portable logging unit operated using Logshell™ software, an MGB–1000 ultralight winch, and an EMA–1000 induction probe. The EMA–1000 induction probe is based on the Geonics EM39 induction probe. In 1998, the MGX portable logger was upgraded by installing a digital MGXII console using Logshell™ software. Beginning in 2000, the Logshell™ software was upgraded to MSLog™ software. The Logshell™ software was used again for the logs collected in 2001 because of the truncation of some of the values recorded in the output files. The EMA–1000 induction probe malfunctioned in 2002, and the logs collected that year were obtained by using an induction probe borrowed from the USGS Tennessee Water Science Center. A new induction probe was purchased and used from 2003 to 2006. The truncation issues related to the software had been addressed by 2002, and instrumentation was operated using MSLog™ software during 2002 to 2006. In 2007, after another probe malfunction, an EM39 induction probe was rented from Colog Borehole Geophysical Services for the collection of logs that year. Currently (2013), a 2PIA–1000 EM39 induction probe, a 4305–1000–120 mini winch, and a 5MXA–1000–120 Matrix™ logging console operated using Matrix™ logging software are being used.

Although there have been a number of modifications to the probes that have been used through time, all of the

probes used were based on the EM39 design. The EM39 probe provides a radius of maximum sensitivity of 28 cm, a radius of minimum sensitivity of 10 cm, and vertical resolution of 65 cm (McNeill, 1986; Mount Sopris Instrument Co., Inc., 2002, p. 17). This means that the probe is insensitive to changes in borehole fluid in wells with a diameter of less than 20 cm. Most of the wells logged during this study had a diameter of 5 cm, and changes in the electrical conductivity of the fluid in these boreholes should not have affected the logs. The probe provides "appreciable sensitivity" out to a radius of 100 cm (McNeill and others, 1990, p. 5). Measurement resolution and accuracy are 0.02 and 5 percent of full scale, respectively (Mount Sopris Instrument Co., Inc., 2002, p. 17). Given the full scale of 1,000 mS/m, the accuracy is about 50 mS/m. The data collected in the study area by the USGS during the last 17 years, using various versions of the EM39 induction probe and varying calibration methods, and coils, however, indicate that much greater accuracy may be possible. Although there were some issues with calibration slope and offset, once they were addressed, the data collected where salinity is not changing tended to agree to within ± 1.0 to 1.5 mS/m even though changes have been made to the hardware and software used to collect these logs.

Corrections of Calibration Slope

A two-point calibration process is used to determine the equation of a straight line that is used by the operating software to convert probe readings (cps) to bulk conductivity. The equation of this line includes a slope and offset. Relatively large errors in the calibration slope of logs were caused during 1996 to 2007 by using a calibration coil that had been marked at the factory with incorrect values and during 1996 to 2001 (excluding 1998) by using a second calibration point that was greater than the full-scale reading of 1,000 mS/m. The calibration coil error was discovered in 2008 when logs were collected using a new calibration coil from the same factory. Both coils were sent back to the factory for examination. This examination revealed that the coil settings labeled 81, 345, and 1,301 mS/m should have been labeled 91, 460, and 1,700 mS/m, respectively, and that given the incorrect labels, the calibrations applied during 1996 to 2007 were generally off by about 11 to 25 percent. After the necessary corrections had been applied to the slope of the affected logs, only minor ±7 mS/m offsets remained between any of logs.

TSEMIL Dataset Processing

Where a time series of EMI logs was collected from a well penetrating freshwater parts of the Biscayne aquifer, the individual EMI logs of the set are nearly identical, with the exception of small and uniform offsets in bulk conductivity between the logs collected on different dates (fig. 5–1). These offsets are generally within ±7 mS/m of the mean of the log set. The offsets are likely caused by the calibration and measurement process rather than by actual changes in aquifer water quality because these offsets are almost perfectly uniform throughout the thickness of freshwater parts of the aquifer. The offsets could be caused by slight differences in calibration resulting from variations in temperature, humidity, and calibration time, because the probe must be removed from the well for calibration. Even though the offsets are small (±7 mS/m), they obscure the ability to identify small but real changes in bulk conductivity that occurred as changes in the salinity of the pore water occurred. A technique was developed, therefore, to remove the offsets to create TSEMIL datasets that could be used to more clearly identify changes in bulk conductivity resulting from saltwater intrusion.

The offsets apparent in the time series of EMI logs (fig. 5–1) are removed on a log-by-log basis. An important consideration of this procedure is that if there are no actual changes in the electrical conductivity of water occurring through time in the aquifer, then the adjustments made to the time series of EMI logs should not alter the mean bulk conductivity of the set of EMI logs. In other words, with few exceptions, the corrected set of EMI logs should not be skewed to the left or right of the mean of the uncorrected set of logs. The offsets between individual EMI logs were nearly constant throughout the freshwater-saturated interval; aligning individual logs to the left or right of the mean bulk conductivity measured at one depth generally created near perfect alignment at all depths in the freshwater-saturated interval. The correction process consisted, therefore, of (1) determining the mean bulk conductivity measured by the full time series of EMI logs at a selected depth within the freshwater-saturated interval, (2) determining the difference between this value and the bulk conductivity measured at this same depth for an individual log of the set, (3) subtracting this difference from each bulk conductivity measurement of that log, and (4) repeating this process for all logs in the set until they were all aligned to the mean bulk conductivity at the selected depth. This process creates near perfect alignment of the set of EMI logs and creates the ability to identify small differences between logs that were otherwise obscured by the offsets that had been present (fig. 5–2).

The first EMI log of the TSEMIL dataset from well G–3611 collected on January 9, 1996, shows slightly elevated bulk conductivity at depths of 6.7 and 16.7 m (fig. 5–2). This change in bulk conductivity is a common observation in many of the TSEMIL datasets from new wells. It likely results from water of greater than normal electrical conductivity entering porous rock layers during the drilling process. Generally, the electrically conductive water dissipates during the first few years of logging the well.

A simple method to ensure that the corrections were applied correctly is to verify that the sum of all corrections applied is zero. By using the corrections that were applied to align individual logs to the mean of all logs at a given depth, the standard deviation of a TSEMIL dataset may also be determined. Simple graphical examinations of the time series of the logs prior to and following these corrections allow the

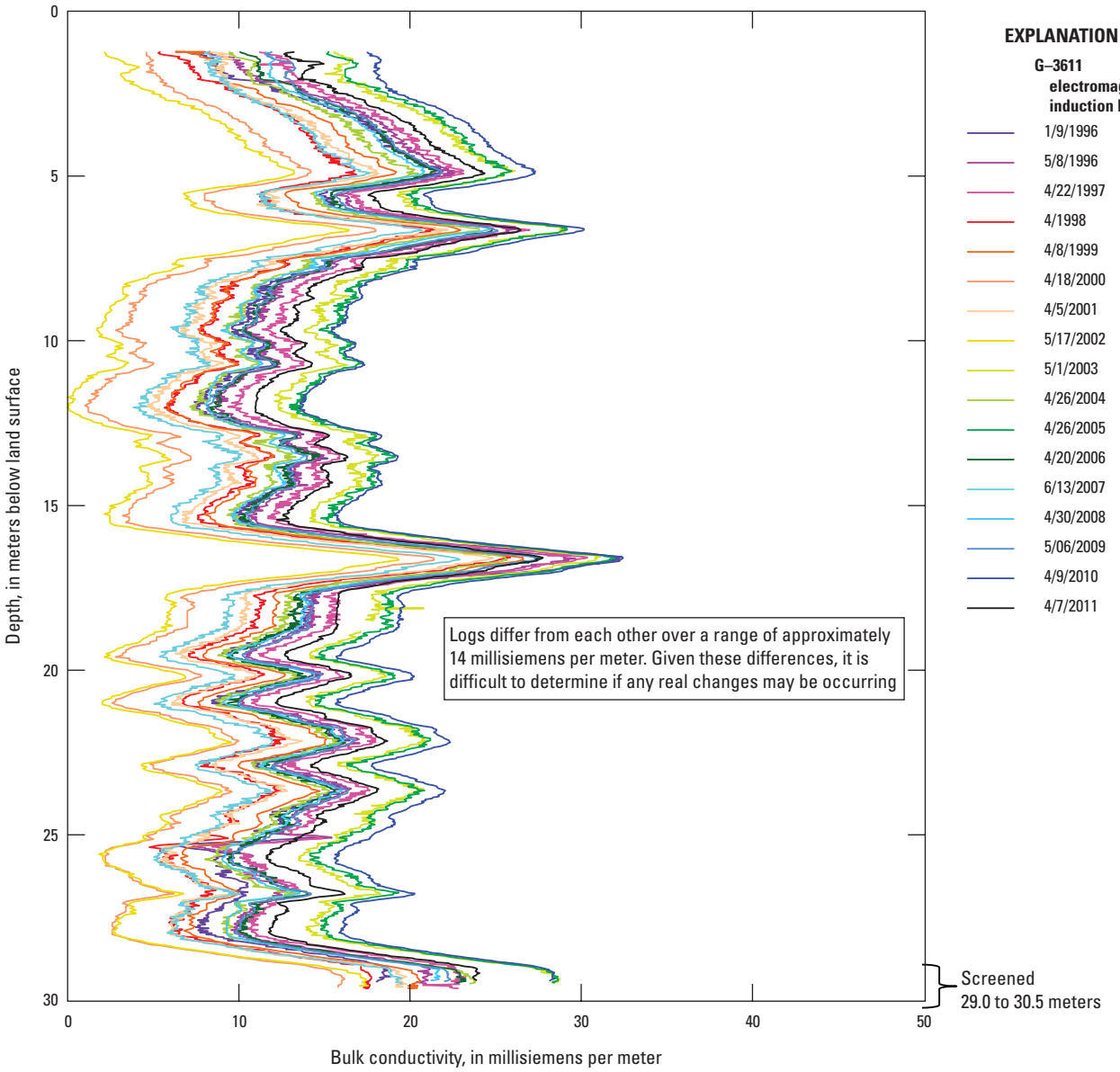

Figure 5–1. Electromagnetic induction logs collected from monitoring well G–3611 from January 1996 to April 2011 prior to bulk conductivity adjustments, Miami-Dade County, Florida.

evaluation of the best overall alignment for a given dataset. Multiple depths may be selected to computationally determine the best overall alignment, and the adjustments computed for each individual log can be averaged. Logs could also be aligned to the median bulk conductivity measured at selected depths if desired. Depending on the goals of the research and aquifer conditions, this method could also be used to establish a baseline to which all future logs would be corrected.

When using the correction procedures described, there generally remains only about ±1 to 1.5 mS/m of completely irregular variation between successive logs that cannot be removed (fig. 5–2). Even if perfect numerical alignment is achieved at one or two depths, the ±1 to 1.5 mS/m of random variation remains at all other depths. This variation is likely the result of random instrumentation noise, but is slightly greater than the manufacturer-specified noise level of less than 0.5 mS/m (Mount Sopris Instrument Co., Inc., 2002); equipment variation, drift, and calibration may have been contributing factors. This random variation is much smaller than the difference in change in bulk resistivity occurring when saltwater enters previously freshwater-saturated materials.

Caution should be used when interpreting the resulting TSEMIL datasets because apparent changes in bulk conductivity are much smaller than the manufacturer-specified precision of the equipment. One way to evaluate the quality of corrections applied to the time series of EMI logs is to compare the evident changes in bulk conductivity in the TSEMIL dataset to chloride concentrations in samples

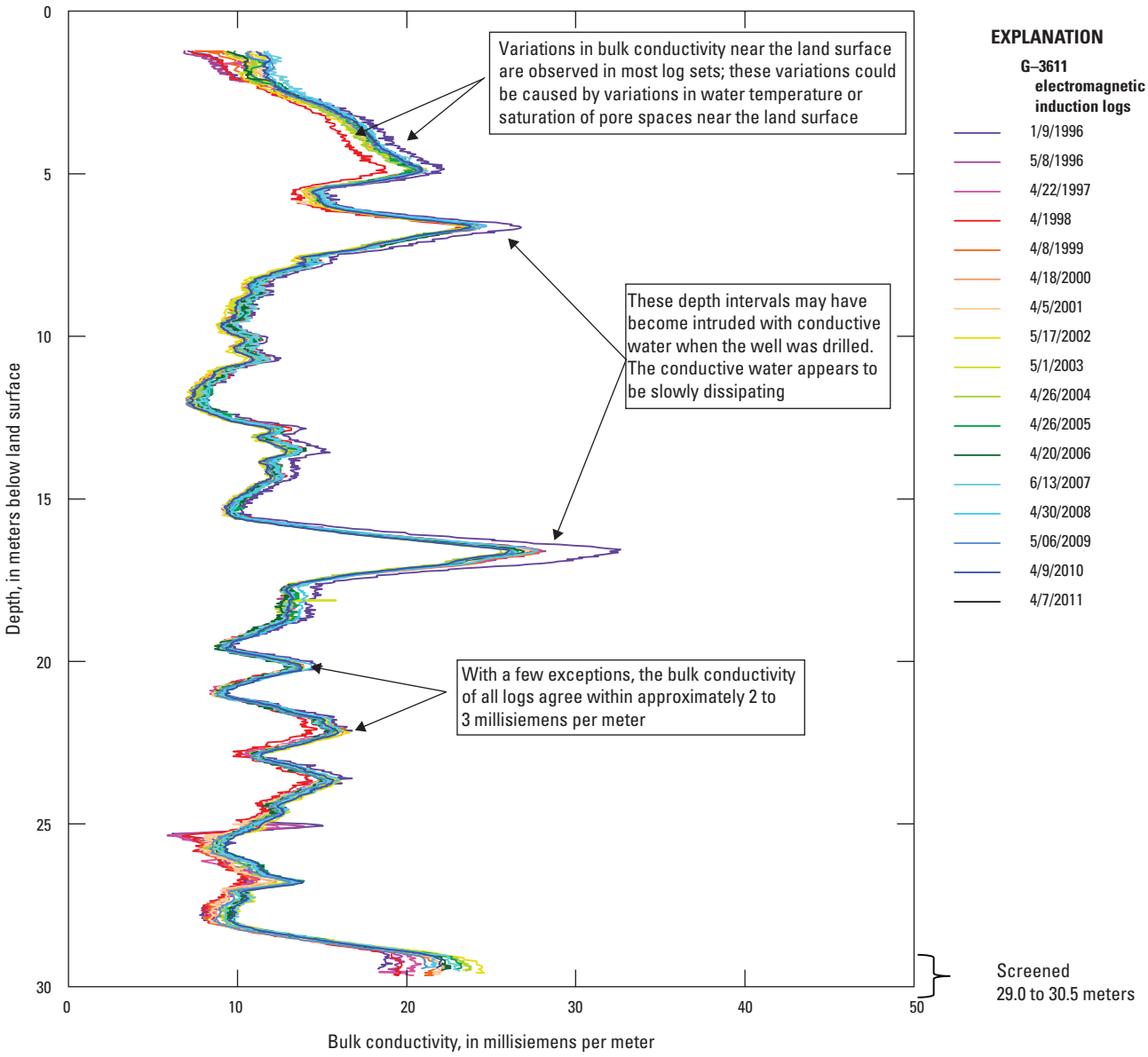

Figure 5–2. Time series electromagnetic induction log dataset that results from correction of errors in the calibration slope and offset. Monitoring well G–3611, January 1996 to April 2011, Miami-Dade County, Florida.

collected from the screen interval of the well. The chloride concentrations in samples collected from well G–3611 were compared to the bulk conductivity measured at a depth of 29.4 m (fig. 5–3). The chloride measurements and EMI logs collected during January and May 1996 have been excluded from the graph, because they were collected on different dates. During 1997 to 2000, changes in chloride concentration were not reflected in the EMI logs, but the 15-mg/L increase in chloride concentration that occurred between 2001 and 2002 corresponds to a 2-mS/m increase in bulk conductivity. The gradual decrease in chloride concentration from 200 to 170 mg/L that occurred between 2002 and 2011 corresponds to a gradual 4-mS/m decrease in bulk conductivity.

Considering the magnitude of corrections that have been applied and all of the other factors that could potentially lead to differences between logs, the correlations observed between chloride and bulk conductivity (fig. 5–3) indicate that the application of this method to the time series of EMI data produces reasonable results. Factors that could lead to differences include (1) a manufacturer-specified measurement accuracy of 5 percent of full scale, or 50 mS/m for a full scale setting of 1,000 mS/m, (2) the relatively small changes in the chloride concentration in water samples, (3) the magnitude of corrections applied to bulk conductivity that are larger than the final range in bulk conductivity data at the depth 29.4 m, (4) the difference in EMI-log measured depth

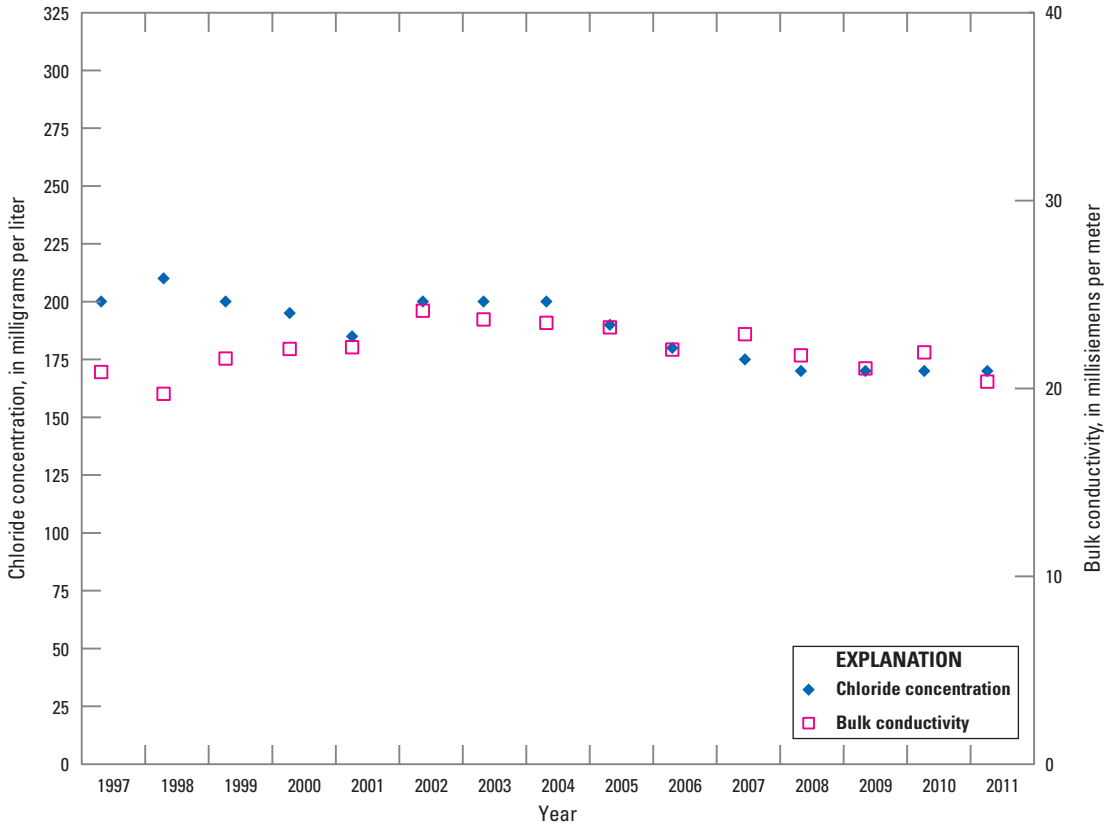

Figure 5–3. Chloride concentrations in water samples collected from well G–3611 and the corrected bulk conductivity measured at a depth of 29.4 meters, Miami-Dade County, Florida.

and the depth of the screened interval, caused by the probe encountering the bottom of the well before a full response can be measured from the open interval and recorded, (5) the number of different EMI logging instruments and calibration methods that have been used, (6) the potential for chloride concentration in water samples to change rapidly if drawn from well-connected pore spaces, while EMI logs would also measure water trapped in finer pores that diffuses more slowly, and (7) the potential for water to be drawn in from outside the radius of investigation of the EMI logging equipment during water sampling. All of these factors could create large differences between the chloride concentration in water samples and measured bulk conductivity. Yet some of the changes in bulk conductivity do correspond to changes in the chloride concentration in water samples (fig. 5–3), and this correspondence is not unique to this site.

The TSEMIL dataset from well G–3609 provides an example of the potential precision of this method. Prior to adjustment, the individual EMI logs were difficult to interpret (fig. 5–4). Once these logs were processed using the methods described, however, the temporal changes in bulk conductivity in the depth interval 19 to 23 m became immediately evident (fig. 42*A*). The changes in bulk conductivity occurring in this depth interval generally agree with the changes in chloride concentration in water samples collected from the open interval of this well, which is 24.4 to 25.9 m (fig. 42*B*). Similar comparisons of chloride concentration sampled and bulk conductivity measured are provided for most of the TSEMI datasets published in this report (figs. 32*B*, 33*B*, 35*B*, 38*B*, 41*B*, 43*B*, 44*B*, and 45*B*). In general, the changes in bulk conductivity measured and chloride concentration samples are similar. The depth intervals from which bulk conductivity data were compiled for comparisons were often a little shallower than the top of the screened interval, where chloride samples were collected. This decision was made because the EMI probe typically encounters the bottom of the well before a full response to aquifer materials can be recorded at the screened interval. The new well design (appendix 7) should allow better comparisons of bulk conductivity measurements and chloride concentrations sampled from the screened interval because the probe will be able to be lowered past the bottom of the screen and will be able to record a full response to aquifer materials within the screened interval.

The TSEMIL datasets collected in the study area frequently indicate changes in bulk conductivity through time, from near the land surface to a depth of about 10 m. These changes may be caused by (1) differences in water temperature over time at shallow depths, (2) differences in the saturation of pore spaces near the water table, and (3) the influence of saline and conductive purge water that may have soaked

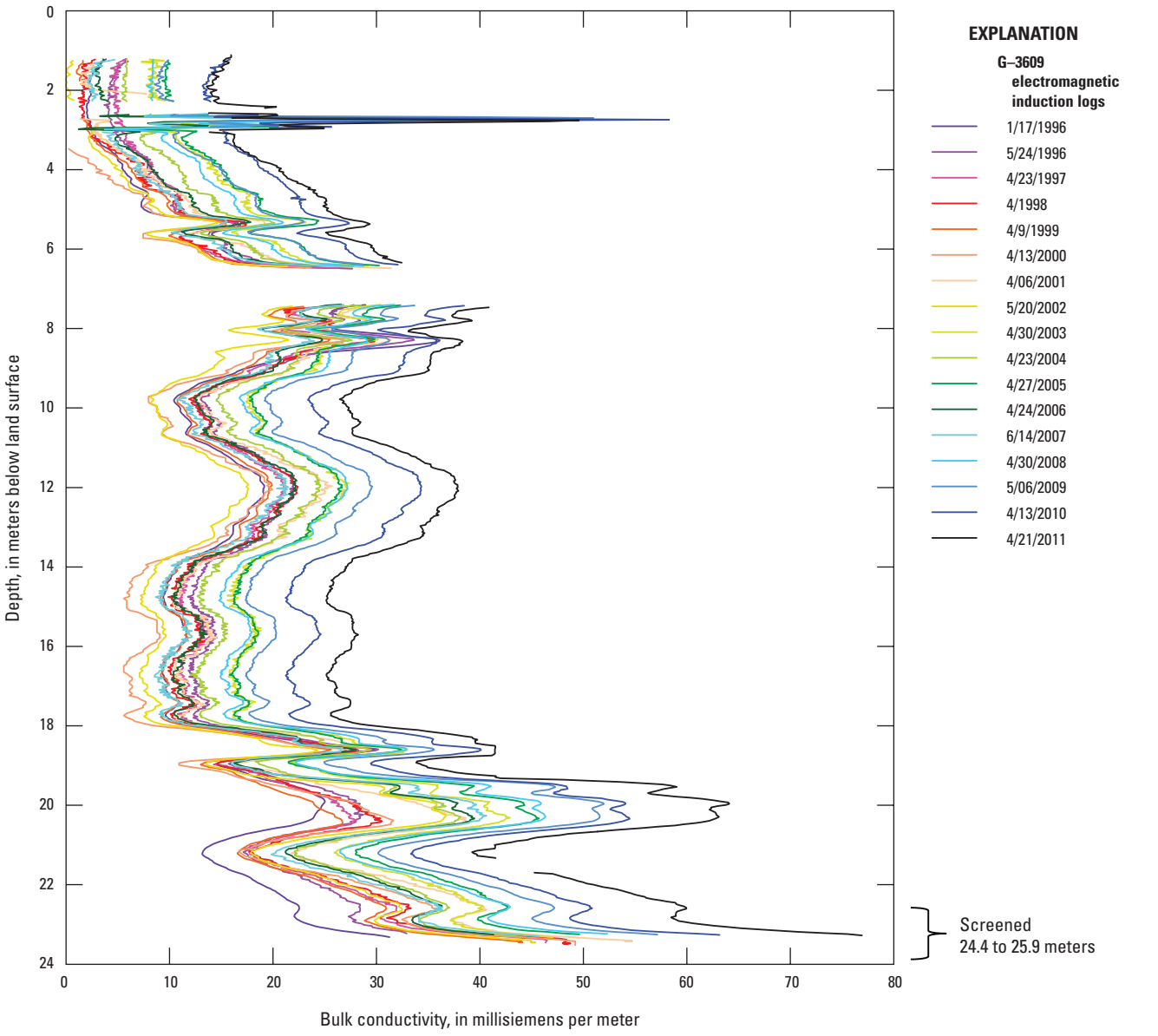

Figure 5–4. Electromagnetic induction logs collected from monitoring well G–3609 from January 1996 to April 2011, Miami-Dade County, Florida.

into the ground near the well. Frequently, where the chloride concentrations in water samples from the well are increasing, the bulk conductivity of the shallow layers is also increasing.

Examination of TSEMIL datasets reveals that the thickness of the saltwater interface in the Biscayne aquifer varies. The TSEMIL dataset collected in well G–3604 (fig. 41*A*) shows a 1.7-m-thick transition between freshwater and water with a chloride concentration of 5,000 mg/L. The TSEMIL dataset collected in well G–3699 (fig. 44*A*) indicates that the transition between freshwater and water with a chloride concentration of 9,700 mg/L is 6.2 m thick.

Although both slope and offset are components of the calibration equation, the procedure described previously generally addresses only the offsets between logs. With the exception of the calibration coil error, it appears that the most of the differences between individual logs can be addressed by removing the apparent offsets between individual logs. Any apparent temporal changes that could be a function of calibration slope should be considered when using TSEMIL datasets to evaluate possible temporal changes in aquifer salinity because the slope corrections generally are not considered during the adjustment process. Slope differences frequently can be ruled out as a significant factor when differences in aquifer salinity apparent in TSEMIL datasets and occurring below the saltwater interface are compared with the parts of the TSEMIL datasets that are above the saltwater interface.

References

ASTM International, 2007, Standard guide for conducting borehole geophysical logging—electromagnetic induction: ASTM International D 6726–01 (reapproved 2007), 8 p.

McNeill, J.D., 1986, Geonics EM39 borehole conductivity meter theory of operation: Geonics Limited, Technical Note TN–20, 9 p., 1 addendum.

McNeill, J.D., Bosnar, M., and Snelgrove, F.B., 1990, Resolution of an electromagnetic borehole conductivity logger for geotechnical and ground water applications: Geonics Technical Note TN–25, 28 p.

Mount Sopris Instrument Co., Inc., 2002, 2PIA–1000 Poly induction probe, 2EMA–1000 conductivity probe (2 EMB–1000 and 2ECM–1000) EMP–2493 and EMP–4493: Golden CO, Mount Sopris, 19 p.

Appendix 6. Evaluation of Depth of the Biscayne Aquifer by Using TEM Soundings

Understanding the depth of the base of the Biscayne aquifer is important for creating maps of saltwater intrusion because saltwater may encroach along the base. At the outset of the current study, existing contour maps of the base of the Biscayne aquifer were available for Broward County (Fish, 1988) and Miami-Dade County (Fish and Stewart, 1991). The TEM results from the current study were evaluated to determine the extent of agreement between the depths of selected model layers and the depth of the Biscayne aquifer mapped by Fish (1988) and Fish and Stewart (1991) (appendix 4).

Wherever possible, the depth to the bases of the Biscayne aquifer mapped by Fish (1988) or Fish and Stewart (1991) was interpolated at each TEM location and compared to the depths of selected model layers of TEM soundings. The values of altitude below sea level provided by Fish and Stewart (1991) were converted to depth by using the altitude of the land surface at each TEM sounding location interpolated from the data provided by a recent light detection and ranging (LIDAR) study (Florida Division of Emergency Management, 2009). The contour intervals of Fish and Stewart (1991) and the 2008 LIDAR study were 3.0 and 0.6 m, respectively. The relations between modeled depths and aquifer depths interpolated from the contours of Fish (1988) or Fish and Stewart (1991) fall into four general categories:

- Type 1 – Model indicates a layer of saltwater (resistivity ≤ 15 ohm-m) occurring within the Biscayne aquifer (fig. 6–1). The bottom of this model layer appears to correspond closely with the depth of the base of the Biscayne aquifer.
- Type 2 – Model does not indicate a layer of saltwater occurring within the Biscayne aquifer (fig. 6–2), but model does indicate a decrease in resistivity that occurs at or near to the depth of the base of the Biscayne aquifer.
- Type 3 – Model does not indicate any layer that is likely associated with the base of the Biscayne aquifer (fig. 6–3). Measurement indicates freshwater (resistivity > 15 ohm-m) throughout the depth modeled, and modeled depth extends at least as deep as the base of the Biscayne aquifer.
- Type 4 – Model does not indicate any layer likely to be associated with the base of the Biscayne aquifer, but a relatively conductive layer (resistivity < 15 ohm-m) occurs well below the base of the Biscayne aquifer. The top of this deeper conductive layer in some instances corresponds to the base of the surficial aquifer (fig. 6–4).

There are also a few subtypes that can be described. These are

- Subtype 1a models are similar to type 1 models in that a conductive layer (resistivity < 15 ohm-m) occurs within the Biscayne aquifer; however, the thickness of the conductive layer could not be determined, and its potential relation with the depth of the base of the Biscayne aquifer could not be evaluated.
- Subtype 1b models have a conductive layer (resistivity < 15 ohm-m) occurring within the Biscayne aquifer, but the thickness of this layer extends below the estimated depth of the Biscayne aquifer and into the semiconfining unit of the surficial aquifer system.
- Subtype 3a models consist of a resistive layer or layers (resistivity > 15 ohm-m) within the Biscayne aquifer that may not fully penetrate the aquifer. It cannot be ascertained whether resistive water extends fully to the base of the Biscayne aquifer or beyond because the thickness of the deepest resistive layer of these models could not be determined.

Appendix 4 provides (1) the resistivity of model layers, (2) the depths of the model layers, (3) the estimated depth of the base of the Biscayne aquifer at each measurement location from Fish and Stewart (1991) or Fish (1988), (4) the model type or subtype, and (5) the difference between the depth of the base of the Biscayne aquifer modeled from the TEM sounding, if evident, and that estimated from Fish and Stewart (1991). Although these relations are subject to interpretation because they rely on previously mapped aquifer depths, this information may be used to assist geologic mapping efforts. Appendix 4 provides a summary of the types of relations between the estimated depth of the base of Biscayne aquifer and the depth of selected model layers. Where such comparisons are possible, table 6–1 provides the minimum, maximum, and average differences between the estimated depth of the base of the Biscayne aquifer and the depth of the selected model layers.

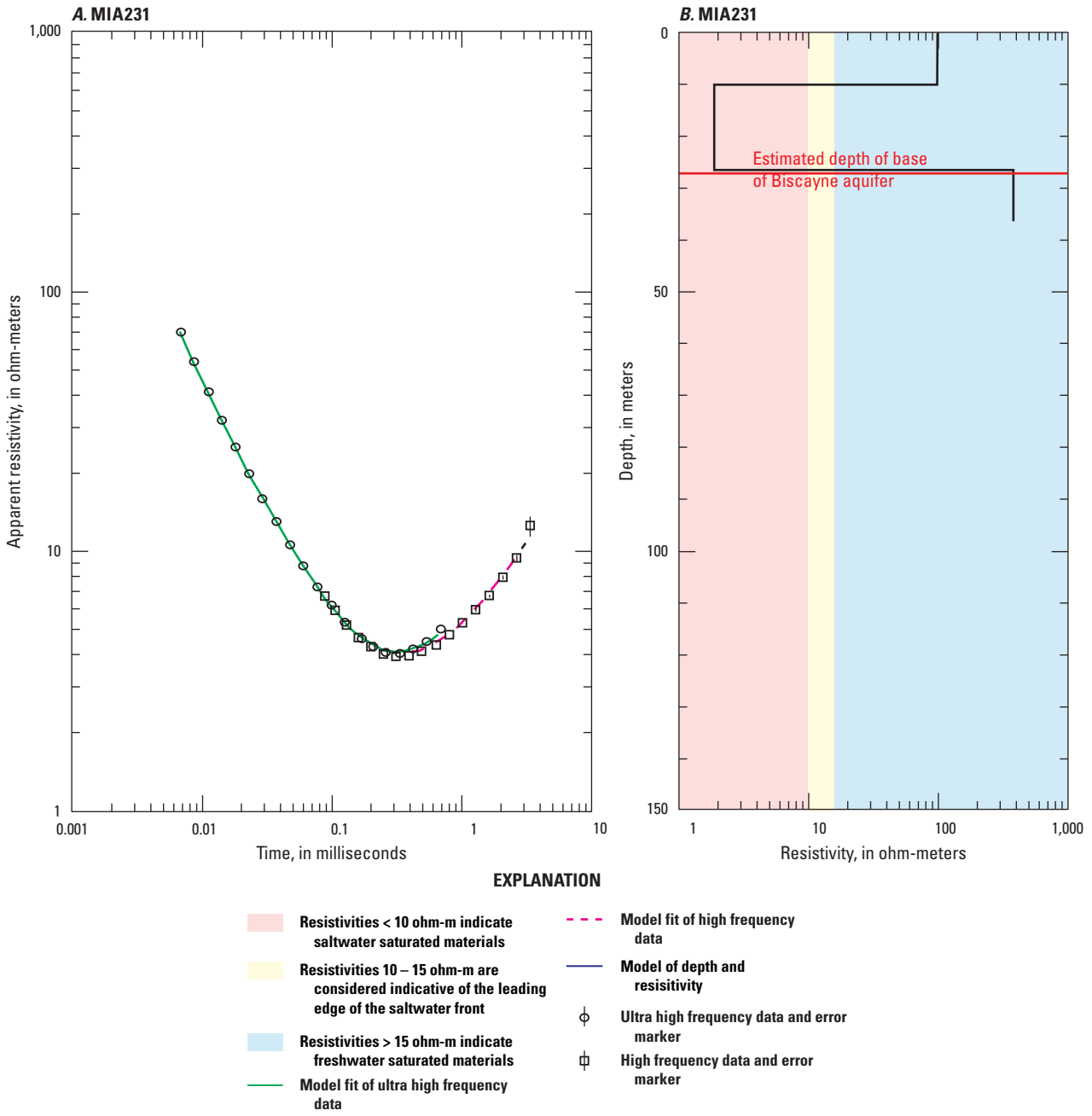

Figure 6–1. Type 1 relation between the depths of model layers and the depth of the base of the Biscayne aquifer. (*A*) Graph of apparent resistivity versus time; (*B*) modeled depth and resistivity. Graph modified from Fitterman and Prinos (2011).

Of the 79 TEM soundings collected, 3 were unusable as a result of anthropogenic interference with the measurements. The remaining 76 were categorized as type 1 (30), type 1a (9), type 1b (2), type 2 (17), type 3 (7), type 3a (1), and type 4 (10) (appendix 4 and appendix 6, table 6–1). Only the 47 type 1 and 2 models have a model layer interface that potentially can be compared to the depth of the base of the Biscayne aquifer (figs. 6–1 and 6–2). The type 1 and type 2 relations are summarized in table 6–1. Of the 47 type 1 and 2 relations, 30, 53, and 81 percent of the models had a model-layer interface that corresponded to the previously mapped base of the Biscayne aquifer within 1.0, 2.0, and 4.0 m, respectively. The average difference was ±2.4 m. Differences could result from (1) imprecision of depth interpolations from contours, (2) variation in the modeled thickness of the conductive layer depth resulting from measurement imprecision or model equivalency, (3) depressions or highs in the paleosurface over which the Biscayne aquifer was deposited that were not captured in the contours of Fish (1988) or Fish and Stewart (1991), (4) intrusion of a portion of the semiconfining unit of the surficial aquifer system by saltwater, (5) imprecision of land-surface altitudes, or (6) potential difficulties in interpreting the depth of the Biscayne aquifer from available stratigraphic information.

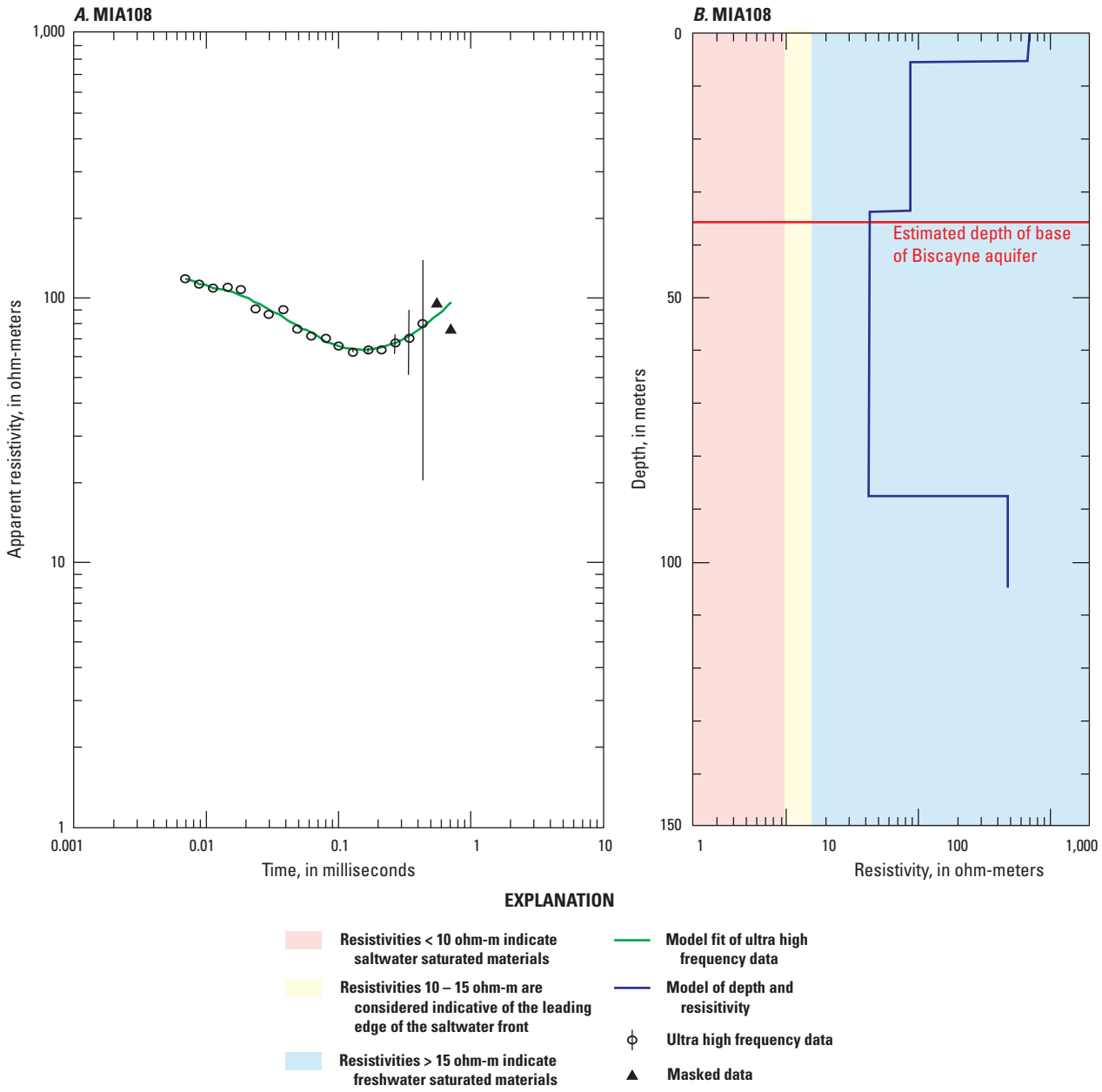

Figure 6–2. Type 2 relation between the depths of model layers and the depth of the base of the Biscayne aquifer. (*A*) Graph of apparent resistivity versus time; (*B*) modeled depth and resistivity. Graph modified from Fitterman and Prinos (2011).

The largest differences between the estimated depth of the base of the Biscayne aquifer and the selected model layer depth were 6.9, and 7.7 m, which occurred at measurement locations MIA122 and MIA202, respectively. The modeled layer thicknesses determined for measurement MIA202 were considered "very good" (Fitterman and Prinos, 2011). Measurement MIA202 may, therefore, indicate the presence of an isolated but deep topographic depression in the paleosurface over which the Biscayne aquifer was deposited, or it may indicate that the differences in resistivity occurring near the base of the Biscayne aquifer were not large enough to detect. Five of the seven sites where the differences ranged between 5 and 7.7 m are in the Model Land area. Fish and Stewart (1991, p. 38) used only three boreholes in this area for their mapping effort, and the sparse distribution of boreholes in their mapping effort may have failed to identify variations in the depth of the base of the Biscayne aquifer.

All of the type 3 and type 4 models determined from measurements in the Model Land area and a few miles north of it indicate a decrease in resistivity occurring between depths of 11.8 and 18.9 m. These models have a highly resistive (184–709 ohm-m) first layer and a less resistive

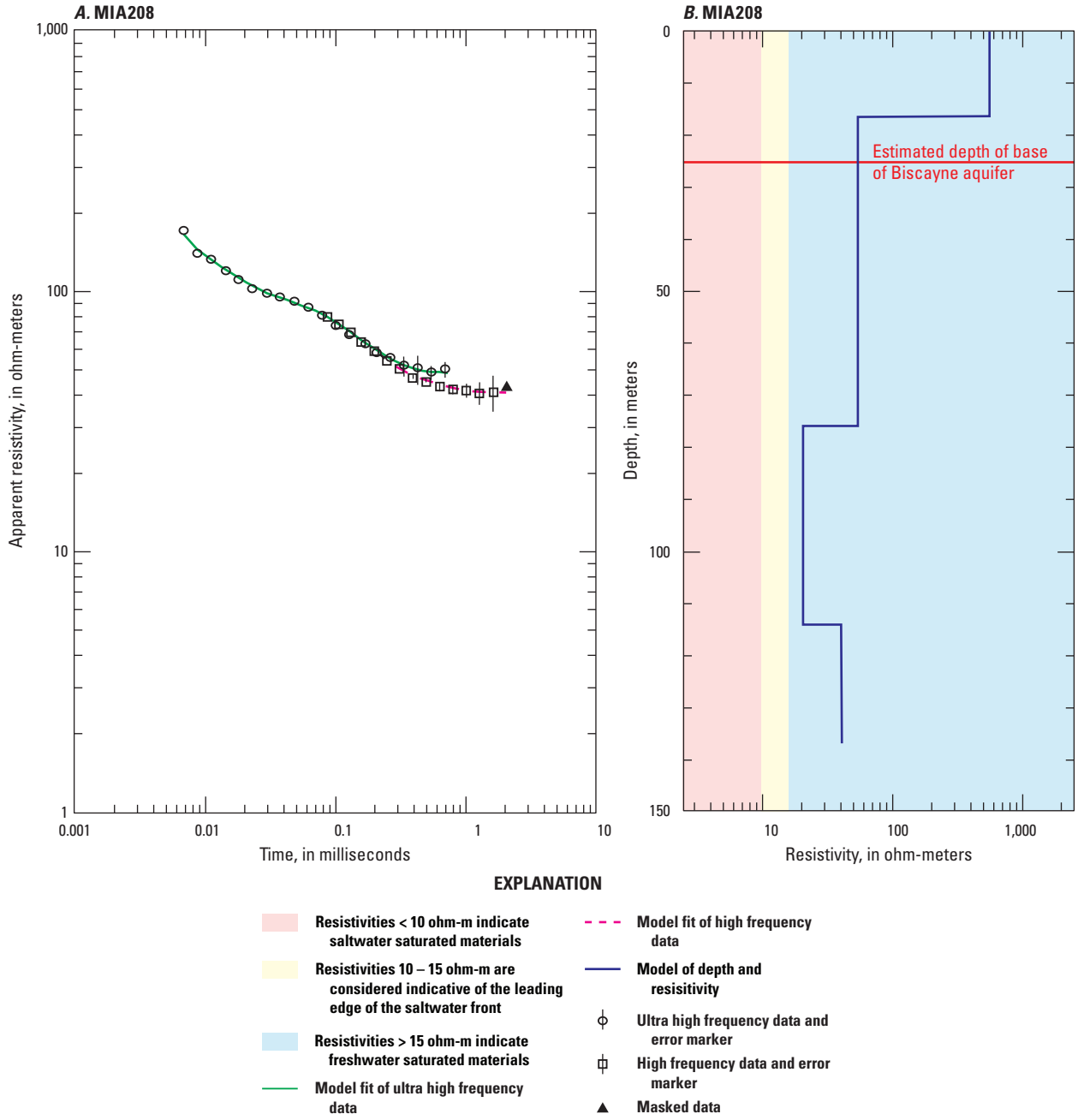

Figure 6–3. Type 3 relation between the depths of model layers and the depth of the base of the Biscayne aquifer. (*A*) Graph of apparent resistivity versus time; (*B*) modeled depth and resistivity. Graph modified from Fitterman and Prinos (2011).

(21.1–60.0 ohm-m) second layer. The decrease in resistivity does not appear to be associated with the base of the Biscayne aquifer because there is ample hydrostratigraphic information available in this area to place the depth of the base of the aquifer between 23 and 29 m. Hydrostratigraphic information includes logs from recently installed monitoring wells and numerous proximal type 1 and type 2 TEM models from which the depth of the base of the Biscayne aquifer can be interpreted. Geophysical logs collected in well G–3946, installed during this study (table 7–1), and test core holes G–3938, G–3939, and G–3940 (appendix 1), installed during a recent USGS and FPL cooperative study (Wacker, 2010), indicated flow zones at depths of approximately 14 to 17 m. Flow zones also were identified in wells G–3939 and G–3940 at depths of approximately 10 to 11 m. If laterally persistent, these flow zones and perhaps the interaction of these flow zones with minor amounts of intruded saltwater (less than that normally associated with the saltwater front) may account for the changes in resistivity detected in the type 3 and type 4 models of TEM soundings.

TEM sounding MIA240 was a two-layer type 3 model that indicated a reduction in resistivity occurring at a depth

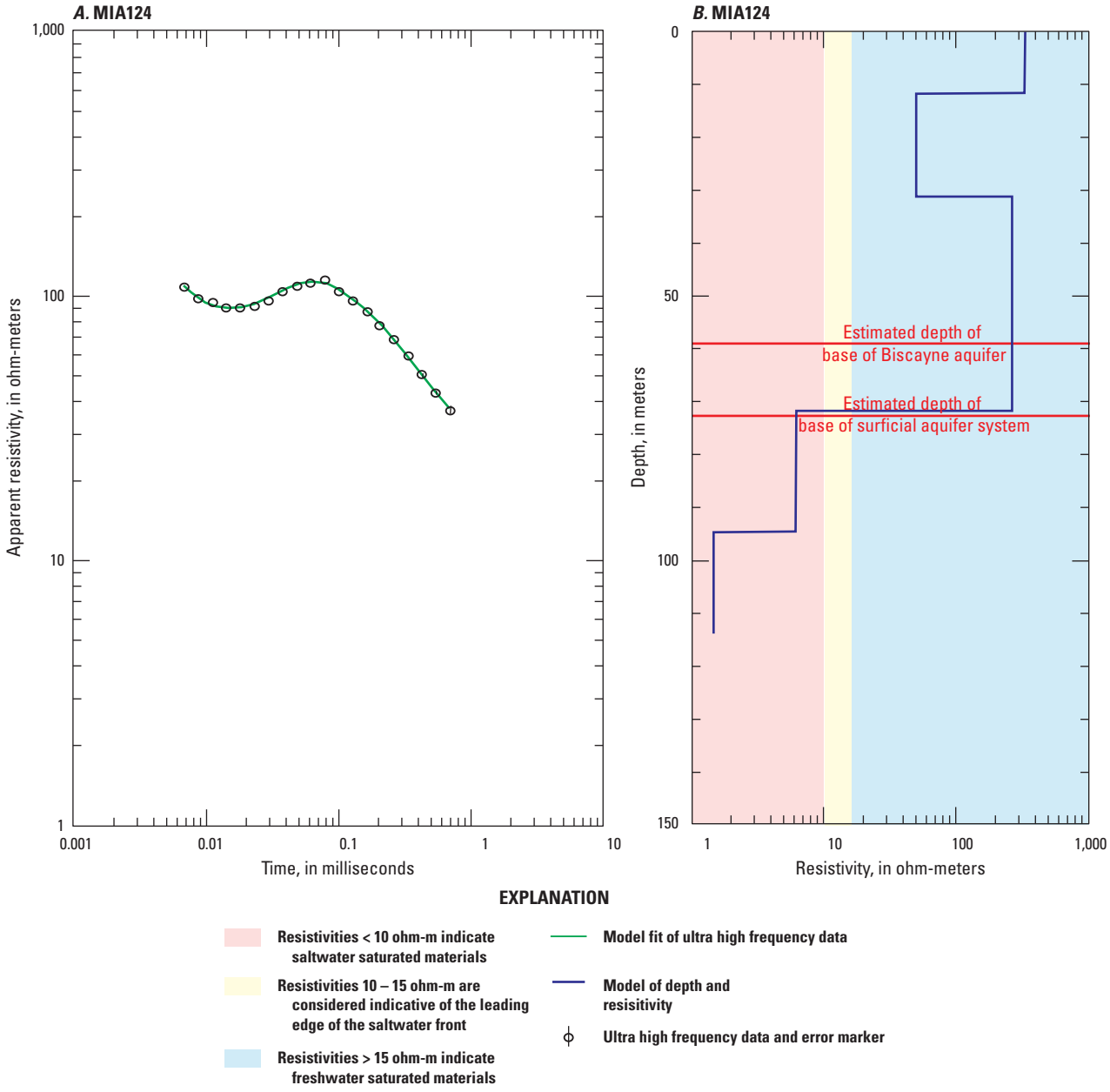

Figure 6–4. Type 4 relation between the depths of model layers and the depth of the base of the Biscayne aquifer. (*A*) Graph of apparent resistivity versus time; (*B*) modeled depth and resistivity. Graph modified from Fitterman and Prinos (2011).

of 72.9 m. Models of measurements MIA241 and MIA242, collected in the same area, also indicated decreases in resistivity occurring at depths of 65.1 and 76.4 m, respectively. The depth of the base of the surficial aquifer in this area is estimated to be 86 m from the contour map of Fish (1988). Considering that the contour in this area was based on only one borehole and that the depth of the base of the surficial aquifer may vary, the decreases in resistivity indicated by the models of these TEM soundings may be associated with the depth of the base of the surficial aquifer.

The conductive layers identified in type 4 models occurred at depths ranging from 49.6 to 98.1 m. These layers correspond within 29 m to the base of the surficial aquifer system in 7 of the 10 type 4 models. It is unknown if the base of the surficial aquifer varies this extensively because the distribution of boreholes used for the mapping effort was relatively sparse (Fish, 1988; Fish and Stewart, 1991). The conductive layers identified in the remaining three type 4 models are at depths ranging from 35 to 45 m below the estimated depth of the base of the surficial aquifer system and may correlate to a unit within the Hawthorn Group.

Table 6–1. Types of model relations and comparisons between the estimated depth of the base of the Biscayne aquifer in Miami-Dade and Broward Counties, Florida, and the depth of the selected model layers.

[NA, not applicable]

Relations between selected model surfaces and estimated depth of base of Biscayne aquifer		Difference between estimated depth of the base of the Biscayne aquifer and depth of applicable model surface			Percentage of relations for which the estimated aquifer depth and selected layer depth are within:		
Relation type	Number of relations of this type	Maximum	Minimum	Average	1 Meter	2 Meter	4 Meter
1	30	7.7	0.1	2.3	33	60	80
1a	9	NA	NA	NA	NA	NA	NA
1b	2	NA	NA	NA	NA	NA	NA
2	17	5.6	0.1	2.7	24	41	82
3	7	NA	NA	NA	NA	NA	NA
3a	1	NA	NA	NA	NA	NA	NA
4	10	NA	NA	NA	NA	NA	NA
1 and 2 combined	47	7.7	0.1	2.4	30	53	81

References

Fish, J.E., 1988, Hydrogeology, aquifer characteristics, and groundwater flow of the surficial aquifer system, Broward County, Florida: U.S. Geological Survey Water-Resources Investigations Report 87–4034, 80 p.

Fish, J.E., and Stewart Mark, 1991, Hydrogeology of the surficial aquifer system, Dade County, Florida: U.S. Geological Survey Water-Resources Investigations Report 90–4108, 50 p., 11 sheets.

Fitterman, D.V., and Prinos, S.T., 2011, Results of time-domain electromagnetic soundings in Miami-Dade and southern Broward Counties, Florida: U.S. Geological Survey Open-File Report 2011–1299, 289 p.

Florida Division of Emergency Management, 2009, Miami-Dade County 2 ft contour lines: Tallahassee, FL, Florida Division of Emergency Management, Shapefile, accessed February 10, 2011, at *http://www.floridadisaster.org/gis/index.asp*.

Wacker, M.A., 2010, Tools and data acquisition of borehole geophysical logging for the Florida Power and Lights Company Turkey Point Power Plant in support of a groundwater, surface-water, and ecological monitoring plan, Miami-Dade County, Florida: U.S. Geological Survey Open-File Report 2010–1260, 5 p., appendixes.

Appendix 7. Description of Installation and Construction of Saltwater Front Monitoring Wells

Site Selection and Depths of New Monitoring Wells

Sites for new saltwater monitoring wells were selected to fill gaps in the existing salinity monitoring network, based on a review of the spatial coverage provided by existing monitoring wells and surface geophysical data. The eight new wells were named G–3885, G–3886, G–3887, G–3888, G–3946, G–3947, G–3948, and G–3949 (fig. 8). Some of the new monitoring wells have sample tubes installed to collect water-quality samples in flow zones above or below the saltwater interface, and “A,” “B,” “C,” “D,” and “S” suffixes are added to the well name to differentiate between the primary well and the sample tubes (table 7–1). In addition to the installation of new saltwater monitoring wells, the study also included the collection of core and borehole geophysical logs (appendixes 8 and 9).

Drilling and Coring

Monitoring wells were drilled and constructed in two phases. Four wells were drilled between June 30, 2009, and

Table 7–1. Construction and logging information from new wells installed in Miami-Dade County, Florida, during 2009–2011.

[NGVD 29, National Geodetic Vertical Datum; m, meters; >, greater than; µS/cm, microsiemens per centimeter; cm, centimeters; NA, not applicable]

Local identifier	Description*	USGS station number	End date of construction	Latitude (North), in degrees, minutes, and seconds	Longitude (West), in degrees, minutes, and seconds	Altitude of ground surface (m)	Altitude of top of casing (m)	Total depth cored from surface (m)	Base of Biscayne aquifer from land surface (m)	Depth to water with > 5,000 µS/cm (m)	Screen interval from land surface (m)	Bottom of tailpipe from land surface (m)	Number of separate stages needed to log well	Internal diameter of PVC pipe (cm)
G-3885	Primary well	253253080221201	8/18/2009	25–32–53.1	080–22–12.7	2.12	1.89	27.74	24.63	NA	23.16–24.69	26.21	1	5.08
G-3886	Primary well	253527080195401	10/2/2009	25–35–27.9	080–19–54.2	3.1	2.91	33.22	27.74	NA	26.21–27.74	30.78	1	5.08
G-3887A	Primary well	253924080174601	9/25/2009	25–39–24.7	080–17–46.8	3.18	2.96	40.84	36.52	23.38	24.38–25.91	39.62	1	5.08
G-3887B	Sample tube	253924080174602	9/25/2009	25–39–24.7	080–17–46.8	3.18	Not Surveyed	40.84	36.52	23.38	19.51–21.03	22.56	1	2.54
G-3888A	Primary well	254542080145901	10/5/2009	25–45–42.7	080–14–59.8	4.31	4.17	45.35	41.76	29.57	31.55–34.59	43.74	2	5.08
G-3888B	Sample tube	254542080145902	10/5/2009	25–45–42.7	080–14–59.8	4.31	Not Surveyed	45.35	41.76	29.57	39.62–41.15	42.67	2	1.91
G-3888C	Sample tube	254542080145903	10/5/2009	25–45–42.7	080–14–59.8	4.31	Not Surveyed	45.35	41.76	29.57	22.86–27.43	28.96	2	1.91
G-3946D	Primary well	252431080261001	6/22/2010	25–24–30.7	080–26–09.7	1.09	1	26.64	20.09	16.73	18.90–20.42	26.52	1	5.08
G-3946S	Sample tube	252431080261002	6/22/2010	25–24–30.7	080–26–09.7	1.09	1.01	26.64	20.09	16.73	15.85–16.76	16.76	1	2.54
G-3947	Primary well	255011080124501	7/16/2010	25–50–11.3	080–12–45.4	3.57	3.48	69.49	54.01	None	51.82–54.86	60.96	1 (below 23.77 m)	5.08
G-3948D	Primary well	255515080103601	10/13/2010	25–55–14.9	080–10–36.2	3.62	3.54	84.8	76.2	65.78	72.24–74.07	83.21	6	5.08
G-3948S	Sample tube	255515080103602	10/13/2010	25–55–14.9	080–10–36.2	3.62	Not Surveyed	84.8	76.2	65.78	35.51–37.03	37.03	6	2.54
G-3949D	Primary well	255733080195601	1/31/2011	25–57–33.6	080–09–56.5	3.75	3.62	106.46	84.04	NA	66.14–67.67	99.06	7	5.08
G-3949I	Sample tube	255733080195602	1/31/2011	25–57–33.6	080–09–56.5	3.75	Not Surveyed	106.46	84.04	NA	44.44–45.96	46.01	7	2.54
G-3949S	Sample tube	255733080195603	1/31/2011	25–57–33.6	080–09–56.5	3.75	Not Surveyed	106.46	84.04	NA	15.24–16.76	16.81	7	2.54

*Monitoring wells with sample tube listed under description were constructed in the same borehole as the primary well with the same local identifier prefix, to obtain water-quality samples only.

October 5, 2009, and the remaining four wells were drilled between June 30, 2010, and February 3, 2011. A USGS Florida Water Science Center hydrologist supervised the coring, data collection, and well construction at each site. Decisions were made during drilling, regarding the need for additional lengths of surface casing and the stability of the borehole. Borehole geophysical logs were collected in stages (table 7–1) during the drilling at some sites. A steel casing was used to keep the borehole open to total depth due to sand infilling the borehole.

Borehole drilling began at each site using a 35.6-cm-diameter auger to drill a hole to the top of the first stable geologic unit, such as a well cemented limestone or sandstone unit. A schedule 2, polyvinyl chloride (PVC) surface casing with a 25.4-cm inside diameter was installed in the hole produced by the auger and was grouted into place. The well was cored from the approximate top of the bedrock using a wire-line coring system to collect a 10.2-cm-diameter core samples to a depth below the base of the Biscayne aquifer and into the uppermost part of the underlying semiconfining unit as determined by the USGS onsite hydrologist. Coring was completed in 1.5-m intervals, and the time required to drill each foot (0.3 m) was recorded in a field log. Each 1.5-m core interval segment was brought to the surface; the core segment was removed from the core barrel by the USGS onsite hydrologist and placed in a 1.5-m-long PVC core-recovery tray while maintaining the correct vertical stratigraphic orientation. The core segment was washed to remove drilling cuttings and fluids and was placed in a 0.6-m-long cardboard core box with wooden blocks marked with the driller's depth placed at the bottom of each core segment. The core segment was then marked by using paint pens with two continuous vertical lines (one black and one red) running parallel to the long axis of the cylindrical core samples. When the core is oriented in the correct vertical orientation with respect to the strata in the aquifer, the red line is on the right side of the core and the black line is on the left. This marking convention prevents inadvertent inversion of core segments. The length of the core segment recovered from each 1.5-m core interval was entered in a field log.

A liquid polymer mud was added as necessary to the drilling fluid to facilitate collection of unconsolidated sand and soft sediment in the core barrel and to allow their extrusion from the barrel at the surface. The polymer mud also provided lubrication and facilitated the removal of cuttings. The polymer breaks down within a few days and is easily removed from the column of borehole fluid during a borehole purging process called airlifting. Once coring was completed to the desired total depth below the Biscayne aquifer, the wire-line coring casing was removed. The borehole was prepared for logging by evacuating loose clay, silt, and sand to cobble-sized (up to 7.6 cm diameter) material from the borehole with an airlift device constructed by the drilling contractor. As water was purged from the borehole by using this device, it was replaced by water from the aquifer. This flow aids removal of drilling fluids and improves water clarity. Any noteworthy samples brought to the surface during airlifting were archived in core boxes and the approximate depth of retrieval, if known, was indicated with wood blocks. Airlifting was considered complete when the borehole was free of obstructions and the water from the borehole was free and clear of suspended solids. Water clarity is an important consideration for optical borehole image (OBI) logging.

At some sites, sand layers within the aquifer bridged across the borehole to create an obstruction. Bridging and infilling with sand required that these boreholes be drilled, logged, and constructed in stages (table 7–1). Some of the geophysical logs, such as the digital OBI logs, were incomplete because of the obstructions caused by the bridging of sand layers in these boreholes. In well G–3949, numerous sand bridges were encountered during drilling.

Borehole Geophysical Logging Prior to Well Construction

Geophysical logging was performed by the USGS in each of the eight boreholes. Geophysical logs similar to those described in Wacker and Cunningham (2008) were collected to help identify (1) the base of the Biscayne aquifer, (2) zones of higher permeability, and (3) depth to water with conductivity, compensated at 20 °C, greater than 5,000 µS/cm, if found within the boreholes. This information was used to determine the optimal design specifications for the new monitoring wells. These new monitoring wells were designed to monitor the deepest preferential groundwater flow zone identified within the formations that comprise the Biscayne aquifer. Additional sample tubes were added if the geophysical logs indicated other permeable zones of interest. Geophysical logging commenced within about 24 hours of completion of airlifting to allow suspended sediment in the borehole fluid column to settle. The 24-hour waiting period was generally sufficient to produce clear formation fluid in the borehole required for the OBI log. In some wells, geophysical logs (caliper, gamma, spontaneous potential, single point resistance, electromagnetic induction, and full waveform sonic) were run immediately after the airlift development because these logs are not affected by borehole water clarity.

Borehole Image Logging

At each borehole drilled for this study, two types of geophysical borehole imaging tools were used: the Mount Sopris OBI MK-IV digital OBI tool and a Mount Sopris ABI–40 digital acoustic borehole imaging (ABI) tool. The OBI log was collected first, using 95 percent light and 720 turns (or every half degree of circumference), and was sampled vertically every 0.82-mm of depth. Then the ABI–40 digital acoustic borehole imaging (ABI) log was collected using 288 turns (or every 1.25 degrees of circumference) and was sampled vertically every 1.68 mm of depth. Both OBI and ABI tools acquired data while logging upward from the bottom of the borehole to the land surface or from the bottom of casing if the borehole was logged in stages.

Borehole Fluid and Caliper Logging

A Mount Sopris Idronaut 303 (Mount Sopris 2IFA–1000) water-quality tool was used at each site to collect logs of fluid temperature, conductivity compensated at 20 °C , pH, dissolved oxygen (in percent), and oxidation reduction potential. The conductivity measured by this probe is not the same as specific conductance because specific conductance is typically normalized to a temperature of 25 °C. The water-quality tool acquired data while logging upward and downward in the borehole. After the first four wells were completed, and before construction of the last four was begun, the water-quality tool was returned to the manufacturer for repairs of a sensor and for re-calibration. The water-quality tool was fully calibrated and functioned properly at all sites. In addition, the water-quality tool calibration was checked with a separate and independently calibrated conductivity meter during logging.

At sites where the borehole was filled with freshwater, a Mount Sopris 2FSB–1000 fluid probe, which was attached to the bottom of a Mount Sopris 2CAA–1000 three-arm caliper tool, was used to acquire fluid temperature and resistivity measurements while logging downward from land surface. Temperature and resistivity were automatically used to compute fluid conductivity and specific conductance (appendix 8). Fluid probe data were used for comparison with the water-quality tool when available. Caliper logging with the caliper tool was then performed to determine the borehole diameter. These logs were collected in an up-hole direction.

Induction, Natural Gamma-Ray, Spontaneous Potential, and Single-Point Resistance Logging

After the caliper log was collected, logs were collected using a Mount Sopris 2PIA–1000 electromagnetic induction tool, an HLP–2375/S natural gamma-ray tool, and a combined spontaneous potential (SP) and single-point resistance (SPR) tool. Induction logs were collected in the up-hole and down-hole directions. The natural gamma-ray log was collected in an up-hole direction, and the spontaneous potential (SP) and single-point resistance (SPR) logs were collected in a down-hole direction. The Mount Sopris 2PIA–1000 electromagnetic induction tool was calibrated as described in preceding sections of this report. A final electromagnetic induction log was collected in each of the completed 5.1-cm-diameter monitoring wells. The natural gamma-ray tool and SP/SPR tool do not require calibration and provide relative values that can be compared with other logs collected with the same tool.

Full Waveform Sonic

Upon completion of induction, natural gamma-ray, SP, and SPR logging, a Mount Sopris 2SAA–1000/F full waveform sonic tool log was collected from each borehole. Two logs were collected by using the sonic tool: one with an acoustic signal transmitted at 15 kilohertz (kHz; used for porosity calculations) and one transmitted at 1 kHz (used for relative permeability estimations). The full waveform sonic logs were not collected from wells that were logged in multiple stages when the length of logging stage was less than 6.1 m because the 3.0-m tool length would not provide useful information in a short interval. The full waveform sonic logs were processed by using Log Cruncher™ software. Log Cruncher is used to determine the mean primary compressional wave and Stoneley wave velocities. The compressional wave velocity is used as input into the Raymer-Hunt porosity equation for calculation of sonic porosity (Raymer and others, 1980). Sonic porosity values calculated from compressional wave velocities are typically higher than whole-core laboratory porosity measurements. Known values of laboratory-measured porosity of rock cores were not available to calibrate a computed porosity curve. The amplitude of the Stoneley wave also was measured from the receiver closest to the transmitter (receiver 1). The Stoneley wave amplitude has a predictable qualitative relation to permeability, which can be used to estimate a qualitative permeability of the rock surrounding the borehole. Generally, low amplitudes can represent relatively high permeability, and high amplitudes can represent relatively low permeability. The computed value, therefore, can be used in a qualitative and conservative sense to estimate zones of relatively high and low permeability.

Flowmeters

Flowmeter logging of each borehole was completed under both ambient (static) and dynamic (pumping) conditions. Three different types of flowmeters were used during the study because of the variability in borehole fluid conditions. Saline fluids are more conductive and appear to have an effect on the performance of the electromagnetic flowmeter and, to a lesser degree, on the performance of the heat-pulse flowmeter. The spinner flowmeter is not affected by the conductivity of the borehole fluid. Each borehole was pumped using a 5.08-cm-intake-diameter centrifugal water pump with the suction line placed below the water table within the open borehole. Flow rates were measured by timing the rate at which discharge water filled a 75.7–L container and are shown on each log heading (appendix 8). Pumping rates during geophysical logging ranged from 121 to 477 L/min. Rates varied depending on depth to water and length of discharge hose. Flowmeter logs were not collected from any boreholes (G–3888, G–3947, G–3948, and G–3949) with geophysical logging intervals less than 6.1 m in length.

Once the image and caliper logs were collected at each borehole, a draft of these logs was plotted in the field to determine optimum depths for the collection of stationary measurements of vertical borehole fluid flow using the flowmeters. A Mount Sopris HPF–2293 heat-pulse flowmeter with an 18-cm petal diverter was set at each predetermined depth, and at least three measurements were collected at each stationary depth under ambient borehole fluid-flow conditions.

Following logging with the heat-pulse flowmeter, a Century Geophysical 9721 electromagnetic flowmeter was used to log by trolling up and down the borehole to create a continuous log of vertical borehole fluid flow under ambient conditions. The electromagnetic flowmeter also contained a sensor to measure borehole fluid temperature and resistivity, which were recorded. After the ambient borehole fluid flow was measured while trolling, a centrifugal pump was used to draw water from the well at a constant rate. Once the flow and drawdown stabilized, the electromagnetic flowmeter log was collected in the borehole under pumping conditions. The electromagnetic flowmeter acquired stationary pumping flow measurements at the same depths as those acquired by the heat-pulse flowmeter under ambient conditions. The electromagnetic flowmeter also provided logs of fluid temperature and resistivity (appendix 8).

In some boreholes that were logged in stages, the lowest stage was logged with either a Mount Sopris FLP–2492 spinner flowmeter or an electromagnetic flowmeter during pumping to determine flow zones. Ambient flow information was not collected in wells where the upper part of the borehole was cased because there would not be a head difference between the lower and upper flow zones to cause ambient flow.

Geophysical Log Analysis

Following acquisition of all geophysical logs in the field, the raw log data were processed and displayed by using Advance Logic Technology, WellCAD version 4.3, and were saved in Adobe Systems Incorporated Portable Document Format (PDF) at 1:48 scale (appendix 8). Final monitoring-well completion zones are shown on the final log montage with depths relative to land surface.

Well Completion

By using the information provided by geophysical and water-quality logging (appendix 8), the monitoring wells were designed to (1) penetrate the full thickness of the aquifer and a shallow depth below it, into the upper portion of the semi-confining unit of the surficial aquifer, (2) provide samples from the deepest flow zone occurring within the formations that comprise the Biscayne aquifer, and (3) allow sampling of shallower flow zones or saltwater interfaces through sample tubes. Table 7–1 provides well construction information for the eight wells installed during this study. The depth to water of conductivity, compensated at 20 °C, greater than 5,000 µS/cm also is provided because water of this conductivity generally has a chloride concentration of 1,000 mg/L or greater. A chloride concentration of 1,000 mg/L has been used historically for mapping the inland extent of saltwater in southeast Florida.

Many of the pre-existing monitoring wells were designed such that the bottom of the well would be at about the same depth of the base of the Biscayne aquifer. In this design, the tip of the induction logging tool usually encounters the bottom of the well before a full response to materials at the aquifer's base can be achieved. To improve the quality of data collected, the new monitoring wells incorporated several design features (fig. 7–1) not previously implemented in the USGS network in this area: (1) additional casing that extended below the screen and somewhat deeper than the base of the Biscayne aquifer, (2) installation of secondary filter packs in zones of high porosity, and (3) installation of secondary sampling tubes in selected secondary filter packs. By adding additional casing below, a full response can be recorded within the screened interval. The additional casing can also allow measurement of changes occurring near the top of the semi-confining unit of the surficial aquifer to determine if saltwater also is intruding into these sediments.

Large solution cavities in the limestone of the Biscayne aquifer likely would allow the cement grout of the annular seal to flow into the formation. This grout could prevent formation water from entering the 20- to 100-cm radius of investigation of the induction logging probe. The installation of secondary filter packs at depths where large solution cavities occur allows formation water to flow unimpeded in close proximity to the well casing so that the formation water can be measured by the induction probe. Small-diameter sample tubes were installed in some of the secondary filter packs so that the water in highly transmissive flow zones could be sampled.

Historically, drill cuttings were used to evaluate the stratigraphy and to help determine the depths of the intakes of some of the monitoring wells used for collection of TSEMIL datasets. Evaluations of drill cuttings alone could result in a well intake too deep to provide water samples from the depth interval where there are changes in bulk conductivity. For example, this situation occurred at well G–3701 (fig. 33*A*). The geophysical logging during this study allowed the identification of the deepest flow zones within the Biscayne aquifer so that the screened interval of the 5.1-cm-diameter monitoring well could be placed in this flow zone. Additional casing was added below the screen to ensure that the induction tool would be able to record data across the boundary between the base of the aquifer and the semi-confining unit of the surficial aquifer. In some instances, such as for well G–3949, the tailpipe extends to a much greater depth below the screened interval so that identified zones of weak flow within the semi-confining unit of the surficial aquifer can be monitored. Secondary sampling tubes were installed in five of the eight boreholes.

Once the well design was completed, construction began by backfilling the borehole with 20–30 grade sand to the designed depth of the bottom of the added casing. Then the well casing and screen were assembled and inserted into the well. More fine sand was added to a depth about 1.2 m below the screen, and then a layer of time-release bentonite pellets and sand was installed that extended to within approximately 0.6 m of the bottom of the screen. A filter pack consisting of pea gravel was used to fill the screened interval from 0.6 m below the interval to 0.6 m above the top of the interval. Then

Depths of screen intervals, and seals are based on results of geophysical logging

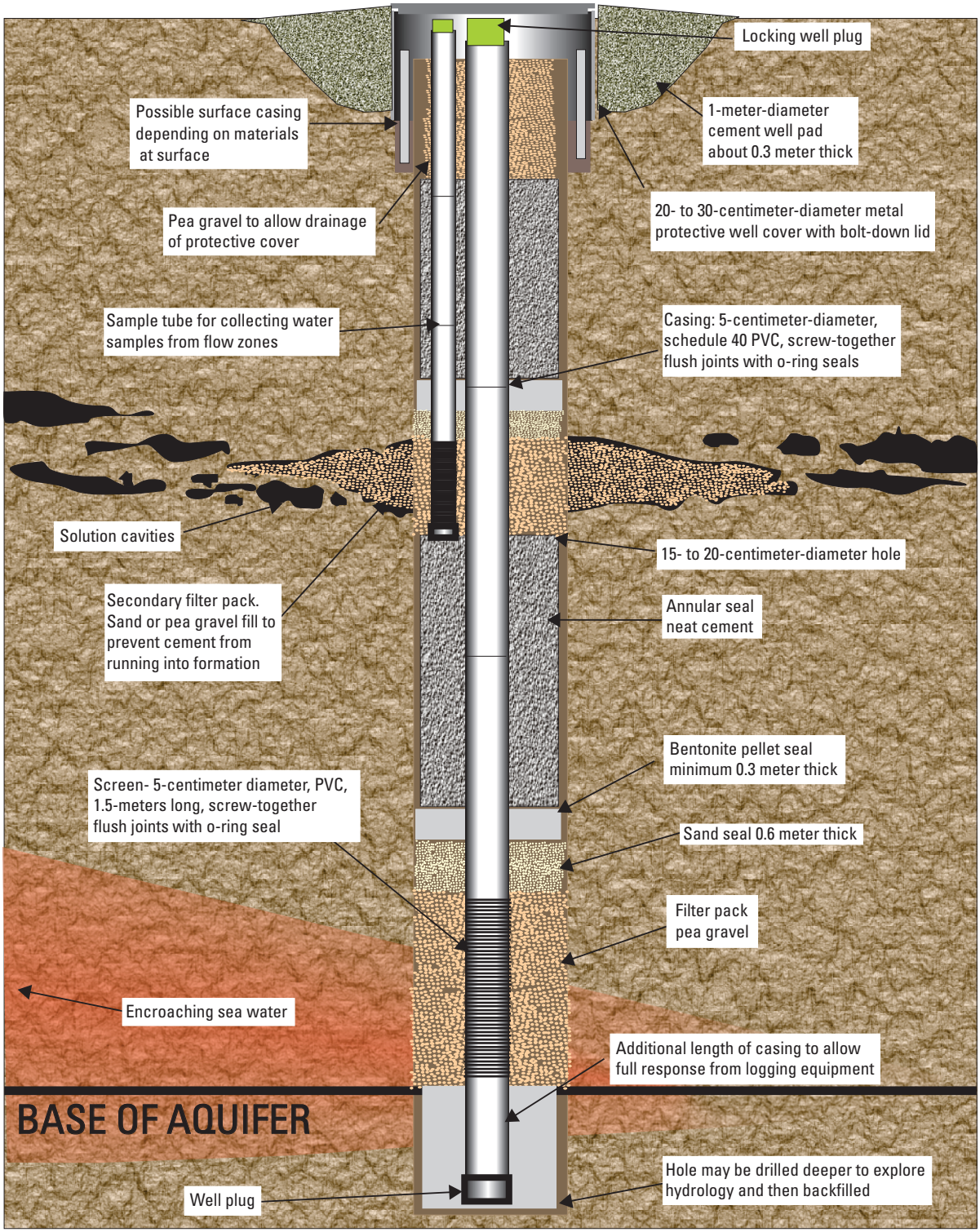

Figure 7–1. Illustration showing design of new monitoring wells installed during the study to monitor saltwater intrusion into the Biscayne aquifer, Miami-Dade County, Florida.

successive layers of sand and bentonite pellets were added to create a seal above the filter pack that would prevent grout from filling the filter pack. In the deeper wells (G–3947, G–3948, and G–3949), the material was added by using a 2.5-cm-diameter PVC tremie pipe. The annular seals of wells were grouted in stages. A 190–L barrel (about 4 bags) of grout was added at a time, and this grout was allowed to set overnight. If a sample tube was installed to monitor a flow zone, the previously described procedure for creating a filter pack was used to complete that interval. If a sample tube was not installed in the identified high flow zone, it was filled with a layer of coarse (6–20 grade) sand that extended about 1 m above and below the flow zone. This layer of sand was capped with a layer of bentonite pellets and grout to prevent the movement of water in the annular space. Pea gravel filter packs, sample tubes, seals, and grout were installed as necessary to complete the well installation. Near the surface, a grout layer was added to within a few feet of land surface to seal the well from surface water. After the grout was set, the manhole was constructed by adding sand above the grout to the base of the manhole to allow for drainage. Then a concrete pad was constructed.

After the wells were completed, Miami-Dade County surveyed the top of each casing and the manhole, and a final electromagnetic induction log was run in each completed monitoring well. Field notes were collected during drilling, logging, and construction, and a PDF file was then made of all logs. Well information was entered into the USGS Ground Water Site Inventory (GWSI) system for future reference, and the geophysical logs were archived for future use.

References

Raymer, L.L., Hunt, E.R., and Gardner, J.S., 1980, An improved sonic transit time-to-porosity transform, paper P, *in* 21st Annual Logging Symposium Transactions: Society of Professional Well Log Analysts, 12 p.

Wacker, M.A., and Cunningham, K.J., 2008, Borehole geophysical logging program—Incorporating new and existing techniques in hydrologic studies: U.S. Geological Survey Fact Sheet 2008–3098, 4 p.

Appendix 8. Geophysical Logs

Geophysical logs collected in the eight new wells were evaluated using WellCAD™ software. WellCAD™ files are provided as supplemental files. Adobe™ Portable Document Format (PDF) files are also provided in the supplement files, but the ability to view all logs in detail is limited by this format.

See supplemental files in the folder *http://pubs.usgs.gov/sir/2014/5025/appendix/sir2014-5025_appendix_08*.

Appendix 9. Hydrostratigraphic Analysis

Continuously drilled core samples from the eight new monitoring sites and related borehole geophysical logs were examined in the USGS core laboratory in Davie, Florida. Geologic, geophysical, and hydrologic data from the eight boreholes form the fundamental basis for a generalized hydrostratigraphic framework of the surficial aquifer in central to northern coastal Miami-Dade County, which is described herein. The information obtained from the new wells was used to map on a two-dimensional section the lithostratigraphic and hydrostratigraphic units (fig. 9–1). The lithology and extent of the lithostratigraphic units were determined by examination of continuously drilled cores and borehole-geophysical logs (especially digital optical borehole wall images).

Correlation of Lithostratigraphy and Hydrostratigraphy of Eight New Boreholes

Correlation of the basic lithostratigraphy represented in the eight boreholes drilled for this study is shown in figure 9–1. Zones of groundwater flow within and delimiting the base of the Biscayne aquifer in these eight wells were defined by using the results of the examination of pore systems in lithologic cores and in digital optical borehole wall images and the evaluation of flowmeter logs combined with borehole-fluid conductivity and temperature log data. Interpretations of this information indicate that the surficial aquifer within the study consists mostly of the Tamiami Formation, Fort Thompson Formation, Miami Limestone, and the intermediate confining unit comprised of the Stock Island Formation (figs. 6 and 9–1). The hydrogeologic cross section displayed in figure 9–1 is oriented oblique to the strike of depositional facies belts of the Pliocene-Pleistocene depositional systems that comprise the Stock Island Formation, Tamiami Formation, Fort Thompson Formation, and Miami Limestone. Thus the lithologies encountered in the southern boreholes represent more shoreward facies belts that are oriented generally parallel to paleoshorelines, and the northern boreholes intersect facies belts mostly parallel and proximal to the Pliocene-Pleistocene paleoshelf margins.

Until recently, the Stock Island Formation was only defined in the western Florida Keys (Cunningham and others, 1998), but is now recognized in Miami-Dade County at the G–3948 and G–3949 test boreholes (fig. 8). In the two test boreholes, the lithology of the Stock Island Formation is characterized by skeletal fragment, planktonic foraminiferal lime packstone and grainstone, which in some cases is very quartz-sand rich. The Stock Island Formation occurs subjacent to the Tamiami Formation in the test boreholes G–3948 and G–3949 (fig. 9–1), but on a regional scale is generally equivalent to the Tamiami Formation. In Broward County, the Stock Island Formation is shown on the Hillsboro Canal

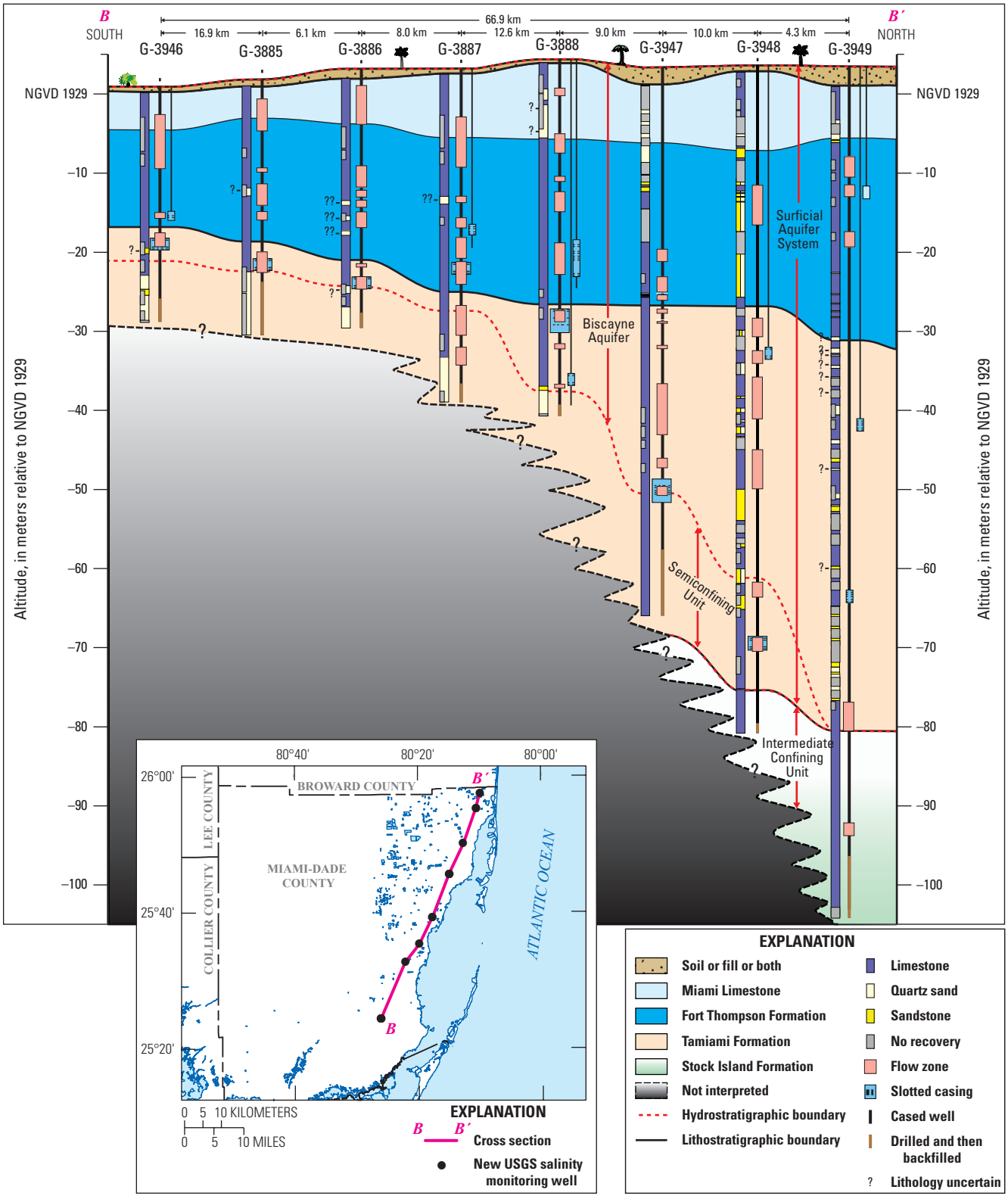

Figure 9–1. Illustration showing the cross section oblique to depositional strike of the upward transition from Pliocene-to-Pleistocene mixed carbonate-siliciclastic ramp to platform that comprise the surficial aquifer system and intermediate confining unit of central and northern coastal Miami-Dade County. The southern part of the cross section is substantially west of the present-day and Plio-Pleistocene shelf margin as compared to the northern part of the cross section.

seismic profile to be, at least in part, equivalent to the Ochopee Limestone Member of the Tamiami Formation. Chronostratigraphy by Guertin (1998) indicated that on Stock Island in the Florida Keys, the Stock Island Formation is mostly the same age as the Tamiami Formation. Cunningham and others (1998) delineated the Stock Island Formation as mainly equivalent to the Long Key Formation, and thus entirely or mostly restricted to a Pliocene age. Minor groundwater flow zones are defined in the Stock Island Formation in these test boreholes and provide examples of minor aquifer zones within the intermediate confining unit. It is likely that the Stock Island Formation is a low permeability, relatively deeper-water, outer-ramp equivalent to units within the Tamiami Formation that are much better defined to the west (Reese and Cunningham, 2000). New continuously drilled cores that span the complete thickness of the Biscayne aquifer, advanced geophysical logs, and new seismic profiles in canals and offshore in Biscayne Bay and the Atlantic Ocean (e.g., Cunningham and Wacker, 2009) are providing the information necessary to reinterpret the hydrogeologic setting described by Causaras (1987) and Fish and Stewart (1991).

Core Descriptions

Core descriptions from the eight new wells installed during the study are provided in a supplementary Adobe Acrobat ™ Portable Document Format file. General information concerning site location, core-hole depth, and available borehole geophysical logs is provided for each of the cores described. The depths to the top of the Miami Limestone, the Fort Thompson Formation, and the Tamiami Formation are included in this general information.

See supplemental file *http://pubs.usgs.gov/sir/2014/5025/appendix/sir2014-5025_appendix_09.pdf*.

References

Causaras, C.R., 1987, Geology of the surficial aquifer system, Dade County, Florida: U.S. Geological Survey Water-Resources Investigations Report 86–4126, 240 p., 2 sheets.

Cunningham, K.J., McNeill, D.F., Guertin, L.A., Ciesielski, P.F., Scott, T.M., and de Verteuil, L., 1998, New Tertiary stratigraphy for the Florida Keys and southern peninsula of Florida: Geological Society of America Bulletin, v. 110, no. 2, p. 231–258.

Cunningham, K.J., and Wacker, C., 2009, Seismic-sag structural systems in Tertiary carbonate rocks beneath southeastern Florida, USA—Evidence for hypogenic speleogenesis? *in* Klimchouk, A.B., and Ford, D.C., eds., Hypogene speleogenesis and karst hydrogeology of artesian basins: Simferopol, Ukraine, Ukrainian Institute of Speleology and Karstology, Special Paper no. 1, p. 151–158.

Fish, J.E., and Stewart Mark, 1991, Hydrogeology of the surficial aquifer system, Dade County, Florida: U.S. Geological Survey Water-Resources Investigations Report 90–4108, 50 p., 11 sheets.

Guertin, L.A., 1998, A late Cenozoic mixed carbonate/siliciclastic system, south Florida—Lithostratigraphy, chronostratigraphy, and sea-level record: Miami, University of Miami, Ph.D. dissertation, 335 p.

Reese, R.S., and Cunningham, K.J., 2000, Hydrogeology of the gray limestone aquifer in southern Florida: U.S. Geological Survey Water-Resources Investigations Report 99–4213, 244 p.

Appendix 10. Geochemical Sampling Methods

A total of 52 groundwater samples were collected from 34 wells, and 17 surface-water samples were collected from 10 surface-water monitoring sites by using a submersible pump, centrifugal suction pump, or Kemmerer water sampler. The sampling method used to collect each sample is provided in table 2–1. Site selection and sampling method were based on type of site (surface water or groundwater), well construction, well installation date, location, and the purpose of each sample. Sites were selected on both sides of the leading edge of the saltwater front. Wells near canals and farther away from canals were selected for comparison purposes.

Wells with short open intervals situated near the base of the aquifer are able to provide the most reliable information concerning the inland extent and age of saltwater in the aquifer. In some areas, however, the only available monitoring wells have long open intervals. In long open-interval wells, water of different ages and chemical compositions potentially could mix, which could greatly reduce the value of samples collected for age dating and evaluation of maximum salinity in the aquifer.

Sampling and decontamination procedures generally adhered to those described in the USGS National Field Manual for the collection of water-quality data (U.S. Geological Survey, variously dated), but procedures documented on the websites of the USGS Chlorofluorocarbon Laboratory in Reston, Virginia (U.S. Geological Survey, 2011a, b, c), and methods similar to those described by Kohout and Hoy (1963) also were used.

A Fultz™ SP–400 submersible pump with 100% Teflon lines was used to collect groundwater samples. Each sample collected using this pump was processed in a chamber that consisted of a clear, virgin, poly-resin, disposable bag. The bag prevented contamination by dust and cross-contamination between samples. Temperature, pH, dissolved oxygen, and specific conductance were monitored with a calibrated YSI Professional Plus™ multimeter and a flow-through chamber. Turbidity samples were periodically collected during purging by using a Hach™ 2100P portable turbidity meter.

Hydrogen sulfide was evaluated with a Hach HS-WR 0- to 11.25-mg/L test kit at selected sites. Samples collected by using the submersible pump were evaluated to determine the concentrations of the full suite of analytes, including barium, boron, bromide, calcium, chloride, fluoride, iron, magnesium, potassium, silica, sodium, strontium, sulfate, tritium, uranium, tritium (^{3}H), alkalinity, pH, temperature, specific conductance, turbidity, dissolved oxygen, and the isotopic ratios of ^{18}O/^{16}O and ^{2}H/^{1}H. Selected sites were sampled to evaluate (1) the age of the water by using ^{3}H/^{3}He and SF_6 age-dating methods, (2) the isotopic ratio of ^{87}Sr/^{86}Sr, (3) dissolved gas composition, and (4) terrigenic helium concentration.

A small, 4-stroke, variable-speed, gasoline-powered Honda™ WX10 centrifugal suction pump was used to sample surface-water sites. The centrifugal pump could pump at rates up to 60 L/min, but could not pump at rates as slow as the Fultz submersible pump. The speed of the centrifugal pump was too great to allow the use of the flow-through chamber, so probes from either the YSI™ Professional Plus multimeter or an Oakton™ pH/Con 10 series multimeter were placed in a bucket receiving discharge from the pump. The flow rate of the suction pump was more than sufficient to exchange water in the bucket as rapidly as the submersible pump had exchanged water in the flow-through cell. Dissolved oxygen was not measured. The centrifugal pump was decontaminated between samples by using the same procedures that were used on the submersible pump. To facilitate sampling, a valve was installed in the discharge line, which allowed a part of the pump discharge to be diverted to a small-diameter sampling line to which a filter could be attached. The centrifugal pump was only used to collect samples for the evaluation of major ion and tritium concentrations and the stable isotope ratios of oxygen and deuterium. These parameters were deemed sufficiently stable for sampling by using this method.

The long open-interval wells FKS4, FKS7, and FKS8 (appendix 1) were sampled with a Kemmerer water sampler. A flow-through cell could not be used with the Kemmerer. Instead, once the Kemmerer was retrieved from the well, a small part of the sample was placed in a cup that held the probes of the multimeter for evaluation of pH, temperature, and specific conductance. Measurements of these parameters in samples collected in this manner may not be fully representative of aquifer conditions because of the changes in pressure and temperature that can occur during measurement. The Kemmerer could only be used to collect samples for analysis of major ion and tritium concentrations and oxygen and deuterium stable isotope ratios because of the small sample volume and because the sample comes into contact with the air when released from the Kemmerer. It should be noted that sampling with a Kemmerer does not avoid the problem of mixing as a result of ambient vertical flow in the borehole. Site set-up and cleaning procedures used for Kemmerer sampling were similar to those used for samples collected with the submersible pump.

Dissolved gas samples (table 2–2) generally were not collected at surface-water sampling sites because they are used to evaluate the temperature of the water at the time that it entered the aquifer. These samples were only collected at selected sites.

Sample Analysis and Quality Assurance

Major and trace ion analyses were conducted at the USGS National Water Quality Laboratory in Denver, Colorado, by using the methods described in Clesceri and others (1998), Fishman and Friedman (1989), Fishman (1993), Garbarino (1999), and Garbarino and others (2006). The tritium concentrations in water samples (table 2–3) were evaluated by the USGS Stable Isotope and Tritium (USGS-SI&T) Laboratory in Menlo Park, California, by using electrolytic enrichment and liquid scintillation. The ^{87}Sr/^{86}Sr isotope ratios were analyzed by the USGS Metal and Metalloid Isotope Laboratory in Menlo Park, California, as described in Katz and Bullen (1996). Alkalinity was analyzed by titration with a Hach Universal Digital Titrator and 1.600 ± 0.008 N sulfuric acid by using the inflection point method. Titrations were usually performed twice for each sample, and the average alkalinity and bicarbonate concentrations were computed. Alkalinity, terrigenic helium, and dissolved gas samples were kept refrigerated until analyzed.

Dissolved gas composition (table 2–2) and SF_6 concentrations (table 2–4) were analyzed by the USGS Chlorofluorocarbon laboratory in Reston, Virginia, following the procedures described in USGS (2011d, i). The USGS Chlorofluorocarbon laboratory also evaluated the terrigenic helium in water samples with a Hewlett Packard 5890 Series gas chromatograph. The isotope compositions of oxygen and hydrogen expressed in terms of δ^{18}O and δ^2H (table 2–7) were determined by the USGS-SI&T as described in Révész and Coplen (2008a, b).

^{3}H/^{3}He age dating was performed by the Lamont-Doherty Earth Observatory Noble Gas laboratory at the Earth Institute at Columbia University (CU-LDEO) in Palisades, New York. The CULDEO laboratory determined the concentration of tritium by helium ingrowth. They also determined the concentrations of helium and neon and the isotope ratios of ^{3}He/^{4}He. Additional information concerning the methods used for mass spectrometry of helium isotopes and for measurement of the tritium concentration in water samples by the ^{3}He ingrowth method is provided by Ludin and others (1997). Ages were determined by using the relation of Schlosser and others (1988):

$$t = \frac{T_{1/2}}{\ln 2} \ln\left[1 + \frac{^3He_{trit}}{^3H}\right], \qquad (10\text{–}1)$$

where t is the ^{3}H/^{3}He age in years, $^3He_{trit}$ is the concentration of tritiogenic helium, *T1/2* is the half-life of tritium, and ^{3}H is the concentration of tritium. The amount of $^3He_{trit}$ derived from radioactive decay of ^{3}H in the water sample is determined by using a helium isotope mass balance (Schlosser and others, 1988). The helium concentration of groundwater can be enriched by terrigenic helium, which can interfere in the mass balance used to compute amount of $^3He_{trit}$ derived from radioactive decay. The neon concentration of the water sample, which is assumed to be derived solely from the

atmosphere, is used to calculate the amount of additional $^3He_{trit}$ (Schlosser and others, 1989). To determine if the terrigenic helium concentration in samples is excessive, the concentrations of helium, hydrogen, and neon in samples were determined by the USGS Reston Chlorofluorocarbon Laboratory (USGS-RCL) using gas-chromatography, and the concentration of helium that is in excess of the air-water equilibrium (Δ^4He) was computed using the relation

$$\Delta^4 He = \left[\frac{^4He_s - ^4He_{eq}}{^4He_{eq}} \right] \times 100 , \qquad (10–2)$$

where ^4He_s is the helium concentration of the sample and $^4He_{eq}$ is the air-water equilibrium concentration of helium. If the Δ^4He is positive, the sample contains excess air or terrigenic helium. If the tritium concentration is greater than 0.5 TU and if Δ^4He is less than 200 percent, $^3H/^3He$ age dating is likely to be successful. Corrections for terrigenic helium were applied to samples that indicated that terrigenic helium was greater than 5 percent. If the Δ^4He is negative by more than a few percent, the sample may have degassed and may not be able to be dated. The precision of analyses of the dissolved gases helium, hydrogen, and neon are respectively 20, 10–20, and 10 percent (Busenberg and others, 2000; Eurybiades Busenberg, U.S. Geological Survey, written commun., May 25, 2011). All but one of the samples (well G–3609) had Δ^4He values of less than 200 percent (table 2–6). The Δ^4He of the samples collected from well G–3609 on July 30, 2009, and December 17, 2009, were 8.5 and 215.3, respectively. Given this large discrepancy, the sample collected on December 17, 2009, may have had an air bubble that was not identified during sampling. Excluding the one sample from G–3609, the Δ^4He ranged from 0.1 to 154.9 percent and averaged 36.6 percent. The Δ^4He was not negative in any of these samples; therefore, these samples potentially could be used for $^3H/^3He$ age dating.

The $^3H/^3He$ age-dating results provided by the CU-LDEO laboratory also included determinations of Δ^4He. The analyses by the CU-LDEO laboratory were generally higher in precision than those that could be obtained by the USGS-RCL using gas chromatography. The Δ^4He in samples determined by the CU-LDEO laboratory ranged from 2.6 to 71.7 percent (table 2–5). Terrigenic helium corrections were applied to $^3H/^3He$ age dates of all samples that had terrigenic helium concentrations that were greater than 5 percent.

Excess air in samples also can potentially interfere with $^3H/^3He$ age-dating analyses. Samples for which the ΔNe and $\Delta^4He/\Delta Ne$ ratios are negative indicate that gas fractionation occurred. Where the $\Delta^4He/\Delta Ne$ ratio is less than 1, it is also possible that some gas fractionation may have occurred. When water comes in contact with air, the helium tends to diffuse more rapidly into the air than neon. If gas fractionation removed parent or daughter products from the system, it could invalidate the determined age. The ΔNe and $\Delta^4He/\Delta Ne$ ratios were computed for samples analyzed by the CU-LDEO laboratory (table 2–5). The ΔNe and $\Delta^4He/\Delta Ne$ ratios in samples from G–3600 were negative, which indicates that gas fractionation has occurred and that the age of this sample is questionable. Analyses of samples collected from wells G–3608, G–896, and G–894 and the C2 Canal at G–3608 indicated respective $\Delta^4He/\Delta Ne$ ratios of 0.7, 0.7, 0.8, and 0.5. These results indicate that gas fractionation may have occurred. Gas fractionation of canal water seems reasonable given that the canal water is always in contact with the atmosphere. The samples from wells G–896 and G–3608, which are 0.38 km and 8 m, respectively, from the Snapper Creek Canal, also could be affected by gas fractionation; however, the locations of these wells relative to the Snapper Creek Canal, the extraordinary permeability of the Biscayne aquifer, and the concordance of the samples collected in this area with respect to the $\Delta^4He/\Delta Ne$ ratios indicate that the $^3H/^3He$ ages from these wells may be reliable. Samples from wells G–896 and G–3608 indicated interpreted piston-flow ages that date to about 1998 and 1997, respectively (table 2–5).

The results of tritium analyses provided by the CU-LDEO lab (table 2–5) were used for $^3H/^3He$ age dating and are of greater precision than analyses provided by the USGS-SI&T laboratory (table 2–3). The analyses by the USGS-SI&T were used to ensure that tritium levels were within the acceptable range for analysis by the CU-LDEO lab and would not contaminate the CU-LDEO lab. Samples analyzed by the USGS-SI&T laboratory also were used to evaluate tritium concentrations in the aquifer. The standard deviation of analyses for all samples evaluated by the CU-LDEO laboratory for this study ranged from 0.04 to 0.91 TU, whereas the standard deviation for analyses by the USGS-SI&T laboratory ranged from 0.4 to 1.7 TU. Analytical results from the CU-LDEO were used to determine analytical ages and interpreted piston-flow ages. The analytical ages were determined using the analytical results of the CU-LDEO, measured salinity of the each sample, the approximate altitude of each sample location, and the recharge average recharge temperature determined from dissolved gas analyses. A crustal terrigenic $^3He/^4He$ ratio of 2.00×10^{-8} was used. The half-life of tritium used was 12.32 years. Interpreted piston-flow ages were determined based on the determined ages and amount of tritium. Samples with very low tritium are considered to provide only a very coarse understanding of age. Samples that have analytical ages older than 1970, which is considered beyond the practical range of this dating method, were assigned interpreted piston-flow ages of < 1970. Most interpreted piston-flow ages are considered approximate, because of the uncertainties in recharge temperature, gas fractionation, and the $^3He/^4He$ ratio.

A $^3H/^3He$ age-dating sample was collected from only one surface-water site because surface water typically is considered to be in relatively close equilibrium with the atmosphere and therefore would have an age near zero. The surface-water sample was collected to determine if older groundwater was flowing into the canal in sufficient quantities to be detected. $^3H/^3He$ age-dating samples were not collected from long screened wells or from newly installed wells where the mixing of water caused by sampling or well installation would affect the ages determined.

Quality-Assurance Samples

Replicate samples consisted of two or more sets of samples collected concurrently so that both samples are assumed to have identical water chemistry. Three replicate samples of major and trace ions were collected (table 2–1). The average difference between analytical results of original and replicate samples of major and trace ions was ±1.9 percent when all constituents were considered. The largest differences were observed for the analyses of fluoride and uranium. The difference between fluoride concentrations in original and replicate samples was ±7.5 percent. The replicate sample from well G–3610 indicated a –19.6 percent difference in uranium concentration from the original sample. The concentrations of fluoride and uranium were low in the replicate and original samples for which large percentage differences were evaluated. The fluoride concentrations of these replicate samples ranged from 0.13 to 0.16 mg/L, and the reporting level for this analysis was 0.08 mg/L. The amounts of uranium measured in the original and replicate samples from well G–3610 were 0.021 and 0.017 µg/L, respectively, and the reporting level for this analysis was 0.008 µg/L. Excluding fluoride and uranium, the analytical results of major and trace ions in original and replicate samples differed by ±4.4 percent.

All of the samples collected to evaluate SF_6, dissolved gases, and $^3H/^3He$ age dating were collected in replicate. Analytic results of the original and replicate samples of dissolved gases and SF_6 are reported (tables 2–2 and 2–4), except when a sample was lost or damaged during transport.

Replicates were collected for all dissolved gas samples, with the exception that the replicate sample from G–894 was lost. The absolute value of the difference between the analytical results of each pair of original and replicate samples was divided by the arithmetic mean of these results to determine percent differences (table 2–2). Replicate estimates of recharge temperature differed by only 0.80 percent, on average, with a maximum difference of 1.91 percent. Replicate samples of methane and oxygen differed by as much as 53.3 and 46.1 percent, respectively, and differences may have been caused by bacterial consumption of oxygen. The determinations of recharge temperature were likely unaffected because the two samples which indicated the largest differences in methane and oxygen (C2 Canal at G–3608 and well G–3607) indicated small differences in the recharge temperatures (1.39 and 0.19 percent, respectively).

Replicate samples were collected for all samples of oxygen and hydrogen stable isotopes. Most of the replicate samples were retained as potential replacement samples in case any of the original samples were lost during shipment to the laboratory for analysis. After results were received from the original samples, thirteen of the replicate samples were selected for analysis to evaluate the precision of the analytical method and the sampling procedures. The absolute value of differences between the original and replicate samples analyzed for δ^2H ranged from 0.54 to 126 percent and averaged 26.0 percent. The absolute value of differences between the original and replicate samples analyzed for $\delta^{18}O$ ranged from 1.32 to 106 percent and averaged 18.9 percent. Although these differences seem large, when evaluted graphically (fig. 10–1) they do not greatly alter the interpretations that can be drawn from the analyses. For example, even though the differences between the original and replicate analyses of

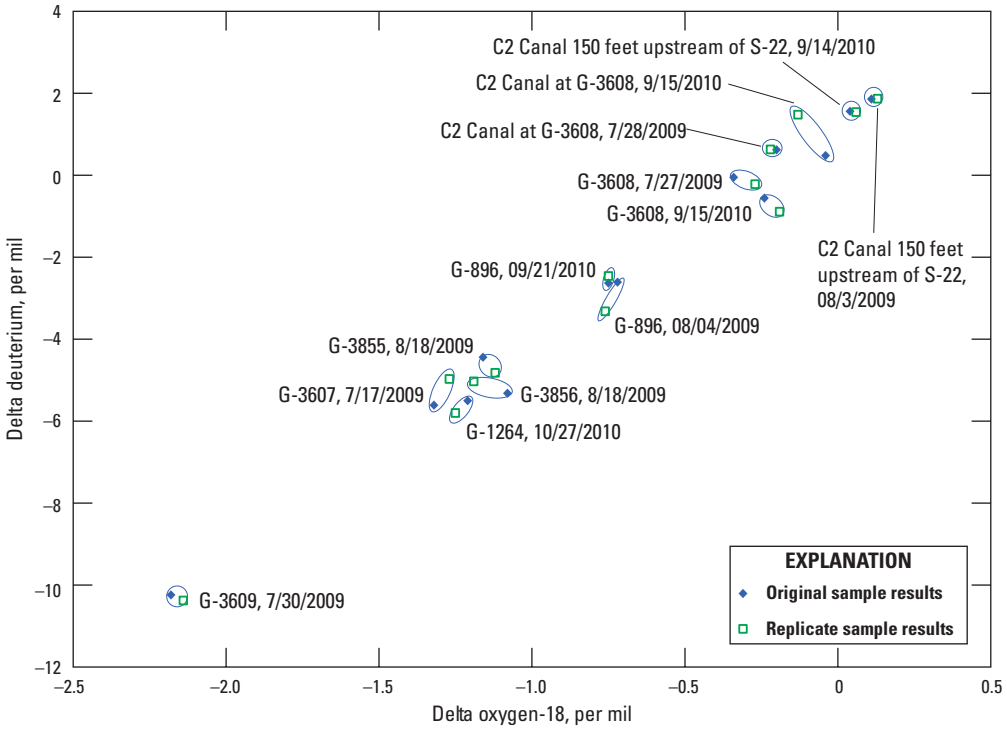

Figure 10–1. Delta oxygen-18 and delta deuterium for samples and replicate samples, 2009–2010, Miami-Dade County, Florida.

δ^2H and $\delta^{18}O$ in well G–3608 collected on July 27, 2009, were 126 and 23.0 percent, respectively, the results still plot within a small area as shown by the blue circles around each original and replicate sample in figure 10–1.

To ensure that the deionized water used for equipment cleaning did not contain the major and trace ions evaluated during the study, quality-assurance samples of deionized water were collected directly from the filtration system on July 16, 2009, and December 15, 2009, and analyzed for all ions of interest. No detections of any major or trace ions were above the minimum reporting levels for any of these ions.

To ensure that the equipment was properly decontaminated between samples, 11 equipment blanks were collected using deionized water from the USGS National Water Quality Laboratory. Minor amounts of iron ranging from an estimated 2.3 to 8 µg/L were detected in 6 of the 11 equipment blanks, but because many of the well casings were constructed of iron and the pump head was constructed of stainless steel, this analyte was not considered for evaluation of aquifer geochemistry. Excluding iron, one or more of the analytes evaluated for this study were detected in 4 of the 11 blanks. The majority of these detections were below or very close to the normal reporting level for the analytes detected. Although calcium, chloride, magnesium, sodium, and strontium were detected in equipment blanks, the detections were only 0.2 to 2.1 percent of the minimum concentrations measured in the groundwater and surface-water samples that were collected, and as such would not significantly affect the results of analyses. The one exception was the detection of 22.8 µg/L of boron in the equipment blank collected at C–5 Canal at NW 32 Court on August 6, 2010. The amount of boron in all other equipment blanks was less than the reporting level of 4 µg/L. The boron concentrations in samples ranged from 27.2 to 2,470 µg/L. Boron averaged 245 µg/L in groundwater samples and 42.4 µg/L in surface-water samples.

References

Busenberg, Eurybiades, Plummer, L.N., Doughten, M.W., Widman, P.K., and Bartholomay, R.C., 2000, Chemical and isotopic composition and gas concentrations of ground water and surface water from selected sites at and near the Idaho National Engineering and Environmental Laboratory, Idaho, 1994–97: U.S. Geological Survey Open-File Report 00–81, 51 p.

Clesceri, L.S., Greenburg, A.E., and Eaton, A.D., eds., 1998, Standard methods for the examination of water and wastewater (20th ed.): Washington, D.C., American Public Health Association, American Water Works Association, and Water Environment Federation, p. 3–37 to 3–43.

Fishman, M.J., ed., 1993, Methods of analysis by the U.S. Geological Survey National Water Quality Laboratory—Determination of inorganic and organic constituents in water and fluvial sediments: U.S. Geological Survey Open-File Report 93–125, 217 p.

Fishman, M.J., and Friedman, L.C., 1989, Methods for determination of inorganic substances in water and fluvial sediments: U.S. Geological Survey Techniques of Water-Resources Investigations, book 5, chap. A1, 545 p.

Garbarino, J.R., 1999, Methods of analysis by the U.S. Geological Survey National Water Quality Laboratory—Determination of dissolved arsenic, boron, lithium, selenium, strontium, thallium, and vanadium using inductively coupled plasma-mass spectrometry: U.S. Geological Survey Open-File Report 99–093, 31 p.

Garbarino, J.R., Kanagy, L.K., and Cree, M.E., 2006, Determination of elements in natural-water, biota, sediment, and soil samples using collision/reaction cell inductively coupled plasma-mass spectrometry: U.S. Geological Survey Techniques and Methods, book 5, sec. B, chap. 1, 88 p.

Katz, B.G., and Bullen, T.D., 1996, The combined use of 87Sr/86Sr and carbon and water isotopes to study the hydrochemical interaction between groundwater and lakewater in mantled karst: Geochimica et Cosmochimica Acta, v. 60, no. 24, p. 5075–5087.

Kohout, F.A., and Hoy, N.D., 1963, Some aspects of sampling salty ground water in coastal aquifers: Ground Water, v. 1, no. 1, p. 28–32.

Ludin, A.I., Weppernig, Ralf, Bonisch, G., and Schlosser, Peter, 1997, Mass spectrometric measurement of helium isotopes and tritium in water samples: Lamont-Doherty Earth Observatory of Columbia University, Technical Report 98.6, accessed May 12, 2011, at *http://www.ldeo.columbia.edu/~etg/ms_ms/Ludin_et_al_MS_Paper.html*.

Révész, Kinga, and Coplen, T.B., 2008a, Determination of the δ(2H/1H) of water: RSIL lab code 1574, chap. C1 of Révész, Kinga, and Coplen, T.B., eds., Methods of the Reston Stable Isotope Laboratory: U.S. Geological Survey Techniques and Methods 10–C1, 27 p.

Révész, Kinga, and Coplen, T.B., 2008b, Determination of the δ(180/160) of water: RSIL lab code 489, chap. C2 of Révész, Kinga, and Coplen, T.B., eds., Methods of the Reston Stable Isotope Laboratory: U.S. Geological Survey Techniques and Methods, 10–C2, 28 p.

Schlosser, Peter, Stute, Martin, Dorr, Helmut, Sonntag, Christian, and Munnich, K.O., 1988, Tritium/3He dating of shallow groundwater: Earth and Planetary Science Letters, v. 89, p. 353–362.

Schlosser, Peter, Stute, Martin, Sonntag, Christian, and Munnich, K.O., 1989, Tritiogenic 3He in shallow groundwater: Earth and Planetary Science Letters, v. 94, p. 245–256.

U.S. Geological Survey, variously dated, National field manual for the collection of water-quality data: U.S. Geological Survey Techniques of Water-Resources Investigations, book 9, chaps. A1–A9, available online at *http://pubs.water.usgs.gov/twri9A*.

U.S. Geological Survey, 2011a, Reston Chlorofluorocarbon Laboratory—SF6 sampling: U.S. Geological Survey, accessed April 29, 2011, at *http://water.usgs.gov/lab/sf6/sampling/*.

U.S. Geological Survey, 2011b, Reston Chlorofluorocarbon Laboratory— Dissolved Gas N2 / Ar and 4He Sampling: U.S. Geological Survey, accessed June 25, 2013, at *http://water.usgs.gov/lab/dissolved-gas/sampling/*.

U.S. Geological Survey, 2011c, Reston Chlorofluorocarbon Laboratory—3H/3He sampling: U.S. Geological Survey, accessed April 26, 2011, at *http://water.usgs.gov/lab/3h3he/sampling/*.

U.S. Geological Survey, 2011d, Reston Chlorofluorocarbon Laboratory—Analytical procedures for SF6: U.S. Geological Survey, accessed April 26, 2011, at *http://water.usgs.gov/lab/sf6/lab/analytical_procedures/*.

U.S. Geological Survey, 2011i, Reston Chlorofluorocarbon Laboratory—Analytical procedures for dissolved gasses N2 / Ar: U.S. Geological Survey, accessed April 26, 2011, at *http://water.usgs.gov/lab/dissolved-gas/lab/analytical_procedures/*.

Appendix 11. Salinity Measurements in Canals

Monthly measurements of salinity in canals collected by the Miami-Dade County Permitting, Environmental, and Regulatory Affairs (M-D PERA); Maria Idia Macfarlane, Water and Sewer Department, written commun., March 7, 2011; Craig Grossenbacher, Miami-Dade County Permitting, Environmental, and Regulatory Affairs, written commun., July 7, 2010) are provided as supplemental files.

See supplemental file *http://pubs.usgs.gov/sir/2014/5025/appendix/sir2014-5025_appendix_11.xlsx*.

Appendix 12. Geographic Information System Files

GIS files for the 2008 and 2011 lines showing the inland extent of saltwater in the Biscayne aquifer are provided as ESRI Arc-GIS shape files in separate electronic files. Metadata are included in these files. Users should view the Federal Geographic Data Committee (FGDC) metadata, because it provides important distribution information that other metadata formats do not include. These files describe the conditions of usage. The column “LINETYPE” in the attribute table should be used to indicate where the lines are shown as solid or dashed. To confirm that users are depicting this line correctly they should compare their maps to the USGS maps of these lines available at: *http://www.envirobase.usgs.gov/FLIMS/SaltFront/viewer.htm* (U.S. Geological Survey, 2011g).

See supplemental files in the folder *http://pubs.usgs.gov/sir/2014/5025/appendix/sir2014-5025_appendix_12*.

Manuscript approved February 17, 2014
Prepared by the Raleigh Publishing Service Center
Kimberly Waltenbaugh, Editor
Kimberly Swidarski, Illustrations and layout

For more information about this publication, contact:
Director
U.S. Geological Survey
Florida Water Science Center
4446 Pet Lane, Suite 108
Lutz, FL 33559
(813) 498-5000

or visit our website at
http://fl.water.usgs.gov

ISSN 2328-0328 (online)
http://dx.doi.org/10.3133/sir20145025